

# **Thin film molecularly imprinted polymers for environmental and biological sample preparations and analysis**

By

© Fereshteh Shahhoseini

A thesis submitted to the School of Graduate Studies in partial fulfillment of the requirements for the degree of

**Doctor of Philosophy**

**Department of Chemistry**

Memorial University of Newfoundland and Labrador

**March 2022**

St. John's, Newfoundland and Labrador

## Abstract

Sample preparation has always been the challenging part of analysis in both environmental and biological samples. The need for trace monitoring of organic pollutants in different water matrices has initiated a lot of research to develop a sensitive sample preparation method. Furthermore, with the advancement in precision medicine facilitating healthy lives, a high throughput and simple biological sample preparation is of prime importance. Besides the challenges in sensitivity, throughput and simplicity, matrix effect is a serious problem in sample preparation techniques which adversely affect the accuracy of the results in both environmental water and biofluid analysis. Molecularly imprinted polymer (MIP) sorbents implementation in sample preparation devices can add selectivity in extraction of targeted analytes and limit the matrix effect.

In this thesis, MIP sorbent were fabricated on a frosted glass and a stainless-steel substrate to produce MIP-thin film microextraction (MIP-TFME) devices for water and plasma samples analysis, respectively. Polycyclic aromatic hydrocarbons (PAHs) pollutants in different water matrices were extracted using a MIP-TFME device previously developed in Dr. Bottaro's research group. The device size was decreased compared to previous studies to accommodate a high throughput method for analysis of sixteen regulated PAHs with detection limits ranging from 2 ng L<sup>-1</sup> to 400 ng L<sup>-1</sup> using gas chromatography with atmospheric pressure chemical ionization mass spectrometry (GC-APCI-MS). As for bioanalysis, a MIP-TFME device was developed for analysis of tricyclic antidepressants (TCAs) in plasma by optimizing different parameters affecting the MIP performance such as template: monomer ratio, monomer:crosslinker ratio and progen

volume. TCAs were extracted using the optimized MIP-TFME device and analytical method from pooled human plasma and patient samples; and quantified using ultra high-performance liquid chromatography-tandem mass spectrometry. The optimized MIP-TFME device showed good selectivity over corresponding non-imprinted polymers (imprinting factors 2.36-4.36). In another bioanalysis study, the applicability of an optimized porous polymer thin film device as a micro-sampling technique for analysis of TCAs was assessed. These devices allowed for analysis of small volume (10  $\mu$ L) of plasma sample using spot extraction procedure. Important factors affecting the extraction efficiency such as sample volume, solvent desorption, washing, and the time of the extraction were studied to develop and validate the analytical method. Two spiked individual plasma samples were analyzed using the validated method and the obtained data proved the acceptable accuracy (86.7% to 114%) and precision (RSD values of 0.1-10%) of this method. Further evaluation such as matrix effect, method of normalization using deuterated compound and preservation of the extracted TCAs were performed. The satisfactory results of these studies provided more confirmation of the suitability of the porous thin film device for microsampling analysis of TCAs in plasma samples.

## **Acknowledgment**

The completion of my Ph.D. program and this thesis would not be possible without people who helped and supported me. It is a genuine pleasure to express my deep sense of thanks and gratitude to my supervisor Dr. Christina Bottaro. Her support, guidance, and advice carried me through the stages of the Ph.D. program. Her effort in providing a growing environment, knowledge, and emotional support gave me the courage to be my best and satisfaction of enjoyable research. I would like to give my warmest thanks to my supervisory committee, Dr. Christopher Kozak and Dr. Christopher Rowley for their valuable comments and suggestions.

I like to thank my truly amazing husband, Ali Azizi. Ali is my best friend, closest advisor, and the love of my life. He supported me every step of this long journey with patience, great insight, and love.

I want to dedicate this thesis to my late father who I am sure is happy for me and watching me through heaven and my mother, brothers, and sisters that have always been supportive and encouraging.

## Table of contents

Abstract	ii
Acknowledgment	iv
List of Tables	xi
List of Figures	xiv
List of Symbols, Nomenclature or Abbreviation	xxiv
Co-authorship Statement	xxxiii
<b>Chapter 1: A critical evaluation of molecularly imprinted polymer (MIP) coatings in solid phase microextraction devices</b>	<b>1</b>
1.1. Introduction to MIP-SPME	2
1.2. Principles of molecularly imprinting	8
1.3. Characterization performance	11
1.4. MIP-SPME fibers	17
1.4.1. MIP-coated fibers	17
1.4.1.1. Surface polymerization from bulk solution	18
1.4.1.2. Molding	23
1.4.1.3. Spraying	25
1.4.1.4. Coating incorporating premade MIP particles	26

1.4.2. Monolithic MIP-fiber	30
1.5. Alternative High Capacity MIP format	36
1.5.1. MIP-SBSE	36
1.5.1.1. Grafting	38
1.5.1.2. Molding	41
1.5.1.3. Monolithic	43
1.5.1.4. Physical attachment	45
1.5.2. MIP-TFME	49
1.5.2.1. Solid substrate supported MIP-TFME	50
1.5.2.2. Membrane supported MIP-TFME	54
1.6. Conclusions on MIP-SPME devices	58
1.7. Instrumental analysis with MIP-SPME devices	60
1.8. Guidelines to validate an analytical method	66
1.9. Thesis objectives	66
1.10. References	68
<b>Chapter 2: Single-use porous thin film extraction with gas chromatography atmospheric pressure chemical ionization tandem mass spectrometry for high-throughput analysis of 16 PAHs</b>	83

2.1. Introduction	84
2.2. Experimental	87
2.2.1. Reagents and Materials	87
2.2.2. Thin film Fabrication	89
2.2.3. Instrumentation	90
2.2.4. Sample preparation procedure	91
2.2.5. Water samples	93
2.3. Results and discussion	93
2.3.1. Method development	93
2.3.1.1. Desorption of PAHS from porous thin films	84
2.3.1.2. Extraction of PAHs from water using porous thin films	96
2.3.2. Potential reusability	99
2.3.3. Selection of internal standard	100
2.3.4. Method validation	106
2.3.5. Matrix-matched calibration for real sample analysis	110
2.4. Conclusion	116
2.5. References	117

<b>Chapter 3: Thin film molecularly imprinted polymer (TF-MIP), a selective and single-use extraction device for high-throughput analysis of biological samples</b>	121
3.1. Introduction	122
3.2. Experimental	125
3.2.1. Materials and Reagents	125
3.2.2. Instrumentation and operating conditions	127
3.2.3. Preparation of the pseudo template	129
3.2.4. Preparation of thin film MIPs	130
3.2.5. Optimization of MIP composition	131
3.2.6. Extraction of TCAs from biological samples using thin film MIPs	132
3.3. Results and discussion	133
3.3.1. Preparation and characterization of thin film MIPs	133
3.3.2. Considerations for the use of thin film MIPs for extraction of TCAs from biological matrices	144
3.3.3. Optimization of extraction of TCAs from biological matrices	148
3.3.3.1. Washing	148
3.3.3.2. Desorption	149
3.3.3.3. Extraction	152

3.3.4. Method validation	159
3.3.4.1. BSA	159
3.3.4.2. Plasma	162
3.3.5. Application to real patient samples for clinical validation	167
3.4. Conclusion	168
3.5. References	168
<b>Chapter 4: Single-use porous polymer thin-film device: a reliable sampler for analysis of drugs in small volumes of biofluids</b>	174
4.1. Introduction	175
4.2. Experimental section	178
4.2.1. Chemicals and materials	178
4.2.2. Instrumentation	181
4.2.3. Manufacture of single-use porous polymeric thin film devices	182
4.2.4. Extracted biofluid spot procedure	183
4.3. Results and discussion	184
4.3.1. Porous thin film for extracted biofluid spot	184
4.3.1.1. Evaluation of coating in extraction of TCAs	185
4.3.2. Optimization of extracted biofluid spot procedure	188

4.3.2.1. Sample volume	188
4.3.2.2. Solvent desorption	190
4.3.2.3. Washing effect	193
4.3.2.4. Extraction time profile	195
4.3.3. Matrix effects	198
4.3.4. Single-use sampling devices: suitability for collection, transport and storage	199
4.3.4.1. Inter-device variability assessment	199
4.3.4.2. Preservation of drugs extracted onto the porous polymeric thin film	202
4.3.5. Reusability of porous thin films	206
4.3.6. Method validation	206
4.3.7. Analysis of real samples	214
4.4. Conclusion	216
4.5. References	217
Chapter 5: Conclusion and future work	222
5.1. Conclusion	223
5.2. Future work	229
5.3. References	230

## List of Tables

### Chapter 1:

**Table 1.1.** MIP-SPME fibers: composition, fabrication technique and performance for applications in aqueous samples. 29

**Table 1.2.** MIP-SPME fiber composition, selectivity and performance fabricated using different techniques with an application in food, plant material, and biological samples. 34

**Table 1.3.** MIP-SBSE composition, fabrication technique, selectivity and performance for specified targeted compounds and matrices 47

**Table 1.4.** Thin film-MIP devices fabrication method, composition, selectivity and performance prepared for targeted compounds in various matrices. 56

### Chapter 2:

**Table 2.1.** Physiochemical properties of target analytes 88

**Table 2.2.** Summary of tandem mass spectrometry parameters using APGC-MS/MS 91

**Table 2.3.** Method validation of porous thin film extraction for determination of PAHs in DI water (n=3) 108

**Table 2.4.** Comparison of proposed thin film extraction with other methods for the determination of PAHs 109

**Table 2.5.** Matched calibration data for analysing Waterford River sample (n=3) 111

**Table 2.6.** Matched calibration data for analysing Harbour sample (n=3) 112

<b>Table 2.7.</b> Matrix effect assessment for real water samples	114
<b>Chapter 3:</b>	
<b>Table 3.1.</b> Target drugs and physical chemical properties	126
<b>Table 3.2.</b> Summary of tandem mass spectrometry parameters of TCAs using LC-MS/MS	128
<b>Table 3.3.</b> Details of prepolymer solutions used for porogen dilution study	135
<b>Table 3.4.</b> Effect of porogen volume on imprinting and repeatability of extraction of TCAs	137
<b>Table 3.5.</b> Effect of porogen volume on recovery and repeatability of extraction of TCAs using MIPs and NIPs	137
<b>Table 3.6.</b> T-test at a 95% confidence level for inter-batch reproducibility of thin film MIPs ( $T_{crit} = 2.776$ )	140
<b>Table 3.7.</b> Figures of merit for quantification of free concentration of TCAs in BSA using thin film MIPs (n=3)	161
<b>Table 3.8.</b> Effect of dilution on the accuracy and precision of the results	162
<b>Table 3.9.</b> Figures of merit for quantification of free concentration of TCAs in pooled plasma using thin film MIP extraction method	164
<b>Table 3.10.</b> Detected concentrations of TCAs in patient samples analyzed by thin film MIP extraction method	167

#### **Chapter 4:**

<b>Table 4.1.</b> Targeted TCAs with physical and chemical properties	179
<b>Table 4.2.</b> Summary of tandem mass spectrometry parameters for determination of tricyclic antidepressants	181
<b>Table 4.3.</b> Details of prepolymer solutions used for monomer study	187
<b>Table 4.4.</b> Matrix effect study of spot sampling using porous thin film device	199
<b>Table 4.5.</b> T-test at a 95% confidence level for inter-batch reproducibility of porous thin films ( $T_{crit} = 2.776$ )	202
<b>Table 4.6.</b> Figures of merit obtained by spot sampling analysis using porous polymeric thin films ( $n=3$ )	208
<b>Table 4.7.</b> Comparison of extracted biofluid spot method with other methods for analysis of TCAs.	213
<b>Table 4.8.</b> Application of spot sampling analysis using porous polymeric thin films for TCA quantitation in two plasma samples ( $n=3$ ).	215

## List of Figures

### Chapter 1:

- Figure 1.1.** The percentage of the papers with the subject of developing fiber, monolithic fiber, SBSE and TFME of MIP-SPME devices published during 2001-2022 (n= 142) 7
- Figure 1.2.** Classification of different formats of MIP-SPME devices based on the method of fabrication. 7
- Figure 1.3.** MIP sorbent fabrication process. 8
- Figure 1.4.** MIP-fiber fabrication techniques. 17
- Figure 1.5.** SEM image of MIP-SPME fiber prepared by bulk polymerization after 5 cycles (A-C) and FTIR characterization (D). Reprinted from Ref. [1], with permission from John Wiley and Sons. 20
- Figure 1.6.** SEM images. (a) MIPs (1000 ×), and (b) NIPs (5000 ×), (c) MIPs-coated fiber (50 ×), and (d) MIPs-coated fiber (1000 ×). Reprinted from Ref. [2], with permission from Elsevier. 28
- Figure 1.7.** Comparison of extraction capacities of TPhP and structural analogues on TPhP-MIPs/GO and NIPs/GO fiber (a), and reusability of monolithic MIP-SPME fiber for extraction of TPhP at 10 ng mL<sup>-1</sup> (b). Reprinted from Ref. [3], with permission from Elsevier. 32
- Figure 1.8.** MIP-SBSE fabrication techniques. 38
- Figure 1.9.** The photo of a bare glass bar (A) and the scanning electron micrographs of the MIP coating of a stir bar (B, C) and the cross-section of a MIP-SB (D). Reprinted from Ref. [4], with permission from Elsevier. 40

<b>Figure 1.10.</b> Thin film MIP fabrication techniques.	49
<b>Figure 1.11.</b> Scanning electron micrographs of prepared thin film MIPs at different magnifications. Reprinted from Ref. [5], with permission from Elsevier.	53
<b>Figure 1.12.</b> Cross-section diagram of APCI ion source	62
<b>Figure 1.13.</b> Ionization mechanisms in APCI-GC ion source	63
<b>Figure 1.14.</b> ESI ion source structure and mechanism	64
<b>Figure 1.15.</b> Fundamental mechanism of tandem mass spectrometry	65
 <b>Chapter 2:</b>	
<b>Figure 2.1.</b> Experimental procedure for fabrication of thin film devices	90
<b>Figure 2.2.</b> Method of extraction and desorption process	92
<b>Figure 2.3.</b> Effect of agitation rate using multi vortex on desorption of PAHs. Extraction: sample 20 mL DI spiked with 50 ng mL <sup>-1</sup> PAHs, 2 hours at 1400 rpm	94
<b>Figure 2.4.</b> Optimization of solvent desorption in 10 min using multi vortex at 1000 rpm; Extraction was performed from 20 mL DI water sample spiked 2000 pg mL <sup>-1</sup> of Naph, Acy, Ace, Flu, Phe, Ant, Flut and Pyr and 250 pg mL <sup>-1</sup> of BaA, Chry, BbF, BkF, BaP, InP, DB(ah)A and BGP for 2 hours and 1400 rpm agitation; Solvents spiked with internal standards to obtain 50000 pg mL <sup>-1</sup> of Naph-d8, Ace-d10 and Phe-d10 and 10000 pg mL <sup>-1</sup> Chry-d12	95
<b>Figure 2.5.</b> Optimization of desorption time in the range of 2-20 mins; Extraction was performed from 20 mL DI water sample spiked 2000 pg mL <sup>-1</sup> of Naph, Acy, Ace, Flu, Phe,	

Ant, Flut and Pyr and 250 pg mL<sup>-1</sup> of BaA, Chry, BbF, BkF, BaP, InP, DB(ah)A and BGP for 2 hours and 1400 rpm agitation; Desorption: hexane (1250 µL) spiked with internal standards to obtain 50000 pg mL<sup>-1</sup> of Naph-d8, Ace-d10 and Phe-d10 and 10000 pg mL<sup>-1</sup> Chry-d12 under 1000 rpm vortex agitation 96

**Figure 2.6.** Investigation of extraction agitation effect on extraction efficiency; Extraction was performed for 2 hours in 20 mL DI water sample spiked with 2000 pg mL<sup>-1</sup> of Naph, Acy, Ace, Flu, Phe, Ant, Flut and Pyr and 250 pg mL<sup>-1</sup> of BaA, Chry, BbF, BkF, BaP, InP, DB(ah)A and BGP; Desorption: 1000 rpm multi-vortex for 5 minutes. Hexane was used as desorption solvent spiked with internal standards to obtain 50000 pg mL<sup>-1</sup> of Naph-d8, Ace-d10 and Phe-d10 and 10000 pg mL<sup>-1</sup> Chry-d12 97

**Figure 2.7.** Extraction time profile of 16 PAHs on polymeric thin film; Extraction was performed at 1400 rpm in 20 mL DI water sample spiked with 2000 pg mL<sup>-1</sup> of Naph, Acy, Ace, Flu, Phe, Ant, Flut and Pyr and 250 pg mL<sup>-1</sup> of BaA, Chry, BbF, BkF, BaP, InP, DB(ah)A and BGP; Desorption: 1000 rpm multi-vortex for 5 minutes. Hexane was used as desorption solvent spiked with internal standards to obtain 50000 pg mL<sup>-1</sup> of Naph-d8, Ace-d10 and Phe-d10 and 10000 pg mL<sup>-1</sup> Chry-d12 98

**Figure 2.8.** Reusability of polymeric thin films. Extraction was performed from 20 mL DI water sample with concentration of 2000 pg mL<sup>-1</sup> of Naph, Acy, Ace, Flu, Phe, Ant, Flut and Pyr and 250 pg mL<sup>-1</sup> of BaA, Chry, BbF, BkF, BaP, InP, DB(ah)A and BGP for 1 hour. Desorption: 1000 rpm multi vortex for 5 minutes, Hexane was used as desorption solvent and spiked with 50000 pg mL<sup>-1</sup> of Naph-d8, Ace-d10 and Phe-d10 and 10000 pg mL<sup>-1</sup> of Chry-d12 100

<b>Figure 2.9.</b> Multiplication of relative errors (RSD%) of normalized peak area of 8 light PAHs during optimization of desorption solvent	102
<b>Figure 2.10.</b> Calibration curve of BGP obtained in deionized water, extraction was performed using 20 mL deionized water sample spiked with BGP in a concentration range between 4-200 pg mL <sup>-1</sup> , and 100 pg mL <sup>-1</sup> of Per-d12 (a) and (b) Chry-d12, for 1 hour and 1400 rpm agitation. Desorption with 1250 µL of Hexane vortexed at 1000 rpm for 5 min	103
<b>Figure 2.11.</b> Calibration curve of BGP obtained in synthetic river water, extraction was performed using 20 mL synthetic river water sample spiked with BGP between 2-200 pg mL <sup>-1</sup> , and 100 pg mL <sup>-1</sup> of Per-d12 (a) and (b) Chry-d12, for 1 hour and 1400 rpm agitation. Desorption with 1250 µL of Hexane vortexed at 1000 rpm for 5 min	104
<b>Figure 2.12.</b> Calibration curve of BGP obtained in synthetic sea water, extraction was performed using 20 mL synthetic sea sample spiked with BGP between 2-200 pg mL <sup>-1</sup> , and 100 pg mL <sup>-1</sup> of Per-d12 (a) and (b) Chry-d12, for 1 hour and 1400 rpm agitation. Desorption with 1250 µL of Hexane vortexed at 1000 rpm for 5 min	105
<b>Figure 2.13.</b> Comparison of relative peak area obtained for matched matrices at added concentration of 2 pg mL <sup>-1</sup> of PAHs and real samples	115

### **Chapter 3:**

<b>Figure 3.1.</b> Chemical structure of the synthesized template	130
---	-----

<b>Figure 3.2.</b> Fabrication of thin film MIP using drop casting technique	131
<b>Figure 3.3.</b> Experimental workflow for analysis of plasma samples using thin film MIPs	133
<b>Figure 3.4.</b> MIP formula development: a) Porogen volume effects, extraction at pH ~7 (T:M:C, 1:4:24); b) Porogen volume effects, extraction with 1% TEA at pH ~11 (T:M:C, 1:4:24); c) Optimization monomer-to-crosslinker ratio (T:M, 1:4); d) Optimization template-to-monomer ratio (M:C, 1:6). All extractions from 20 mL of 50 ng mL <sup>-1</sup> aqueous TCAs (n=3)	138
<b>Figure 3.5.</b> Inter-batch reproducibility of 2 sets of thin film MIPs. All extractions from 20 mL of 50 ng mL <sup>-1</sup> of TCAs with 1% TEA at pH ~11	140
<b>Figure 3.6.</b> Side view of exemplary a) thin film MIP, and b) thin film NIP prepared on stainless steel substrates obtained at 2500x magnification	141
<b>Figure 3.7.</b> SEM of prepared thin film MIPs a) at 5000x, c) at 40,000x, and e) at 80000x; SEM of prepared thin film NIPs, b) at 5,000x, d) at 40000x, and f) at 80000x. (T:M:C, 1:2:24)	142
<b>Figure 3.8.</b> BET isotherm for a) optimized thin film MIP and b) its corresponding NIP	144
<b>Figure 3.9.</b> The summary process for assessment of protein binding of TCAs	145
<b>Figure 3.10.</b> Effect of PBS and BSA on recoveries of TCAs following 1 h incubation at 37 °C at neutral pH (TCA are protonated under these conditions)	146

**Figure 3.11.** Effect of type of base on TCA recoveries following 1 h incubation at 37 °C of 100 ng mL<sup>-1</sup> of TCAs in 1% MS-compatible base with either water, PBS, or BSA solution.

BA – butylamine 147

**Figure 3.12.** Wash optimization. Wash: 8 s immersion in 20 mL DI water, 0.1 % aqueous FA or 1% aqueous TEA. Sample extraction: 700 µL of 100 ng mL<sup>-1</sup> of TCAs in BSA with 1% TEA, extraction for 20 min at 1000 rpm, Desorption conditions: 700 µL MeOH, 20 min at 1000 rpm 149

**Figure 3.13.** Comparison of the extracted mass of TCAs by using different solvents for desorption. Sample extraction: 700 µL of 100 ng mL<sup>-1</sup> of TCAs in BSA with 1% TEA, extraction for 20 min at 1000 rpm, washing: 8 sec immersion in water with 1%TEA, Desorption conditions: 700 µL, 20 min at 1000 rpm 151

**Figure 3.14.** Desorption time profile. Sample extraction: 700 µL of 100 ng mL<sup>-1</sup> of TCAs in BSA with 1% TEA, extraction for 20 min at 1000 rpm, washing: 8 sec immersion in water with 1%TEA, Desorption conditions: 700 µL of ACN/water (1:1) with 0.1% FA at 500 rpm 151

**Figure 3.15.** The effect of agitation on the recovered TCAs. Sample extraction: 700 µL of 100 ng mL<sup>-1</sup> of TCAs in BSA with 1% TEA, extraction for 20 min at various agitation, washing: 8 sec immersion in water with 1%TEA, Desorption conditions: 700 µL of ACN/water (1:1) with 0.1%FA, 20 min at 500 rpm 152

<b>Figure 3.16.</b> Adsorption Kinetics of TCAs. Extraction: 700 $\mu\text{L}$ of BSA sample spiked with 100 $\text{ng mL}^{-1}$ of TCAs at 1500 rpm. Desorption: 700 $\mu\text{L}$ of 0.1 % FA in 50% aqueous ACN (20 min at 500 rpm)	154
<b>Figure 3.17.</b> Comparison of the chromatograms of (a) thin film MIPs, and (b) thin film NIPs. Extraction: 700 $\mu\text{L}$ of BSA sample spiked with 100 $\text{ng mL}^{-1}$ of TCAs (60 min at 1500 rpm); Desorption: 700 $\mu\text{L}$ of 0.1 % FA in 50% aqueous ACN (20 min at 500 rpm)	156
<b>Figure 3.18.</b> Calibration curves obtained for extraction of a) nortriptyline, b) desipramine, c) amitriptyline, d) doxepin, e) imipramine, f) trimipramine, and g) clomipramine; h) the ratio of slopes of calibration curve for TCAs using thin film MIPs versus NIPs for extraction from BSA	157
<b>Figure 3.19.</b> RSD percentage for extraction of TCAs using 15 individual devices with and without normalization	159
Figure 3.20. External calibration curve of thin film MIP device in pooled human plasma samples	165
<b>Figure 3.21.</b> Calibration curves obtained for extraction of a) nortriptyline, b) desipramine, c) amitriptyline, d) doxepin, e) imipramine, f) trimipramine, and g) clomipramine using thin film MIPs from plasma solutions without internal standard correction	166
<b>Chapter 4:</b>	
<b>Figure 4.1.</b> Schematic presentation for fabrication of porous thin films.	183

- Figure 4.2.** Analytical workflow for the developed biofluid spot procedure coupled with LC-MS/MS analysis. 184
- Figure 4.3.** Side view of porous thin film prepared by MAA at 5000x magnification 186
- Figure 4.4.** Effect of different monomers on recovery of TCAs. Extraction: 5 min from 100 ng mL<sup>-1</sup> TCAs in BSA solution, washing: 10 s immersion in 1 mL water 1%TEA, desorption: 300 μL ACN/water 0.1% FA for 20 min at 500 rpm (n=3) 188
- Figure 4.5.** Effect of different sample volume on extracted mass (a) and recovery (b) of TCAs. Extraction: 5 mins from 100 ng mL<sup>-1</sup> TCAs in BSA solution, washing: 10 s immersion in 1 mL water 1%TEA, desorption: 300 μL of ACN/Water 0.1% FA for 20 mins at 500 rpm (n=3) 189
- Figure 4.6.** Desorption solvent study performed at 10 mins at 1500 rpm using 500 μL of ACN 0.1% FA at 1500 rpm; Extraction: 10 μL of 100 ng mL<sup>-1</sup> TCAs in BSA solution for 5 mins; Washing: 10 secs immersion in 1 mL water 1%TEA (n=3) 191
- Figure 4.7.** Desorption solvent volume effect on a) recovery and b) signal intensity (peak area) performed using ACN 0.1% FA at 1500 rpm for 10 mins; Extraction: 10 μL of 100 ng. mL<sup>-1</sup> TCAs in BSA solution for 5 mins; Washing: 10 secs immersion in 1 mL water 1%TEA (n=3) 192
- Figure 4.8.** Desorption time profile using 500 μL of ACN 0.1% FA at 1500 rpm; Extraction: 10 μL of 100 ng mL<sup>-1</sup> TCAs in BSA solution for 5 mins; Washing: 10 secs immersion in 1 mL water 1%TEA (n=3) 193

**Figure 4.9.** Washing effect on the percentage recovery of TCAs. Five mins static extraction of 10  $\mu\text{L}$  of 100  $\text{ng mL}^{-1}$  TCAs in plasma solution for 5 mins, desorption: 500  $\mu\text{L}$  of ACN 0.1% FA for 2 mins at 1500 rpm. Washing with 1 mL of 1% TEA (n=3) 195

**Figure 4.10.** Extraction time profile TCAs in BSA solution. Static extraction of 10  $\mu\text{L}$  of 100  $\text{ng mL}^{-1}$ , washing: 10 s static wash in 1 mL water 1% TEA, desorption: 500  $\mu\text{L}$  ACN 0.1% FA, 2 mins at 1500 rpm (n=3) 197

**Figure 4.11.** Extraction time profile in pooled plasma. Static extraction (3 min) of 10  $\mu\text{L}$  of 100  $\text{ng mL}^{-1}$  TCAs, washing: 10 s static wash in 1 mL water 1% TEA, desorption: 500  $\mu\text{L}$  ACN 0.1% FA, 2 min at 1500 rpm (n=3) 197

**Figure 4.12.** a) Effect of normalization using a deuterated standard applied into spot sampling method with different approaches (A: analyte, S: surrogate, IS: internal standard). b) acquired RSD values for inter-device variability without using IS and different approaches of loading IS. Extraction: static for 3 min, washing: 10 secs in 1 mL water 1% TEA at 1000 rpm, desorption: 500  $\mu\text{L}$  ACN 0.1% FA, 2 min at 1500 rpm (n=10 for each method) 201

**Figure 4.13.** Inter-batch reproducibility of two different batches of porous thin films. Sample: 10  $\mu\text{L}$  of plasma spiked with TCAs (100  $\text{ng mL}^{-1}$ ) and imipramine-D3 (50  $\text{ng mL}^{-1}$ ); Extraction: 3 min static extraction by porous thin films; Washing: 1 mL 1% TEA in water at 1000 rpm for 10s, Desorption: 200  $\mu\text{L}$  ACN 0.1% FA at 1500 rpm for 2 min (n=3 for each batch) 202

**Figure 4.14.** Stability assessment results using spot sampling obtained for a) desipramine and b) imipramine at various storage conditions; Sample: 10  $\mu\text{L}$  of plasma spiked with

TCA<sub>s</sub> (100 ng mL<sup>-1</sup>) and IS (imipramine-D3 at 50 ng mL<sup>-1</sup>); Extraction: 3 min static extraction by porous thin films; Washing: 1 mL 1% TEA in water at 1000 rpm for 10s, Desorption: 200 μL ACN 0.1%FA at 1500 rpm for 2 min (n=3) 204

**Figure 4.15.** Stability assessment results using spot sampling obtained for cocaine at room temperature; Sample: 10 μL of plasma spiked with cocaine (100 ng mL<sup>-1</sup>); Extraction: 3 min static extraction by two different compositions of porous thin films; Washing: 1 mL water at 1000 rpm for 10s, Desorption: 200 μL MeOH 0.1%FA at 1500 rpm for 2 min (n=3) 205

**Figure 4.16.** Reusability of porous thin films for spot sampling; Sample: 10 μL of plasma spiked with TCA<sub>s</sub> (100 ng mL<sup>-1</sup>); Extraction: 3 min static extraction by porous thin films; Washing: 1 mL 1% TEA in water at 1000 rpm for 10s, Desorption: 200 μL ACN 0.1%FA at 1500 rpm for 2 min (n=3) 206

**Figure 4.17.** Quantitative analysis of plasma spiked with TCA<sub>s</sub> and imipramine-D3 (50 ng mL<sup>-1</sup>). Red triangles represent the obtained accuracy levels (30, 150 and 750 ng mL<sup>-1</sup>) (n=3) 209

**Figure 4.18.** Quantitative analysis of plasma spiked with TCA<sub>s</sub> based on instrumental response (n=3) 211

**Figure 4.19.** Variations of instrumental response (peak area) for extraction from plasma spiked with TCA<sub>s</sub> for inter-day validation experiments (n=3) 212

## List of Symbols, Nomenclature or Abbreviation

<b>1-Vim</b>	1-Vinylimidazole
<b>2,4-D</b>	2,4-Dichlorophenoxyacetic acid
<b>3-MBT</b>	3-Methylbenzothiophene
<b>4, 6-DMDBT</b>	4,6-Dimethyldibenzothiophene
<b>4-VBA</b>	4-Vinyl benzoic acid
<b>4-VP</b>	4-Vinyl pyridine
<b>AA</b>	Acrylic acid
<b>AAm</b>	Allylamine
<b>Ace</b>	Acenaphthene
<b>Ace-d10</b>	Acenaphthene-d10
<b>Acy</b>	Acenaphthylene
<b>ACN</b>	Acetonitrile
<b>ACVA</b>	2,2'-Azo-biscyanovaleric acid
<b>AIBN</b>	Azo(bis)-isobutyronitrile
<b>AIMN</b>	2,2'-Azobis-(2-methyl-butyronitrile)
<b>AIVN</b>	4,4'-Azobis (4-cyanovaleric acid)
<b>AM</b>	Acrylamide
<b>Ami</b>	Amitriptyline
<b>Ant</b>	Anthracene
<b>APCI</b>	Atmospheric pressure chemical ionization

<b>APGC</b>	Atmospheric pressure gas chromatography
<b>APTES</b>	3-Aminopropyl triethoxysilane
<b>BA</b>	Butylamine
<b>BaA</b>	Benzo(a)anthracene
<b>BaP</b>	Benzo(a)pyrene
<b>BbF</b>	Benzo(b)fluoranthene
<b>BGP</b>	Benzo(ghi) perylene
<b>BkF</b>	Benzo(k)fluoranthene
<b>BPA</b>	Bisphenol A
<b>BPADMA</b>	Bisphenol A dimethacrylate
<b>BPAF</b>	Bisphenol AF
<b>BPB</b>	Bisphenol B
<b>BPF</b>	Bisphenol F
<b>BPS</b>	Bisphenol S
<b>BSA</b>	Lyophilized bovine serum albumin
<b>BT</b>	Benzothiophene
<b>CAR</b>	Carbamazepine
<b>CBS</b>	Coated blade spray
<b>CBZ</b>	Carbendazim
<b>CBZ-desipramine</b>	(3-(10,11-dihydro-5H-dibenzo[b,f]azepin-5-yl)propyl)(methyl) carbamate
<b>CEL</b>	Celecoxib
<b>Chry</b>	Chrysene

<b>Chry-d12</b>	Chrysene-d12
<b>CIP</b>	Ciprofloxacin
<b>Clo</b>	Clomipramine
<b>DAD</b>	Diode array detector
<b>DART</b>	Direct analysis in real time
<b>DB(ah)A</b>	Dibenzo(a,h) anthracene
<b>DBP</b>	Dibutyl phthalate
<b>DBS</b>	Dried blood spot
<b>DBT</b>	Dibenzothiophene
<b>DC</b>	Doxycycline
<b>DCM</b>	Dichloromethane
<b>DEP</b>	Diethyl phthalate
<b>Des</b>	Desipramine
<b>DI</b>	Deionized
<b>DLLME</b>	Dispersive liquid-liquid microextraction
<b>DMAC</b>	N,N-dimethylacetamide
<b>DMC</b>	Dimethoxycoumarin
<b>DMF</b>	Dimethyl formamide
<b>DMPA</b>	2,2-dimethoxy-2-phenylacetophenone
<b>DMS</b>	Dried matrix spot
<b>DMSO</b>	Dimethyl sulfoxide
<b>Dox</b>	Doxepin
<b>DPS</b>	Dried plasma spot

<b>DVA</b>	2,5-Divinylterephthalaldehyde
<b>DVB</b>	Divinylbenzene
<b>EBS</b>	Extracted blood spot
<b>EDCs</b>	Endocrine disruptors
<b>EDMA</b>	Ethylene dimethacrylate
<b>EGDMA</b>	Ethylene glycol dimethacrylate
<b>EHDPP</b>	2-Ethylhexyl diphenyl phosphate
<b>EME</b>	Electro membrane extraction
<b>ENR</b>	Enrofloxacin
<b>EP</b>	Ethyl-p-hydroxybenzoate
<b>ESI</b>	Electrospray ionization
<b>EU</b>	European Union
<b>FA</b>	Formic acid
<b>FID</b>	Flame ionization detector
<b>Flu</b>	Fluorene
<b>Flut</b>	Fluoranthene
<b>FPD</b>	Flame photometric detector
<b>GC</b>	Gas chromatography
<b>GAT</b>	Gatifloxacin
<b>HEMA</b>	Hydroxyethyl methacrylate
<b>HF-LPME</b>	Hollow fiber liquid phase microextraction
<b>HREA</b>	Health Research Ethics Authority
<b>HREB</b>	Health Research Ethics Board

<b>IF</b>	Imprinting factor
<b>Imi</b>	Imipramine
<b>Imi-D3</b>	Imipramine-D3
<b>InP</b>	Indeno(1,2,3-cd) pyrene
<b>IS</b>	Internal standard
<b>KH-560</b>	3-(2-cyclooxypropoxyl) propyltrimethoxysilane
<b>LC</b>	Liquid chromatography
<b>LDH</b>	Layered double hydroxide
<b>LDR</b>	Linear dynamic ranges
<b>LLE</b>	Liquid-liquid extraction
<b>LOD</b>	Limit of detection
<b>LOQ</b>	Limit of quantification
<b>LR</b>	Linear range
<b>MAA</b>	Methacrylic acid
<b>MAPS</b>	3-Methacryloxypropyltrimethoxysilane
<b>MCLs</b>	Maximum contamination levels
<b>ME</b>	Matrix effect
<b>MeOH</b>	Methanol
<b>MEPS</b>	Microextraction by packed sorbent
<b>MIPs</b>	Molecular imprinted polymers
<b>MIP-SBSE</b>	Molecularly imprinted polymer-stir bar sorptive extraction
<b>MIP-TFME</b>	Molecularly imprinted polymer-thin film microextraction
<b>MMIPSPE</b>	Magnetic molecularly imprinted solid phase extraction

<b>MOFs</b>	Metal organic frameworks
<b>MP</b>	Methylparaben
<b>MRM</b>	Multiple reaction monitoring
<b>MS</b>	Mass spectrometry
<b>MS/MS</b>	tandem MS
<b>N<sub>2</sub></b>	Nitrogen
<b>NAB</b>	Nabumetone
<b>Nap</b>	Naproxen
<b>Naph</b>	Naphthalene
<b>Naph-d8</b>	Naphthalene-d8
<b>NFZ</b>	Nitrofurazone
<b>Nor</b>	Nortriptyline
<b>NIPAM</b>	N-isopropylacrylamide
<b>NIP</b>	Non-imprinted polymer
<b>NPD</b>	Nitrogen phosphorus detector
<b>NVCL</b>	N-vinylcaprolactam
<b>OH-TSO</b>	Hydroxy-terminated silicone oil
<b>OPPs</b>	Organophosphorus pesticides
<b>OTC</b>	Oxytetracycline
<b>PAHs</b>	Polycyclic aromatic hydrocarbons
<b>PAN</b>	Polyacrylonitrile
<b>PASHs</b>	Polycyclic aromatic sulfur heterocycles
<b>PBS</b>	Phosphate-buffered saline solution

<b>PDMS</b>	Polydimethylsiloxane
<b>PEG</b>	Polyethylene glycol
<b>PETA</b>	Pentaerythritol triacrylate
<b>PFAS</b>	Polyfluoroalkyl substances
<b>Phe</b>	Phenanthrene
<b>Phe-d10</b>	Phenanthrene-d10
<b>PMHS</b>	Poly(methylhydrosiloxane)
<b>PP</b>	Protein precipitation
<b>PPZ</b>	Propazine
<b>PQ</b>	Paraquat
<b>Pry-D12</b>	Perylene-d12
<b>PTFE</b>	Polytetrafluoroethylene
<b>PTMOS</b>	Phenyltrimethoxysilane
<b>PT-SPE</b>	Solid phase extraction in pipette tips
<b>PVC</b>	Polyvinyl chloride
<b>Pyr</b>	Pyrene
<b>R<sup>2</sup></b>	Correlation coefficients
<b>RAMIP</b>	Restricted access molecularly imprinted polymer
<b>RR</b>	Relative recovery
<b>RSD</b>	Relative standard deviation
<b>SBSE</b>	Stir bar sorptive extraction
<b>SC</b>	Semicarbazide
<b>SDM</b>	Sulfadimethoxine

<b>SDZ</b>	Sulfadiazine
<b>SEM</b>	Scanning electron microscopy
<b>SMD</b>	Sulfamotoxydiazine
<b>SM-FTN</b>	Sample manager flow-through needle
<b>SMM</b>	Sulfamonomethoxine
<b>SMZ</b>	Sulfamethazine
<b>SPE</b>	Solid phase extraction
<b>SPME</b>	Solid phase microextraction
<b>Sty</b>	Styrene
<b>TAP</b>	Thiamphenicol
<b>TBZ</b>	Thiabendazole
<b>TC</b>	Tetracycline
<b>TCAs</b>	Tricyclic antidepressants
<b>TCEP</b>	Tri (2-chloroethyl) phosphate
<b>TDM</b>	Therapeutic drug monitoring
<b>TEA</b>	Triethylamine
<b>TEOS</b>	Tetraethoxysilane
<b>TFA</b>	Trifluoroacetic acid
<b>TFME</b>	Thin film microextraction
<b>TF-MIP</b>	Thin film molecularly imprinted polymer
<b>TF-SPME</b>	Thin film SPME
<b>TMP</b>	Trimethyl phosphate
<b>TPhP</b>	Triphenyl phosphate

<b>TPPO</b>	Triphenylphosphine oxide
<b>Tri</b>	Trimipramine
<b>TRIM</b>	Trimethylol propane trimethacrylate
<b>TSM</b>	Triflusulfuron-methyl
<b>US EPA</b>	United States Environmental Protection agency
<b>UHPLC</b>	Ultra high-performance liquid chromatography
<b>UV</b>	Ultra-violet
<b>β-CD</b>	β-cyclodextrin

## Co-authorship statement

The principal author has conducted the literature review and research in all the chapters of this thesis for the degree of Doctor of Philosophy under supervision of Prof. Christina Bottaro.

Chapter 1: Fereshteh Shahhoseini, Ali Azizi, Christina Bottaro, “A critical evaluation of molecularly imprinted polymer (MIP) coatings in solid phase microextraction devices”, manuscript is accepted as a review paper in *Trends in Analytical Chemistry (TrAC)*. The first author proposed the idea and wrote the first draft, tables, and figures. Dr. Ali Azizi had edited the first draft by reviewing and add some discussions to the manuscript. The final version was edited by Prof. Christina Bottaro.

Chapter 2: Fereshteh Shahhoseini, Ali Azizi, Stefana N. Egli, Christina Bottaro, “Single-use porous thin film extraction with gas chromatography atmospheric pressure chemical ionization tandem mass spectrometry for high-throughput analysis of 16 PAHs” *Talanta* 207 (2020) 1203202. This published paper contains all the discussions in Chapter 2. The first author proposed the idea of the shape of the device and method structure. She also performed all the steps of this work such as: planning the experiment, preparation of MIP thin film devices, method development and validation, carrying out extraction and desorption, data analysis, manuscript writing, submission and revision. The second author’s (Dr. Ali Azizi) contribution was carrying out extraction and desorption, performing instrumental analysis, and writing the manuscript. The third author (Stefana Egli) peer reviewed the first draft of the manuscript. The final version of the manuscript was reviewed by Prof. Christina Bottaro.

Chapter 3: Fereshteh Shahhoseini, Evan Langille, Ali Azizi, Christina Bottaro. “Thin film molecularly imprinted polymer (TF-MIP), a selective and single-use extraction device for high-throughput analysis of biological samples” *Analyst*, 2021, 146, 3157–3168. This published work forms the basis of discussions in Chapter 3. The first author contributed to all stages of the manuscript preparation process such as planning the experiment, preparing the MIP-thin film devices, performing extraction, desorption, method development and validation, instrumental and data analysis and writing the first draft of the manuscript. Second author (Evan Langille) synthesized the pseudo template and purified that to be used for MIP-thin film fabrication. Third author (Dr. Ali Azizi) had contribution in performing extraction and desorption, planning some parts of method validation, data analysis and writing the manuscript. The final version of manuscript was reviewed by Prof. Christina Bottaro.

Chapter 4: Fereshteh Shahhoseini, Ali Azizi, Christina Bottaro. “Single-use porous polymer thin-film device: a reliable sampler for analysis of drugs in small volumes of biofluids” *Analytica Chimica Acta*, 2022, 1203,339651. The accepted manuscript forms the basis for the work described in Chapter 4. The contribution of the first author was in the first idea, planning the experiment, performing extraction, desorption, method development and validation, instrumental analysis, data analysis, and writing the first draft of the manuscript. Second author (Dr. Ali Azizi) had contribution in planning some part of experiment, data analysis and peer reviewing the first draft of the manuscript. The final draft was reviewed by Prof. Christina Bottaro.

## **Chapter 1: A critical evaluation of molecularly imprinted polymer (MIP) coatings in solid phase microextraction devices**

Fereshteh Shahhoseini, Ali Azizi, Christina S. Bottaro “A critical evaluation of molecularly imprinted polymer (MIP) coatings in solid phase microextraction devices” *accepted in TrAC Trends in Analytical Chemistry*

## 1.1. Introduction to MIP-SPME

The step between sampling and instrumentation is sample preparation, which continues to present a challenge for trace analysis, particularly for complex matrices [6]. The term trace is considered as concentration of nanogram (ng) or microgram ( $\mu\text{g}$ ) per litre range ( $\mu\text{g L}^{-1}$ ) [7]. Sample preparation methods have various objectives, but they are all designed to provide a sample for instrumental analysis that preserves the analyte integrity while minimizing interference with instrument performance. Often these methods involve the transfer of the analyte from one phase to another, for example from an aqueous sample to an organic solvent (i.e., liquid-liquid extraction, LLE) or from liquid to solid (i.e., solid phase extraction, SPE). Although LLE is still common, SPE features a wide range of sorbents for improved selectivity and analyte recovery, reduces the use of toxic solvents and is easily automated. Traditional SPE cartridge systems have some downsides including the need for specialized equipment to control flow rates, which are typically slow. They also involve additional manipulation steps with concomitant sources of error, such as sample filtration to prevent cartridge clogging, and analyte elution with organic solvent. Excess solvent can be evaporated to improve method sensitivity, but with the risk of irreproducible analyte loss [8]. A huge amount of effort has been devoted to tackle these problems by introducing the miniaturized forms of LLE and SPE under the umbrella of microextraction techniques [9]. Of these, solid phase microextraction (SPME) has gained prominence for its simplicity and potential to reduce or eliminate the organic solvent consumption. The first application of SPME used a fused silica fibre as the substrate with a coating of polyimide as the extraction phase [10]. Although SPME is non-exhaustive,

extracting only a fraction of the analyte from the sample, the entire extracted mass can be introduced directly into the analytical instrument reducing sample handling and improving method sensitivity. Thanks to the numerous positive characteristics of SPME (i.e., simple operation, portability, compatibility with an array of instruments and on-line analysis), in the three decades since its invention thousands of papers have reported headspace and direct immersion SPME for numerous organic analytes [11]. The extraction mechanism in SPME is based on analyte transfer from the sample matrix to the boundary layer and then to the extraction phase through diffusion. The amount of analyte extracted is based on an equilibrium between the sample and coating [12, 13]. This amount can be expressed by the Eq. (1), where  $e$  denotes the sorptive phase and  $s$  the sample phase.  $n$  is extracted amount at equilibrium which is proportional to the partition coefficient ( $K_{es}$ ), volume of the extraction phase ( $V_e$ ), volume of sample ( $V_s$ ), and the analyte concentration in the sample ( $C_s$ ).

$$n = \frac{K_{es}V_eV_s}{K_{es}V_e + V_s} C_s \quad (1)$$

In SPME based techniques, where sample volume is very large compared with the volume of extraction phase ( $V_s \gg V_e$ ), Eq. (1) can be articulated as Eq. (2), where extracted amount of analyte is directly proportional to analyte concentration in solution.

$$n = K_{es}V_eC_s \quad (2)$$

Given this equation, the method sensitivity (extracted analytes) can be enhanced by using larger volume of sorbent or improved affinity of extraction phase for targeted analytes. Often the aim is to increase the volume of extraction phase in SPME devices with innovative formats, for example, multiple coated fibers have been bundled together as a

multi-fibre extraction device [14] and surface area and phase thickness is increased using stir bar sorptive extraction (SBSE) [15]. However, a thick coating delays equilibration as defined in Eq. (3):

$$t_{95\%} = 3 \times \frac{\delta K_{es}(b-a)}{D} \quad (3)$$

In this equation,  $t_{95\%}$  is the equilibrium time,  $\delta$  is the thickness of the boundary layer,  $b - a$  is the thickness of the extraction phase, and  $D$  is the diffusion coefficient. Consequently, the sorptive phases have been applied as a thin coating over a large surface area to improve the efficiency without compromising the extraction time [16]. This approach is typically called thin film microextraction (TFME) to distinguish it from traditional SPME. The high surface area in thin film also accelerates the extraction rate according to Eq. (4).

$$\frac{dn}{dt} = \left(\frac{DA}{\delta}\right) C_s \quad (4)$$

This equation shows that initial extraction rate  $\frac{dn}{dt}$  (mass of the analyte ( $n$ ) extracted over the sampling time ( $t$ )) is proportional to surface area of the extraction phase [13]. However, according to Eq. 2 further improvements in sensitivity are still limited by affinity of the analyte for the sorbent.

The composition of the coating material used in SPME has an important role in extraction efficiency and discrimination against matrix components needed for clean-up of complex samples, notably biological fluids, and wastewater. Common commercially available SPME coatings are polydimethylsiloxane (PDMS), divinylbenzene (DVB), carboxen, polyacrylate, and a combination of these materials [17, 18]. A vast range of materials and composites have been proposed to address selectivity, such as carbon

nanotubes and other carbon nanomaterials, metal organic frameworks (MOFs), molecularly imprinted polymers (MIPs), and ionic liquids for biological and environmental samples [11, 17, 19]. Among these coatings, MIPs have gained attention due to their tunable selective adsorption properties, combined with adaptable fabrication strategies suited for use with most common sorbent formats, including, particulate and monolithic materials for SPE and chromatography, freestanding membranes, and thin film coatings on solid substrates, which have been incorporated into an array of miniaturized extraction techniques [20, 21].

Use of MIPs in SPME devices are widely reported in the literature for sample preparation. A few excellent review papers are available which highlight the applications of MIP-SPME [22-24]. A. Sarafraz-Yazdi and N. Razavi reviewed the applications of various SPME modes (i.e., fiber, in-tube, monolith, dispersed particle, membrane) as well as innovations in optical and electrochemical sensors using MIP-SPME fibers until 2015 [22]. In another review, S. Ansari and M. Karimi focused on application of MIP-SPME sorbents for extraction of drugs by describing each technique and discussing their advantages and disadvantages [23]. Recently, E. Turiel and A. Martín-Esteban reviewed MIP microextraction techniques including SPME that used MIP as the extraction media along with their advantages and disadvantages [24]. However, the application of MIP-SPME devices has not been fully accepted by the analytical community due to suspicions regarding the performance of MIP-SPME such as the selectivity of coatings, range of analytes (i.e., polarity and hydrophobicity), application in real samples, lifetime of the devices, obstacles for sample manipulation and limited applicability for only extraction of hydrophobic analytes.

In this review, a short introduction to molecular imprinting technology and its major features is provided, accompanied by a critical assessment of reported MIP-microextraction devices used for sample preparation in advance of chromatographic and mass spectrometric analysis. All the MIP-based devices presented can be categorized as SPME devices (Figure 1.1) and follow the principles of extraction established for fiber-SPME [25-27]. MIP-SPME fibers, monolithic fibers, SBSE and TFME are the most common techniques to be discussed. A search of the literature from the past two decades reveals that the majority (54%) of the papers on this topic emphasized MIP fiber devices and their applications (Figure 1.1, sum of MIP coated and monolithic fibers). However, there has also been a dramatic rise in the number of papers reporting MIP-SBSE as a robust solution to microextraction, which now numbers second most common on the list at 34% of the published manuscripts. Another highlight is the growth in publications featuring MIP-TFME, first introduced in 2010. Focusing on papers published over the last three years, the following aspects will be discussed: 1) fabrication methods; 2) the imprinting process; 3) chemical composition and optimization of MIP composition; 4) physiochemical properties of analytes and successful molecular imprinting; 5) evaluation of aspects of selectivity for MIP-SPME; 6) real world applications (genuine sample analyses and durability); and 7) other common concerns, such as recognition in aqueous matrices, and fouling of the MIP coating in biological matrices, and possible solutions using MIP-SPME devices will be presented.

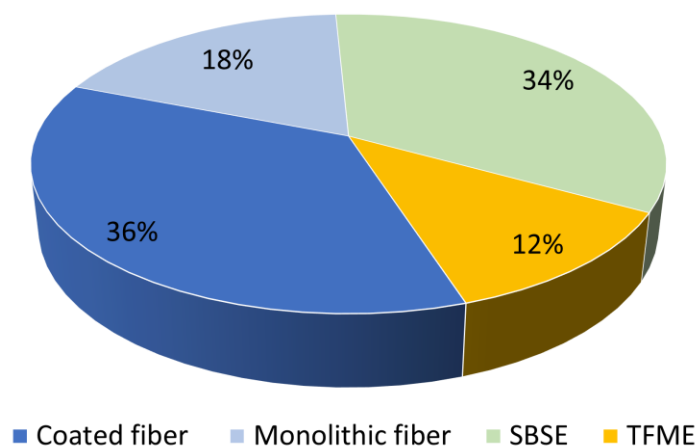


**Figure 1.1.** The percentage of the papers with the subject of developing fiber, monolithic fiber, SBSE and TFME of MIP-SPME devices published during 2001-2022 (n = 142).

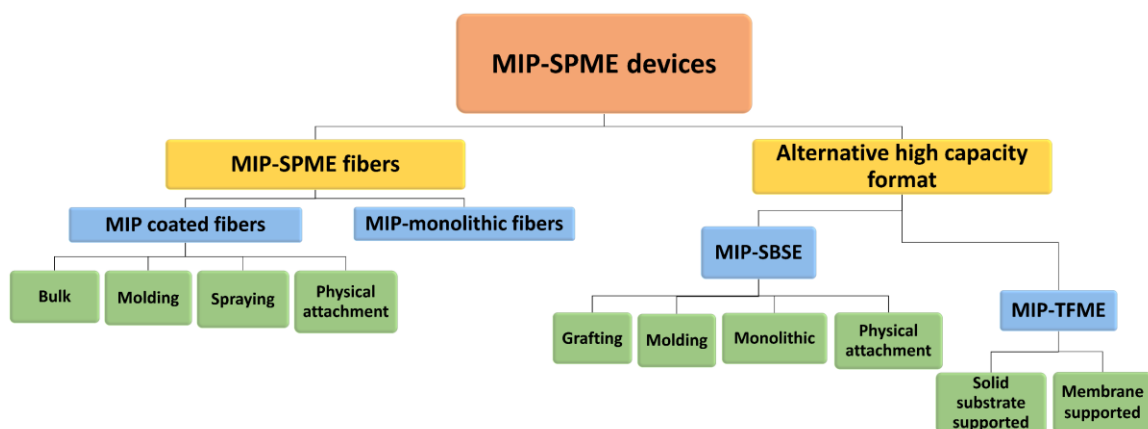


**Figure 1.2.** Classification of different formats of MIP-SPME devices based on the method of fabrication.

In this review, MIP-SPME devices are divided into two main groups (Figure 1.2): MIP-SPME fibers and formats introduced to achieve higher capacity while solving other issues (SBSE and TFME). In Figure 1.2, the two main groups are subdivided based on similar formats along with the different fabrication approaches used in each category.

## 1.2. Principles of molecular imprinting

The concept of molecular imprinting first was introduced by Pauling in 1940 in the discussion of the theory of antibodies [28]. Based on that theory, an antibody should have two or more distinct regions with surface configuration complementary to that of antigen. Later, Dickey used this mechanistic theory to imprint silica (analogous to antibody) with methyl orange as the template (antigen analogue) [29]. Molecular imprinting can be described as assembling selective binding sites in synthetic polymers using a template as a scaffold. A template (atom, ion, molecule or complex) is selected to impart specific order to the orientation of functional monomers, which is conserved during the polymerization process. The bonds formed between the template and matching functional monomer is locked in place through crosslinking of the monomers into a three-dimensional covalent network. After polymerization and removal of the template, vacant recognition sites are left that can rebind target molecules identical or similar to the template (Figure 1.3) [30].

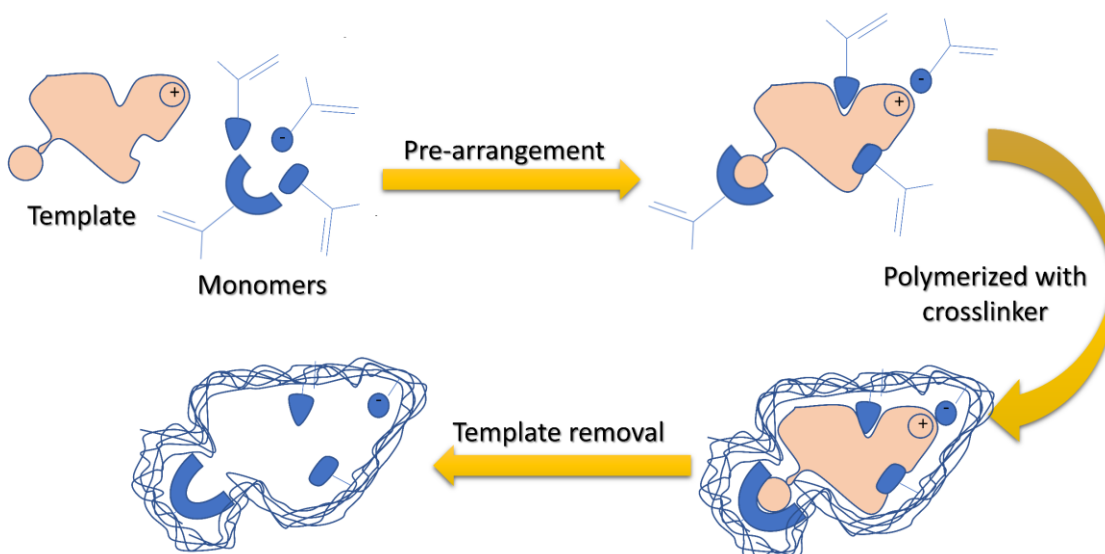


**Figure 1.3.** MIP sorbent fabrication process.

Based on the types of bonds between the monomer and template, MIP fabrication is typically classified as covalent or noncovalent. In covalent imprinting, templates are covalently bound to one or more polymerizable groups. After polymerization, templates are cleaved to leave functional groups in the correct orientation to bind the target molecule either by reforming the covalent bonds (fully covalent MIP) or through non-covalent interactions like hydrogen bonding (semi-covalent MIP). For fully covalent MIPs, specific conditions are required to covalently bind the analytes to the MIPs, which is an impediment to use in analytical chemistry [31]. Semi-covalent methods circumvent some of these issues, but the options with respect to suitable template-monomer pairs in the pre-polymer solution can be limiting [32]. Noncovalent imprinting is the most popular MIP synthetic procedure due to the relatively mild synthetic conditions and rapid template removal and rebinding. In this approach, templates and monomers form complexes through noncovalent bonds (i.e., electrostatic interactions, hydrogen bonding, van der Waals forces, and  $\pi$ - $\pi$  interactions). Analyte rebinding relies on the same interactions. However, these bonds are sensitive to even slight changes in the chemical environment that can disturb the stability of the complex, which requires careful optimization of the system [33]. Even with a potentially laborious optimization, noncovalent MIPs are the prominent type in analytical chemistry and the focus of this review.

There is no single set of conditions that will yield a perfect MIP fabricated by non-covalent approach, however there are some characteristics of each polymer component that are generally accepted as desirable. Preparation of noncovalent MIPs with suitable recognition properties and mechanical and chemical stabilities depends on a multitude of factors, such as, the chemistry and relative amounts of polymer components (i.e., template,

monomer, crosslinker, polymerization initiator, porogen) and the polymerization conditions that influence the complex stability and the rate of polymer growth (e.g., temperature, activation of initiator) [34]. The starting point in MIP formula optimization is always based on the chemistry of the analyte, which is typically also used as the template. However, if the MIP is to be used for trace analysis, residual template can be a source of positive errors. In such a case the template can be replaced with a structurally-related molecule (dummy or pseudo template) [35]. Pseudo-templates are also used if the target analyte is incompatible with MIP fabrication, e.g., unstable under the reaction conditions. An ideal pseudo-template must share a similar geometric orientation of some functionalities present in the analyte, in essence replicating the geometry of the functional monomer-template complex [32]. The success of imprinting is measured by the affinity of the analyte for the binding sites, which depends on the fidelity of the binding sites after polymerization and that is attributed to the stability of the template-monomer complex prior to polymerization [36]. The selection of the monomer is interconnected to the nature of template (acidic monomers for basic templates and basic monomers for acidic templates) [37]. Three monomers that commonly appear in the literature are methacrylic acid (MAA, acidic compound), 4-vinyl pyridine (4-VP, alkaline compound) and styrene (Sty, neutral compound). Although the template-monomer complex is central to molecular imprinting, the bulk of the polymer typically comes from the crosslinking agent. The primary role of the crosslinker is to form the 3-dimensional network that preserves the shape of the binding site, but it also influences surface polarity (wettability), surface area, pore size, and adsorption capacity. [38]. The relationship between adsorption capacity and the crosslinker loading is complex as contributes to the accessibility of the binding sites and also

can be a source of non-selective interactions. There is a minimum amount of crosslinker necessary to form a rigid polymer, but high amounts make the structure too rigid or lead to infilling of pore structures, both impair the kinetics of template removal and rebinding [39]. Although the literature has primarily focused on the components discussed thus far, one cannot ignore the role of the porogen serving to control pore formation during polymerization. As a solvent, the porogen must solubilize the components, but not interfere with the template-monomer interactions, so for example if hydrogen bonding is the dominant interaction, an aprotic solvent is used [40]. Typically, nonpolar aprotic solvents are preferable in non-covalent imprinting because they have low capacity to be hydrogen bond donors and acceptors [41]. The porogen also can affect the recognition properties, enantioselectivities, and physical properties of MIP such as surface area, pore volume and swelling [42].

### **1.3. Characterizing performance**

The performance of MIPs as sorbents in analytical devices must be characterized to demonstrate their efficiency (adsorption capacity, equilibrium kinetics, etc.) and since they should be selective towards the imprinted molecules, their selectivity should also be demonstrated. A brief overview of these methods is given below as a guide to the data that will be discussed in the evaluation of MIP-SPME devices reported in the literature. It is notable that in some papers reporting MIP particles in composite coatings (particles immobilized in a polymeric matrix), performance may be determined for the particles rather than the composite material or device itself.

1. *Adsorption capacity*. The adsorption of analytes by MIP-SPME devices [43] or MIP particles [44], is the amount of analyte adsorbed at equilibrium from analyte solution. The extracted amount is calculated directly by determining the amount adsorbed to the sorbent or indirectly by determining how much analyte is left in solution. For the latter approach, adsorption capacity ( $q$ ) is calculated based Eq. (5).

$$q = \frac{(C_0 - C_f)V}{m} \quad (5)$$

Where  $C_0$  is the initial concentration,  $C_f$  is the analyzed concentration,  $V$  is the volume of the solution and  $m$  is the mass of the polymer [44]. As can be seen from Eq. (5), the adsorption capacity is obtained by normalizing the mass of adsorbed analytes against the mass of polymer, which is normally consistent for a batch of MIP-SPME devices. In instances where the mass of the adsorbent is reproducible between devices this normalization can be omitted, and the adsorption capacity can be calculated using Eq. (6) [45].

$$q = (C_0 - C_f)V \quad (6)$$

The adsorption capacity is proportional to the sorbate concentration in solution, until the sorbent begins to reach saturation. As such, it is useful to fit adsorption data from a range of concentrations using various binding models which are plotted based on relationship between bound analyte and free analyte in the sample. The binding models are divided into discrete or continuous distribution models. Discrete models benefit from a simplified approach to MIPs characterization, suggesting that there is a finite number of binding site types (uniform binding site energies) that can be modeled using simple tools (e.g.,

Scatchard plots). However, for non-covalent imprinted polymers, measurements of binding site energies over a range of loading concentrations have shown a heterogeneous distribution of site energies and thus continuous models, such as Freundlich and Langmuir–Freundlich are preferred [46]. Continuous distribution models provide measures of the distributions of binding site energies and the magnitude of the binding site energies over a specified analyte loading [47]. High average binding site energies result from successful imprinting, leading to the high partition coefficients (K) needed for SPME. However, if the MIPs show a high degree of site heterogeneity, one can assume that the highest energy sites will be saturated at low loadings. Thus, MIP-SPME will perform best in trace analysis and reduction in performance should be anticipated with high analyte concentrations.

2. *Imprinting*. Commonly, the success of imprinting is defined by figures of merit, such as, imprinting factor (*IF*) and selectivity factor ( $\alpha$ ). *IF* is defined as the ratio of adsorption by a MIP relative to adsorption to by an identical control sorbent but without imprinting (non-imprinted polymer, NIP) [48]. Thus, calculation of *IF* from the adsorption capacities can be straightforward (Eq. 7):

$$IF = \frac{q_{MIP}}{q_{NIP}} \quad (7)$$

This proportionality will be constant over a range of concentrations provided that the adsorption behaviours for the two materials are consistent over a range of concentrations. If this is not the case the *IF* values can vary depending on the sorbate concentration ranges studied. Ideally, *IF* will be higher if imprinting successfully creates higher energy binding sites. However, differences in surface area can also result in non-unity *IF* values. One should also note that it is rare to produce a system that shows no adsorption by the NIP. In

fact, adsorption by a NIP is a means to assess the non-selective adsorption capacity of a specific polymer system, therefore, if  $q_{MIP}$  is higher than  $q_{NIP}$ , that increased capacity can be fairly attributed to imprinting.

The selectivity factor ( $\alpha$ ) compares the affinity of a target analyte to a reference compound for a given MIP (Eq. 8); where affinity is measured as the distribution coefficient ( $K_d$ ), which relates the amount of analyte adsorbed ( $q_e$ ) at equilibrium to the analyte concentration remaining ( $C_e$ ) in solution (Eq. 9) [49].

$$\alpha = \frac{K_d(\text{analyte})}{K_d(\text{ref})} \quad (8)$$

$$K_d = \frac{q_e}{C_e} \quad (9)$$

Values of  $\alpha > 1$  imply that the MIP is selective toward the analytes of interest; whereas values  $\leq 1$  show that the MIP shows no preferential uptake of the target compared to the specific reference compounds [50, 51]. This measure of selectivity is highly dependent on the choice of reference compound and the context in which it is applied. For example, selectivity measuring how well a MIP excludes a particularly problematic matrix component is very different than selectivity toward an enantiomer. If the reference compound is chosen judiciously, it can provide insight into the influence of structure and functionality on imprinting and recognition.

3. *Adsorption Kinetics*: The kinetics of adsorption are important as these influence equilibration rates and ultimately determine analysis time. In these studies, the adsorption capacity ( $q$ ) data is collected over a range of time intervals up to equilibrium and fitted to various kinetic models. Based on SPME theory, if the extraction recovery is negligible, the

kinetics should follow a first order model where the mass of analyte adsorbed is directly proportional to the solution concentration [52, 53]. For MIP-SPME devices, pseudo-first order model is reported in the literature when extraction efficiency is low, i.e. the concentration in solution does not decrease substantially as the system approaches equilibrium [54]. While pseudo-second order model is reported for MIP-SPME devices that provided exhaustive extraction efficiency and depletion of analytes [55, 56]. While there is no explicit advantage to having first or second order adsorption kinetics, particularly if operating under equilibrium conditions, MIPs that follow first order kinetics are better suited to fast methods using fixed pre-equilibrium adsorption times. Kinetic modeling experiments can also be used to evaluate the affinity of MIP and NIP toward the analyte both by looking at rate of adsorption and by the equilibrium adsorption capacity ( $q_e$ ) [57].

4. *Other types of selectivity evaluation:* There are different ways to evaluate an extraction technique for performance under real world conditions, where matrix components can influence analyte partitioning. At minimum, extraction efficiencies from analysis of authentic samples should be compared to those using standards in solutions with known composition [2, 5]. Signal detection can also be impacted by co-extracted matrix components, for example, enhancing or suppressing ionization in mass spectrometry (MS) or contributing to background in spectrophotometry. Because of their intrinsic selectivity, MIPs offer some advantages in these situations by providing a mechanism to exclude interfering substances [58]. A common procedure to assess selectivity of MIP-SPME in sample clean-up is to compare the results (total ion chromatogram, selected ion monitoring, or UV chromatogram) for extraction of analytes from genuine samples to the results from

other non-MIP devices, for example, NIP-SPME [59, 60] or commercial SPME devices [43].

Although, MIP theory suggest that imprinted cavities are selective toward only the templated analyte, MIPs—like natural molecular recognition elements (e.g., enzymes)—can have affinity for other compounds with related structures that also complement the imprinted site functionality. This type of cross-reactivity can be an advantage for analysis, e.g., detecting precursors and their metabolites or a class of compounds sharing a common functionality. In this regard, the selectivity of the prepared MIP sorbent is evaluated by extracting the targeted analyte(s) in the presence of the other compounds [3, 61]. Hence cross-reactivity is not really a matrix effect; as long as the sorption capacity is not exceeded, the target has a higher affinity for the imprinted binding sites than its analogues and the detection method can discriminate the specified target from other compounds, performance will be ensured.

The guiding principle in evaluating MIP performance is to determine whether the extraction efficiency for the target analytes is preserved regardless with changing sample composition. Thus, performance in simple systems should always be compared to that in complex samples. The use of a suitable evaluation criteria can provide proof of imprinting and evidence for MIP selectivity.

## 1.4. MIP-SPME fibers

### 1.4.1. MIP-coated fibers

Early applications of MIP-SPME devices included fabrication of MIP coating onto a solid substrate as a selective alternative to commercial SPME fibers. Various strategies have been used to prepare MIP-SPME fibers (Figure 1.4).

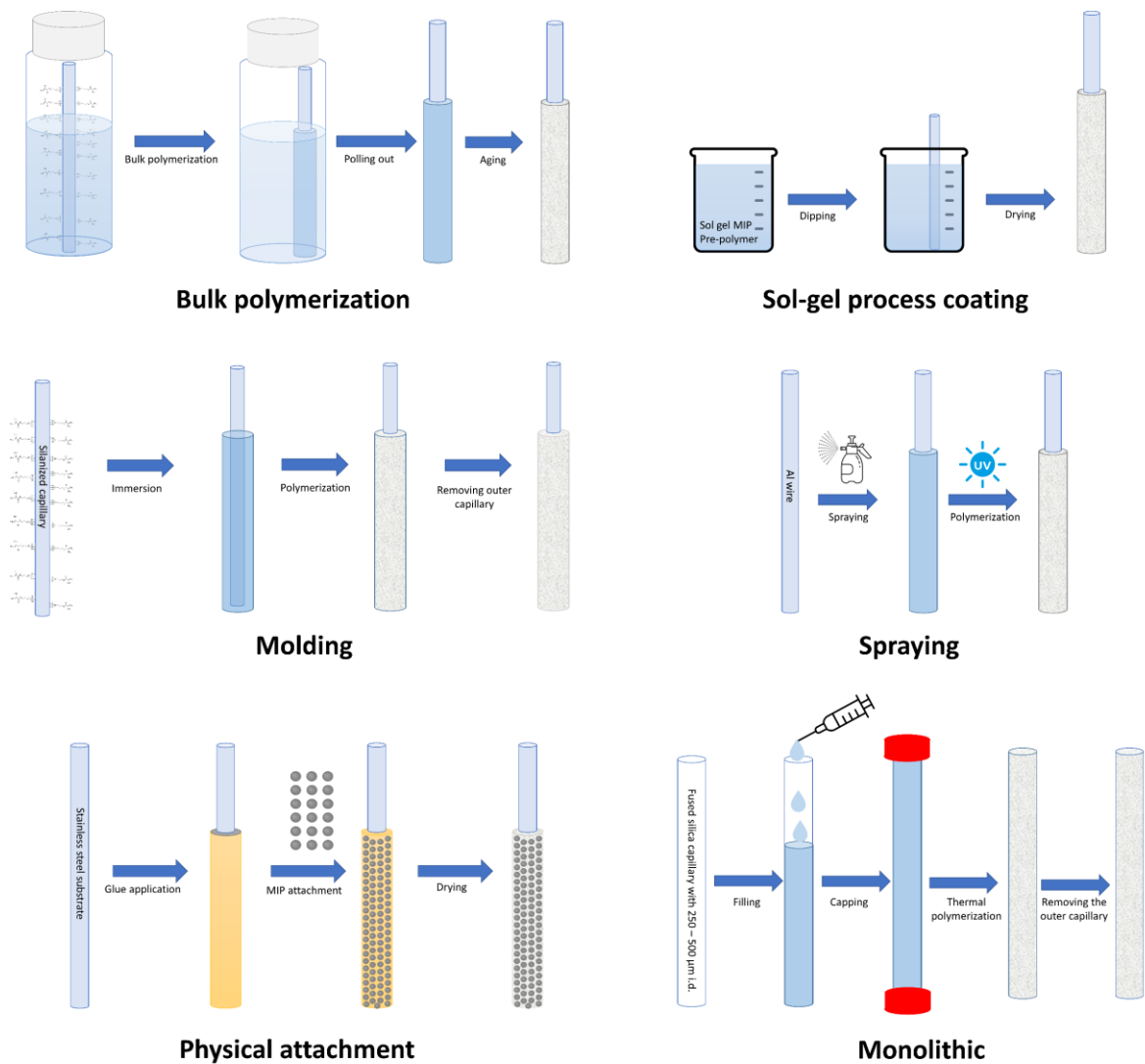


Figure 1.4. MIP-fiber fabrication techniques.

Note that for each of the studies cited in this section, readers may refer to Tables 1.1 and 1.2 for summary of conditions and key figures of merit.

#### *1.4.1.1. Surface polymerization from bulk solution*

Polymerization onto fibers from a bulk solution was one of the first methods used in fabrication of MIP-SPME devices and because of its simplicity and reliability has retained its popularity [62]. The first step in this technique is typically modification (etching, functionalization, etc.) of the fiber surface to promote formation of a polymer coating on the surface. Then these devices were made by deposition of the MIP onto silanized silica fibers, much like traditional SPME. Silanization using vinyl functionalities allows covalent bonding of the MIP layer to the substrate by participating the vinyl groups in polymerization reaction. In the bulk process, the fiber is inserted into a MIP pre-polymerization solution and a coating forms following thermally-initiated radical polymerization; thermal aging of the coated fiber stabilizes the MIP coatings [63]. The polymer thickness can be increased by the optimization of polymerization conditions and by layering of the polymer through repetition of the polymerization process. Zhang et al. [1] studied layering by cycled polymerization (each time using a fresh pre-polymer mixture) and found that analyte extraction was improved when the coating thickness was increased from 0.61  $\mu\text{m}$  after one cycle to 19.7  $\mu\text{m}$  after 5 cycles. However, by using fibers prepared by 8 cycles (35.8  $\mu\text{m}$  thickness) the peak area of the extracted targeted compound decreased. Although authors explained that the reason can be a lower physical stability and change in the balance of the adsorption and desorption processes, another possible explanation is infilling of the formed pores by the new layers of polymer thereby reducing

accessibility of the binding sites. The SEM images of the optimized MIP device and FTIR characterization are presented in Figure 1.5.

To overcome the fragility of silica fibers, stainless steel was introduced as an inert and stable substrate for SPME devices. Hu et al. [64] coated MIPs onto an oxidized and silanized steel wire by inserting it into a pre-polymer solution of metolachlor (template), MAA, trimethylol propane trimethacrylate (TRIM) and azo(bis)-isobutyronitrile (AIBN) for analysis of chloroacetanilide herbicides in soybean and corn samples. The MIP-SPME devices coupled with HPLC-UV presented limits of detection (LOD) in the range of 3-38  $\mu\text{g L}^{-1}$  and acceptable relative standard deviation (RSD) values of 3.2-9.5%. The MIP coating (14.8  $\mu\text{m}$ ) showed excellent performance even when reused (<200 times). Another group created a hydrophilic MIP-SPME device by cycled layering of a MIP MAA/hydroxyethyl methacrylate (HEMA)/copolymer/ethylene glycol dimethacrylate (EGDMA) onto stainless steel for extraction of trace quantities of highly polar tetracycline (TC) in animal-derived foods [65]. The treated stainless steel wire was exposed to three cycles of polymerization at 60 °C for 3 h followed by removal and thermal aging at 85 °C for 2 h gave a coating of a suitable thickness (15  $\mu\text{m}$ ). The hydrophilicity of the MIP fiber was shown by extracting TC with log P -1.3 from solutions in different media: water, water-methanol (20, 40, and 60%), methanol, and acetonitrile (ACN), with the best adsorption capacity from water. Reported IF for TC and oxytetracycline (OTC), doxycycline (DC) with similar structures to TC, sulfamethazine (SMZ), and thiamphenicol (TAP) were 3.23, 1.73, 0.96, 1.25, and 1.18. The poor IF of 0.96 for DC is mainly due to the orientation of the heteroatoms, which in this case seems to hinder interaction with cavities imprinted by

TC. The extraction time profile showed that adsorption increased up to 60 min, and then decreased. Similarly, increased stirring rates had a negative effect on the extraction efficiency. These results are counter-intuitive and differ from expectations for equilibrium-based extractions with SPME. The authors attributed such results to back desorption at long intervals and lack of strong interactions between sorbent and analytes at higher agitation speeds. However, one can surmise that reduction in extraction efficiency with time may be due to lack of polymer stability over time and degradation at high speed agitations. Competition for adsorption sites by other sample components is another possible explanation.

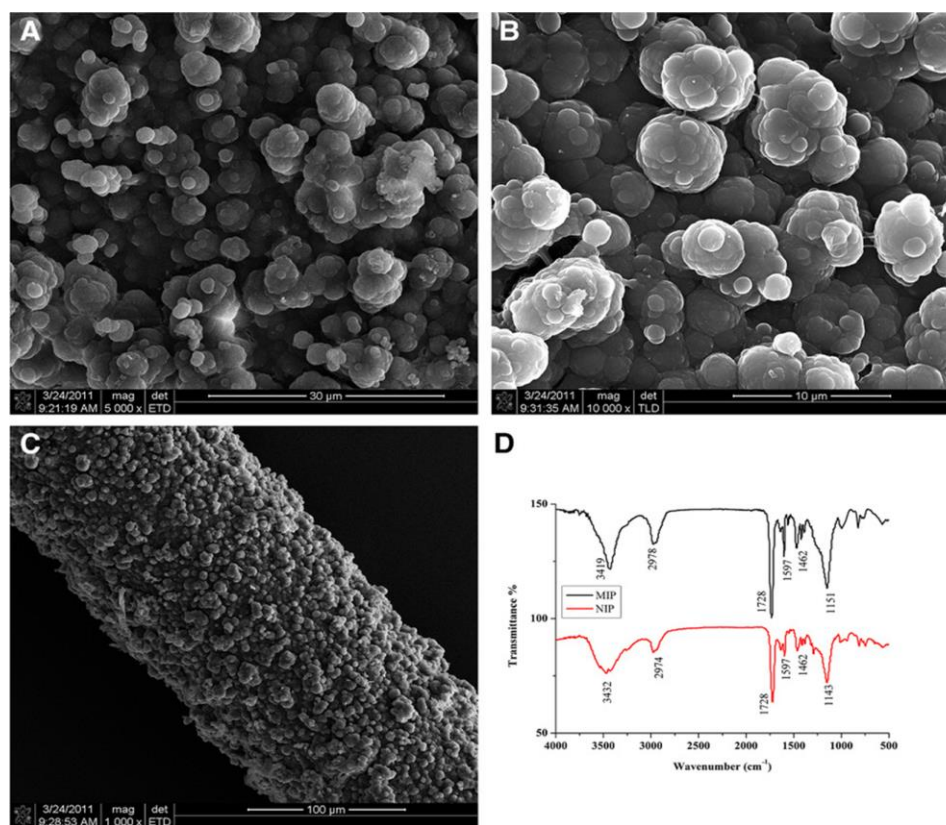


**Figure 1.5.** SEM image of MIP-SPME fiber prepared by bulk polymerization after 5 cycles (A-C) and FTIR characterization (D). Reprinted from Ref. [1], with permission from John Wiley and Sons.

Inorganic and hybrid sol-gel materials have been reported as extraction phases for sample preparation including preparing stable and efficient SPME coatings [66]. Incorporating molecular imprinting can improve the selectivity of this organic-inorganic network for adsorption of analytes. The sol solution consists of one or more precursors which are typically a metal alkoxide, solvent to disperse the precursors, catalyst (acid or base) and water [67]. Sol-gel process includes hydrolysis of the precursors, followed by polycondensation (alcohol or water) reactions. Molecularly imprinted sol-gel organosilica sorbents are made by mixing the sol solution and the targeted template. The R' fragment of alkyl alkoxy silane group in the precursor,  $(RO)_mSiR'_{4-m}$ , interacts with the template and the alkoxy silane fragment acts as a crosslinker [33]. The fabrication process is started by immersing the support (fiber) in the prepared mixture; once the MIP coating has formed, the fibers are left at room temperature to dry, then thermal conditioning is used to drive the polycondensation process to completion. The coating thickness is controlled by the number of immersion and drying cycles. MIP-fibers using the sol-gel technique have been reported for a range of targets including organophosphorus pesticides (OPPs) [68, 69], quercetin [70], and simazine [71]. The sol-gel technique for use in MIP fabrication is attractive because thermally- and mechanically-stable sorbents can be made under mild conditions (e.g., room temperature and ambient pressure) [72]. Additionally, the porous structures with high surface area can yield a higher number of accessible imprinted cavities and more efficient template removal [73]. A good example of such a sol-gel-MIP-SPME fiber was reported by Dowlatshah and Saraji [74] for extraction of difenoconazole from wheat and fruit samples (Table 1.2). The pre-polymerization solution combined mesoporous silica MCM-41, ammonia, ethanol, water, tetraethoxysilane (TEOS), 3-aminopropyl

triethoxysilane (APTES) phenyltrimethoxysilane (PTMOS); to which the difenoconazole template was then added. In this application, the support was silanized nichrome wire coated with a fast 1 min immersion in the aforementioned solution. Incorporation of mesoporous silica enhanced adsorption and imprinting (IF for difenoconazole from 2.38 to 6.04, log P 4.3) and the device reached equilibrium quickly (10 min). This paper also reported IF values for analogous compounds, illustrating both cross-reactivity and the influence of structure and hydrophobicity on adsorption phenomena: thiabendazole (TBZ, IF 1.02, log P 2.47), diniconazole (IF 1.07, log P 4.4), chlorpyrifos (IF 1.20, log P 4.96), and cypermethrin (IF 1.62, log P 6.6). In this example, the IF for the non-template molecules is correlated with increased hydrophobicity, although this is not the case for all MIPs [69].

Another advantage of sol gel technique is that the polarity of the prepared sorbent using this technique can be tailored towards a specific analyte by incorporating appropriate organic compounds in the coating [75]. Xiang et al. developed polar MIP-SPME fibers by using polyethylene glycol (PEG) as the monomer in the sol solution, and applied them for analysis of OPPs in fruits and vegetables [76]. Single template MIP-fibers were prepared by adding diazinon, parathion-methyl, and isocarbophos in separate sol solutions, while multi-template fibers used a sol solution containing all three templates. Selectivity of the one-template fiber, multi-template fiber and a bundle containing a collection one-template fibers (combined together with a home-made handle) was investigated by equilibrium extraction from a solution of diazinon (log P 3.81), quinalphos (log P 4.4), pirimiphos-methyl (log P 4.2); parathion-methyl (log P 2.86), and isocarbophos (log P 2.7). The highest imprinting was obtained using the multi-fibre-one-template-MIP device: IFs 3.89, 3.49, 2.51, 3.1, and 2.95 for diazinon, parathion-methyl, pirimiphos-methyl, quinalphos, and

isocarbophos, respectively. The multi-template fiber and single template fibers did not show good imprinting. It is worth mentioning that, the reported imprinting effects are best for adsorption from low concentration solutions, and IFs decreased at higher analyte loadings, which is consistent with theory suggesting that non-covalent imprinting gives a range of binding-site affinities [77]. Further details on MIP-SPME fibers prepared by surface polymerization from bulk solutions for extraction from various matrices are provided in Tables 1.1 and 1.2.

#### *1.4.1.2. Molding*

Molding is an alternative to layering by polymerization cycles, in which a silanized fiber substrate is inserted into a glass capillary filled with pre-polymer solution. After thermal polymerization (at 60 °C for 24 h), the outer glass capillary is removed to leave the coated extraction device [78, 79]. A MIP coating of an acrylamide (AM) and EGDMA copolymer was formed on a glass capillary in the presence of different template molecules for extraction of endocrine disruptors chemicals (EDCs) from water [78]. The authors tested different MIPs using one, two or three of the targeted compounds (i.e., ethyl-p-hydroxybenzoate (EP), dibutyl phthalate (DBP), and bisphenol A (BPA)) as templates. The MIP formed using a double template system of EP and DBP had the best extraction efficiency for all three targets, with IFs of 1.40, 1.44 and 1.49 for BPA, EP and DBP, respectively. The optimized double template MIP fibers also provide higher efficiency for related structural analogues (bisphenol B (BPB), diethyl phthalate, methylparaben (MP) and diphenyl ether). The performance of developed fibers was consistent after 200 times

extraction cycles demonstrating the suitability of the molding approach to fabricate robust MIP-SPME fibers.

Stainless steel is an appropriate substrate for molded MIP-SPME fibers, however, increasing the stability of MIP coatings on steel is crucial. One successful strategy is the use of bridging agents that can bind to the surface of the metal while leaving an available functional group to hold the coating. For example, dopamine binds to the steel while leaving an available hydroxyl group to act as a bridging agent [80]. Wang et al. [61] applied this treatment method before silanization with 3-methacryloxypropyltrimethoxysilane (MAPS) for preparation of MIP-SPME fibers for analyzing hesperetin and its metabolites for in-vivo applications. MIP-fibers were fabricated by injection moulding between the functionalized metal and glass capillary using a pre-polymer solution of hesperetin in chloroform/dimethyl sulfoxide (DMSO) (2:1 v/v), the monomer N-isopropylacrylamide (NIPAM), EDGMA (cross-linker) and AIBN (radical initiator), with polymerization at 62 °C for 24 h under nitrogen. The authors also took an additional step to make the fibers more compatible with vivo analysis by pretreating the MIP-SPME fiber with bovine serum albumin (BSA) as a restricted access agent, which may reduce biofouling by other serum proteins to form a material they call restricted access MIP (RAMIP). The mechanism of protein exclusion by RAMIP is based on combination of factors e.g., physical barriers, hydrophilic layer, and electrostatic repulsion [81]. RAMIP-SPME and its NIP analogue were tested for the adsorption of hesperetin (log P 2.6) from rat liver, adsorption capacities of 106.09 µg for the MIP and only 34.66 µg for the NIP (IF 3.06) were obtained, although they both reached equilibrium at the same point (~90 min). The cross selectivity of analogous compounds was also assessed, baicalein (similar functional groups with different

spatial orientation and a more planar structure) yielded an IF of  $<2$ , demonstrating that the selectivity is at least in part attributable to the geometry of the key functional groups. Note that the IF values reported here are extracted from the data presented [61].

Surface polymerization and molding techniques are the most common procedure to prepare MIP-coated fibers, in the following sections, two less common approaches that are rather promising will be presented.

#### *1.4.1.3. Spraying*

Compared to the methods discussed so far, the thickness of MIP layer can more easily be adjusted by using a spray method as simple as a home-made pneumatic spray device. Having good control over the thickness of the MIP coating on SPME devices can improve reproducibility as thickness dictates both the volume of the extracting phase (device capacity) and the accessibility of the binding sites through diffusion (porous materials) or permeation (non-porous coatings), i.e., equilibration time. In this method, the pre-polymerization solution is sprayed over the metal substrate and radical polymerization is initiated under UV irradiation. One device for adsorption of triazines pesticides from water and food samples was created by spraying the MIP solution onto a chemically-modified aluminum wire [82]. The wire was first anodized to oxidize the Al surface to form  $\text{Al}_2\text{O}_3$ , which was treated with NaOH to generate hydroxyl groups, then these were silanized prior to spraying. The optimized thickness and extraction capability was achieved by controlling spraying distance, polymerization time and the number of spraying/polymerization cycles. Other authors have proposed alternative treatment of the metal surface to improve the MIP-SPME coating and enhance the sensitivity of a MIP-

SPME, for example, Piryaei et al. created a layered double hydroxide (LDH) coating prior to silanization to improve the porosity of the Al surface [83]. These MIP-SPME devices were designed to analyze digoxin in urine and blood samples using a sprayed digoxin-imprinted polymer comprised of MAA and EGDMA in ACN, with the LDH devices showing 1.3 times higher extraction efficiency compared to a fiber made of anodized and silanized Al. Their device gave a 4.5-5.5 times signal enhancement compared to a commercial PDMS accompanied by high durability with good performance even after 80 uses [83].

#### *1.4.1.4. Coatings incorporating premade MIP particles*

SPME devices with various chemistries can be prepared by immobilizing adsorptive particles on the substrate using a polymeric binder [26]. Using this fabrication method solves two issues for MIP-SPME devices. One is to ensure the MIP is stable on the fiber. Secondly, the greatest advantage is that there is much greater control over the way the MIP can be prepared, allowing for the use of a range of polymerization approaches such as suspension polymerization [44] or precipitation polymerization [2, 84] to enhance the selectivity and repeatability.

One of the seminal works for this technique was reported by Shaikh et al. [44]. They used polyvinyl chloride (PVC) glue to prepare MIP fiber for extraction of endosulfan I and II from water. Here, MIP particles were prepared by polymerization onto the surface of Fe<sub>3</sub>O<sub>4</sub>@SiO<sub>2</sub>-methacrylamide core-shell nanoparticles. The pre-polymer solution constituents of magnetic particles dispersed in dimethyl formamide (DMF)/water solution, endosulfan (template), N,N'-methylene-bis-acrylamide and ammonium persulfate. After

template removal, these core shell MIP particles demonstrated a significant IF of 10.1 and 9.1 for endosulfan I (log P 3.8) and II (log P 3.8), respectively. MIP-functionalized particles (1 mg) were dispersed in DMF (1 mL) and mixed with PVC adhesive (0.4 mg) for application to the stainless-steel fiber substrate by dipping. The coating was cured by ultrasonic solvent evaporation.

Other binding agents have been used to attach MIP particles to stainless steel wire such as silicon sealant [2]. For example, a steel wire treated with hydrogen fluoride and polished was dipped into silicon sealant to create a thin adhesive layer, which was then dipped into MIP particles and dried (12 h) to obtain a stable MIP-fiber. The MIPs particles were formed by thermally initiated (60 °C for 24 h) precipitation polymerization of 2,5-divinylterephthalaldehyde (DVA) as a cross-linking functional monomer with estradiol as the template from ACN. As shown in Figure 1.6, both MIP and NIP particles were spherical, and formed a uniform coating on the steel wire. The device demonstrated excellent selectivity towards estrogens with IFs ranging from 2.94 to 4.42, with only weak matrix effect (8.5%–16.8% reduction in the slopes relative to water) in milk. The reusability of the MIP fiber was confirmed for as many as 60 adsorption/desorption cycles.

A novel approach for incorporation of MIP particles into a host matrix for fiber coating is based on electrospinning [84, 85]. Demirkurt et al. [84] made benzyl paraben imprinted particles by precipitation polymerization from MAA and TRIM in ACN (4,4'-Azobis (4-cyanovaleric acid) (AIVN) was used to initiate polymerization). Once the template was removed, the MIP particles were mixed with polystyrene and DMF to prepare electrospinning solution. This solution was then electro-deposited onto a silica fiber as polystyrene knitted MIP microspheres for selective extraction of parabens from water

samples, IFs 2 to 4. The electrospinning process seems to create a more open polymer host structure compared to the usual methods to imbed the particles into an adhesive matrix, making diffusion to the MIPs more accessible.

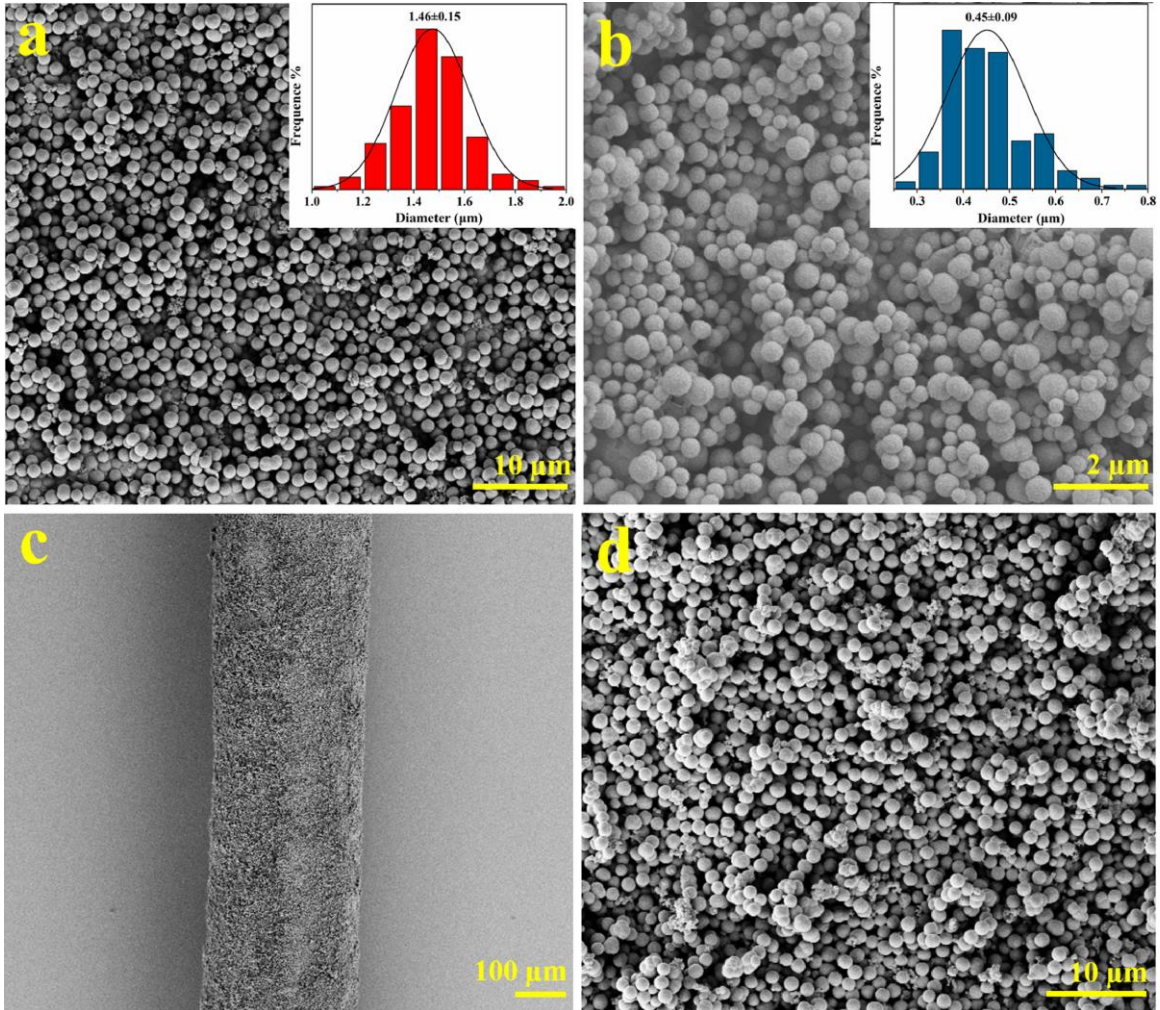


**Figure 1.6.** SEM images. (a) MIPs (1000 ×), and (b) NIPs (5000 ×), (c) MIPs-coated fiber (50 ×), and (d) MIPs-coated fiber (1000 ×). Reprinted from Ref. [2], with permission from Elsevier.

**Table 1.1.** MIP-SPME fibers: composition, fabrication technique and performance for applications in aqueous samples.

Targeted analytes	T:M:CL:Por:In	Selectivity	Figures of merit	Other highlights	Ref
<b>Surface Polymerization from Bulk Solution</b>					
Phthalate esters	DBP/diethyl phthalate (DEP) (0.045 g): NIPAM (1g): N,N'-methylenebisacrylamide (0.045 g): ACN (10 mL): AIBN(20 mg)	IF for di(2-ethylhexyl) phthalate, DEP, DBP and dimethyl phthalate were 1.5, 1.8, 2.1 and 2.8 respectively.	LR: 1-20 $\mu\text{g L}^{-1}$ LOD: 0.12 $\mu\text{g L}^{-1}$ Accuracy: 90.1% to 96.44 % RSD: 6.1% Analysis: GC-flame ionization detector (FID)	N/A	[86]
Simazine	Simazine (12 $\mu\text{mol}$ ): Methyltriethoxysilane (25 $\mu\text{L}$ , 0.12 mmol): Toluene (15 mL): Water (2 $\mu\text{L}$ ): HCl (32%, v/v, 2 $\mu\text{L}$ )	IF for simazine, terbuthylazine, ametryn, cyanazine, and desmetryn were 4.6, 2.8, 2.3, 2 and 2.3 respectively.	LR: 0.02-20 $\mu\text{g L}^{-1}$ LOD: 0.005 $\mu\text{g L}^{-1}$ Accuracy: 94.5% to 96.9 % RSD: <4.8% Analysis: GC-MS	N/A	[71]
<b>Molding</b>					
EDCs	Various templates (1 mmol): AM (4 mmol): EGDMA (20 mmol): methanol (5 mL): AIBN (20 mg)  Templates: Bisphenol F (BPF); MP, DEP	IF of 1.46 was reported for BPF.	LR: 0.01- 200 $\mu\text{g L}^{-1}$ LOD: 0.003- 0.016 $\mu\text{g L}^{-1}$ Accuracy: 80.8% and 114.1% RSD: <12.4% (n = 3) Analysis: HPLC- diode array detector (DAD)	Various array configurations tested, with best comprised of 2 BPF, 1 MP and 1 DEP fibers	[87]
EDCs	Template (1 mmol): AM (4 mmol): EGDMA (30 mmol): ACN: AIBN (50 mg)  Template: EP and DBP	IFs for BPA, EP and DBP, were 1.40, 1.44 and 1.49 respectively.	LR: 0.1–125 $\mu\text{g L}^{-1}$ LOD: 0.03 $\mu\text{g L}^{-1}$ Accuracy: 87%-120% RSDs (n=5) < 10%. Analysis: HPLC-DAD	N/A	[78]
Polychlorophenols	Triclosan (1mmol): Mono-(6-ethylenediamine-(N-methylacryloyl)-6-deoxy)- $\beta$ -CD and MAA (4 mmol): EGDMA (60 mmol): DMSO (20 mL): AIBN (012 mmol)	IF for 2,4-dichlorophenol, hexachlorophene, and triclosan were 2.73, 2.29 and 2.18 respectively.	LR: 1–200 $\mu\text{g L}^{-1}$ LOD: 0.3 $\mu\text{g L}^{-1}$ Accuracy: 83.71% to 109.98% RSD: 2.83% to 12.19% Analysis: HPLC-DAD	N/A	[55]
2,6-dichloro-1,4-benzoquinone (disinfection by-product)	2,6-dichloroindole-4-chloroimine (0.05 mmol): MAA (0.25 mmol): EGDMA (2.25 mmol): ACN (0.5 mL ): AIBN (15.0 mg)	IF of 4.7 for the template was obtained.	LR: 5.0 to 600.0 ng mL <sup>-1</sup> LOD: 2.3 ng mL <sup>-1</sup> Accuracy: 96.2% to 112% RSDs: 1.0%–13% (n = 3) Analysis: HPLC-ultra-violet (UV)	N/A	[88]
<b>Coatings incorporating premade MIP particles</b>					
Parabens	Benzyl paraben (1 mmol): MAA (4 mmol): TRIM (16 mmol): ACN (200 mL): AIVN 2.0 % (mol/mol)	IF of 2-4 for parabens were reported.	LR: 2-50 $\mu\text{g L}^{-1}$ LOQ: 0.26–0.29 $\mu\text{g L}^{-1}$ Accuracy: 92.2% to 99.8% RSD: <5.4% Analysis: HPLC-DAD	Cross selectivity study in presence of non analogous compound (triclosan and triclocarban) showed no selectivity.	[84]
<b>MIP monolithic fiber</b>					
Triphenyl phosphate (TPhP) in water	TPhP (0.05 mmol): AM (0.25 mmol): EGDMA (2.5 mmol): DMF (500 $\mu\text{L}$ ): 0.15 mmol AIBN Modifier: silanized graphene oxide (5 mg) was dispersed in	IF for TPhP, triphenylphosphine oxide, 2-ethylhexyl diphenyl phosphate (EHDPP), TCEP, trimethyl phosphate (TMP) were of 10.3, 5.0, 3.6, 1.5 and 1.3 were obtained	LOD: 0.0001 ng mL <sup>-1</sup> LR: 0.0007-124 ng mL <sup>-1</sup> Accuracy: 78- 110 %. RSD: 3.3% and 12.1% Fiber to Fiber RSD: 8.5 % Analysis: GC-flame photometric detector (FPD)	N/A	[3]

**Table 1.1** (Continued)

Targeted analytes	T:M:CL:Por:In	Selectivity	Figures of merit	Other highlights	Ref
<b>MIP monolithic fiber</b>					
Organophosphate flame retardants	Template (0.0625mmol): AM (0.25 mmol); EGDMA (2.5 mmol); DMF (500 $\mu$ L): AIBN (0.15 mmol) Templates: TMP, tri (2-chloroethyl) phosphate (TCEP), TPhP	IF of TMP-MIP fiber for TMP, TECP-MIP fiber for TCEP and TPhP-MIP fiber for TPhP were 4.3, 4.5, and 10.3, respectively.	LR: 0.004- 70 ng mL <sup>-1</sup> LOD: 0.0005 - 0.0015 ng mL <sup>-1</sup> Accuracy: 72.4% to 112.0% RSDs: 3.3% and 9.6% Analysis: GC-FPD	Graphene oxide was used as substrate for grafting MIP particles to have a larger amount of adsorbent.	[89]
TMP	TMP (0.15 mmol): AM (0.60 mmol); EGDMA (3 mmol); methanol (0.5 mL):AIBN (0.13 mmol)	IF for TMP was 2.28.	LR: 0.02–50 $\mu$ g L <sup>-1</sup> LOD: 0.00036 $\mu$ g L <sup>-1</sup> Accuracy: 88.7% to 103.2 % RSD: 4.5% and 6.9% (n = 6) Analysis: GC- nitrogen phosphorus detector (NPD)	IF for structural analogous of TMP O,O,O-trimethyl thiophosphate, O,O,S-trimethyl phosphorothioate, TCEP and TPhP were 1.43, 1.36, 1.10, and 1.03.	[90]

#### 1.4.2. Monolithic MIP-fiber

MIP coated SPME fibers have some limitations such as low porosity, surface area (accessible adsorption sites), and small sorbent volume. Furthermore, the MIP coating may detach from the solid substrate or degrade in myriad ways after multiple uses, requiring use of a new fiber and the concomitant calibration and quality checks [91]. Monolithic MIP-fiber is the format which address these issues [92, 93]. The fabrication of this fiber is quite simple and starts by introducing the pre-polymerization solution (template, monomer, crosslinker and porogen) containing an initiator to a glass capillary. Both ends of the capillary are sealed, e.g., using small pieces of rubber. Radical polymerization is usually thermally-initiated for relatively long intervals in an oven or water bath (e.g.  $\geq 12$  h) [56], though others have shown that the use of microwave heating can shorten the time significantly (30 min [94]). A monolithic fiber is liberated from the glass chemically or physically, and the template removed. Recent reports of monolithic MIP-SPME fibers for extraction of various contaminants are summarized in Tables 1.1 (water) and 1.2 (other

matrices). Extraction with monolithic polymers depends on mass transfer dynamics, which is limited by diffusion of analytes from the bulk sample through the porous or permeable material to the binding sites. The performance of monolithic MIP-SPME fibers has been improved by incorporating nanostructured supports, such as graphene oxide, into the polymer to improve porosity and increase mass transfer; a nice example of this has been reported for adsorption of TPhP from water [3]. In this work, silanized graphene oxide was dispersed in DMF and mixed the TPhP template and typical MIP components, AM, EGDMA and AIBN. The authors tested various porogenic solvents for this work, the solvent must dissolve the MIP components while suspending the modifier homogeneously, however only DMF was successful. A kinetic study revealed that the equilibrium adsorption by the MIP-fiber fabricated using GO was higher ( $\times 2$ ) than the MIP-fiber without GO or the NIP-fiber. Adsorption isotherms showed a higher adsorption capacity for MIP ( $7 \text{ mg TPhP g}^{-1}$ ) compared to NIP ( $1.2 \text{ mg TPhP g}^{-1}$ ). They also studied the cross-reactivity of these MIPs toward structural analogues (triphenylphosphine oxide (TPPO), and EHDPP); the best IF (10.3) was for the template (moderately hydrophobic TPhP), with weaker adsorption for the most hydrophobic (EHDPP) (IF 3.6) (Figure 1.7-a). MIP adsorbed TMP and TCEP (different compounds but with same functionality) slightly higher than NIP. The authors attribute the lack of correlation between IF and hydrophobicity to successful imprinting. We also reviewed their data and saw that the improved adsorption by MIPs relative to the NIPs for the hydrophobic compounds cannot be explained by surface area differences, thus the imprinted cavities must also show some, though weaker, affinity for analytes with similar functionalities. The developed MIP-fiber was very robust and could preserve the performance even after 110 extractions (Figure 1.7-b).

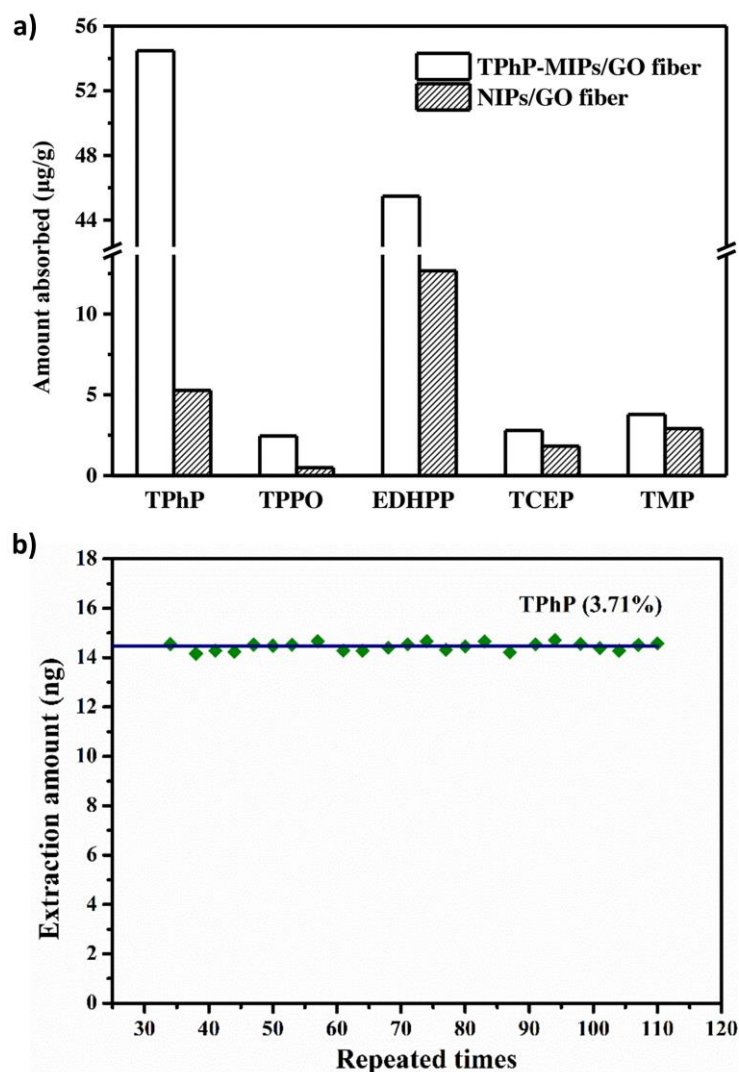


**Figure 1.7.** comparison of extraction capacities of TPhP and structural analogues on TPhP-MIPs/GO and NIPs/GO fiber (a), and reusability of monolithic MIP-SPME fiber for extraction of TPhP at  $10 \text{ ng mL}^{-1}$  (b). Reprinted from Ref. [3], with permission from Elsevier.

The role of solvent in monolithic MIPs goes beyond than the solubilization of pre-polymer mixture. The volume of solvent (porogen) is very important in reducing polymer brittleness and controlling pore size and volume. This parameter was assessed for a monolithic MIP-fiber developed for extraction benzodiazepines from plasma samples [54].

The pre-polymer components consisting of diazepam, MAA, EGDMA, and 2,2'-azobiscyanovaleric acid (ACVA) were dissolved in chloroform (optimal values can be found Table 1.2) with different polymer loadings at dilutions reported as volume of solvent. The best fibers were formed with 3.0 mL of chloroform, but for more concentrated pre-polymerization solutions (< 3 mL) fibers became brittle, likely due to reduced void volume and thus reduced flexibility in the network. However, volumes > 3 mL yielded particles in the capillary instead of a monolith since these are the conditions required for precipitation polymerization. Flexibility in a monolithic MIP is advantageous for high throughput manufacturing as flexible fibers are more robust (resist breakage) and can be used to prepare long capillaries, which can be used to improve analyte loading or be cut into smaller pieces that speeds the manufacturing process.

Applications of monolithic MIP fibers in biological samples requires considerations of compatibility with unique biological matrix components; for example, the binding sites can be easily occupied due to interactions between polymer functionality and macromolecules in high protein-content samples like plasma [95]. One interesting recent solution is to pre-coat the polymer with a layer of BSA to prevent binding of sample proteins; this restricted access blocks large molecules from accessing imprinted binding sites in monolithic MIP similar to molded MIP-SPME fibers mentioned in this article. Abrão and Figueiredo reported that this modification masked some analyte binding sites but improved protein exclusion by as much as 98 % (28 µg protein per 1 mL sample). They also compared binding efficiencies for the template diazepam to analogous psychoactive molecules, showing significant cross-reactivity and high imprinting factors for both coated and non-coated monoliths [54].

**Table 1.2.** MIP-SPME fiber composition, selectivity and performance fabricated using different techniques with an application in food, plant material, and biological samples.

Targeted analytes	T:M:CL:Por:In	IF	Figures of merit	Notes	Ref
<b>Surface Polymerization from Bulk Solution</b>					
OPPs in fresh and dry foods	Chlorpyrifos (25.4 mg): $\beta$ -cyclodextrin ( $\beta$ -CD, 65.8 mg) and AM solution (16.5 mg): TEOS (7.2 mmol): Mixture of dichloromethane (DCM)/DMF (4:1) (4 mL): 1.1 mL acetic acid	IF were in the range of 2-5 for targeted OPPs compounds.	LR: 0.25-25 $\mu\text{g L}^{-1}$ LOD: 0.02-0.07 $\mu\text{g L}^{-1}$ Accuracy: 81.2% to 97.7% RSD: <6.3% Analysis: GC-FPD	N/A	[96]
OPPs in vegetable samples	Diazinon (86mg): Hydroxy-terminated silicone oil (OH-TSO, 90 mg): Poly(methylhydrosiloxane) (PMHS, 10 mg): 3-(2-cyclooxypropoxyl) propyltrimethoxysilane (KH-560, 50 $\mu\text{L}$ ): TEOS (100 $\mu\text{L}$ ): Toluene (700 $\mu\text{L}$ ): Trifluoroacetic acid (TFA)/water (95/5, 80 $\mu\text{L}$ )	IF for diazinon, pirimiphos-methyl, pirimiphos-ethyl, parathion-methyl, isocarbophos were 3.06, 3.08, 3.70, 2.54, 2.51 respectively.	LR:2 -1600 $\mu\text{g kg}^{-1}$ LOD: 0.017-0.77 $\mu\text{g kg}^{-1}$ Accuracy: 81.2-113.5% RSD: 2.66% to 11.65% Analysis: GC-NPD	N/A	[68]
OPPs in fruits	Parathion-methyl (11.2 mg): monomer (30 mg): OH-TSO (90 mg): PHMS (10 mg): KH-560 (50 $\mu\text{L}$ ): TEOS (100 $\mu\text{L}$ ): DCM (600 $\mu\text{L}$ ): TFA/water (95/5, 80 $\mu\text{L}$ )	IF for fonofos, parathion-methyl, fenitrothion, and parathion were 1.44, 1.63, 1.48, 1.40 respectively.	LR: 0.2- 1000 $\mu\text{g kg}^{-1}$ LOD: 0.0019 to 0.065 $\mu\text{g kg}^{-1}$ Accuracy: 84.0% to 109.0% RSD: 3.4 – 7.0 % Analysis: GC-NPD	5,11,17,23-tetra- <i>tert</i> -butyl-25,27-dicyanomethoxyl-26,28-dihydroxy calix[4]arene was synthesized to be used as monomer.	[69]
Pyrrrolizidine alkaloids in herbal medicine	Monocrotaline (50 $\mu\text{M}$ ): sodium allylsulfonate (200 $\mu\text{M}$ ): EGDMA (0.5 mM): Methanol: ACN (50:50%, 5 mL): AIBN (2 mg)	IF for echimidine, europine, heliotrine, and lasiocarpine were 2.4, 2.6, 4.7and 4.5, respectively.	LR: 5 to 500 $\mu\text{g L}^{-1}$ LODs: 0.32 to 0.60 $\text{ng}\cdot\text{g}^{-1}$ Accuracy: 89.1-104.7% RSDs:< 8.1%: Analysis: LC-MS	Selectivity factor of MIP fiber for lasiocarpine, heliotrine, europine, and echimidine were 2.9, 2.1, 2.3, and 2, respectively compare to sinomenine (reference compound)	[97]
Auxins in tobacco	Indole-3-acetic acid (31 mg): 4-VP (150 $\mu\text{L}$ ): TRIM (225 $\mu\text{L}$ ): Toluene (2.1 mL): AIBN (17.5mg)	Selectivity factor for indole-3-acetic acid, indole-3-propionic acid were 2.78 and 2.59 respectively compared to the reference compound of Indole-3-pyruvic acid (0.95).	LR: 0.001-0.1 $\mu\text{g mL}^{-1}$ LOD: 0.0005 $\mu\text{g mL}^{-1}$ Accuracy: 82.5%-120.6%. RSD: 12.4 and 10.2%. Analysis: HPLC-UV	N/A	[1]
Quercetin in tea and coffee	Quercetin (50 mg): APTES (0.2 mL): TEOS (1mL): Ethanol (9mL): Acetic acid (1.1 mL)	IF of 2 for quercetin was reported.	LR: 0.05 to 100 $\mu\text{g mL}^{-1}$ LOD: 0.09 $\mu\text{g mL}^{-1}$ Accuracy:94.92%-98.50% RSD:2.09%-4.83% Analysis: HPLC-UV	Cross selectivity compared to gallic acid and caffeic acid using MIP and NIP fiber, showed no selectivity for competing compounds and 7 times more recovery for quercetin compared to NIP and competing compounds.	[70]
Chloroacetanilide herbicides in soybean and corn	Metolachlor (13 $\mu\text{L}$ ): MAA (17 $\mu\text{L}$ ): TRIM (255 $\mu\text{L}$ ): Toluene (2.5 mL): AIBN (3.9 mg)	IF for metolachlor was 5.5.	LR: 10 -1000 $\mu\text{g L}^{-1}$ LOD: 3-38 $\mu\text{g L}^{-1}$ Accuracy: 74.3%-96.4% RSD: 4.1-7.6% Analysis: HPLC-UV	Selectivity factor of metolachlor, hydroxymetolachlor, deschlorometolachlor and desmethylmetolachlor compared to toluene as reference compound were 4.60, 4.27, 3.88 and 3.24 respectively.	[64]
TC in animal derived food	TC (0.4 mmol): MAA (1.2 mmol) and HEMA (0.4 mmol): EGDMA (10 mmol): ACN (12 mL) and methanol (4mL): AIBN (120 mg)	IF for TC and its analogous compound OTC, and DC, and its non-analogous compound SMZ, and TAP were 3.23, 1.73,	LR: 5-1000 $\mu\text{g L}^{-1}$ LOD: 0.38-0.72 $\mu\text{g kg}^{-1}$ Accuracy: 77.3 to 104.4% RSD: 1.2 to 7.2% Analysis: HPLC-UV	Selectivity coefficient for OTC, DC, SMZ, and TAP were 1.38, 2.32, 4.30 and 9.55 respectively.	[65]

		0.96, 1.25, and 1.18 respectively.		
--	--	------------------------------------	--	--

**Table 1.2. (Continued)**

Targeted analytes	T:M:CL:Por:In	IF	Figures of merit	Notes	Ref
<b>Surface Polymerization from Bulk Solution</b>					
Difenoconazole in wheat and fruit samples	Difenoconazole (0.1 mol L <sup>-1</sup> ): APTES (0.2 mL) and PTMOS (0.2 mL): TEOS (3.0 mL): Ethanol (3.0 mL) and water (1.0 mL): Concentrated ammonia (0.1 mL)  Modifier: mesoporous silica MCM-41 (30 mg)	IF for difenoconazole, chlorpyrifos, thiabendazole, diniconazole, and cypermethrin were 6.04, 1.20, 1.02, 1.07, and 1.62.	LR: 0.01–1 ng mL <sup>-1</sup> LOD: 0.002 ng mL <sup>-1</sup> Accuracy: 73%–103% RSD: 3.4–7.2% Analysis: GC-ECD	N/A	[74]
OPPs in fruits and vegetables	Template: PEG (100 mg): OH-TSO (90 mg): TEOS (100 µL): PMHS (10 mg): KH-560 (50 µL): Toluene (700 µL): TFA solution containing 5% water (80 µL)  Template: Diazinon (74 µL), parathion-methyl (74.8 µL), and isocarbophos (82 µL).	IF were 3.89, 3.49, 2.51, 3.1, and 2.95 for diazinon, parathion-methyl, pirimiphos-methyl, quinalphos, and isocarbophos, respectively.	LR: 0.1–100 µg kg <sup>-1</sup> LOD: 0.0052–0.23 µg kg <sup>-1</sup> Accuracy: 75.1–123.2% RSD: 1.1–11.8 % Analysis: GC-NPD	Multi-fibre-one-template bundle was used as extraction device.	[76]
<b>Spraying</b>					
Digoxin in urine and blood samples	Digoxin (2.2 mmol): MAA (30 mmol): EGDMA (120 mmol): ACN (30 mL): AIBN (280 mg)	higher peak area using MIP versus NIP for digoxin, morphine, heroin, and codeine	LR: 0.1–10 ng mL <sup>-1</sup> LOD: 0.03 ng mL <sup>-1</sup> Accuracy: 102%–112 % RSD: <15% Analysis: HPLC-PDA	MIP-fiber compared to PDMS fiber and showed 4.5–5.5 times higher intensity in the chromatographic response	[83]
<b>Molding</b>					
Hesperetin and its metabolites for in-vivo applications.	Hesperetin (0.03 mmol): NIPAM (0.18 mmol): EDGMA (0.37 mmol): chloroform/DMSO (2:1 v/v, 4.5 mL): AIBN (10 mg)	IF of 6, 3, 2, and 2 were obtained for hesperetin, uteolin, quercetin, and baicalein respectively.	LR: 0.05–83.59 µg mL <sup>-1</sup> LOD: 0.02 µg mL <sup>-1</sup> Accuracy: 81.40% to 92.90% RSD: 4.92%–7.01% Analysis: UPLC-tandem mass	Comparison of RA-MIP with commercial PDMS and DVB fibers showed higher selectivity of RA-MIP for extraction of hesperetin and its metabolites	[61]
<b>Coatings incorporating premade MIP particles</b>					
Estrogens from milk	Estradiol (0.3 mmol): DVA (2.4 mmol, as monomer and crosslinker): ACN (40 mL): AIBN (10 mg)	IF values of 17β-estradiol, estriol, ethinyl estradiol, estrone, estradiol benzoate, and chloramphenicol were 4.42, 3.52, 3.29, 3.11, 2.94, and 1.01, respectively.	LR: 0.5–10000 ng kg <sup>-1</sup> LOD: 0.08–0.26 ng kg <sup>-1</sup> Accuracy: 84.3%–105% RSD: 3.2–8.1% Analysis: UHPLC-tandem mass	N/A	[2]
<b>MIP monolithic fiber</b>					
Steroid hormones from complex food samples	Progesterone (0.2 mmol): MAA (0.8 mmol): EGDMA (4 mmol): ACN and DMF (v/v, 3/1) mixture (50 mL): AIBN (20 mg)	IF for progesterone, testosterone, β-sitosterol, cholesterol and campesterol was about 5 times.	LR: 0.01–1000 µg L <sup>-1</sup> LODs: 3–5 ng L <sup>-1</sup> Accuracy: 95% and 101.0% RSD: 3.4–4.1% Analysis: HPLC-UV	Peak area difference of extracted non-analogous compounds such as ciprofloxacin, norflorxacin, ofloxacin, lovefloxacin, phenatherme, and anthracene obtained using MIP and NIP was less than 2.	[98]
Valproic acid in human serum and pharmaceutical formulations	Valproic acid (2.1 mmol): MAA (30 mmol): EGDMA (120 mmol): ACN (30 mL): AIBN (280 mg)	Higher peak area (300) of extracted valproic compared to extracted 1-octanol, octane, and decanoic acid (≤50) using MIP fiber were demonstrated.	LR: 0.03 to 100 µg L <sup>-1</sup> LODs: 0.01 µg L <sup>-1</sup> Accuracy: 90% and 97.5% RSD: 7.9% Fiber-to-fiber RSD: 9.3% Analysis: GC-FID	N/A	[99]
Sulfonylurea herbicides in soya milk and grape juice samples	Triflurosulfuron-methyl (TSM, 5.0 mg): 1-vinyl-3-octylimidazolium tetrafluoroborate (60 mg):	Selectivity factor values of TSM, metsulfuron-methyl, chlorsulfuron,	LR: 0.50–200.0 µg·L <sup>-1</sup> LODs: 14–91 ng·L <sup>-1</sup> Accuracy: 75.2% to 102% RSD: 1.8–9.2%	Four MIP fiber were tied up as an array for analysis.	[100]

	Ethylene dimethacrylate (EDMA, 90 mg): DMSO (150 mg): AIBN (30 mg)	prosulfuron and halosulfuron methyl are 8.1, 2.7, 1.3, 2.3 and 1.5, respectively.	Analysis: HPLC-DAD		
--	--	---	--------------------	--	--

**Table 1.2.** (Continued)

Targeted analytes	T:M:CL:Por:In	IF	Figures of merit	Notes	Ref
<b>MIP monolithic fiber</b>					
Benzodiazepines in human plasma	Diazepine (0.1 mmol): MAA (0.4 mmol): EGDMA (2 mmol): Chloroform (3 mL): ACVA (0.03 mmol)	The peak areas of targeted benzodiazepines using MIP were higher than NIP.	LR: 15-2600 $\mu\text{g L}^{-1}$ LOD: 5-30 $\mu\text{g L}^{-1}$ Accuracy: 84.4% - 121.6% RSD: 0.5%-20.0% Analysis: HPLC-DAD	N/A	[54]

## 1.5. Alternative High Capacity MIP Formats

Along with development of SPME fiber technology, other geometries have been introduced to improve the shortcomings of fibers leading to the introduction of MIP devices with larger effective surface area, higher adsorption capacity, improved robustness, simple operation, straightforward fabrication, and the possibility for high-throughput manufacturing. Among various MIP-based microextraction techniques there are two geometries which seem to be promising formats for SPME devices, specifically MIP-SBSE and MIP-thin films.

### 1.5.1. MIP-SBSE

The concept for MIP-SBSE is quite simple, to produce a MIP extraction device that can be used simultaneously for sample agitation. This serves two purposes; it facilitates quicker mass transport from the bulk sample to the sorbent surface and provides increased sorbent volume and surface area. Since SBSE is based on the equilibrium between the analyte in the sample and the coating material, the higher volume of extraction phase results in higher adsorption capacity and extraction efficiency [101]. The simple operation and excellent reproducibility of SBSE have advanced many application methods since its

introduction, however, most SBSE papers have used the commercial PDMS coated stir bar, which limits applications to hydrophobic analytes [102]. New research incorporates novel extractive phases such as carbon nanotechnology (e.g., graphene, graphene oxide, and carbon nanotubes), MOFs, and organic polymers [103]. Among these, MIPs have the advantage of molecular imprinting and are easily adapted to improve sample compatibility (e.g. to create hydrophilic polymers) due to the wide selection of suitable monomers, cross-linkers and solvents available.

The first report of MIP-SBSE was described by Zhu et al. using surface polymerization grafting of a MIP coating onto a PDMS-coated magnetic stir bar [100]. In this instance, the MIP formed was Nylon-6 imprinted with monocrotophos through hydrogen bonding with the amine functionality. Although this MIP-SBSE showed poor analyte recognition in aqueous media due to disruption of hydrogen bonding, this work inspired several fabrication methods (Figure 1.8) for MIP-SBSE devices which will be discussed here. Table 1.3 summarizes the analytical performance and condition of the referenced papers in this section and more examples of publications in MIP-SBSE.

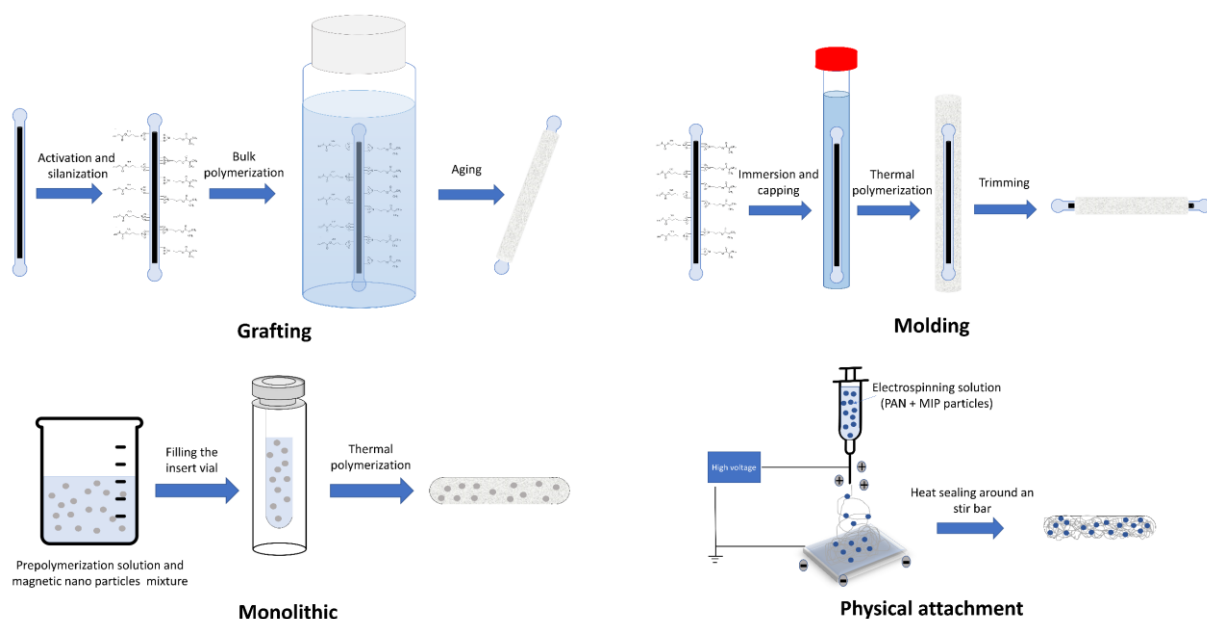


**Figure 1.8.** MIP-SBSE fabrication techniques.

#### 1.5.1.1. Grafting

Chemical grafting of MIP coatings onto a functionalized stir bar has been successful for selective recognition from environmental [104], biological [105], and food [106] samples (Figure 1.8). Tang et al. [4] used this approach to analyze semicarbazide (SC) in fish samples. To form a glass stir bar, iron wire was inserted into a glass tube (3.0 cm  $\times$  5.0 mm id) that was then heat-sealed at the ends. The glass was activated and silanized to add vinyl functionality to which the MIP could be tethered. The modified stir bar was immersed in a tube containing the pre-polymer solution of SC, MAA, EGDMA, and AIBN in methanol:water (4:1, v/v) and held at 60 °C for 18 h. They also tested acrylic acid (AA) and 4-VP. The device was washed and aged at 100 °C for 10 h to yield a thin (1.4  $\mu$ m) MIP coating (Figure 1.9). The authors reported their efforts to optimize the MIP formulae and the fabrication conditions (temperature and time of the polymerization and aging) using

theory (modeling template-monomer interactions with Gaussian) and experiments. They found that along with the fabrication and aging conditions monomer selection affected the MIP homogeneity (e.g., poor with 4-VP) and quality; as well they confirmed that the ratio of template to monomer was crucial in optimizing adsorption capacity (e.g., optimal molar ratio of 1:3 for SC:MAA). Selectivity of the MIP-stir bar relative to a NIP-stir bar was assessed for using SC at  $0.17 \mu\text{M}$  ( $13 \text{ ng mL}^{-1}$ ,  $\log P -2.75$ ) as a neat solution and in the presence of potential interferences: urea ( $\log P -2.1$ ), N,N-dimethylacetamide (DMAC,  $\log P -0.77$ ), cysteine ( $\log P -2.49$ ) and nitrofurazone (NFZ,  $\log P 0.23$ ). The MIP-stir bars performed much better than the NIP-stir bars under all conditions with 95% of SC recovered by the MIP and less than 25% by the NIP (IF 4.13), with only a small change in recoveries attributable to the presence of spiked interferences. Unfortunately, these polymers were not very robust, with recoveries reduced to 86% after only three extractions.

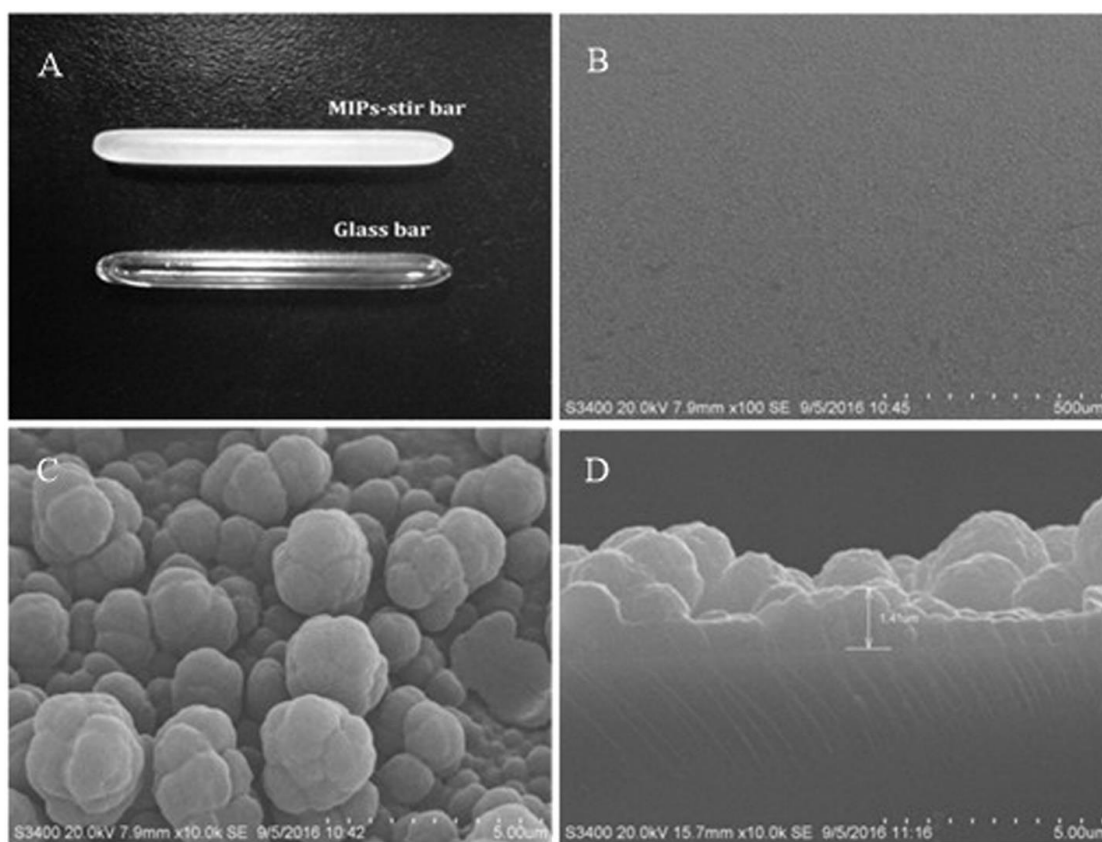


**Figure 1.9.** The photo of a bare glass bar (A) and the scanning electron micrographs of the MIP coating of stir bar (B (100 ×), C (10.0k ×) and the cross-section of a MIP-SB (D (10.0k ×)). Reprinted from Ref. [4], with permission from Elsevier.

Concerns regarding template removal and rebinding efficiency due to low porosity and restricted diffusion into the grafted MIP film coating has led to alternative fabrication strategies to improve surface area and binding site accessibility. One innovative approach uses boranate-affinity imprinting of the surface of Janus nanosheets (e.g., amino groups on one side and vinyl groups on the other) with catechol (template) and 4-vinyl phenyl boronic acid (monomer) in the presence of EDGMA to imprint the vinyl face of the sheets [107]. The SBSE device was created by immersing an aldehyde modified glass stir bar into an aqueous mixture of the MIP-coated Janus nanosheets, with grafting occurring via a reaction

of the aldehyde groups on the glass with the amino groups on the second face of the Janus nanosheets. A robust device that could be reused at least 7 times was produced. Study of the adsorption kinetics, showed that the MIPs reached equilibrium more quickly than the NIP, which the authors cite as proof of accessibility to the imprinted sites in MIP-SBSE provided by the nanosheets. We add a further interpretation to the data; the catechol template likely also plays a part in the formation of pores which improves accessibility to the binding sites and equilibration rate. The kinetic data fit a pseudo-second order model which as discussed in Section 3 is consistent with exhaustive extractions; here recoveries were near 90%. The adsorption isotherms fit the Langmuir model, suggesting monolayer adsorption and that the strength of interactions (binding site energy) between the catechol and the MIP are homogenous, at least over the narrow concentration range studied (20-200 mg L<sup>-1</sup>). The adsorption capacities of the MIP-SBSE and NIP-SBSE devices for catechol (log P 0.88) were compared to data for other phenolic compounds (2,4,6-trichlorophenol, log P 3.69; quercetin, log P 1.48; hydroquinone, log P 0.59), finding that the MIPs and NIPs favoured adsorption of catechol due to favourable interactions between the diol of the catechol and the oxygen of the deprotonated borate moiety. Using this data, we also calculated the IF values for each of the adsorbates, finding that only catechol had strong evidence for imprinting (IF 2.7), though a small amount of recognition for 2,4,6-trichlorophenol (IF 1.25) is noted, possibly related to improved surface area for the MIPs.

#### *1.5.1.2. Molding*

As with fibers, a mold—typically glass or polytetrafluoroethylene (PTFE)—provides a facile means to control volume and dimensions of the extracting phase in the

production of these larger MIP-SBSE devices. As with the grafting procedures, a substrate was prepared on a glass stir bar (usually fabricated in-house) which is positioned concentrically within the mold, which is filled with pre-polymerization solution. The thickness of the MIP sorbent on the stir bar can easily be controlled using different diameters of mold. Thickness, surface area and porosity of the extraction phase influence analytical performance, particularly sensitivity and reproducibility. Although PTFE mold is reusable, glass capillaries are inexpensive and can be broken or dissolved for easy liberation of the SBSE device after polymerization [50]. The fabrication and application of molded MIP-SBSE devices have been the subject of several literature publications, for example, for the analysis melamine in animal feed and milk [108] and propanol in urine [109].

Fan et al. [108] employed a PTFE mold of three parts of bottom cap, body, and top cap with thermal polymerization to control the thickness of MIP layer over a glass stir bar for analysis of melamine in animal feed and milk. In this work, cyromazine (pseudo template) was mixed with MAA, EGDMA, and AIBN in ACN to prepare the pre-polymerization solution. The reported IF for adsorption of melamine from methanolic extract was 4.0 [108]. Another exemplary MIP-SBSE fabricated via molding technique was applied for analysis of EDCs in environmental water samples [110]. Using glass capillary (1.8-2.2 mm) molds, several different monomers, including functionalized  $\beta$ -CD and common MIP monomers (4VP, MAA and AM), were tested in a pre-polymerization mixture of BPA (log P 3.32, template), EGDMA, and AIBN in DMF. A 2:2 ratio of diallyamine derivatized  $\beta$ -CD to AM had the highest extraction efficiency for BPA and IF of 1.5. The cross-reactivity reported as IF was studied for extraction of other compounds

similar to bisphenol: bisphenol AF (BPAF, log P 4.47), BPB (log P 4.13), BPF, (log P 2.91), bisphenol S (BPS, log P 1.65), and MP (log P 1.96) with modest results (Table 1.3) ranging from 1.04-1.21. Here the results can be compared to those reported using fiber MIP-SPME for analysis of EDCs in water samples (Table 1.1).

#### *1.5.1.3. Monolithic*

Typical preparation methods for coating MIP onto a substrate for SBSE, e.g., grafting and molding, require fabrication of the glass stir bar followed by surface activation and silanization to ensure a stable coating layer. An alternative is the fabrication of MIP-monoliths that incorporate the magnetic element as dispersed magnetic nanoparticles. In principle, this is very similar to the fabrication of monolithic SPME-fibers, with special attention given to homogeneous integration of the magnetic particles and mechanical robustness needed for use as a stir bar.

Díaz-Álvarez et al. [111] mixed vinyl modified magnetic nanoparticles (at ~7% (w/v)) into a pre-polymerization solution of MAA, EGDMA, and AIBN in toluene with propazine (PPZ) as the template for extraction of triazine herbicides from soil extracts. The authors found that the loading magnetic nanoparticles amount was key, where too little resulted in a device with poor stirring response, while too many nanoparticles interfered with polymerization and reduced the stability of the monolith. Similarly, sufficient cross-linking was required for mechanical stability, but too much affected the recognition properties. The optimum template-monomer-crosslinker ratio that yielded stable MIP stir bars was 1:4:11 of PPZ: MAA:EGDMA. Extraction time profiles showed that the MIP-SBSE adsorbed all triazines faster than NIP-SBSE, and chromatographic data showed that

the MIP-SBSE devices effectively reduced noise from soil matrix components when compared to direct injection of soil extracts [111]. In a similar study, a monolithic MIP-stir bar was fabricated for enrichment of TBZ (log P 2.47) and carbendazim (CBZ, log P 1.52) from orange peel extracts [112]. The pre-polymer mixture was prepared with TBZ (template), MAA, EGDMA, and AIBN in toluene (70:30 v/v), with ~7 % (w/v) of methacrylate-modified magnetic nanoparticles (synthesized in a 3-step process). The use of 30% ACN in the pre-polymerization solution was necessary to dissolve the TBZ template, but its use reduced the device stability. It was found that storage of the device in ACN prior to use, helped to avoid degradation and improved mechanical stability of the monolith. Due to a large number of non-specific interactions in water, both MIP and NIP strongly adsorbed TBZ, therefore, the device was tested in ACN extracts of orange peel. The absolute recovery of TBZ using MIP stir bar was almost twice as that of NIP-stir bar, 19% and 8%, respectively. A competitive study for extraction of TBZ and the structurally-similar CBZ showed that the slope of the calibration curve for each analyte was not influenced by the other analyte in the concentration range studied (25 – 1000  $\mu\text{g L}^{-1}$ ). Moreover, peel extract chromatograms before and after the MIP-SBSE process demonstrated that significant clean-up was achieved using this device. Díaz-Bao et al. [113] suggested that by combining a protic solvent (e.g. methanol) with a non-polar solvent (toluene) the compatibility of the MIP coating with aqueous media could be improved. In this work, a MIP-stir bar was prepared using  $\text{Fe}_3\text{O}_4$  nanoparticles dispersed in an optimized pre-polymerization solution of MAA, EGDMA, template (5,7-dimethoxycoumarin (DMC, log P 1.89)), and initiator (2,2'-azobis-(2-methyl-butynitrile), AIMN) in

methanol:toluene (9:1). The prepared MIP-stir bar was employed for extraction of aflatoxins (mycotoxins) (i.e., M1 (log P 0.5), B<sub>1</sub> (log P 1.23), B<sub>2</sub> (log P 1.45), G1 (log P 0.5), and G2 (log P 0.71)), from baby foods. Although the pseudo-template (a.k.a “dummy” template) used, DMC, is not a mycotoxin, the aflatoxins share many similarities with this coumarin. One of the more interesting findings was the success in forming a hydrophilic sorbent, with exhaustive recovery (97%) of DMC from an aqueous solution and no recovery from methanol:toluene. Recoveries for the aflatoxins ranged from 39% to 60% with good precision (RSDs<10%). Although the material was effective for adsorption of these key food contaminants, imprinting was modest; the MIP-stir bar provided on 5-10% higher recoveries than the NIP-stir bar for DMC.

#### *1.5.1.4. Physical attachment*

SBSE devices can be prepared by physical attachment of premade MIP particles to the stir bar substrate, which allows for incorporation of the broadest range MIP functionalities and fabrication methods. For example, MIPs were fabricated by emulsion polymerization then incorporated into a nanofiber membrane via electrospinning; this membrane was then affixed to a magnetic stir bar by heat-sealing and used for extraction of sulfonamides from animal feeds [114]. In this work, the MIPs were formed using a mixture of sulfamonomethoxine (SMM), MAA, Sty, EGDMA, and AIBN in DMSO dispersed into an aqueous solution of 0.25% SDS and 0.8% octadecanol (stabilizer). After template removal, 0.4 g of the MIP particles were added to the electrospinning solution containing polyacrylonitrile (PAN) and DMF. Then, nanofiber membrane containing MIP particles were prepared by electrospinning using a syringe with an applied potential of 18

kV, with a feed rate of 0.3 mL h<sup>-1</sup>. Specific masses of these membranes were heat sealed around the stir bar. Prior to use, the devices were soaked in ethyl acetate. Adsorption performance was tested on extracts of feed (extraction by sonication in ethyl acetate) that were spiked with standards as needed; absolute recoveries of SMM (log P 0.7), sulfadiazine (SDZ, log P -0.9), sulfamoxidyazine (SMD, log P 0.41), and sulfadimethoxine (SDM, log P 1.63) exceeded 80%. In a selectivity study of the MIP membrane on its own, 10 mg of each of the MIP and NIP membranes were exposed to 1 mL of a solution of standards that also contained the reference compound aniline (log P 0.9), a substructure of the analytes. Adsorption was determined indirectly by LC-MS/MS analysis of the supernatant. The IFs for SDZ, SMD, SMM, and SDM were 3, 2.5, 2.6, 2.8 and selectivity factors versus aniline were 2.3, 2.7, 2.6, and 2.8, respectively. Given that the reference compound was such a good probe for imprinting (sharing a large functionality with the analytes and similar hydrophobicity), the lack of selectivity for the MIP toward aniline (IF is 1) demonstrates that the imprinting is likely dominated by the sulfonamide functionality.

**Table 1.3.** MIP-SBSE composition, fabrication technique, selectivity and performance for specified targeted compounds and matrices

Targeted analytes	T:M:CL:Por:In	Selectivity	Figures of merit	Other highlights	Ref
<b>Grafting</b>					
SC in fish samples	SC (0.1 gr): MAA (230 $\mu$ L): EGDMA (1.52 mL): Methanol: water (4:1, v/v) (3. mL): AIBN (28 mg)	IF of 4.13 for SC was obtained in separate and mixed solutions of urea, DMAC, cysteine and NFZ.	LR: 1-100 ng mL <sup>-1</sup> LOD: 0.59 ng mL <sup>-1</sup> Accuracy: over 80% RSDs: <10% Analysis: HPLC-UV	Consistency of recovery in presence of other compounds is a proof of low matrix effect of MIP-stir bar.	[4]
Nabumetone (NAB) in tap water, serum and urine	NAB (0.3 mmol): MAA (3 mmol): EGDMA (6 mmol): toluene (30 mL): AIBN (15 mg)	IF of 5 was reported for NAB.	LR: 1.5–20.0 $\mu$ g L <sup>-1</sup> LOD: 0.20 $\mu$ g L <sup>-1</sup> Accuracy:98-105 % RSD: 4.6 and 8.1% (n = 6) Analysis: UV	MIP-SBSE recovery for NAB (5.0 $\mu$ g L <sup>-1</sup> ) and diclofenac, furazolidone and naproxen (20 $\mu$ g L <sup>-1</sup> ) from separate solutions was 90 % for NAB and less than 10% for other compounds.	[115]
Cationic paraquat (PQ) in environmental water and vegetable samples	PQ (100 mg): onohydroxylcucurbit[7]uril (300 mg). 20 mg of the T:M complex was mixed in sol gel mixture of DCM (700 $\mu$ L): OH-PDMS (300 $\mu$ L): PMHS (50 $\mu$ L): MTMOS (50 $\mu$ L): KH-560 (300 $\mu$ L): 98% TFA (300 $\mu$ L)	IF for PQ, ethyl viologen, diquat, difenzoquat were 2.56, 0, 0, and 0.24 respectively.	LR: 100 to 10,000 ng L <sup>-1</sup> LOD: 8.2 ng L <sup>-1</sup> LR: 0.02–0.85 mg kg <sup>-1</sup> LOD of 0.005 mg kg <sup>-1</sup> Accuracy:70-95.5 % RSD:<7.6% Analysis: HPLC-UV	The pre-polymerization solution was used for 15 times coating.	[43]
Chlorophenols from Seawater	2-chlorophenol (0.129 g, 1 mmol): 4-VP (0.4 mL, 4 mmol): EDMA (3.8 mL, 20 mmol): ACN (6 mL): AIBN (60 mg)	IF for 2-chlorophenol, 2,4-dichlorophenol and 2,4,6-trichlorophenol were 3.	LR: 1.0–100.0 $\mu$ g L <sup>-1</sup> LOD:0.17-0.38 $\mu$ g L <sup>-1</sup> Accuracy:84.3 % - 99.1% RSD:<7.4% Analysis: HPLC-UV	Extraction recovery for the three chlorophenols was same.	[116]
Naphthalene sulfonate in seawater	1- naphthalene sulfonic acid:4-VP (0.34 mL): EDMA (2.93 mL): Methanol/water (4:1, V/V) (13.33 mL): AIBN (166.7 mg)	IF for 1-naphthalene sulfonic acid, 2-naphthalene sulfonate, and 1-naphthol-3,6-disulfonic acid disodium salt was almost same (2.5) and for 5-Amino-1-naphthalenesulfonic acid was 4.5.	LR: 5-250 $\mu$ g L <sup>-1</sup> LOD: 1.20- 2.97 $\mu$ g L <sup>-1</sup> Accuracy 81.8%-99.5%. RSDs: 1–9.4% Analysis: UV	N/A	[117]
Diclofenac in seawater and commercial tablet samples	Diclofenac (0.20 g): 4-VP (0.27 mL): EGDMA (2.62 mL): Toluene (8 mL): AIBN (40 mg)	IF for diclofenac was 2-3 in different concentration	LR:0.5-500 $\mu$ g L <sup>-1</sup> LOD: 0.15 $\mu$ g L <sup>-1</sup> Accuracy: 94.2%-100.0 % RSD: 0.7-4.6% Analysis: HPLC-UV	N/A	[118]
$\beta$ -Agonist residues in animal-derived food	Clenbuterol (139.0 mg): MAA (0.20 mL): EGDMA (1.60 mL): ACN (5 mL): AIBN (20.0 mg )	IF of clenbuterol, salbutamol, ractopamine, mabuterol, brombuterol, and terbutaline were 3.8, 2.9, 3.1, 3.5, 3.2, and 3.3 respectively	LR:0.5-35 $\mu$ g L <sup>-1</sup> LOD: 0.05–0.15 $\mu$ g L <sup>-1</sup> Accuracy: 75.8–97.9% RSD: 2.6-5.3%. Analysis: HPLC-DAD	N/A	[4]
<b>Molding</b>					
Naproxen (Nap) enantiomer in pharmaceuticals personal care products	s-Nap (1 mmol): R-cysteine hydrochloride monohydrate (4 mmol): EGDMA (30 mmol): Methanol-DMSO (5:5, v/v) (15 mL): AIBN (20 mg)	IF for S-Nap and its similar compounds R-Nap, S-ibuprofen and its dissimilar structure phenol were 1.32, 1.31, 1.09 and 0.99 respectively.	LR: 0.01-200 $\mu$ g L <sup>-1</sup> LOD: 0.005 and 0.08 $\mu$ g L <sup>-1</sup> Accuracy: 83.98 %–118.88%. RSD <13.08% Analysis: HPLC-UV	Selectivity factor for S-Nap, R-Nap, S-ibuprofen and phenol (reference compound) were 14.24, 13.62, 11.13 and 1.0 respectively.	[50]

**Table 1.3. (Continued)**

Targeted analytes	T:M:CL:Por:In	Selectivity	Figures of merit	Other highlights	Ref
<b>Molding</b>					
EDCs in environmental water	BPA (1 mmol): $\beta$ -CD (2 mmol) and AM (2 mmol); EGDMA (60 mmol): DMF (26 mL): AIBN (20 mg)	IF of 1.21, 1.16, 1.09, 1.04, 1.10 and 1.06 were obtained for BPA BPAF, BPB, BPF, BPS, and MP.	LR: 0.1-200 $\mu\text{g L}^{-1}$ LOD: 0.004 – 0.01 $\mu\text{g L}^{-1}$ Accuracy: 92% to 119 % RSD: < 9.7 % Analysis: HPLC-DAD	N/A	[110]
Secbumeton and triazine herbicides in peppermint and tea samples	Secbumeton (1:12 ratio to methacrylate monomers): 30 wt% of methacrylate monomers (30 wt% EDMA and 70 wt% MAA); Chloroform (30 wt%): 2 wt% of lauroyl peroxide	IF for Secbumeton was about 1.5.	LR: 0.02-8.6 $\mu\text{g L}^{-1}$ LOD: 0.4 $\mu\text{g L}^{-1}$ - 2.5 $\mu\text{g L}^{-1}$ Accuracy: 74% and 122%. RSD: < 13%. Analysis: GC-MS	Water/Oil medium internal phase emulsion (40/60 w/w%) containing multi-walled carbon nanotubes (2 wt%) was used in fabrication.	[119]
<b>Monolithic</b>					
Triazines from soil	PPZ: (106.6 mg): MAA (159.8 $\mu\text{L}$ ): EGDMA (1.015 mL): Toluene (3 mL): AIBN (33.5 mg) Modifier: vinyl-modified magnetic nanoparticles (0.035 g of) was added to 0.5 mL of pre-polymer solution	The difference in slope of the extraction time profile graphs in MIP and NIP was significant and higher in MIP which shows the selectivity of imprinted sites in MIP-stir bar.	LR: 1 to 50 $\mu\text{g L}^{-1}$ LOD: 3.6-7.5 $\text{ng g}^{-1}$ Absolute recoveries ranged from 2.4% to 15.4% RSDs: <10% Analysis: HPLC-DAD	Another assessment of selectivity was demonstrated by comparing much less noisy LC-UV chromatograms from soil extracted samples enriched with MIP-stir bar with direct injection of extracts.	[111]
TBZ and CBZ from orange samples	TBZ (58.4 mg): MAA (157.4 $\mu\text{L}$ ): EGDMA (1.0 mL): Toluene: ACN 70:30 (v/v) (3.46 mL): AIBN (33.5 mg)	IF of 2.4 for TBZ.	LR: 25 to 1000 $\mu\text{g L}^{-1}$ LODs: 0.10 and 0.13 $\text{mg kg}^{-1}$ RSD: <10% Recovery: 21% - 33%. Analysis: HPLC-DAD	Cross-selectivity of TBZ and CBZ was tested by obtaining isotherms using MIP which shown there was no difference in their slopes. Note: 0.035 g of methacrylate modified magnetic nanoparticles was used in pre-polymer solution.	[112]
Aflatoxins from baby foods	DMC (0.1 mmol): MAA (0.4 mmol): EGDMA (2 mmol): methanol: toluene (9:1) (1 mL): AIMN (0.25 mmol)	MIP-stir bar provided on 5-10% higher recoveries for DMC than the NIP-stir bar	LR: 0.5-8 $\text{ng kg}^{-1}$ LOD: 0.3-1.7 $\text{ng kg}^{-1}$ RSD: <10% Recovery: 39%-60% Analysis: HPLC- Q-Trap MS	The device provided 97% recovery for the extraction of DMC Note: 0.5 g $\text{Fe}_3\text{O}_4$ nanoparticles was used in pre-polymer solution	[113]
<b>Physical attachment</b>					
Sulfonamides from animal feeds	SMM (0.5 mmol): MAA (2 mmol) and Sty (1 ml): EGDMA (8 mmol): DMSO (10 ml): AIBN (0.05 gr)	IF for SDZ, SMD, SMM, and SDM were 3, 2.5, 2.6, 2.8 and selectivity factor versus aniline were 2.3, 2.7, 2.6, and 2.8 respectively.	LR: 10-1000 $\text{ng g}^{-1}$ LOD: 1.5-3.4 $\text{ng g}^{-1}$ Accuracy: 72%-90% RSD: 2.8% to 7.9% Analysis: LC-MS/MS	Pre-polymer solution dissolved in 100 mL of 0.25% SDS aqueous solution containing 0.8 gr of octadecanol as stabilizer for emulsion polymerization.	[114]

### 1.5.2. MIP-TFME

As mentioned previously, TFME uses a large sorbent volume in a thin layer to improve the effective surface area to volume while retaining the favourable mass transfer kinetics. This geometry improves the extraction capacity without long intervals to reach equilibrium [120]. TFME devices are usually prepared by immobilizing SPE packing materials (e.g., C18, HLB, DVB) using a polymer binder. Due to the flexibility in formulation and fabrication, MIPs are excellent candidates to be used as TFME devices either as solid substrate-supported or membrane-supported thin films (Figure 1.10).

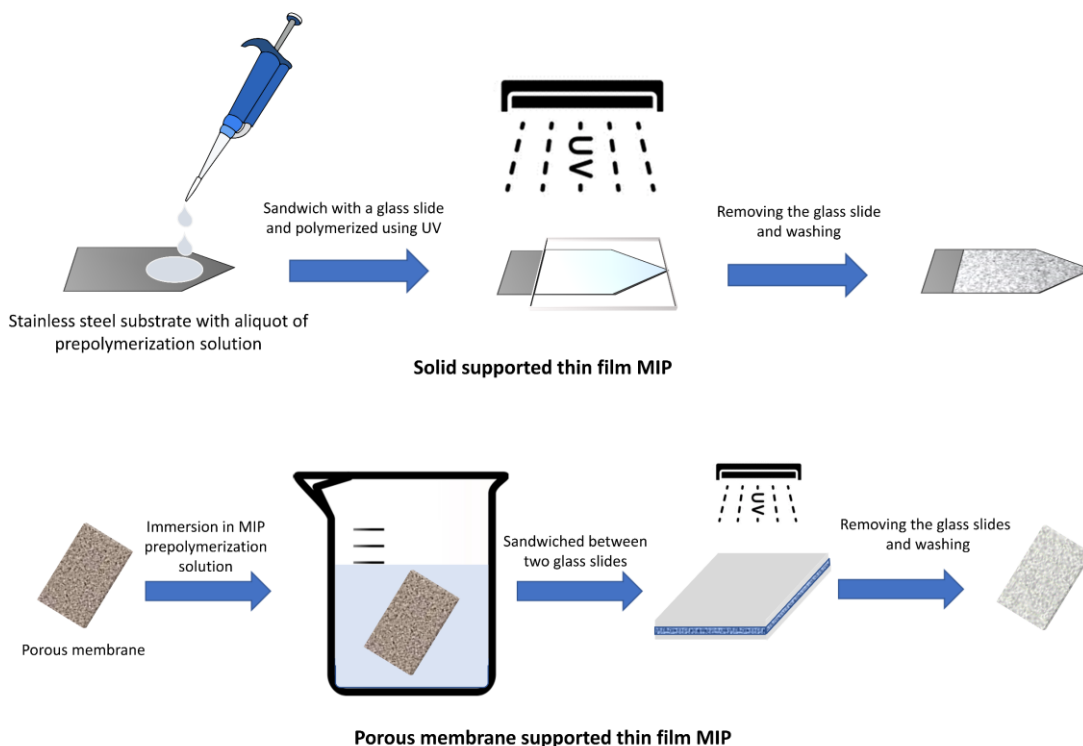


**Figure 1.10.** Thin film MIP fabrication techniques.

Readers can find the information regarding the performance and compositions of the MIP-TFME devices referenced here in Table 1.4.

### *1.5.2.1. Solid substrate supported MIP-TFME*

MIPs have been fabricated in thin film format using a solid substrate (e.g., microscopic glass slide) for sensor applications [121]. One of the first MIP TFME applications for use with mass spectrometry was reported by Van Biesen et al. [122], since then MIPs in this format have been extended to sample enrichment and cleanup for chromatography. In a typical fabrication procedure, MIPs are prepared by drop-casting of a few  $\mu\text{L}$  of pre-polymer solution between a silanized glass microscope slide (cut to  $25 \times 22 \text{ mm}^2$ ) and a glass cover slide. This sandwich then is exposed to UV light to initiate polymerization. Fabricated thin films are then washed in proper organic solvents to remove the template and unreacted polymer components; drop-casting is simple, adaptable to different shapes and sizes using a range of polymer compositions and allows for simultaneous fabrication of multiple devices.

One of the classes of compounds for which thin film MIPs have been developed is phenols and alkyl phenols. A thin film MIP for phenols was developed based on Sty as the monomer to maintain the hydrophobic binding and pentaerythritol triacrylate (PETA) to form a tighter, hydrophilic network [123], these were imprinted with phenol and 2,2-dimethoxy-2-phenylacetophenone (DMPA, photoinitiator) in methanol:water (5:1, v/v). The highest IF obtained for extraction of phenol ( $0.5 \text{ mg L}^{-1}$ ) from water was only 1.16. It was concluded from the results that it is difficult to achieve imprinting effect for phenols due their small size, simple shape and only one weakly acidic hydroxyl group. Additionally, the selective binding of phenol via hydrogen bonding is suppressed in aqueous environments, which drove the choice of Sty as the functional monomer to avail of

hydrophobic and  $\pi$ - $\pi$  interactions between the aromatic structures of the monomer and phenols.

In comparison, Abu-Alsoud [124] developed a MIP-TFME based on 4-vinyl benzoic acid (4-VBA) as the monomer imprinted with o-catechol for analysis of phenol, alkyl phenols, and chlorophenols; these can undergo hydrogen binding and  $\pi$ - $\pi$  interactions with the monomer functionality rather than only  $\pi$ - $\pi$  interactions reported in other work. Arriving at this composition followed fabrication and characterization of MIPs and NIPs using five monomers (4-VBA, 4-vinylaniline, N-allylaniline, 4-VP and Sty), various pseudo-templates (hydroquinone, 4-hydroxy benzoic acid and catechol), cross-linkers, porogens and ratios thereof. Another innovation here, was the addition of linear polymers to the porogen—specifically PEG in methanol and water (5:1)—to improve pore formation during the phase separation process. Thin film MIP selectivity towards phenol compounds was demonstrated by noticeable difference in the slope of adsorption isotherms for the MIPs and NIPs, with IFs ranging from 1.25 to 1.47, with excellent performance characteristics (Table 1.4).

MIP-TFME devices on glass for analysis of polycyclic aromatic sulfur heterocycles (PASHs) in seawater [125] have been reported using a pseudo-template, 2-thiophene-carboxaldehyde, with 1-vinylimidazole (1-Vim), bisphenol A dimethacrylate (BPADMA), PEG, and DMPA in ACN. These devices were used under pre-equilibrium conditions (2 h) and demonstrated the highest extraction efficiencies for benzothiophene (BT, log P 3.12), 3-methylbenzothiophene (3-MBT, log P 3.71), dibenzothiophene (DBT, log P 4.38). An interesting finding was that the MIPs showed lower, but similar capacity for adsorption of indole (log P 2.14) and 4,6-dimethyldibenzothiophene (4,6-DMDBT, log P 5.5) despite the

much higher hydrophobicity of the latter; this was attributed to possible steric hindrance associated the two methyl groups on 4,6-DMDBT. Indole is the nitrogen analogue of the sulfur bearing BT. IFs for the targeted analytes were calculated at 3.0, 2.8, 2.9, and 2.3 for BT, 3-MBT, DBT, and 4,6-DMDBT, respectively.

MIP-TFME devices have also be fabricated using more robust substrates, such as stainless steel, which is mechanically stable, durable, does not need any treatment or modification prior to deposition of the polymer precursors, and can be easily cut-to-fit [5]. MIP-TFME devices fabricated on stainless steel (sword shaped  $0.5 \times 35 \text{ mm}^2$ ) via the sandwich method (Figure 1.10) were used for extraction of OPPs from water and fruit juices. The pseudo template was synthesized specifically by the authors, and used with MAA, EDGMA, and DMPA in 1-octanol. In this work, the importance of the porogen volume relative to the mass of the pre-polymer components in controlling porosity, surface area, capacity and selectivity was highlighted in a pseudo-phase diagram. Using this diagram, we showed that relatively small changes (3%) in the porogen-to-polymer ratio resulted in materials with very different pore morphologies and analytical behaviour, e.g., a macroporous polymer with low selectivity was formed at 49.8% porogen loading, whereas at slightly higher loadings (52.8%) a micro-gel polymer formed with smaller pores, higher surface area, and superior selectivity toward the targets. Figure 1.11 shows the SEM images the developed MIP-TFME. A study of adsorption capacity at equilibrium demonstrated that the IF for fenamiphos (log P 3.2) was 3.5, while for some of the more hydrophobic OPPs, such as chlorpyriphos (log P 5.0) showed low imprinting. Of note, the incorporation of the EGDMA cross-linker imbues the devices with excellent water-compatibility, allowing for use without preconditioning. A comparison of adsorption

without conditioning the MIP-TFME to conditioning with 50% methanol in water prior to extraction provided no evidence of difference in performance. The selectivity for targeted OPPs in the presence of other compounds (i.e., tricyclic antidepressants (TCAs), acidic herbicides) was tested and demonstrated a slight decrease in extraction efficiency for MIP-TFME. However, using the same data to calculate selectivity gave improved IFs, which were associated with a relative decrease in adsorption of the OPPs by the NIPs. The effect of humic acid on performance was also examined; even at 100 ppm humic acid extraction recoveries were unimpaired. The devices reported in this work were used for a minimum of 15 consecutive extractions with no decrease in performance [5].

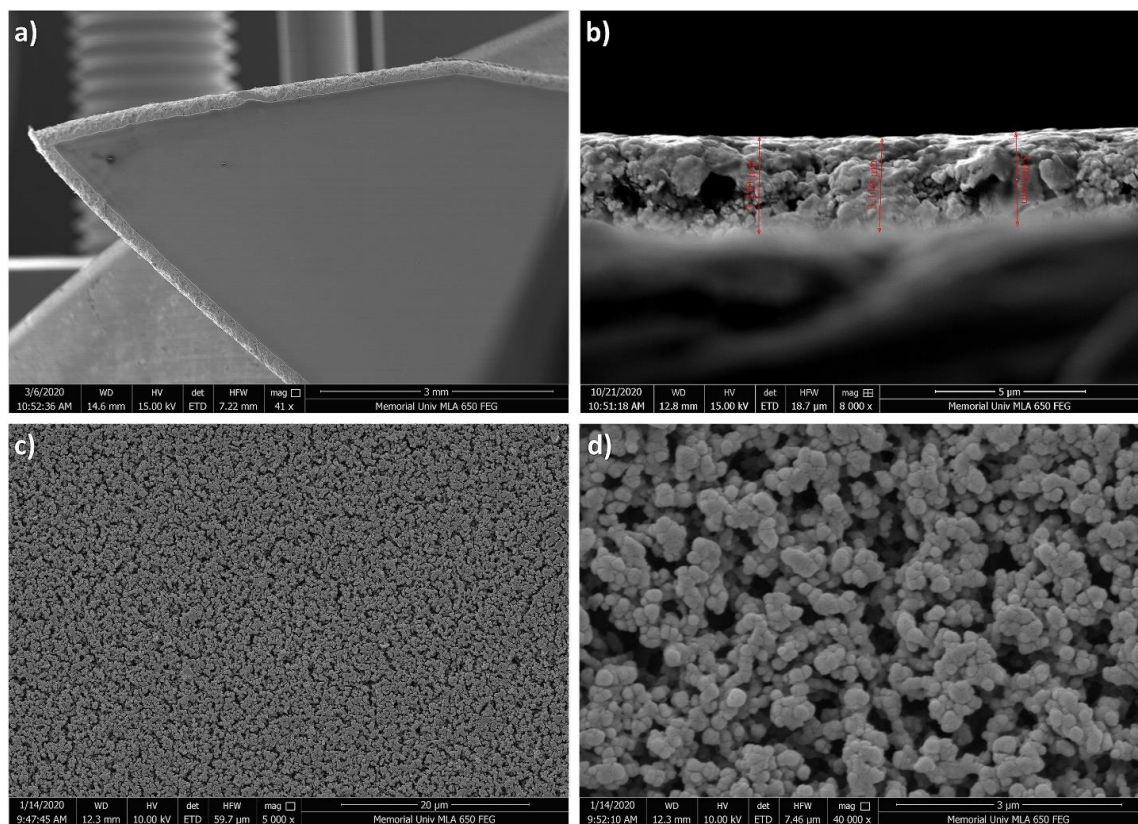


**Figure 1.11.** Scanning electron micrographs of prepared thin film MIPs at different magnifications. Reprinted from Ref. [5], with permission from Elsevier.

### *1.5.2.2. Membrane supported MIP-TFME*

Membrane supported MIP-TFME devices are fabricated by immersing a porous membrane into the MIP pre-polymerization solution. After withdrawal, the membrane is sandwiched between a glass substrate and a cover glass or between two cover glasses. The polymerization can be UV- or thermally initiated [51, 57, 126]. Although the term of molecularly imprinted membrane has been used for these devices, the applications of the devices does not fit the strict definition of a membrane, which is flow-through device [127]. Therefore, the MIP coated membranes are categorized here as MIP-TFME devices.

Yazdanian et al. fabricated MIPs on a polyvinyl fluoride membrane for analysis of celecoxib (CEL) in urine, plasma, and pharmaceutical preparations [126]. The pre-polymerization solution consisted of CEL as the template, a binary monomer system HEMA and N-vinylcaprolactam (NVCL), EGDMA, and AIBN in methanol. An IF of 2 was reported for the extraction of CEL, and a selectivity factor of 3.6 was reported for simultaneous extraction of CEL against levothyroxine (no similarities in structure). Their device showed excellent reproducibility over 10 extraction and desorption cycles. Yuan et al. [51] used a commercial nylon-66 membrane as a support to make MIP-TFME devices for analysis of enrofloxacin (ENR) and ciprofloxacin (CIP) in eggs. The nylon was used as the substrate to provide a flexible device for use with containers of different shapes and sizes. They also developed a novel method of fabricating the MIP on the polymer substrate, where the nylon-66 membranes were first immersed in a solution of initiator in ACN, dried, then dipped into the pre-polymerization solution of gatifloxacin (GAT, pseudo-template), 1-Vim, EGDMA and DMPA in ACN:1-octanol (1:1, v/v), and sandwiched between two cover glasses. The sandwiched membranes were exposed to UV from both sides. Although

many porogens were tested, (methanol, ACN, 1-octanol, and mixtures of these), only ACN:1-octanol could dissolve the pseudo-template effectively. MAA was tested as a monomer but was found to precipitate from the pre-polymerization solution. Selectivity, kinetic and reuse studies relied on indirect analysis of adsorption through measurement of the supernatant concentration after incubation with devices. Under optimal conditions, 1-Vim gave IFs of 1.52-1.62 and selectivity factors against competitive compounds (i.e., ofloxacin and daidzein) in the range of 1.71- 2.15. The MIP-TFME devices showed good performance for up to three cycles of extraction and desorption.

**Table 1.4.** Thin film-MIP devices fabrication method, composition, selectivity and performance prepared for targeted compounds in various matrices.

Targeted analytes	T:M:CL:Por:In	Selectivity	Figures of merit	Other highlights	Ref
<b>Solid substrate supported</b>					
TCAs in plasma	Synthesized pseudo template (0.4 mmol): MAA (0.8 mmol): EGDMA (4.8 mmol): Octanol (1000 $\mu$ L): DMPA (16 mg)	Ratio of the slope of the isotherm for MIP and NIP, considered as IF for nortriptyline, desipramine, amitriptyline, doxepin, imipramine, trimipramine and clomipramine were 3.7, 3.8, 4, 4.3, 3.5, 3, and 4.5.	LR: 1-500 $\mu$ g L <sup>-1</sup> LOD: 0.3-1.6 $\mu$ g L <sup>-1</sup> Accuracy: 90%-110% RSD: <10% Analysis: UPLC-MS/MS	Pseudo template, benzyl (3-(10,11-dihydro-5H-dibenzo[b,f]azepin-5-yl)propyl)(methyl)carbamate) was synthesized by the authors.	[128]
Phenols and alkyl phenols in water	Phenol (0.4 mmol, 37.6 mg): Sty 0.8 mmol (92.0 $\mu$ L): PETA 2.67 mmol (674 $\mu$ L): 1 mL of Methanol: water (5:1, v/v, 1mL): DMPA (0.06 mmol (15.4 mg)	IF obtained at initial concentration of 0.5 mg L <sup>-1</sup> was 1.16	N/A	N/A	[123]
Phenol, alkyl phenol and chlorophenol in water	O-catechol (0.024 mmol): 4-VBA (0.096 mmol): EGDMA (0.48 mmol): DMPA (0.012 mmol): Methanol and water (5:1, 200 $\mu$ L) with PEG as a solvent modifier (0.22 g mL <sup>-1</sup> )	IFs using the optimized formula were in the range of 1.25-1.47	LR: 0.5–1000 $\mu$ g L <sup>-1</sup> LODs: 0.1 to 2 $\mu$ g L <sup>-1</sup> Accuracy: 81%-107% RSDs: <14% Analysis: UPLC-PDA	N/A	[124]
PASHs in seawater	2-thiophene- carboxaldehyde (0.27 mmol, 25.6 $\mu$ L): 1-Vim (1.10 mmol,99.4 $\mu$ L): BPADMA (2.20 mmol, 800mg): ACN (930 $\mu$ L): DMPA (0.05 mmol, 12.1 mg)	IFs for BT, 3-MBT, DBT and 4,6-DMDBT were reported as 3.0, 2.8, 2.9, and 2.3 respectively.	LR: 0.5 –40 $\mu$ g L <sup>-1</sup> LODs:0.029-0.166 $\mu$ g L <sup>-1</sup> Accuracy: 77% to 121% RSDs: <6% Analysis: GC-MS	PEG (average MW20,000, 300 mg) added as modifier to the pre-polymerization solution.	[125]
Semi-volatile thiophene compounds in water	2-thiophene- carboxaldehyde (0.27 mmol, 25.6 $\mu$ L)/ 1-Vim (1.10 mmol,99.4 $\mu$ L)/ BPADMA (2.20 mmol, 800mg)/DMPA (0.05 mmol, 12.1 mg)	The IF for BT, 3-MBT, DBT and 4,6-DMDBT were 2.93, 2.74, 2.86, and 2.21 respectively.	LR: 5-100 $\mu$ g L <sup>-1</sup> LOD: 0.24–0.82 $\mu$ g L <sup>-1</sup> RSD: $\leq$ 7.0% Analysis: GC-sulfur chemiluminescent detector	N/A	[129]
ENR and CIP in egg samples	GAT (0.07 mmol):1-Vim (0.28 mmol): EGDMA (1.4 mmol): ACN: 1-octanol (1:1 v/v, 1.4 mL ): DMPA (8.4 mg)	Selectivity factor in the presence of competitive compounds such as ofloxacin and daidzein which were in the range of 1.71- 2.15	LR:5-5000 $\mu$ g kg <sup>-1</sup> LODs: 0.3 and 0.7 $\mu$ g kg <sup>-1</sup> Accuracies: 84.5%-97.0% RSDs: 1.9%-10.2% Analysis: UHPLC-UV	N/A	[51]
OPPs from water and beverage samples	Synthesized pseudo template (0.3 mmol, 68.16 mg): MAA (1.2 mmol, 101.8 mL), 4.8 mmol): EDGMA (905 mL): DMPA (62 mmol, 16 mg.): 1-octanol (1125 mL)	IFs varied from 1.5 for chlorpyrifos ( the most hydrophobic OPP) to 42.8 for fenamiphos (the most water soluble of the OPPs)	LR: 0.002-0.02 ng mL <sup>-1</sup> LODs: 0.001-0.005 ng mL <sup>-1</sup> Accuracies: 79%–120% RSDs: <15% Analysis: UPLC-MSMS		[5]

**Table 1.4.** (Continued)

Targeted analytes	T:M:CL:Por:In	Selectivity	Figures of merit	Other highlights	Ref
<b>Membrane supported</b>					
2,4-dichlorophenoxyacetic acid (2,4-D) in environmental water samples	2,4-D (1 mmol): 4-VP (4 mmol): EGDMA (20 mmol): Methanol and water (v/v, 4:1) (5 mL): AIBN (0.31 mmol)	IF of about 2 for 2,4-D. Cross selectivity study by extracting target compound and its analogues: 2,4-dichlorophenylacetic acid, 4-chloroxyphenylacetic acid and 4-chlorophenylacetic acid using MIP and NIP sorbents. No selectivity was observed for analogues.	N/A	N/A	[57]
Carbamazepine (CAR) in blood	CAR (42 mM): Sty (220 $\mu$ L): Tetramethyl orthosilicate (390 $\mu$ L): ACN (4mL):AIBN (50 mg) and 0.1 M HCl (390 $\mu$ L)	Chromatograms with less background noise and higher S/N ratio was obtained using MIP-TFME compared with two other commercialized collection cards for dried blood spot analysis.	LR: 4-800 $\mu$ g mL <sup>-1</sup> LOD: 1.3 $\mu$ g mL <sup>-1</sup> Accuracy:88.4 % to 94.5 % RSD: <5.1 %, Analysis: Capillary electrophoresis	N/A	[130]
CEL in urine, plasma and pharmaceutical tablet	CEL (1 mmol): HEMA (4 mmol), NVCL (4 mmol): EGDMA (20 mmol): Methanol (20 mL): AIBN (0.1 gr)	IF of 2 was reported for CEL. Cross selectivity study showed a selectivity factor of 3.86 compared to levothyroxine as reference compound.	LR: 0.5-80 $\mu$ g mL <sup>-1</sup> LOD: 0.0009 $\mu$ g mL <sup>-1</sup> Accuracy:90.7%-93.3% RSD: 1.2%-4.7% Analysis: HPLC-UV	N/A	[126]

## 1.6. Conclusions on MIP-SPME devices

The ultimate goal of advances in analytical instrumentation and sample preparation is to provide more accurate and precise results. Trends toward more robust, user-friendly, and high throughput techniques with reduced sample volumes and solvent consumption have given rise to SPME devices. The adaptability of MIP sorbents has enhanced SPME by improving selectivity, robustness, solvent/sample/pH compatibility, thermal stability, method and fabrication simplicity, while diminishing matrix effects [24]. MIP-SPME devices have been fabricated in a few common formats: fibers, stir bars and thin films coated on flat substrates. The different formats have necessitated innovations in fabrication, however, many of these methods are complicated and time-consuming, which hinder translation from research laboratories to commercial production and widespread availability of MIP-SPME. Some of challenges include device fragility (e.g., fibers), controlling mass-transfer dynamics related to reproducibly porosity and sorbent mass (e.g., the performance of MIP particles can be reduced when immobilized in adhesive materials) and establishing high selectivity through non-covalent molecular imprinting.

The fabrication of MIP-SPME devices should be fast, simple, and reproducible, and must result in a user-friendly, rugged, reusable, and mechanically- and chemically-stable device. In general, MIPs are applied in SPME-devices as MIP particles incorporated into a host or as a MIP monolith (stand-alone device or as a coating). Although MIP particles represent a great opportunity for tailorable chemistries, the demerits associated with application of particles are related to reduction in the effectiveness of hard-fought gains in molecular recognition by adding another polymer into the system and changes in partition

dynamics (e.g., surface wetting, diffusion into pores, etc.). This is a significant complication to the preparation and characterization of performance of MIP-SPME devices since the MIP is not the sole sorbent in such a configuration. In fact, most publications on particle-based MIP-SPME devices reported selectivity (i.e., IF) for the MIP particles alone without comparison to selectivity after inclusion in the device. Even the loading of the MIP particles into a host matrix is subject to a trade off between compromised coating stability at high particle loadings and low analyte capacity with low particle loading [44]. By developing devices with only the MIP to act as the sorbent, the number of factors can be reduced. This is not a trivial task, the fabrication of an ideal MIP coating in one step (i.e., one pre-polymer solution formed into a coating by a single polymerization step) must simultaneously produce high affinity binding sites and a suitably porous material compatible with the sample matrix for favourable mass transfer characteristics from a single pre-polymer solution. There are crucial equilibria that must be optimized, including formation of a stable template-monomer complex and phase separation process to controls porosity, both of which are perturbed by the composition of the pre-polymer solution (e.g., porogen, cross-linkers, etc.) and fabrication conditions (e.g., substrate, temperature, time, mode of polymerization) [131, 132]. As has been discussed, the selection of the template must also be considered particularly for applications in trace analysis. Although the perfect template is the target analyte, exhaustive template removal to eliminate the possibility of template bleed (positive bias) is difficult to attain and can impact polymer morphology [133]. Moreover, cross-reactivity toward a class of compounds is often desirable. As such we have highlighted the use of pseudo-templates (also called dummy templates) in this review but note that inferior molecular recognition is a potential outcome. Ultimately, high

selectivity can be achieved, though it requires insight into the dominant intermolecular forces to predict suitable pseudo-templates and can require extensive iterative testing and sometimes a background in organic synthesis. Although these challenges can be daunting, they represent boundless possibilities for further innovation in MIP-SPME.

### **1.7. Instrumental analyses with MIP devices**

The US-EPA has suggested that analysis of polycyclic aromatic hydrocarbons (PAHs) can be achieved using gas chromatography (GC) or liquid chromatography (LC). GC considered the best choice of chromatographic condition for analysis of volatile and thermally stable PAHs due to selectivity and the efficiency of GC separations. GC is a chromatographic technique in which gaseous analytes are transported through a column by a gaseous mobile phase called the carrier gas. Volatile liquid and gaseous samples are injected through a rubber disk (septum) into a heated port from which they are evaporated. Vaporized samples then carried to and through the column by N<sub>2</sub>, H<sub>2</sub> or He carrier gas [134].

The standard methods use GC with flame ionization detection (FID) and MS or LC coupled to UV and fluorescence detectors. These standard methods are also reported in literature for analysis of PAHs [135, 136]. LC can also be coupled with atmospheric pressure photo-ionization (APPI) as an alternate ionization source for MS analysis of PAHs [137]. In the case of GC-FID, background interferences from other carbonaceous sources may increase the noise level and therefore reduce the sensitivity. MS analyzers have more selectivity compared to FID and are more desirable in PAHs analysis.

The most common combination of GC and MS includes using GC with electron ionization (EI) with quadrupole mass analyser. EI-MS is a sensitive technique that can result in a relatively high ionization efficiency and extensive fragmentation of ions. EI provides higher sensitivity for PAHs which are hard to ionize. Chemical ionization (CI), which uses a reagent gas, is a softer ionization technique that has been reported in combination with GC. However, limitations with respect to suitable analyte classes and lower sensitivity due to use of reagent gas restricts more widespread application of CI. Atmospheric pressure chemical ionization (APCI) coupled with GC (APCI-GC) has received a lot of attention recently particularly due to development of commercial ionization sources coupled conventional MS analyzers. APCI is one of the atmospheric pressure ionization (API) techniques which has been introduced in 1973 for use with LC [138]. APCI requires low energy and favours generation of protonated and molecular ions with little fragmentation [139].

Prevailing API instrumentation uses plasma discharge from a corona pin to promote ionization under atmospheric pressure. The considerable advantage of this soft ionization technique compared to classical EI is higher abundance of molecular ions. The mechanism of ionization in APCI for GC applications is comparable to APCI in LC/MS instrument. Two ionization mechanisms are charge transfer and protonation. Protonation can be operated by using water and methanol in ionization chamber. Another benefit of APCI-GC is that there is no limitation on carrier gas flow rate in development of a GC method as the flow exits into the AP source that can accommodate much higher pressure than a typical EI source. APCI ion sources have been used for various applications such as pollutants and pesticides in environmental samples (i.e., soil, and water) [140, 141], pharmaceutical in

environmental samples (water samples) [142], pesticide [143] and contaminants [144] in food samples. In addition, triple quadrupole instrument has been applied for PAHs quantification in previous studies which can increase the sensitivity of analysis due to reduced noise level of samples in multiple reaction monitoring (MRM) experiments [145, 146].

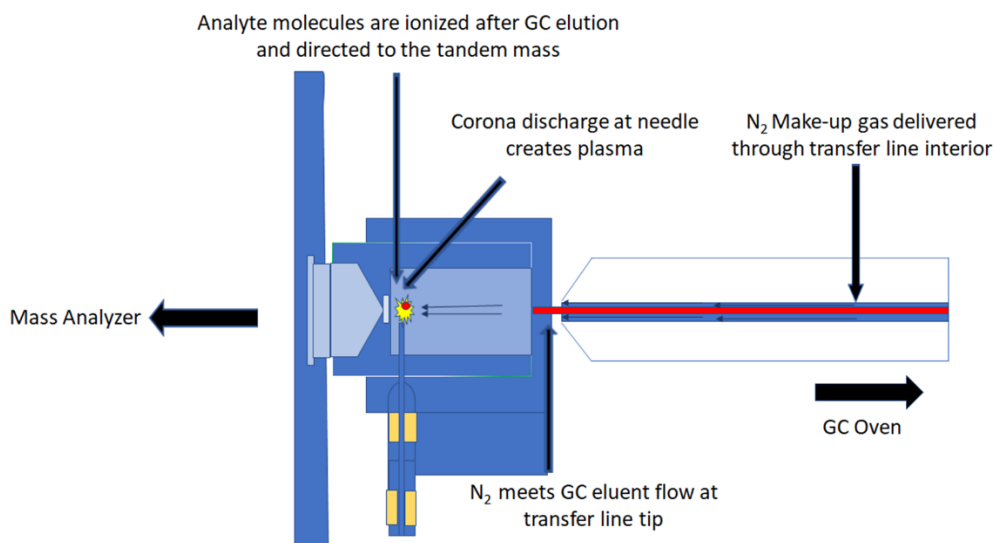


**Figure 1.12.** Cross-section diagram of APCI ion source.

Figure 1.12. shows a cutaway view of an APCI ionization/reaction chamber interfacing GC with MS. The GC and APCI source are connected via a transfer line which also provides nitrogen as makeup gas flow into the source environment. Effective parameters in ionization are corona pin position and current, as well as cone gas and axillary gas flow rates. Figure 1.13 illustrates the two primary mechanisms employed in APCI positive ionization mode. Charge transfer can take place in the absence of water and using nitrogen as a reagent gas which results in formation of molecular ions. Other reagents such as CS<sub>2</sub> and benzene can be employed to enhance charge exchange ionization. A protonation mechanism is also possible using H<sub>2</sub>O or methanol as reagents.

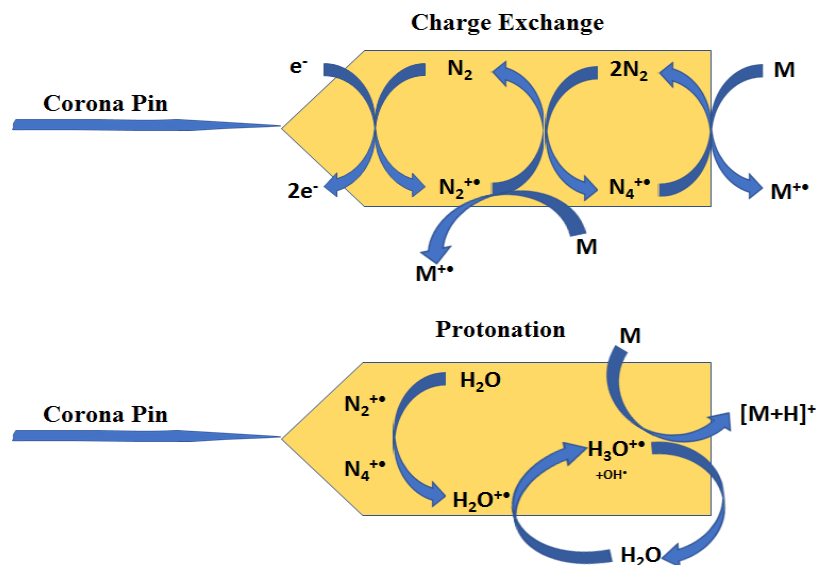


**Figure 1.13.** Ionization mechanisms in APCI-GC ion source.

Tricyclic antidepressants (TCAs) have been a target of analytical studies in many fields, such as emergency toxicology screening, forensics, and clinical pharmacology, using high performance liquid chromatography (HPLC) and high resolution gas chromatography (HRGC) [147]. However, HPLC instrumentation especially with MS has been favored because of its sensitivity, simplicity and short time of analysis relative to GC methods. The study of drugs, their metabolites, and impurities has been assisted by the introduction of electrospray ionization (ESI)-MS in 1984 [148]. The combination of HPLC and ESI-MS has been the widely and successfully used for analyzing N-containing pharmaceutical compounds like TCAs in biological matrices. A schematic representation of ESI ion source is shown in Figure 1.14. In general, a dilute analyte solution from LC is injected through a stainless-steel capillary. A high voltage (3-6 kV relative to the source sampling cone or heated capillary) is applied to the tip of the metal capillary spray needle. With the help of the coaxial sheath gas ( $N_2$ ), the strong electric field cause dispersion of

sample solution into an aerosol of highly charged droplets. Charged analytes are released from these droplets and pass through the sampling cone or the orifice of the heated capillary to the analyzer of the MS.

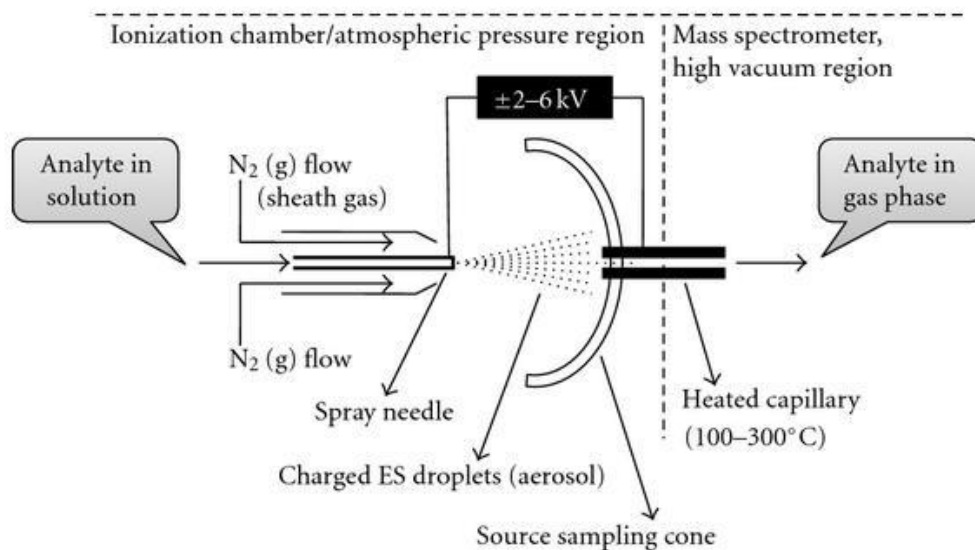


**Figure 1.14.** ESI ion source structure and mechanism [149].

In MS, analytes after ionization in proper ion source are separated based on the ratio of the mass to the charge ( $m/z$ ) of the ions in mass analyzers. One of the most common mass analyzers is quadrupole. Wolfgang Paul received the Nobel prize in 1989 for his conception of a quadrupole mass analyzer. A transmission quadrupole MS consists of four parallel metal rods that a constant voltage and a radiofrequency oscillating voltage are applied to them. Ions drift axially in a complex trajectory during migration from ion source to the detector, letting only ions with particular mass to charge ratio reach the detector. Other non- resonant ions hit the rods and are lost before reaching detector. Ions with different masses can reach the detector because of quickly altered voltage. [150]

Triple quadrupole MS (Figure 1.15), also called tandem MS, MS/MS or MS<sup>2</sup>, is a sensitive mass analysis system that can increase the signal to noise ratio via transmission methods such as selected reaction monitoring (SRM) or multiple reaction monitoring (MRM). Operationally, ionized species generated from a sample enter the first quadrupole mass filter which selects ions with particular mass (precursor or parent ions) for fragmentation. The selected ions are fragmented in second quadrupole, which is a RF-only quadrupole that can be pressurized with a collision gas. This results in collision induced dissociation (CID), a process in which ions can gain internal energy by collision with a neutral molecule [151]. The resulting fragment ions (product or daughter ions) then undergo mass analysis and detected with an electron multiplier.

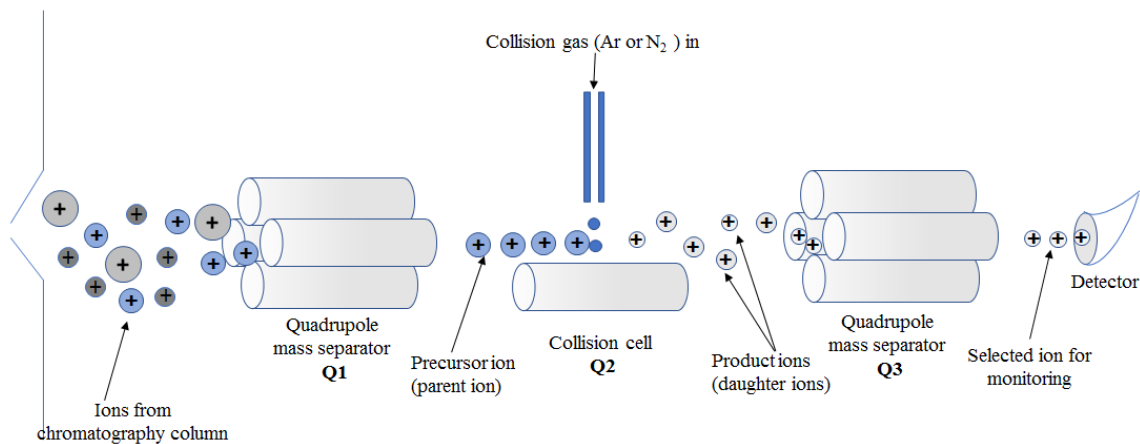


**Figure 1.15.** Fundamental mechanism of tandem mass spectrometry

## **1.8. Guidelines to validate an analytical method**

Method validation is the process of demonstrating that an analytical method is suitable for its intended use. However, the process to establish this should follow some guidelines to conform to regulations and thus be allowable for adoption by other labs.

The US EPA has several documented method validation policies and guidelines which describe general principles for determining and demonstrating that an analytical method is suitable for its aimed purpose. One of these guidelines is chemical method validation and peer review policy which is a good source for developing and validating any new analytical method, for example, for analyzing pollutants in water samples [152]. The document and its referenced guidelines described the level of detailed information about the method should be supplied, including the methods to determine limits of detection (LOD,  $3 \times$  blank standard deviation), limits of quantification (LOQ,  $10 \times$  blank standard deviation), working range, trueness, and precision ( $\pm 17\% - 20\%$ ) [153].

Development and validation of bioanalytical methods are performed base on the most recent guideline published in 2018 by US department of Health and Human services, Food and Drug administration (FDA) [154]. This guideline defines the design, operation condition, limitations, and suitability of the method for its planned use. In general, the acceptable precision in bioanalytical analysis (20 %– 25%) is higher than environmental analysis (17 %- 20%) and include more consideration in LOD, and LOQ determination. Further explanation on acceptable values is mentioned in the method validation section in the following chapters.

## 1.9. Thesis objectives

Implementation of MIP in SPME devices has been proven to have tremendous effects in reducing matrix effect, increasing the selectivity towards targeted compounds and enhancing the sensitivity of the analytical methods. Objectives of this thesis are the further assessment of the thin film-MIP SPME format which has received the least attention between researchers and the advantages that it can add to the environmental and biological samples preparation.

**Literature review to explore MIP-SPME devices pros and cons.** Chapter 1 includes a review paper about all the recent MIP-SPME devices. Different aspects of these devices such as fabrication method, composition, selectivity assessment, analytical method, performance of these devices and their validated method for analyzing real samples (environmental water, biological, and food) have been discussed. The manuscript of this review paper has been submitted to *Trends in Analytical Chemistry* (TrAC).

**Application enhancement of thin film-MIP for environmental analysis.** Analytical performance of a previously thin film-MIP used in the Bottaro group was enhanced for analyzing PAHs in water samples. Changes in the previous format such as smaller size, elimination of chemical treatment and replacing physical treatment of glass substrate, altering the extraction format and optimizing the extraction and desorption process led to a reliable, high throughput, sensitive and simple method of analysis.

**Introducing the first thin film-MIP for biological sample preparation.** Thin film-MIP devices can have an important role in reducing matrix effect in biological samples.

Additionally, these devices can facilitate the sample preparation process due to some features such as single usage and the possibility of being employed in a high throughput sample preparation process. In chapter 3 single-use thin film-MIP devices for analyzing TCAs as model compounds in human plasma samples with an optimized formula were fabricated.

**Application of thin film-MIP as microsampling devices.** In chapter 4, we took one step further in investigating the applicability of porous thin film as a device for small volume analysis and microsampling purposes. One of the disadvantages of microsampling devices is the lack of biopreservation capability. Thin film-MIP can provide biopreservation by maintaining specific interactions in the polymer structure and trapping the targeted compound. This feature makes them a perfect device for microsampling in the case of delayed analysis or archiving the extracted samples. Beside biopreservation, thin film-MIP sample preparation process after microsampling is very simple and includes a washing step which removes the co-extracted salts and leads to more reliable results in mass spectrometry analysis

## 1.10. References

- [1] Q. Zhang, L. Fan, Q. Lu, X. Yu, M. Liang, J. Nie, N. Li, L. Zhang, Preparation and application of molecularly imprinted polymer solid-phase microextraction fiber for the selective analysis of auxins in tobacco, *J. Sep. Sci.* 42(16) (2019) 2687-2695.
- [2] S. Wang, Y. Geng, X. Sun, R. Wang, Z. Zheng, S. Hou, X. Wang, W. Ji, Molecularly imprinted polymers prepared from a single cross-linking functional monomer for solid-phase microextraction of estrogens from milk, *J. Chromatogr. A* 1627 (2020) 461400.

- [3] Y. Jian, L. Chen, J. Cheng, X. Huang, L. Yan, H. Li, Molecularly imprinted polymers immobilized on graphene oxide film for monolithic fiber solid phase microextraction and ultrasensitive determination of triphenyl phosphate, *Anal. Chim. Acta* 1133 (2020) 1-10.
- [4] T. Tang, F. Wei, X. Wang, Y. Ma, Y. Song, Y. Ma, Q. Song, G. Xu, Y. Cen, Q. Hu, Determination of semicarbazide in fish by molecularly imprinted stir bar sorptive extraction coupled with high performance liquid chromatography, *J. Chromatogr. B Analyt. Technol. Biomed. Life Sci.* 1076 (2018) 8-14.
- [5] A. Azizi, F. Shahhoseini, E.A. Langille, R. Akhoondi, C.S. Bottaro, Micro-gel thin film molecularly imprinted polymer coating for extraction of organophosphorus pesticides from water and beverage samples, *Anal. Chim. Acta* 1187 (2021) 339135.
- [6] S. Knoll, T. Rösch, C. Huhn, Trends in sample preparation and separation methods for the analysis of very polar and ionic compounds in environmental water and biota samples, *Anal. Bioanal. Chem.* 412 (2020) 6149–6165.
- [7] K.E. Murray, S.M. Thomas, A.A. Bodour, Prioritizing research for trace pollutants and emerging contaminants in the freshwater environment, *Environ. Pollut.* 158(12) (2010) 3462-3471.
- [8] M.A. Farajzadeh, A. Yadeghari, L. Khoshmaram, Combination of dispersive solid phase extraction and dispersive liquid–liquid microextraction for extraction of some aryloxy pesticides prior to their determination by gas chromatography, *Microchem. J.* 131 (2017) 182-191.
- [9] V. Jalili, A. Barkhordari, A. Ghiasvand, Bioanalytical applications of microextraction techniques: a review of reviews, *Chromatographia* 83(5) (2020) 567-577.
- [10] C.L. Arthur, J. Pawliszyn, Solid phase microextraction with thermal desorption using fused silica optical fibers, *Anal. Chem.* 62(19) (1990) 2145-2148.
- [11] V. Jalili, A. Barkhordari, A. Ghiasvand, A comprehensive look at solid-phase microextraction technique: A review of reviews, *Microchem. J.* 152 (2020) 104319.
- [12] G. Ouyang, J. Pawliszyn, A critical review in calibration methods for solid-phase microextraction, *Anal. Chim. Acta* 627(2) (2008) 184-97.
- [13] R. Jiang, J. Pawliszyn, Thin-film microextraction offers another geometry for solid-phase microextraction, *TrAC, Trends Anal. Chem.* 39 (2012) 245-253.
- [14] X.R. Xia, R.B. Leidy, Preparation and characterization of porous silica-coated multifibers for solid-phase microextraction, *Anal. Chem.* 73(9) (2001) 2041-7.

- [15] E. Baltussen, P. Sandra, F. David, C. Cramers, Stir bar sorptive extraction (SBSE), a novel extraction technique for aqueous samples: Theory and principles, *Journal of Microcolumn Separations* 11(10) (1999) 737-747.
- [16] I. Bruheim, X. Liu, J. Pawliszyn, Thin-film microextraction, *Anal. Chem.* 75(4) (2003) 1002-10.
- [17] M. Lashgari, Y. Yamini, An overview of the most common lab-made coating materials in solid phase microextraction, *Talanta* 191 (2019) 283-306.
- [18] H. Piri-Moghadam, M.N. Alam, J. Pawliszyn, Review of geometries and coating materials in solid phase microextraction: Opportunities, limitations, and future perspectives, *Anal. Chim. Acta* 984 (2017) 42-65.
- [19] A. Azizi, C.S. Bottaro, A critical review of molecularly imprinted polymers for the analysis of organic pollutants in environmental water samples, *J. Chromatogr. A* 1614 (2020) 460603.
- [20] V. Pichon, N. Delaunay, A. Combès, Sample preparation using molecularly imprinted polymers, *Anal. Chem.* 92(1) (2019) 16-33.
- [21] H. Santos, R.O. Martins, D.A. Soares, A.R. Chaves, Molecularly imprinted polymers for miniaturized sample preparation techniques: strategies for chromatographic and mass spectrometry methods, *Anal. Methods* 12(7) (2020) 894-911.
- [22] A. Sarafraz-Yazdi, N. Razavi, Application of molecularly-imprinted polymers in solid-phase microextraction techniques, *TrAC, Trends Anal. Chem.* 73 (2015) 81-90.
- [23] S. Ansari, M. Karimi, Recent progress, challenges and trends in trace determination of drug analysis using molecularly imprinted solid-phase microextraction technology, *Talanta* 164 (2017) 612-625.
- [24] E. Turiel, A. Martín-Esteban, Molecularly imprinted polymers-based microextraction techniques, *TrAC, Trends Anal. Chem.* 118 (2019) 574-586.
- [25] H. Prosen, L. Zupančič-Kralj, Solid-phase microextraction, *TrAC, Trends Anal. Chem.* 18(4) (1999) 272-282.
- [26] N. Reyes-Garces, E. Gionfriddo, G.A. Gomez-Rios, M.N. Alam, E. Boyaci, B. Bojko, V. Singh, J. Grandy, J. Pawliszyn, Advances in Solid Phase Microextraction and Perspective on Future Directions, *Anal. Chem.* 90(1) (2018) 302-360.
- [27] H. Lord, J. Pawliszyn, Evolution of solid-phase microextraction technology, *J. Chromatogr. A* 885(1-2) (2000) 153-93.

- [28] L. Pauling, A theory of the structure and process of formation of antibodies, *J. Am. Chem. Soc.* 62(10) (1940) 2643-2657.
- [29] T. Cowen, E. Stefanucci, E. Piletska, G. Marrazza, F. Canfarotta, S.A. Piletsky, Synthetic mechanism of molecular imprinting at the solid phase, *Macromolecules* 53(4) (2020) 1435-1442.
- [30] H. Yan, K.H. Row, Characteristic and synthetic approach of molecularly imprinted polymer, *Int. J. Mol. Sci.* 7(5) (2006) 155-178.
- [31] C. Alexander, H.S. Andersson, L.I. Andersson, R.J. Ansell, N. Kirsch, I.A. Nicholls, J. O'Mahony, M.J. Whitcombe, Molecular imprinting science and technology: a survey of the literature for the years up to and including 2003, *J. Mol. Recognit.* 19(2) (2006) 106-80.
- [32] L. Chen, S. Xu, J. Li, Recent advances in molecular imprinting technology: current status, challenges and highlighted applications, *Chem. Soc. Rev.* 40(5) (2011) 2922-42.
- [33] J.E. Lofgreen, G.A. Ozin, Controlling morphology and porosity to improve performance of molecularly imprinted sol-gel silica, *Chem. Soc. Rev.* 43(3) (2014) 911-933.
- [34] L. Chen, X. Wang, W. Lu, X. Wu, J. Li, Molecular imprinting: perspectives and applications, *Chem. Soc. Rev.* 45(8) (2016) 2137-211.
- [35] A. Speltini, A. Scalabrini, F. Maraschi, M. Sturini, A. Profumo, Newest applications of molecularly imprinted polymers for extraction of contaminants from environmental and food matrices: A review, *Anal. Chim. Acta* 974 (2017) 1-26.
- [36] A.N. Hasanah, N. Safitri, A. Zulfa, N. Neli, D. Rahayu, Factors Affecting Preparation of Molecularly Imprinted Polymer and Methods on Finding Template-Monomer Interaction as the Key of Selective Properties of the Materials, *Molecules* 26(18) (2021) 5612.
- [37] I.S. Ibarra, J.M. Miranda, I. Perez-Silva, C. Jardinez, G. Islas, Sample treatment based on molecularly imprinted polymers for the analysis of veterinary drugs in food samples: a review, *Anal. Methods* 12(23) (2020) 2958-2977.
- [38] A. Mueller, A note about crosslinking density in imprinting polymerization, *Molecules* 26(17) (2021) 5139.
- [39] D.A. Spivak, Optimization, evaluation, and characterization of molecularly imprinted polymers, *Adv Drug Deliv Rev* 57(12) (2005) 1779-94.
- [40] M.R. Gama, C.B. Bottoli, Molecularly imprinted polymers for bioanalytical sample preparation, *J. Chromatogr. B Analyt. Technol. Biomed. Life Sci.* 1043 (2017) 107-121.

- [41] F. Meier, B. Schott, D. Riedel, B. Mizaikoff, Computational and experimental study on the influence of the porogen on the selectivity of 4-nitrophenol molecularly imprinted polymers, *Anal. Chim. Acta* 744 (2012) 68-74.
- [42] L. Wu, K. Zhu, M. Zhao, Y. Li, Theoretical and experimental study of nicotinamide molecularly imprinted polymers with different porogens, *Anal. Chim. Acta* 549(1-2) (2005) 39-44.
- [43] J. Yao, L. Zhang, J. Ran, S. Wang, N. Dong, Specific recognition of cationic paraquat in environmental water and vegetable samples by molecularly imprinted stir-bar sorptive extraction based on monohydroxylcucurbit [7] uril–paraquat inclusion complex, *Microchim. Acta* 187(10) (2020) 1-10.
- [44] H. Shaikh, N. Memon, M.I. Bhangar, S.M. Nizamani, A. Denizli, Core–shell molecularly imprinted polymer-based solid-phase microextraction fiber for ultra trace analysis of endosulfan I and II in real aqueous matrix through gas chromatography–micro electron capture detector, *J. Chromatogr. A* 1337 (2014) 179-187.
- [45] R. Mirzajani, F. Kardani, Fabrication of ciprofloxacin molecular imprinted polymer coating on a stainless steel wire as a selective solid-phase microextraction fiber for sensitive determination of fluoroquinolones in biological fluids and tablet formulation using HPLC-UV detection, *J. Pharm. Biomed. Anal.* 122 (2016) 98-109.
- [46] R.J. Umpleby II, S.C. Baxter, A.M. Rampey, G.T. Rushton, Y. Chen, K.D. Shimizu, Characterization of the heterogeneous binding site affinity distributions in molecularly imprinted polymers, *J. Chromatogr. B* 804(1) (2004) 141-149.
- [47] R.J. Umpleby, 2nd, S.C. Baxter, Y. Chen, R.N. Shah, K.D. Shimizu, Characterization of molecularly imprinted polymers with the Langmuir-Freundlich isotherm, *Anal. Chem.* 73(19) (2001) 4584-91.
- [48] E.N. Ndunda, Molecularly imprinted polymers—A closer look at the control polymer used in determining the imprinting effect: A mini review, *J. Mol. Recognit.* 33(11) (2020) e2855.
- [49] S. Dai, M.C. Burleigh, Y. Shin, C.C. Morrow, C.E. Barnes, Z. Xue, Imprint Coating: A Novel Synthesis of Selective Functionalized Ordered Mesoporous Sorbents, *Angew. Chem. Int. Ed. Engl.* 38(9) (1999) 1235-1239.
- [50] Y. Liu, Y. Liu, Z. Liu, X. Zhao, J. Wei, H. Liu, X. Si, Z. Xu, Z. Cai, Chiral molecularly imprinted polymeric stir bar sorptive extraction for naproxen enantiomer detection in PPCPs, *J. Hazard. Mater.* 392 (2020) 122251.
- [51] Y. Yuan, X. Yuan, Q. Hang, R. Zheng, L. Lin, L. Zhao, Z. Xiong, Dummy molecularly imprinted membranes based on an eco-friendly synthesis approach for

- recognition and extraction of enrofloxacin and ciprofloxacin in egg samples, *J. Chromatogr. A* 1653 (2021) 462411.
- [52] W.H.J. Vaes, E. Urrestarazu Ramos, H.J.M. Verhaar, W. Seinen, J.L.M. Hermens, Measurement of the free concentration using solid-phase microextraction: Binding to protein, *Anal. Chem.* 68(24) (1996) 4463-4467.
- [53] J. Xu, S. Huang, S. Wei, M. Yang, C. Cao, R. Jiang, F. Zhu, G. Ouyang, Study on the Diffusion-Dominated Solid-Phase Microextraction Kinetics in Semisolid Sample Matrix, *Anal. Chem.* 88(18) (2016) 8921-8925.
- [54] L.C. de Carvalho Abrão, E.C. Figueiredo, A new restricted access molecularly imprinted fiber for direct solid phase microextraction of benzodiazepines from plasma samples, *Analyst* 144(14) (2019) 4320-4330.
- [55] Y. Liu, Y. Liu, Z. Liu, X. Hu, Z. Xu, beta-Cyclodextrin molecularly imprinted solid-phase microextraction coatings for selective recognition of polychlorophenols in water samples, *Anal. Bioanal. Chem.* 410(2) (2018) 509-519.
- [56] L. Chen, X. Huang, Preparation and application of a poly (ionic liquid)-based molecularly imprinted polymer for multiple monolithic fiber solid-phase microextraction of phenolic acids in fruit juice and beer samples, *Analyst* 142(21) (2017) 4039-4047.
- [57] X. Yang, T. Muhammad, J. Yang, A. Yasen, L. Chen, In-situ kinetic and thermodynamic study of 2, 4-dichlorophenoxyacetic acid adsorption on molecularly imprinted polymer based solid-phase microextraction coatings, *Sens. Actuators A Phys.* 313 (2020) 112190.
- [58] H. Lan, N. Gan, D. Pan, F. Hu, T. Li, N. Long, L. Qiao, An automated solid-phase microextraction method based on magnetic molecularly imprinted polymer as fiber coating for detection of trace estrogens in milk powder, *J. Chromatogr. A* 1331 (2014) 10-18.
- [59] X. Hu, Y. Fan, Y. Zhang, G. Dai, Q. Cai, Y. Cao, C. Guo, Molecularly imprinted polymer coated solid-phase microextraction fiber prepared by surface reversible addition-fragmentation chain transfer polymerization for monitoring of Sudan dyes in chilli tomato sauce and chilli pepper samples, *Anal. Chim. Acta* 731 (2012) 40-48.
- [60] R. Koeber, C. Fleischer, F. Lanza, K.-S. Boos, B. Sellergren, D. Barceló, Evaluation of a multidimensional solid-phase extraction platform for highly selective on-line cleanup and high-throughput LC-MS analysis of triazines in river water samples using molecularly imprinted polymers, *Anal. Chem.* 73(11) (2001) 2437-2444.
- [61] D.D. Wang, D. Gao, Y.K. Huang, W.J. Xu, Z.N. Xia, Preparation of restricted access molecularly imprinted polymers based fiber for selective solid-phase microextraction of hesperetin and its metabolites in vivo, *Talanta* 202 (2019) 392-401.

- [62] E.H. Koster, C. Crescenzi, W. den Hoedt, K. Ensing, G.J. de Jong, Fibers coated with molecularly imprinted polymers for solid-phase microextraction, *Anal. Chem.* 73(13) (2001) 3140-5.
- [63] X. Hu, J. Pan, Y. Hu, Y. Huo, G. Li, Preparation and evaluation of solid-phase microextraction fiber based on molecularly imprinted polymers for trace analysis of tetracyclines in complicated samples, *J. Chromatogr. A* 1188(2) (2008) 97-107.
- [64] X. Hu, G. Dai, J. Huang, T. Ye, H. Fan, T. Youwen, Y. Yu, Y. Liang, Molecularly imprinted polymer coated on stainless steel fiber for solid-phase microextraction of chloroacetanilide herbicides in soybean and corn, *J. Chromatogr. A* 1217(38) (2010) 5875-82.
- [65] Y. Lu, L. Lu, J. He, T. Zhao, Preparation of hydrophilic molecularly imprinted solid-phase microextraction fiber for the selective removal and extraction of trace tetracyclines residues in animal derived foods, *J. Sep. Sci.* 43(11) (2020) 2172-2179.
- [66] A. Kumar, A.K. Malik, D.K. Tewary, B. Singh, A review on development of solid phase microextraction fibers by sol-gel methods and their applications, *Anal. Chim. Acta* 610(1) (2008) 1-14.
- [67] A. Amiri, Solid-phase microextraction-based sol-gel technique, *TrAC, Trends Anal. Chem.* 75 (2016) 57-74.
- [68] Y.-L. Wang, Y.-L. Gao, P.-P. Wang, H. Shang, S.-Y. Pan, X.-J. Li, Sol-gel molecularly imprinted polymer for selective solid phase microextraction of organophosphorous pesticides, *Talanta* 115 (2013) 920-927.
- [69] J.W. Li, Y.L. Wang, S. Yan, X.J. Li, S.Y. Pan, Molecularly imprinted calixarene fiber for solid-phase microextraction of four organophosphorous pesticides in fruits, *Food Chem.* 192 (2016) 260-7.
- [70] M. Rahimi, S. Bahar, R. Heydari, S.M. Amininasab, Determination of quercetin using a molecularly imprinted polymer as solid-phase microextraction sorbent and high-performance liquid chromatography, *Microchem. J.* 148 (2019) 433-441.
- [71] M. Saraji, N. Mehrafza, A simple approach for the preparation of simazine molecularly imprinted nanofibers via self-polycondensation for selective solid-phase microextraction, *Anal. Chim. Acta* 936 (2016) 108-15.
- [72] N.P. Kalogiouri, A. Tsalbouris, A. Kabir, K.G. Furton, V.F. Samanidou, Synthesis and application of molecularly imprinted polymers using sol-gel matrix imprinting technology for the efficient solid-phase extraction of BPA from water, *Microchem. J.* 157 (2020) 104965.

- [73] M.M. Moein, A. Abdel-Rehim, M. Abdel-Rehim, Recent Applications of Molecularly Imprinted Sol-Gel Methodology in Sample Preparation, *Molecules* 24(16) (2019) 2889.
- [74] S. Dowlatshah, M. Saraji, A silica-based three-dimensional molecularly imprinted coating for the selective solid-phase microextraction of difenoconazole from wheat and fruits samples, *Anal. Chim. Acta* 1098 (2020) 37-46.
- [75] A.M. Shearrow, S. Bhansali, A. Malik, Ionic liquid-mediated bis [(3-methyldimethoxysilyl) propyl] polypropylene oxide-based polar sol-gel coatings for capillary microextraction, *J. Chromatogr. A* 1216(36) (2009) 6349-6355.
- [76] X. Xiang, Y. Wang, X. Zhang, M. Huang, X. Li, S. Pan, Multifiber solid-phase microextraction using different molecularly imprinted coatings for simultaneous selective extraction and sensitive determination of organophosphorus pesticides, *J. Sep. Sci.* 43(4) (2020) 756-765.
- [77] E. Caro, N. Masque, R.M. Marce, F. Borrull, P.A. Cormack, D.C. Sherrington, Non-covalent and semi-covalent molecularly imprinted polymers for selective on-line solid-phase extraction of 4-nitrophenol from water samples, *J. Chromatogr. A* 963(1-2) (2002) 169-78.
- [78] D. Wang, Y. Liu, Z. Xu, D. Zhao, Y. Liu, Z. Liu, Multitemplate molecularly imprinted polymeric solid-phase microextraction fiber coupled with HPLC for endocrine disruptor analysis in water samples, *Microchem. J.* 155 (2020) 104802.
- [79] Y. Liu, Y. Liu, Z. Liu, F. Du, G. Qin, G. Li, X. Hu, Z. Xu, Z. Cai, Supramolecularly imprinted polymeric solid phase microextraction coatings for synergetic recognition nitrophenols and bisphenol A, *J. Hazard. Mater.* 368 (2019) 358-364.
- [80] T. Zhao, X. Guan, W. Tang, Y. Ma, H. Zhang, Preparation of temperature sensitive molecularly imprinted polymer for solid-phase microextraction coatings on stainless steel fiber to measure ofloxacin, *Anal. Chim. Acta* 853 (2015) 668-675.
- [81] T.V. Mendes, M.A. Rosa, E.C. de Figueiredo, Restricted Access Molecularly Imprinted Polymers for Biological Sample Preparation, *Braz. J. Anal. Chem.* 9(35) (2021).
- [82] D. Djozan, B. Ebrahimi, M. Mahkam, M.A. Farajzadeh, Evaluation of a new method for chemical coating of aluminum wire with molecularly imprinted polymer layer. Application for the fabrication of triazines selective solid-phase microextraction fiber, *Anal. Chim. Acta* 674(1) (2010) 40-8.
- [83] M. Piryaeei, H. Nazemiyeh, Preconcentration of digoxin using a synthetic imprinted polymer deposited upon the surface of double-layered hydroxides on porous anodised

aluminium wire a triple solid-phase microextraction fibre, *Phytochem. Anal. Spectrochimica Acta Part A: Molecular Spectroscopy* 31 (2020) 636–642.

[84] M. Demirkurt, Y.A. Olcer, M.M. Demir, A.E. Eroglu, Electrospun polystyrene fibers knitted around imprinted acrylate microspheres as sorbent for paraben derivatives, *Anal. Chim. Acta* 1014 (2018) 1-9.

[85] V. Mohammadi, M. Saraji, M.T. Jafari, Direct molecular imprinting technique to synthesize coated electrospun nanofibers for selective solid-phase microextraction of chlorpyrifos, *Mikrochim. Acta* 186(8) (2019) 524.

[86] H. Hashemi-Moghaddam, S. Maddah, Coating of optical fiber with a smart thermosensitive polymer for the separation of phthalate esters by solid-phase microextraction, *J. Sep. Sci.* 41(4) (2018) 886-892.

[87] D. Wang, Z. Xu, Y. Liu, Y. Liu, G. Li, X. Si, T. Lin, H. Liu, Z. Liu, Molecularly imprinted polymer-based fiber array extraction of eight estrogens from environmental water samples prior to high-performance liquid chromatography analysis, *Microchem. J.* 159 (2020) 105376.

[88] W. Xue, N. Li, Z. Zhang, G. Li, Dummy template based molecularly imprinted solid-phase microextraction coating for analysis of trace disinfection by-product of 2,6-dichloro-1,4-benzoquinone using high-performance liquid chromatography, *Talanta* 239 (2022) 123065.

[89] L. Chen, Y. Jian, J. Cheng, L. Yan, X. Huang, Preparation and application of graphene oxide-based surface molecularly imprinted polymer for monolithic fiber array solid phase microextraction of organophosphate flame retardants in environmental water, *J. Chromatogr. A* 1623 (2020) 461200.

[90] C. Cai, P. Zhang, J. Deng, H. Zhou, J. Cheng, Ultrasensitive determination of highly polar trimethyl phosphate in environmental water by molecularly imprinted polymeric fiber headspace solid-phase microextraction, *J. Sep. Sci.* 41(5) (2018) 1104-1111.

[91] Y. Jian, J. Deng, H. Zhou, J. Cheng, Fabrication of graphene oxide incorporated polymer monolithic fiber as solid phase microextraction device for determination of organophosphate esters in soil samples, *J. Chromatogr. A* 1588 (2019) 17-24.

[92] E. Turiel, J.L. Tadeo, A. Martin-Esteban, Molecularly imprinted polymeric fibers for solid-phase microextraction, *Anal. Chem.* 79(8) (2007) 3099-104.

[93] D. Djozan, T. Baheri, Preparation and evaluation of solid-phase microextraction fibers based on monolithic molecularly imprinted polymers for selective extraction of diacetylmorphine and analogous compounds, *J. Chromatogr. A* 1166(1-2) (2007) 16-23.

- [94] S. Xu, X. Zhang, Y. Sun, D. Yu, Microwave-assisted preparation of monolithic molecularly imprinted polymeric fibers for solid phase microextraction, *Analyst* 138(10) (2013) 2982-7.
- [95] G. de Oliveira Isac Moraes, L.M. da Silva, A.J. dos Santos-Neto, F.H. Florenzano, E.C. Figueiredo, A new restricted access molecularly imprinted polymer capped with albumin for direct extraction of drugs from biological matrices: the case of chlorpromazine in human plasma, *Anal. Bioanal. Chem.* 405(24) (2013) 7687-96.
- [96] J.K. Ma, X.C. Huang, S.L. Wei, Preparation and application of chlorpyrifos molecularly imprinted solid-phase microextraction probes for the residual determination of organophosphorous pesticides in fresh and dry foods, *J. Sep. Sci.* 41(15) (2018) 3152-3162.
- [97] Z. Luo, G. Chen, X. Li, L. Wang, H. Shu, X. Cui, C. Chang, A. Zeng, Q. Fu, Molecularly imprinted polymer solid-phase microextraction coupled with ultra high performance liquid chromatography and tandem mass spectrometry for rapid analysis of pyrrolizidine alkaloids in herbal medicine, *J. Sep. Sci.* 42(21) (2019) 3352-3362.
- [98] R. Mirzajani, F. Kardani, Z. Ramezani, A nanocomposite consisting of graphene oxide, zeolite imidazolate framework 8, and a molecularly imprinted polymer for (multiple) fiber solid phase microextraction of sterol and steroid hormones prior to their quantitation by HPLC, *Microchim. Acta* 186(3) (2019) 129.
- [99] R. Zakerian, S. Bahar, Molecularly imprinted based solid phase microextraction method for monitoring valproic acid in human serum and pharmaceutical formulations, *J. Iran. Chem. Soc.* 16(4) (2019) 741-745.
- [100] X. Zhu, J. Cai, J. Yang, Q. Su, Y. Gao, Films coated with molecular imprinted polymers for the selective stir bar sorption extraction of monocrotophos, *J. Chromatogr. A* 1131(1-2) (2006) 37-44.
- [101] F. David, N. Ochiai, P. Sandra, Two decades of stir bar sorptive extraction: A retrospective and future outlook, *TrAC, Trends Anal. Chem.* 112 (2019) 102-111.
- [102] C.K. Hasan, A. Ghiasvand, T.W. Lewis, P.N. Nesterenko, B. Paull, Recent advances in stir-bar sorptive extraction: Coatings, technical improvements, and applications, *Anal. Chim. Acta* 1139 (2020) 222-240.
- [103] M. He, Y. Wang, Q. Zhang, L. Zang, B. Chen, B. Hu, Stir bar sorptive extraction and its application, *J. Chromatogr. A* 1637 (2021) 461810.
- [104] S.H. Hashemi, M. Kaykhaii, F. Tabehzar, Molecularly imprinted stir bar sorptive extraction coupled with high-performance liquid chromatography for trace analysis of naphthalene sulfonates in seawater, *J. Iran. Chem. Soc.* 13(4) (2016) 733-741.

- [105] Y. Lei, G. Xu, F. Wei, J. Yang, Q. Hu, Preparation of a stir bar coated with molecularly imprinted polymer and its application in analysis of dopamine in urine, *J. Pharm. Biomed. Anal.* 94 (2014) 118-24.
- [106] L. Zhu, G. Xu, F. Wei, J. Yang, Q. Hu, Determination of melamine in powdered milk by molecularly imprinted stir bar sorptive extraction coupled with HPLC, *J. Colloid Interface Sci.* 454 (2015) 8-13.
- [107] X. Chen, F. Wu, J. Tang, K. Yang, Y. Ma, J. Pan, Anisotropic emulsion constructed boronate affinity imprinted Janus nanosheets for stir bar sorptive extraction of cis-diol-containing catechol, *Chem. Eng. J.* 395 (2020) 124995.
- [108] W. Fan, M. Gao, M. He, B. Chen, B. Hu, Cyromazine imprinted polymers for selective stir bar sorptive extraction of melamine in animal feed and milk samples, *Analyst* 140(12) (2015) 4057-67.
- [109] W. Fan, M. He, L. You, X. Zhu, B. Chen, B. Hu, Water-compatible graphene oxide/molecularly imprinted polymer coated stir bar sorptive extraction of propranolol from urine samples followed by high performance liquid chromatography-ultraviolet detection, *J. Chromatogr. A* 1443 (2016) 1-9.
- [110] Z. Liu, Z. Xu, Y. Liu, Y. Liu, B. Lu, L. Ma, Supramolecular imprinted polymeric stir bar sorptive extraction followed by high-performance liquid chromatography for endocrine disruptor compounds analysis, *Microchem. J.* 158 (2020) 105163.
- [111] M. Díaz-Álvarez, E. Turiel, A. Martín-Esteban, Molecularly imprinted polymer monolith containing magnetic nanoparticles for the stir-bar sorptive extraction of triazines from environmental soil samples, *J. Chromatogr. A* 1469 (2016) 1-7.
- [112] M. Díaz-Álvarez, E. Turiel, A. Martín-Esteban, Molecularly imprinted polymer monolith containing magnetic nanoparticles for the stir-bar sorptive extraction of thiabendazole and carbendazim from orange samples, *Anal. Chim. Acta* 1045 (2019) 117-122.
- [113] M. Díaz-Bao, P. Regal, R. Barreiro, C.A. Fente, A. Cepeda, A facile method for the fabrication of magnetic molecularly imprinted stir-bars: A practical example with aflatoxins in baby foods, *J. Chromatogr. A* 1471 (2016) 51-59.
- [114] Y. Cui, L. Jiang, H. Li, D. Meng, Y. Chen, L. Ding, Y. Xu, Molecularly imprinted electrospun nanofibre membrane assisted stir bar sorptive extraction for trace analysis of sulfonamides from animal feeds, *J. Ind. Eng. Chem.* 96 (2021) 382-389.
- [115] R. Afsharipour, S. Dadfarnia, A.M.H. Shabani, E. Kazemi, Design of a pseudo stir bar sorptive extraction using graphenized pencil lead as the base of the molecularly imprinted polymer for extraction of nabumetone, *Spectrochim. Acta, Pt. A: Mol. Biomol. Spectrosc.* 238 (2020) 118427.

- [116] S.H. Hashemi, F. Najari, Response surface methodology of pre-concentration of chlorophenols from seawater samples by molecularly imprinted stir bar sorptive extraction combined with HPLC: Box–Behnken design, *J. Chromatogr. Sci.* 57(3) (2019) 279-289.
- [117] S.H. Hashemi, M. Kaykhaii, F. Tabehzar, Spectrophotometric determination of four naphthalene sulfonates in seawater after their molecularly imprinted stir bar sorptive extraction, *J. Chil. Chem. Soc.* 63(3) (2018) 4057-4063.
- [118] S.H. Hashemi, Z. Monfaredzadeh, Molecularly imprinted stir bar sorptive extraction coupled with high-performance liquid chromatography for trace analysis of diclofenac in different real samples, *Iran. J. Chem. Chem. Eng.* 38(1) (2019) 173-183.
- [119] B. Fresco-Cala, S. Cardenas, Facile preparation of carbon nanotube-based molecularly imprinted monolithic stirred unit, *Anal. Bioanal. Chem.* 412(24) (2020) 6341-6349.
- [120] Y.A. Olcer, M. Tascon, A.E. Eroglu, E. Boyacı, Thin film microextraction: Towards faster and more sensitive microextraction, *TrAC, Trends Anal. Chem.* 113 (2019) 93-101.
- [121] D.R. Kryscio, N.A. Peppas, Surface imprinted thin polymer film systems with selective recognition for bovine serum albumin, *Anal. Chim. Acta* 718 (2012) 109-15.
- [122] G. Van Biesen, J.M. Wiseman, J. Li, C.S. Bottaro, Desorption electrospray ionization-mass spectrometry for the detection of analytes extracted by thin-film molecularly imprinted polymers, *Analyst* 135(9) (2010) 2237-40.
- [123] A.O. Gryshchenko, C.S. Bottaro, Development of molecularly imprinted polymer in porous film format for binding of phenol and alkylphenols from water, *Int. J. Mol. Sci.* 15(1) (2014) 1338-57.
- [124] G.F. Abu-Alsoud, C.S. Bottaro, Porous thin-film molecularly imprinted polymer device for simultaneous determination of phenol, alkylphenol and chlorophenol compounds in water, *Talanta* 223(Pt 2) (2021) 121727.
- [125] H.Y. Hijazi, C.S. Bottaro, Molecularly imprinted polymer thin-film as a micro-extraction adsorbent for selective determination of trace concentrations of polycyclic aromatic sulfur heterocycles in seawater, *J. Chromatogr. A* 1617 (2020) 460824.
- [126] N. Yazdaniyan, B. Akbari-Adergani, M. Kazemipour, H.A. Panahi, M. Javanbakht, Improving the determination of celecoxib in body fluids and pharmaceuticals using a new selective and thermosensitive molecularly imprinted poly (vinylidene fluoride) membrane, *Anal. Methods* 12(16) (2020) 2185-2195.
- [127] J.Å. Jönsson, L. Mathiasson, Membrane-based techniques for sample enrichment, *J. Chromatogr. A* 902(1) (2000) 205-225.

- [128] F. Shahhoseini, E.A. Langille, A. Azizi, C.S. Bottaro, Thin film molecularly imprinted polymer (TF-MIP), a selective and single-use extraction device for high-throughput analysis of biological samples, *Analyst* 146(10) (2021) 3157-3168.
- [129] H.Y. Hijazi, C.S. Bottaro, Selective determination of semi-volatile thiophene compounds in water by molecularly imprinted polymer thin films with direct headspace gas chromatography sulfur chemiluminescence detection, *Analyst* 143(5) (2018) 1117-1123.
- [130] N. Nuchtavorn, M. Dvorak, P. Kuban, Paper-based molecularly imprinted-interpenetrating polymer network for on-spot collection and microextraction of dried blood spots for capillary electrophoresis determination of carbamazepine, *Anal. Bioanal. Chem.* 412(12) (2020) 2721-2730.
- [131] X. Song, S. Xu, L. Chen, Y. Wei, H. Xiong, Recent advances in molecularly imprinted polymers in food analysis, *J. Appl. Polym. Sci.* 131(16) (2014).
- [132] S. Ansari, S. Masoum, Ultrasound-assisted dispersive solid-phase microextraction of capecitabine by multi-stimuli responsive molecularly imprinted polymer modified with chitosan nanoparticles followed by HPLC analysis, *Mikrochim. Acta* 187(6) (2020) 366.
- [133] F.G. Tamayo, E. Turiel, A. Martin-Esteban, Molecularly imprinted polymers for solid-phase extraction and solid-phase microextraction: recent developments and future trends, *J. Chromatogr. A* 1152(1-2) (2007) 32-40.
- [134] D.C. Harris, *Quantitative chemical analysis*, Macmillan 2010.
- [135] A. Amiri, F. Ghaemi, Graphene grown on stainless steel mesh as a highly efficient sorbent for sorptive microextraction of polycyclic aromatic hydrocarbons from water samples, *Analytica chimica acta* 994 (2017) 29-37.
- [136] H. Wang, X. Zhao, W. Meng, P. Wang, F. Wu, Z. Tang, X. Han, J.P. Giesy, Cetyltrimethylammonium bromide-coated Fe<sub>3</sub>O<sub>4</sub> magnetic nanoparticles for analysis of 15 trace polycyclic aromatic hydrocarbons in aquatic environments by ultraperformance, liquid chromatography with fluorescence detection, *Analytical chemistry* 87(15) (2015) 7667-7675.
- [137] S.-C.C. Lung, C.-H. Liu, Fast analysis of 29 polycyclic aromatic hydrocarbons (PAHs) and nitro-PAHs with ultra-high performance liquid chromatography-atmospheric pressure photoionization-tandem mass spectrometry, *Scientific reports* 5 (2015) 12992.
- [138] E.C. Horning, M.G. Horning, D.I. Carroll, I. Dzidic, R.N. Stillwell, New picogram detection system based on a mass spectrometer with an external ionization source at atmospheric pressure, *Analytical Chemistry* 45(6) (1973) 936-943.

- [139] J. Fang, H. Zhao, Y. Zhang, M. Lu, Z. Cai, Atmospheric pressure chemical ionization in gas chromatography-mass spectrometry for the analysis of persistent organic pollutants, *Trends in Environmental Analytical Chemistry* 25 (2020) e00076.
- [140] K.L. Organtini, L. Haimovici, K.J. Jobst, E.J. Reiner, A. Ladak, D. Stevens, J.W. Cochran, F.L. Dorman, Comparison of atmospheric pressure ionization gas chromatography-triple quadrupole mass spectrometry to traditional high-resolution mass spectrometry for the identification and quantification of halogenated dioxins and furans, *Analytical chemistry* 87(15) (2015) 7902-7908.
- [141] M.G. Pintado-Herrera, E. González-Mazo, P.A. Lara-Martín, Atmospheric pressure gas chromatography–time-of-flight-mass spectrometry (APGC–ToF-MS) for the determination of regulated and emerging contaminants in aqueous samples after stir bar sorptive extraction (SBSE), *Analytica chimica acta* 851 (2014) 1-13.
- [142] T. Bristow, M. Harrison, M. Sims, The application of gas chromatography/atmospheric pressure chemical ionisation time-of-flight mass spectrometry to impurity identification in Pharmaceutical Development, *Rapid Communications in Mass Spectrometry* 24(11) (2010) 1673-1681.
- [143] M.I. Cervera, T. Portolés, F.J. López, J. Beltrán, F. Hernández, Screening and quantification of pesticide residues in fruits and vegetables making use of gas chromatography–quadrupole time-of-flight mass spectrometry with atmospheric pressure chemical ionization, *Analytical and bioanalytical chemistry* 406(27) (2014) 6843-6855.
- [144] S. Lv, Y. Niu, J. Zhang, B. Shao, Z. Du, Atmospheric Pressure Chemical Ionization Gas Chromatography Mass Spectrometry for the Analysis of Selected Emerging Brominated Flame Retardants in Foods, *Scientific reports* 7 (2017) 43998.
- [145] Y. Xing, M. Wang, T. Li, Y.x. Fu, X. Wang, Determination of polycyclic aromatic hydrocarbons in water samples by gas chromatography coupled to triple quadrupole tandem mass spectrometry using macroporous resin solid-phase extraction, *Journal of separation science* (2018).
- [146] T. Portolés, B. Garlito, J. Nácher-Mestre, M.H.G. Berntssen, J. Pérez-Sánchez, Multi-class determination of undesirables in aquaculture samples by gas chromatography/tandem mass spectrometry with atmospheric pressure chemical ionization: A novel approach for polycyclic aromatic hydrocarbons, *Talanta* 172 (2017) 109-119.
- [147] C. Alves, A.J. Santos-Neto, C. Fernandes, J.C. Rodrigues, F.M. Lanças, Analysis of tricyclic antidepressant drugs in plasma by means of solid-phase microextraction-liquid chromatography-mass spectrometry, *J. Mass Spectrom.* 42(10) (2007) 1342-1347.
- [148] W.F. Smyth, Recent studies on the electrospray ionisation mass spectrometric behaviour of selected nitrogen-containing drug molecules and its application to drug

analysis using liquid chromatography–electrospray ionisation mass spectrometry, *J. Chromatogr. B* 824(1-2) (2005) 1-20.

[149] S. Banerjee, S. Mazumdar, Electrospray ionization mass spectrometry: a technique to access the information beyond the molecular weight of the analyte, *Int. J. Anal. Chem.* 2012 (2012).

[150] F.W. McLafferty, F. Tureček, F. Turecek, *Interpretation of mass spectra*, University science books 1993.

[151] R.A. Yost, C.G. Enke, Triple quadrupole mass spectrometry for direct mixture analysis and structure elucidation, *Analytical chemistry* 51(12) (1979) 1251-1264.

[152] E.A. Mishalanie, B. Lesnik, R. Araki, R. Segall, M. Hunt, Validation and peer review of US Environmental Protection Agency chemical methods of analysis, *Environ Prot Agency* (2005).

[153] B. Magnusson, *The fitness for purpose of analytical methods: a laboratory guide to method validation and related topics* (2014), Eurachem, 2014.

[154] F.a.D. Administration, *Bioanalytical Method Validation Guidance for Industry*, 2018.

**Chapter 2: Single-use porous thin film extraction with gas chromatography atmospheric pressure chemical ionization tandem mass spectrometry for high-throughput analysis of 16 PAHs**

Fereshteh Shahhoseini, Ali Azizi, Stefana N. Egli Christina S. Bottaro. "Single-use porous thin film extraction with gas chromatography atmospheric pressure chemical ionization tandem mass spectrometry for high-throughput analysis of 16 PAHs" *Talanta*, 2020, 207, 1203202.

## 2.1. Introduction

A range of organic contaminants in water pollution cause adverse effects on environment and human health. Trace analysis and determination of these compounds in drinking water and surface water are of foremost importance. Oil spills, oil and gas leaks during storage and transportation, and incomplete combustion of organic materials introduce polycyclic aromatic hydrocarbons (PAHs) into the environment [1]. PAHs are highly lipophilic and bioaccumulate; they can be adsorbed by mammals through the gastrointestinal tract or be ingested through consumption of lipid-rich foods contaminated with PAHs [2]. They have been shown to have toxic, carcinogenic, teratogenic and genotoxic effects properties [3, 4]. Therefore, regulatory agencies recommend monitoring PAHs in water, soil and biota, the number depends on the jurisdiction. For example, the United States Environmental Protection agency (US EPA) list 16 PAHs as priority pollutants [5] with maximum contamination levels (MCLs) in the  $\text{pg mL}^{-1}$  range [6, 7]. To meet these criteria, analytical methods must rely on efficient preconcentration, careful treatment to minimize matrix effects and highly sensitive detection.

Traditional methods such as liquid-liquid extraction (LLE) [8, 9] and solid phase extraction (SPE) [10, 11] have been used for extraction of PAHs. LLE, used in the EPA Method 610, is time consuming, laborious and makes use of large amounts of organic solvents [9]. EPA Method 525, which is performed by SPE, shows good sensitivity and efficiency for the analysis of PAHs. However, cartridge conditioning and the sample handling steps, such as filtration are time consuming and reduce the accuracy and reliability of the method [12]. Recent innovations in sample preparation techniques have focused on

high throughput methods with automation, reducing the sample size, improving selectivity, and developing more environmentally-friendly approaches [13].

Solid phase microextraction (SPME) is the most recent solvent-less commercially available extraction technique, and is used widely for environmental monitoring because of its simplicity and high sensitivity [14]. SPME has shown a great potential for the determination of PAHs in environmental [15] and biological [16] matrices and can be used for on-site sampling [17]. The limitations of SPME are the low extraction capacity, fragile fibres, lack of selectivity, and low stability in organic solvents [18], motivating research to develop new formats and coating materials. Bruheim et al. [19] introduced thin film microextraction (TFME) which is a thin film geometry of SPME, using a thin sheet of polydimethylsiloxane (PDMS) membrane as the extraction phase. This format provides a higher surface area to volume ratio, which increases the efficiency of extraction and sensitivity of quantification. To improve the adsorption properties of thin films, several novel coatings were developed by impregnating sorptive particles in polymeric binders such as divinylbenzene in PDMS [20] or C<sub>18</sub> in polyacrylonitrile (PAN) [21]. These particle loaded thin films have been reported in the literature for consecutive extraction purposes[22, 23]; however; the long preparation time for the coating limits the application of this technique.

With respect to high throughput, sorbent clean up using serial washing steps should be quick and efficient, and carryover minimal [23]. Interference and cross-contamination between the samples caused by carry-over effects, can be eliminated if single-use extraction devices with a simple coating process are employed [24].

In this study, a porous molecularly imprinted polymer (MIP) thin film previously developed in our group [25] is used as a sorbent for the extraction of the 16 US EPA Priority PAHs in water. The thin films are prepared on a glass substrate using a drop-casting method followed by UV-initiated radical polymerization, for a simple, fast, low-tech and low-cost fabrication technique. The MIP thin film reported in our previous paper was designed specifically for light PAHs, as they were identified as important components of produced water from oil fields. However, we found that these MIPs were also good sorbents for heavier PAHs and we extended the use of these MIPs for analysis of the 16 PAHs. In this work, we take advantage of the sensitivity afforded by the use of gas chromatography (GC) with atmospheric pressure chemical ionization (APCI) and tandem mass spectrometry. APCI is a soft ionization method that produces molecular ions of the PAHs with little fragmentation. MRM also improves the signal to noise ratio (sensitivity) and selectivity of the method. The thin films are used directly for extraction from samples without any preconditioning steps. The enriched analytes are eluted in a small volume of organic solvent and directly injected into Waters Corp. atmospheric pressure gas chromatography (APGC) system coupled with tandem MS (APGC-MS/MS). After optimization of the extraction protocol, the thin film-APGC-MS/MS method is evaluated in terms of analytical figures of merit, such as sensitivity, linearity, accuracy and precision. Excellent performance for the determination of PAHs in river water and seawater samples using matrix-matched calibration is demonstrated.

## 2.2. Experimental

### 2.2.1. Reagents and Materials

The US EPA 16 priority PAHs including naphthalene (Naph, 99%) , acenaphthylene (Acy, 99%), acenaphthene (Ace, 99%), fluorene (Flu, 98%), phenanthrene (Phe,  $\geq 99.5$  %), anthracene (Ant,  $\geq 99.0$ % GC), fluoranthene (Flut, 98.7 % GC), pyrene (Pyr,  $\geq 99.0$ % GC), chrysene (Chry, Analytical standard), benzo(a)anthracene (BaA, 99%), benzo(b)fluoranthene (BbF, 98%), benzo(k)fluoranthene (BkF,  $\geq 99$  %), benzo(a)pyrene (BaP,  $\geq 96$ % HPLC), dibenzo(a,h) anthracene (DB(ah)A, Analytical standard), benzo(ghi) perylene (BGP, 98%) and indeno(1,2,3-cd) pyrene (InP, Chromatographic Purity) and deuterated PAHs including naphthalene-d8 (Naph-d8, 99 atom % D), acenaphthene-d10 (Ace-d10, 99 atom % D), phenanthrene-d10 (Phe-d10, 98% CP), chrysene-d12 (Chry-d12) and perylene-d12 (Pry-D12, 98 atom %D) were purchased from Sigma-Aldrich (Oakville, ON, Canada). Details on the physiochemical properties such as vapour pressure, solubility and Log P of the standards used are available in Table 2.1. Methanol (MeOH), acetonitrile (ACN), acetone, hexane, toluene, and dichloromethane (DCM) were purchased in Optima grade from Sigma-Aldrich (Oakville, ON, Canada). Ethyleneglycol dimethacrylate (EGDMA, 98%), 2,2-dimethoxy-2-phenylacetophenone (DMPA, 99%) and 4-vinyl pyridine (4-VP, 95%) monomer were purchased from Sigma-Aldrich (Oakville, ON, Canada) in analytical grade and used to prepare the films without further purification. High purity nitrogen (5.0UH, 99.999% purity), used for solvent evaporation, and ultra high purity helium (5.0UH), used as carrier gas for GC, were supplied by Praxair (Mississauga, ON, Canada). Argon with the purity of 99.999% used as collision gas was supplied by Praxair

(Hamilton, ON, Canada). Microscopic glass slides ( $25 \times 75 \text{ mm}^2$ ) used as substrate for the thin films were purchased from Fisher Scientific (Burlington, ON, Canada); cover slips ( $18 \times 18 \text{ mm}^2$ ) were purchased from VWR (Mississauga, ON, Canada). Deionized (DI) water ( $18 \text{ M}\Omega \text{ cm}$ ) was produced by a SYBRON/Barnstead N ( $18 \text{ M}\Omega$ ) water purification system (Boston, MA, USA).

**Table 2.1.** Physiochemical properties of target analytes.

Compound	MW ( $\text{g mole}^{-1}$ )	Solubility ( $\text{mg L}^{-1}$ )	Log P	Boiling point ( $^{\circ}\text{C}$ )	Vapor pressure ( $\text{mm Hg}$ )
Naph	128.17	31	3.3	218	$8.89 \times 10^{-2}$
Acy	152.20	16.1	3.93	280	$2.90 \times 10^{-2}$
Ace	154.21	3.8	3.92	279	$3.75 \times 10^{-3}$
Flu	166.22	1.9	4.18	294	$3.24 \times 10^{-3}$
Phe	178.23	1.1	4.46	338.4	$6.80 \times 10^{-4}$
Ant	178.23	0.045	4.45	341.3	$2.55 \times 10^{-5}$
Flut	202.26	0.26	5.16	384	$8.13 \times 10^{-6}$
Pyr	202.26	0.132	4.88	394	$4.25 \times 10^{-6}$
BaA	228.29	0.011	5.76	437.6	$1.54 \times 10^{-7}$
Chry	228.29	0.0015	5.73	448	$7.80 \times 10^{-9}$
BbF	252.32	0.0015	5.78	481	$8.06 \times 10^{-8}$
BkF	252.32	0.0008	6.11	480	$9.59 \times 10^{-11}$
BaP	252.32	0.0038	6.13	496	$4.89 \times 10^{-9}$
InP	276.34	0.062	6.70	536	$1.40 \times 10^{-10}$
DB(ah)A	278.35	0.0005	6.50	524	$2.10 \times 10^{-11}$
BGP	276.34	0.00026	6.63	550	$1.00 \times 10^{-10}$

Stock solutions of 1000 ppm of individual PAHs were prepared in 50/50 ACN and acetone, monthly and stored at  $-25 \text{ }^{\circ}\text{C}$ . Working standards, used to spike water samples, were prepared from stock solutions by dilution in ACN at least every two weeks. Stock solutions and working solutions to build the instrument calibration curves were prepared in toluene. All standards and samples were stored at  $4 \text{ }^{\circ}\text{C}$  until use. A quality control check solution (middle concentration of calibration curve) was injected daily to monitor the

instrument response. Certified Riverine Water SLRS-3 and Coastal Seawater CASS-3 reference samples from the National Research Council of Canada were used for matrix-matched analysis studies.

### **2.2.2. Thin film Fabrication**

A thin film polymer was prepared based on a previously described method [25], with slight modifications (Figure 2.1). Size of the film was reduced by 4 times to decrease the required volumes of sample and organic solvent for desorption. Precut 5×30 mm<sup>2</sup> frosted glass slides were washed with detergent and DI water, sonicated in MeOH, and dried at 50 °C. A prepolymerization solution prepared from 4-VP, EDGMA, toluene, DMPA and 1-octanol was sonicated for 10 min followed by degassing for 10 min to remove oxygen that interferes with free radical polymerization. A 4-μL aliquot of the prepolymerization solution was dispensed on the glass substrate, overlaid with an 18×18 mm<sup>2</sup> microscope cover-slide aligned with the bottom of the glass substrate, and placed under a UV lamp for 30 min. Following polymerization, the cover slide was removed to reveal a thin layer of solid polymer coating of 5×18 mm<sup>2</sup>. Unreacted components were extracted from the polymer with MeOH stirred for 30 min, repeated three times, then air-dried and stored under ambient conditions until use.

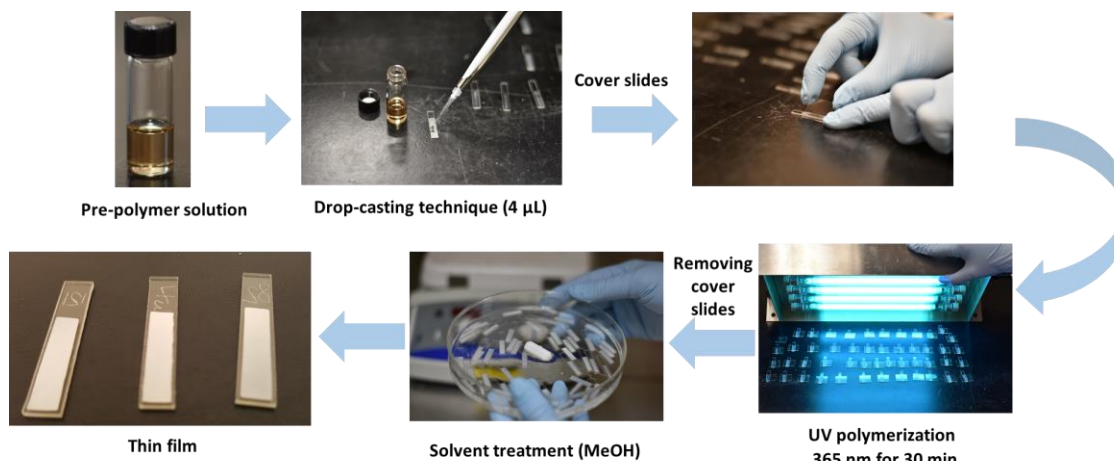


**Figure 2.1.** Experimental procedure for fabrication of thin film devices

### 2.2.3. Instrumentation

Analysis of PAHs was carried out using a Waters Xevo TQ-S (Waters Corporation, Ontario, Canada) equipped with an atmospheric pressure chemical ionization (APGC-MS/MS) ion source and coupled to Agilent 7890B GC instrument (Agilent Technologies, CA, U.S.A.). APGC is Waters' solution for interfacing GC with a soft ion source for their Xevo TQ-S triple quadrupole MS. This results in a configuration with high sensitivity for a range of quantitative analysis applications. A 1- $\mu\text{L}$  of sample was injected in pulsed splitless mode (25 psi, 1 min) with a liner temperature of 280  $^{\circ}\text{C}$  with helium carrier gas at a constant flow rate of 1.2  $\text{mL min}^{-1}$ . An Agilent DB-5MS column (30  $\text{m}\times 0.250$  mm, 0.25  $\mu\text{m}$ ) was used for separation with the following oven program: after injection the column was held at 80  $^{\circ}\text{C}$  for 2 min, increased to 220  $^{\circ}\text{C}$  at 25  $^{\circ}\text{C min}^{-1}$ , to 240  $^{\circ}\text{C}$  at 10  $^{\circ}\text{C min}^{-1}$ , to 280  $^{\circ}\text{C}$  at 3  $^{\circ}\text{C min}^{-1}$  and finally raised to 300  $^{\circ}\text{C}$  at 10  $^{\circ}\text{C min}^{-1}$  then held at 300  $^{\circ}\text{C}$  for 2.5 min. The eluate from the GC passed through a heated transfer line (300  $^{\circ}\text{C}$ ) to the source; transfer flow was assisted with a nitrogen make-up gas (Peak Scientific, UK) at 280

mL min<sup>-1</sup>. The APGC source was kept at 150 °C and the N<sub>2</sub> auxiliary and cone gas flow rates were set at 200 and 190 L h<sup>-1</sup>, respectively. The APGC corona pin was operated in constant current mode at 2 μA. MRM transitions, cone voltages and collision energy used for all compounds are included in Table 2.2.

**Table 2.2.** Summary of tandem mass spectrometry parameters using APGC-MS/MS.

Compound	RT (min)	MRM ( <i>m/z</i> )	Cone (V)	Collision (eV)
Naph-d8	5.81	136>108	55	20
Naph	5.84	128>102	55	20
Acy	7.41	152>151	65	28
Ace-d10	7.55	164>162	40	20
Ace	7.58	154>153	40	20
Flu	8.11	166>165	35	20
Phe-d10	9.18	188>186	65	25
Phe	9.21	178>177	65	25
Ant	9.28	178>177	65	25
Flut	11.05	202>201	70	35
Pyr	11.50	202>201	70	35
BaA	14.90	228>228	30	15
Chry-d12	14.93	240>240	30	15
Chry	15.02	228>228	30	15
BbF	19.28	252>252	30	15
BkF	19.41	252>252	30	15
BaP	20.71	252>252	30	15
Per-d12	20.98	264>264	30	15
InP	25.41	276>276	40	15
DB(ah)A	25.58	278>278	40	15
BGP	26.30	276>276	40	15

#### 2.2.4. Sample preparation procedure

Extraction experiments were carried out on 18 samples simultaneously with the aid of three 6-position stirrers. Although such an intensive schedule is not necessary, performing 6 triplicates experiments at the same time allows for rapid optimization of each effective parameter while minimizing variability associated with drift in ambient

conditions. Aqueous standards were prepared in 20 mL deionized water and used immediately to avoid adsorption of PAHs to the glass vial. The volume of standard solution used for spiking was kept below 1% of the sample volume to minimize changes in matrix composition. The prepared thin film devices were directly exposed to the aqueous solutions with no preconditioning treatment of the sorbent. The extraction was performed by stirring at 1400 rpm for 60 min at room temperature. After extraction of PAHs, the thin films were washed in small aliquots of DI water and allowed to dry. All evaporation, reconstitution and injection steps were carried out in-vial to reduce errors from sample transfer and manipulation. Desorption was carried out in 1250  $\mu$ L hexane at vortex stirred at 1000 rpm for 5 min. The solvent was evaporated to near complete dryness under a stream of nitrogen for 10 min, the extract was reconstituted in 100  $\mu$ L of toluene and transferred to a 250  $\mu$ L glass conical insert vial for injection to the APGC (Figure 2.2).

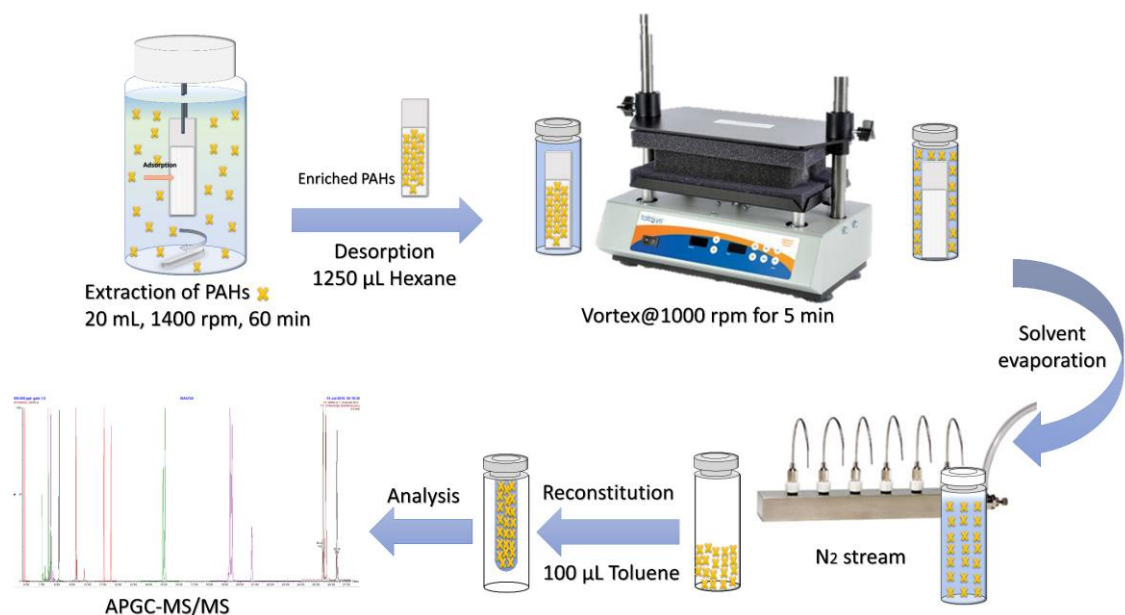


**Figure 2.2.** Method of extraction and desorption process

### **2.2.5. Water samples**

River water and seawater were from the Waterford River and St. John's Harbour (both located in St. John's, Newfoundland, Canada) were collected into pre-cleaned, amber bottles. Each sample was used directly without filtration or other pretreatment.

## **2.3. Results and discussion**

### **2.3.1. Method development**

#### *2.3.1.1. Desorption of PAHs from porous thin films*

Quantitative desorption of analytes from the sorbent guarantees sensitive and reproducible quantification. For desorption of PAHs from thin films, vortex agitation was chosen over magnetic stirring to eliminate the use of a magnetic stir bar, which reduces the potential for sample contamination or loss, allows for use of smaller sample vials and TFME devices, and provides high velocity stirring in a simple apparatus. The dependence of desorption efficiency on stirring is illustrated in Figure 2.3. Efficiency and precision of the desorption improved with increased agitation from 250 to 1000 rpm. Agitation rates higher than 1250 rpm caused physical damage to the polymer. Hence, 1000 rpm was chosen for optimization and validation studies.

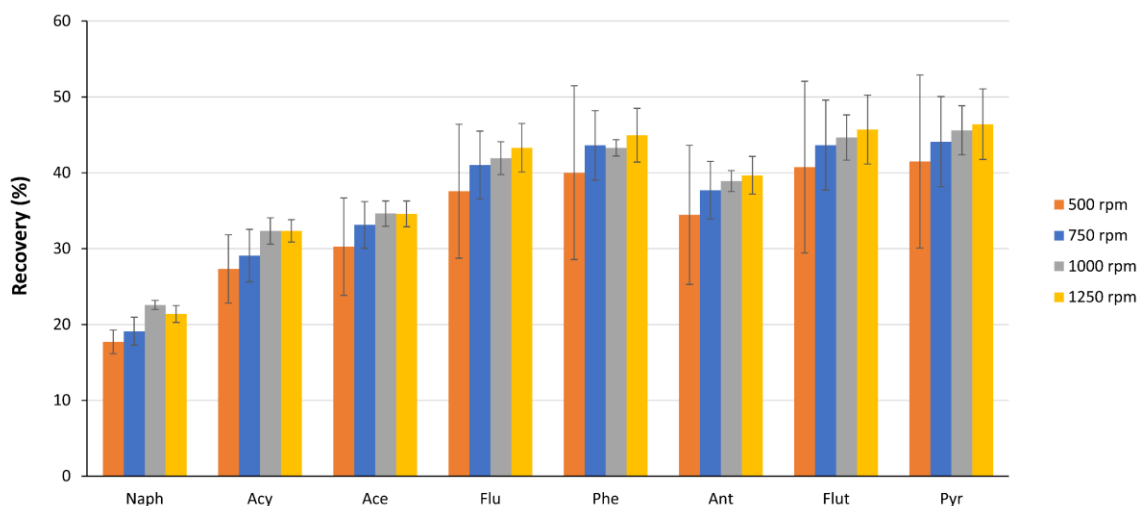


**Figure 2.3.** Effect of agitation rate using multi vortex on desorption of PAHs. Extraction: sample 20 mL DI spiked with 50 ng mL<sup>-1</sup> PAHs, 2 hours at 1400 rpm.

To ensure maximum efficiency, the desorption solvent type and the time required for desorption should be optimized. The solvent should extract all adsorbed analytes from the sorbent and not lead to loss of volatile analytes during the evaporation step. Five different solvents were examined, namely: hexane, ACN, MeOH, toluene and DCM. Hexane gave the best desorption efficiency and most reproducible results as can be seen in Figure 2.4. The data for MeOH was highly irreproducible; we attribute this to losses during the evaporation step due to the potential for azeotrope formation, MeOH forms azeotropes with both benzene and toluene, thus the results are not reported.

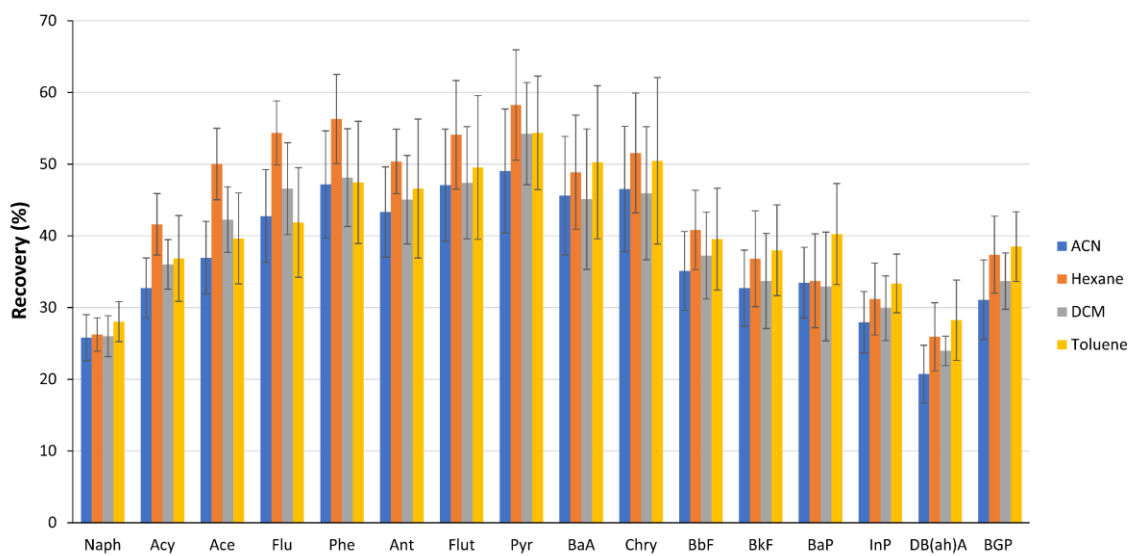


**Figure 2.4.** Optimization of solvent desorption in 10 min using multi vortex at 1000 rpm; Extraction was performed from 20 mL DI water sample spiked 2000 pg mL<sup>-1</sup> of Naph, Acy, Ace, Flu, Phe, Ant, Flut and Pyr and 250 pg mL<sup>-1</sup> of BaA, Chry, BbF, BkF, BaP, InP, DB(ah)A and BGP for 2 hours and 1400 rpm agitation; Solvents spiked with internal standards to obtain 50000 pg mL<sup>-1</sup> of Naph-d8, Ace-d10 and Phe-d10 and 10000 pg mL<sup>-1</sup> Chry-d12.

Investigation of desorption time from 2 to 20 min (Figure 2.5) reveals that there is no significant difference between desorption intervals. This can be related to the highly porous structure of the polymeric sorbent that allows for fast desorption when compared to other sorbents used for SPME [21, 26]. Though lowest desorption time is preferable for throughput, it may result in irreproducible results; 5 min yielded excellent recovery of analytes with lower standard deviations and was thus considered optimum.

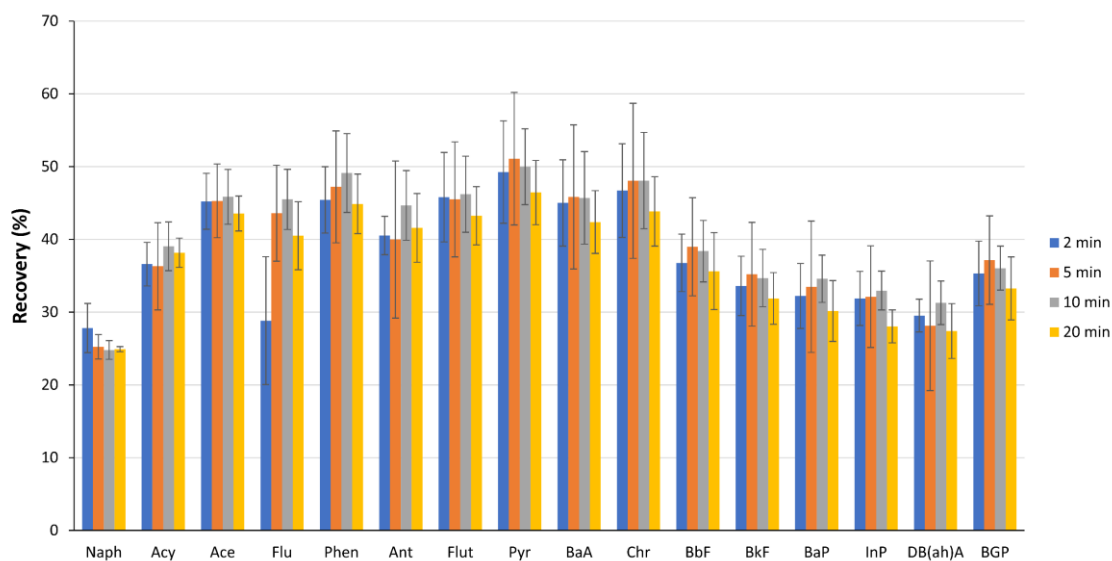


**Figure 2.5.** Optimization of desorption time in the range of 2-20 mins; Extraction was performed from 20 mL DI water sample spiked  $2000 \text{ pg mL}^{-1}$  of Naph, Acy, Ace, Flu, Phe, Ant, Flut and Pyr and  $250 \text{ pg mL}^{-1}$  of BaA, Chry, BbF, BkF, BaP, InP, DB(ah)A and BGP for 2 hours and 1400 rpm agitation; Desorption: hexane ( $1250 \text{ }\mu\text{L}$ ) spiked with internal standards to obtain  $50000 \text{ pg mL}^{-1}$  of Naph-d8, Ace-d10 and Phe-d10 and  $10000 \text{ pg mL}^{-1}$  Chry-d12 under 1000 rpm vortex agitation.

### 2.3.1.2. Extraction of PAHs from water using porous thin films

Extraction of PAHs using porous thin films is based on SPME theory where the analytes are partitioned between the sample solution and extraction phase [27]. The amount of analyte extracted onto the polymer coating is increased by exposure time and reached to an equilibrium after a certain amount of time [28]. By employing agitation, the time required to reach equilibrium can be reduced and extraction efficiency in pre-equilibrium conditions is improved. Rapid agitation facilitates the analyte mass transfer from the bulk solution to the surface of the sorbent and decreases the thickness of the stagnant boundary layer at the surface of the sorbent [28, 29]. The extraction efficiency of all PAHs, shown in Figure 2.6, increased with agitation rates from 200 to 1400 rpm. The results obtained at

highest agitation rate (1400 rpm) gave the shortest extraction times, therefore, a 1400 rpm was selected as optimal.

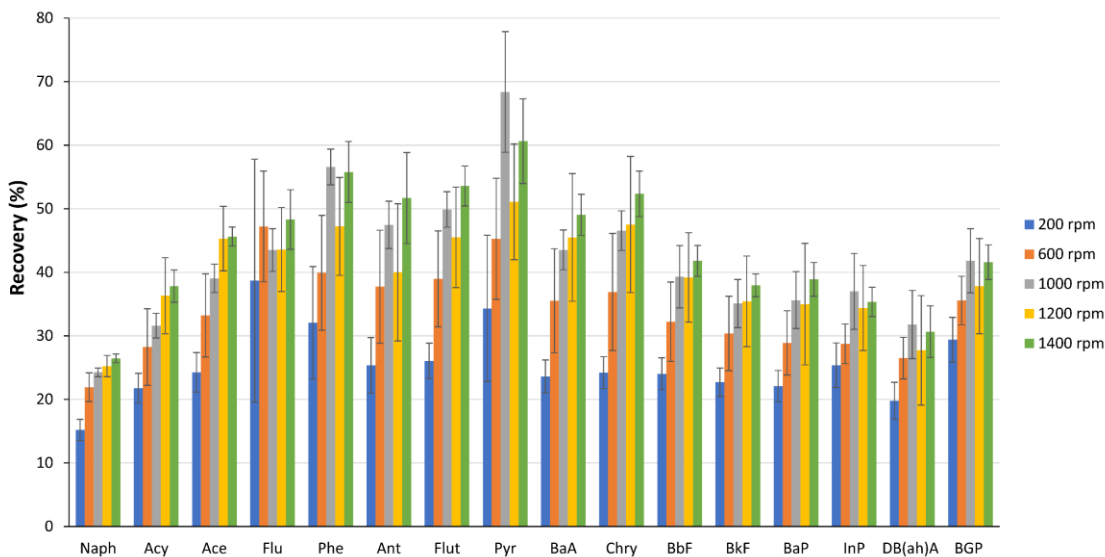


**Figure 2.6.** Investigation of extraction agitation effect on extraction efficiency; Extraction was performed for 2 hours in 20 mL DI water sample spiked with 2000 pg mL<sup>-1</sup> of Naph, Acy, Ace, Flu, Phe, Ant, Flut and Pyr and 250 pg mL<sup>-1</sup> of BaA, Chry, BbF, BkF, BaP, InP, DB(ah)A and BGP; Desorption: 1000 rpm multi-vortex for 5 minutes. Hexane was used as desorption solvent spiked with internal standards to obtain 50000 pg mL<sup>-1</sup> of Naph-d8, Ace-d10 and Phe-d10 and 10000 pg mL<sup>-1</sup> Chry-d12.

Extraction time should be optimized based on requirements for sensitivity and throughput. When the polymer is exposed to the sample during the pre-equilibrium conditions, the amount of analyte extracted increases linearly with time. However as equilibrium is approached the rate of adsorption decreases, thus the interval over which extraction is linear must be studied for new sorbents to account for factors that affect analyte partitioning [27, 30]. For these porous thin films, the extraction time profile for 16 PAHs using maximum agitation were obtained. As shown in Figure 2.7, the equilibrium between extraction phase and water sample was established within 3 h for the more soluble,

lighter analytes, i.e. Naph, Acy, Ace and Ant. However, for compounds with larger Log P values (listed in Table 2.1), a longer extraction time is required. The difference in the kinetic regime between the low and high MW PAHs is caused by differences in the diffusion coefficient between two phases, with the higher molecular weight PAHs requiring a longer extraction time. As a compromise, good sensitivity and shorter analysis time are possible using 60 min for extraction. Although, the extracted mass of analytes recovered is less than 50% of the total, it is linear with sampling time and provides good results. Because many samples can be treated simultaneously, high throughput can be achieved; for example, for 18 samples extracted in parallel with a 60 min extraction time, one sample can be processed every 4 min.

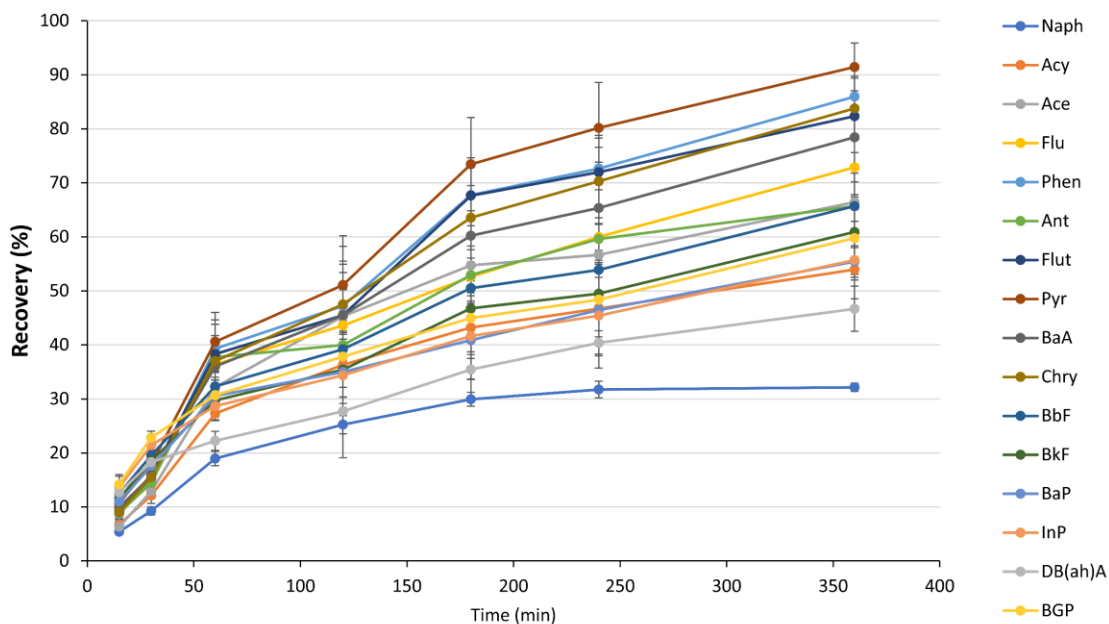


**Figure 2.7.** Extraction time profile of 16 PAHs on polymeric thin film; Extraction was performed at 1400 rpm in 20 mL DI water sample spiked with 2000 pg mL<sup>-1</sup> of Naph, Acy, Ace, Flu, Phe, Ant, Flut and Pyr and 250 pg mL<sup>-1</sup> of BaA, Chry, BbF, BkF, BaP, InP, DB(ah)A and BGP; Desorption: 1000 rpm multi-vortex for 5 minutes. Hexane was used as desorption solvent spiked with internal standards to obtain 50000 pg mL<sup>-1</sup> of Naph-d8, Ace-d10 and Phe-d10 and 10000 pg mL<sup>-1</sup> Chry-d12.

### **2.3.2. Potential reusability**

Although the porous thin films were developed for high throughput using batch processing and single use (e.g., to avoid dealing with carryover), these devices can be reused. The carryover for optimized conditions was evaluated by performing two subsequent desorption of thin films uploaded with analytes. There were no carryover effects for 14 PAHs, only Pyr and BaP were detected, though this was still negligible at ~around 2 %). To assess reusability and robustness of the sorbent, three films were tested for five separate extractions from water samples. Due to excellent desorption of PAHs from thin films, a simple wash step with MeOH was enough to eliminate the minimal carryover for Pyr and BaP. The % recovery and the error for the 5 extractions were calculated and the results for each film were compared (Figure 2.8). The %RSD for reused thin films was impressive, giving experimental errors very similar to the inter-device values, where the %RSD were less than 20%, which is considered acceptable. After several more extractions, physical damage of the polymer film was observed, likely caused by vigorous shaking during desorption. The polymer robustness may be overcome by improving adhesion of polymer to the substrate, but this is out of the scope of this study.

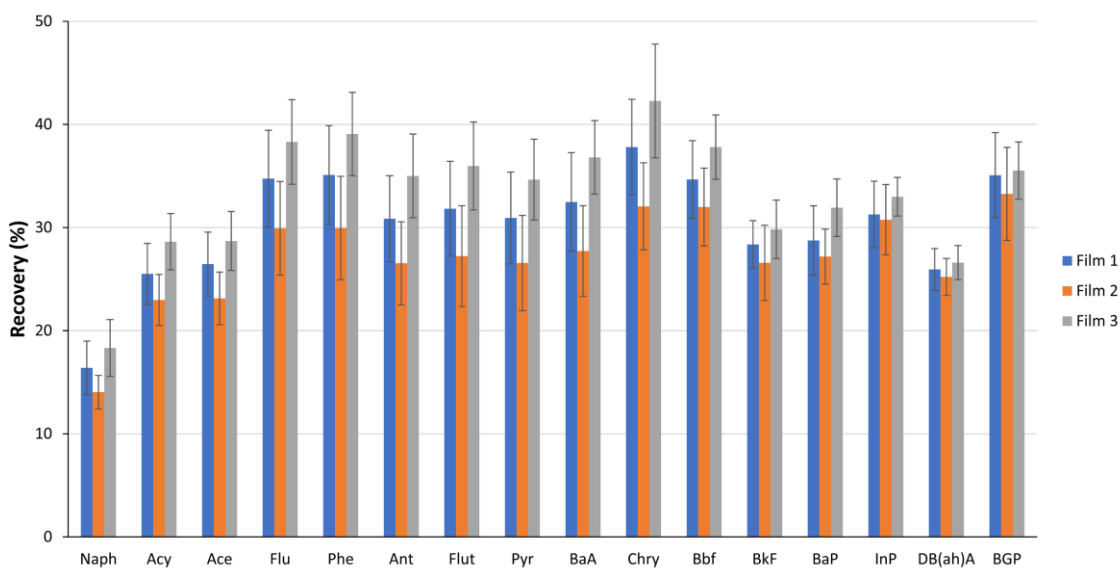


**Figure 2.8.** Reusability of polymeric thin films. Extraction was performed from 20 mL DI water sample with concentration of 2000 pg mL<sup>-1</sup> of Naph, Acy, Ace, Flu, Phe, Ant, Flut and Pyr and 250 pg mL<sup>-1</sup> of BaA, Chry, Bbf, BkF, BaP, InP, DB(ah)A and BGP for 1 hour. Desorption: 1000 rpm multi vortex for 5 minutes, Hexane was used as desorption solvent and spiked with 50000 pg mL<sup>-1</sup> of Naph-d8, Ace-d10 and Phe-d10 and 10000 pg mL<sup>-1</sup> of Chry-d12.

### 2.3.3. Selection of internal standard

To develop an analytical method, selection of internal standards is crucial especially for a group of compounds with a wide range of physiochemical properties such as PAHs. As shown in Table 2.1, the maximum solubility of these compounds in water varies from ng to mg per liter. Such a wide range of solubility makes it difficult to optimize and develop one extraction method for all targeted compounds. Additionally, the difference in vapor pressure and boiling points of PAHs from low-molecular weights to high-molecular weights could affect the efficiency in the recovery during nitrogen blow-down. The US EPA methods recommend several deuterated PAHs to reduce errors associated with sample preparation and detection. A lower number of internal standards is preferable if they can

compensate for correlated random errors and systematic errors. Internal standards were selected based on similarities in structure to the analytes and their capability to reduce random errors associated with ionization efficiency in MS.

To select the appropriate internal standard two main strategies were adopted. First, the internal standards for volatile and semi-volatile compounds were selected based on the abilities to decrease the errors due to analyte loss during solvent evaporation. For this purpose, the obtained signals for 8 light PAHs during optimization of desorption solvent were normalized against the signal intensity of the 3 first internal standards (Naph-d8, Ace-d10, Phe-d10). Then the relative standard deviation (RSD%) between three replicants for each desorption solvent (ACN, MeOH, DCM, hexane, and toluene) were calculated. By combining these RSD values for each analyte, a relative measure of error associated with the use of each internal standard were obtained and showed in Figure 2.9. Obviously, Naph-d8 is the best internal standard for Naph while Ace-d10 is the most appropriate internal standard for Acy and Ace. It is worth mentioning that the random errors associated with Flu can not be corrected using Ace-d10 due to its higher vapour pressure and lower boiling point. Therefore, Phen-d10 was selected as the internal standard for Flu, Phe, Ant, Flut, and Pyr.

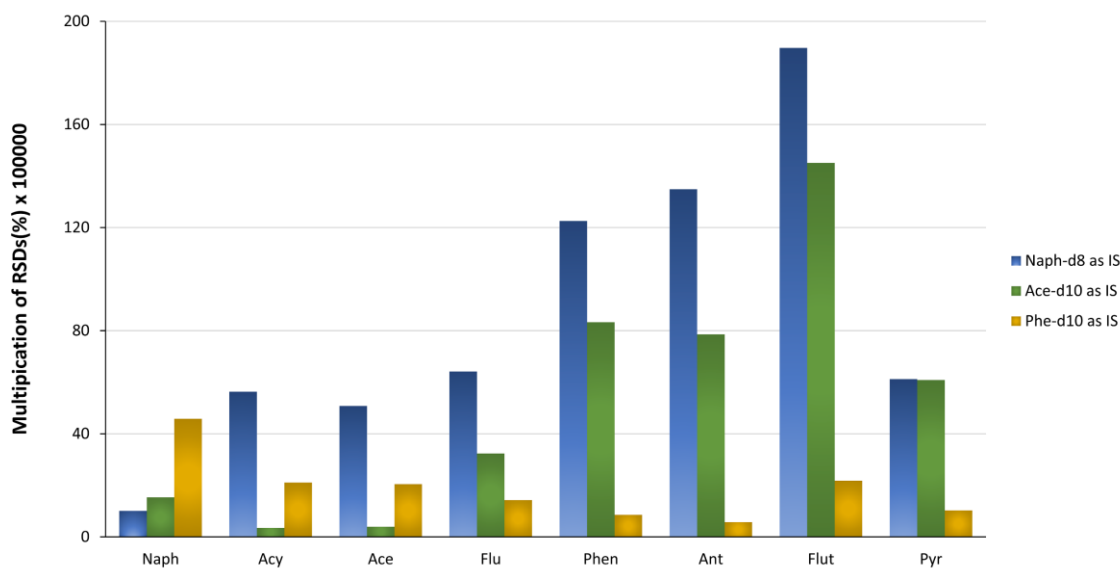


**Figure 2.9.** Multiplication of relative errors (RSD%) of normalized peak area of 8 light PAHs during optimization of desorption solvent

For the next 8 heavier PAHs, two recommended internal standards including Chry-d12 (for BaA and Chry) and Per-d12 (BbF, BkF, BaP, InP, DB(ah)A and BGP) were used for method development steps and validation studies in deionized water and synthetic river water, as shown in Figure 2.10 a and Figure 2.11 a. In the validation studies using synthetic sea water, the Per-d12, added at  $100 \text{ pg mL}^{-1}$  could not compensate for the random errors associated with the extraction of 5 corresponding analytes. As illustrated in Figure 2.12 a, a reasonable linear range can not be calculated using Per-d12 as internal standard for BGP. This is due to excessive variations in extraction efficiency and difficulty to detect/quantify signal intensity of Per-d12 in synthetic sea water. Thus Chry-d12 was chosen as the internal standard for 8 heavy PAHs and used for calculation of extraction efficiency during method development as well as relative peak areas for validation and real sample studies. By using Chry-d12 as internal standard for BGP, a good linearity was calculated in synthetic sea

water which is illustrated in Figure. 2.12 b. Furthermore, the linearity of other later eluted analytes was improved in synthetic sea water as well.

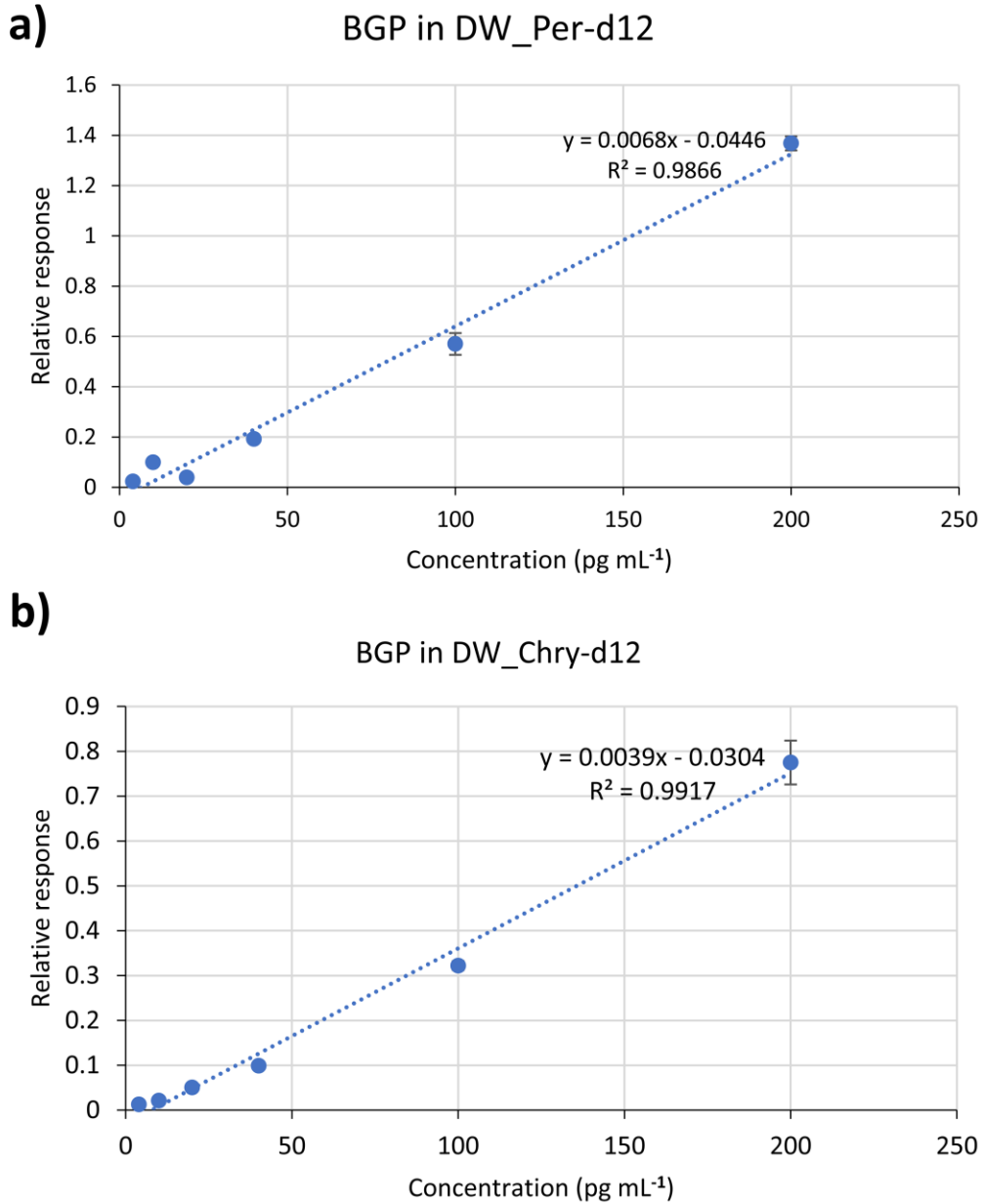


**Figure 2.10.** Calibration curve of BGP obtained in deionized water, extraction was performed using 20 mL deionized water sample spiked with BGP in a concentration range between 4-200  $\text{pg mL}^{-1}$ , and 100  $\text{pg mL}^{-1}$  of Per-d12 (a) and (b) Chry-d12, for 1 hour and 1400 rpm agitation. Desorption with 1250  $\mu\text{L}$  of Hexane vortexed at 1000 rpm for 5 min.

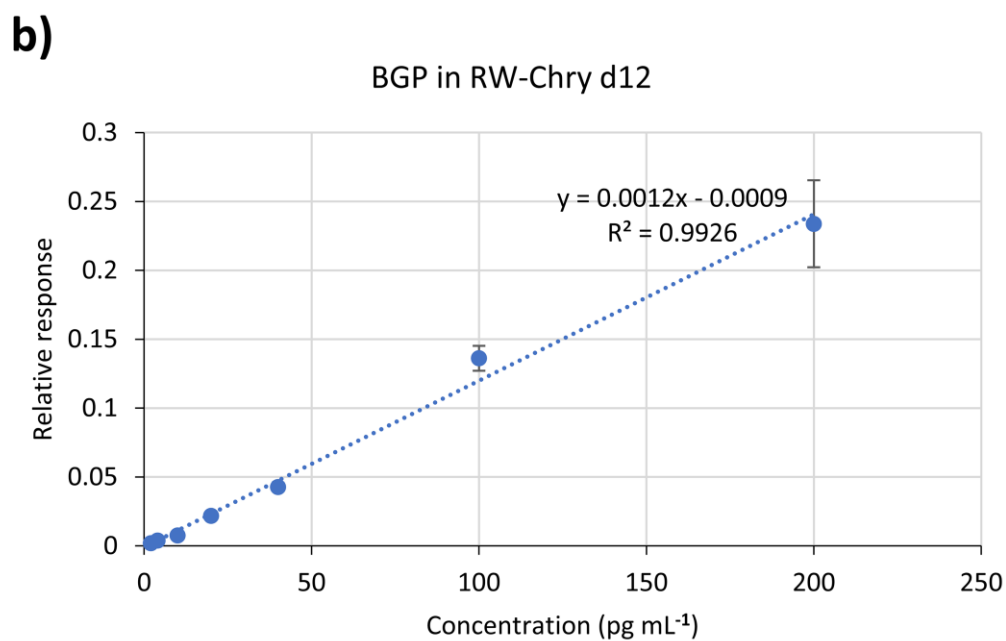
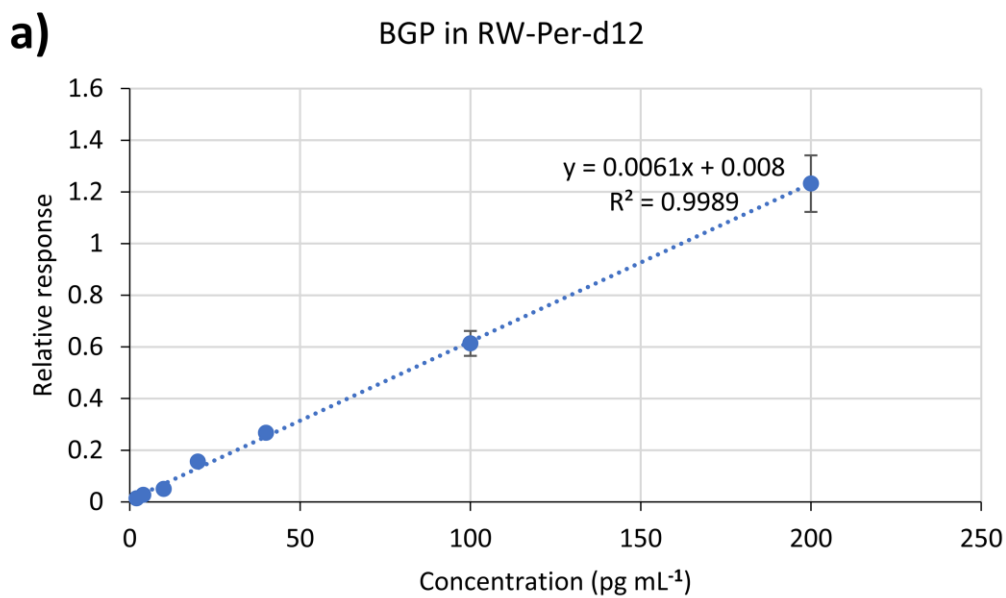


**Figure 2.11.** Calibration curve of BGP obtained in synthetic river water, extraction was performed using 20 mL synthetic river water sample spiked with BGP between 2-200  $\text{pg mL}^{-1}$ , and 100  $\text{pg mL}^{-1}$  of Per-d12 (a) and (b) Chry-d12, for 1 hour and 1400 rpm agitation. Desorption with 1250  $\mu\text{L}$  of Hexane vortexed at 1000 rpm for 5 min.

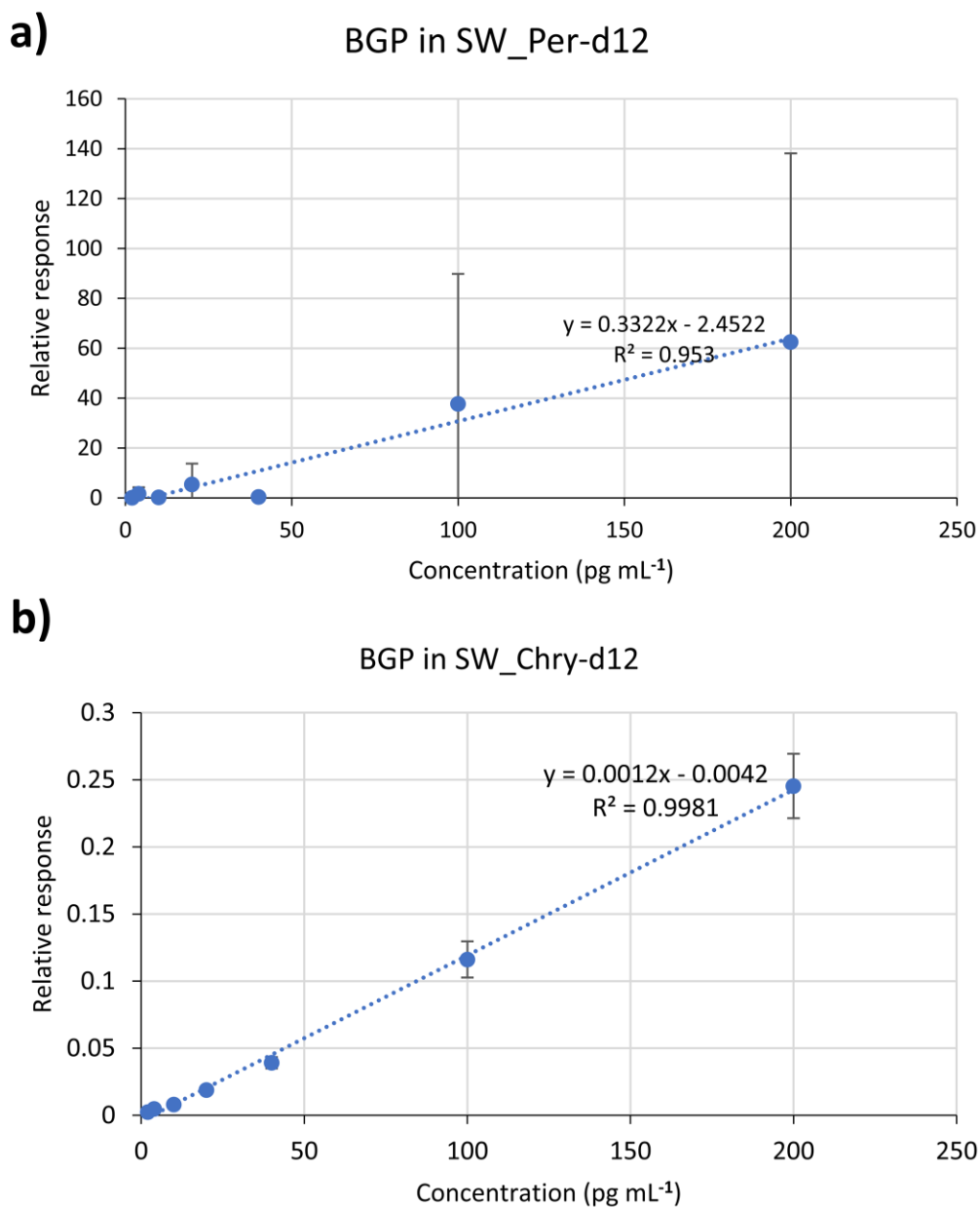


**Figure 2.12.** Calibration curve of BGP obtained in synthetic sea water, extraction was performed using 20 mL synthetic sea sample spiked with BGP between 2-200  $\text{pg mL}^{-1}$ , and 100  $\text{pg mL}^{-1}$  of Per-d12 (a) and (b) Chry-d12, for 1 hour and 1400 rpm agitation. Desorption with 1250  $\mu\text{L}$  of Hexane vortexed at 1000 rpm for 5 min.

#### 2.3.4. Method Validation

The optimized analytical method was validated using DI water spiked with PAH standards and deuterated internal standards. The figures of merit were obtained and shown in Table 2.3. The limit of quantification (LOQ) using the proposed method is defined as the lowest concentration of spiked samples with RSD of triplicate analysis less than 20%.

The LOD and LOQ values for the 16 PAHs were 1-100 pg mL<sup>-1</sup> and 2-400 pg mL<sup>-1</sup>, respectively. The lower limits of the linear dynamic ranges (LDR) were determined based on LOQ and upper limits were based on aqueous solubility or detector saturation; the best being 100 - 50,000 pg mL<sup>-1</sup> for lighter PAHs like Acy, Phen, Ant and Flut. The lowest LDRs were found for heavy PAHs BkF, BaP with ranges of 10-400 pg mL<sup>-1</sup>. The linear fit for all calibrations was very good with R<sup>2</sup> values higher than 0.9978. The LOQ values are at the pg mL<sup>-1</sup> (ppt) level, which is lower than the US-EPA maximum contamination limits (MCL) [5], European Union (EU) limits for human consumption [7], and EU environmental quality standard [6]. For example, EU Council Directive 98/83/EC (quality of water intended for human consumption) indicates parametric values of 10 pg mL<sup>-1</sup> for BaP and of 100 pg mL<sup>-1</sup> for the sum BbF, BkF, BGP and InP [7]. Therefore, this method based on thin film extraction is suitable compliance with US-EPA and EU guidelines. The figures of merits in Table 2.3 were obtained using a relatively short extraction time; sensitivity can be improved with longer extractions.

Additional method validation was completed to assess accuracy and precision of the recoveries at a range of concentrations. Recovery concentrations were calculated using calibration data acquired on a previous day and fit using weighted linear regression [31]. The data was robust even though analysis was performed in different days. The accuracy

and precision assessments were carried out at 15 pg mL<sup>-1</sup>, 80 pg mL<sup>-1</sup>, 250 ng mL<sup>-1</sup>, for the heavy PAHs and 250 pg mL<sup>-1</sup> to 25000 pg mL<sup>-1</sup> for the light PAHs to cover the available linear ranges. The obtained results show good accuracy and suitable precision, which made assessment for environmental applications pertinent.

A comparison of our proposed thin films with previously reported TFME methods [19, 32, 33] for extraction of PAHs is shown in Table 2.4. The current method provides similar or better LODs for trace analysis of PAHs in water samples particularly for high MW PAHs for which other methods did not provide analytical results. Our proposed methodology for fabrication of thin films is straightforward while PDMS- [32] and cellulose triacetate-based [33] sorbents require long preparation time. Furthermore, preparation of the sorbent on glass support resulted in robust extraction devices which can be implemented for highly turbulent sampling media. This robustness has also advantage of easy use in the lab. The porous thin films are water compatible and can be directly employed for sample preparation in comparison to other sorbents [32, 33] which needs a solvent conditioning prior to direct immersion for extraction. This leads to higher throughput and reduces the time for pretreatment of each sample.

**Table 2.3.** Method validation of porous thin film extraction for determination of PAHs in DI water (n=3).

PAHs	Linear range <sup>a</sup>	Function	R <sup>2</sup>	Accuracy (%)					Precision (%)				
				15	80	250	250 0	2500 0	15	80	250	250 0	2500 0
Naph	200-50000	$y = 0.0013x + 0.22$	0.9998	NQ <sup>b</sup>	NQ	108	88.7	104	-	-	6.2	3.6	8.0
Acy	100-50000	$y = 0.00020x + 0.013$	0.9999	NQ	NQ	110	116	107	-	-	2.1	2.3	3.5
Ace	200-50000	$y = 0.00090x + 0.19$	0.9998	NQ	NQ	99.7	109	99.7	-	-	4.1	2.4	2.3
Flu	400-50000	$y = 0.0045x + 0.35$	0.9995	NQ	NQ	106	102	115	-	-	3.1	3.4	2.9
Phen	100-50000	$y = 0.0011x + 0.036$	1.0000	NQ	NQ	107	101	107	-	-	8.2	1.3	9.3
Ant	100-50000	$y = 0.00060x + 0.046$	0.9998	NQ	NQ	113	94.8	103	-	-	9.4	7.1	9.2
Flut	100-50000	$y = 0.0015x + 0.047$	0.9987	NQ	NQ	108	119	102	-	-	9.9	6.0	8.8
Pyr	200-50000	$y = 0.0015x + 0.32$	0.9996	NQ	NQ	113	120	113	-	-	19	6.6	19
BaA	2-2000	$y = 0.012x - 0.072$	0.9997	85.5	86.4	86.2	NL <sup>c</sup>	NL	4.1	3.1	0.60	-	-
Chry	4-1000	$y = 0.012x + 0.062$	0.9999	121	107	92.7	NL	NL	2.4	7.6	4.9	-	-
BbF	10-1000	$y = 0.011x - 0.071$	0.9998	100	77.8	77.7	NL	NL	9.3	7.2	8.8	-	-
BkF	10-400	$y = 0.011x + 0.0018$	0.9978	135	97.7	118	NL	NL	16	9.9	4.6	-	-
BaP	10-400	$y = 0.0086x - 0.035$	0.9988	108	80.0	81.1	NL	NL	8.4	9.0	15	-	-
InP	10-1000	$y = 0.0037x - 0.020$	0.9996	80.9	72.6	75.3	NL	NL	2.0	0.30	13	-	-
D(ah)A	4-400	$y = 0.0031x - 0.0073$	0.9981	90.0	100	93.7	NL	NL	3.7	11	18	-	-
BGP	10-400	$y = 0.0037x - 0.033$	0.9985	110	82.4	83.9	NL	NL	3.9	14	14	-	-

<sup>a</sup> Spiked concentrations of PAHs are from 1.0 to 50000 pg mL<sup>-1</sup>, and Naph-d8, Ace-d10 and Phen-d10 at 1000 pg mL<sup>-1</sup> and Chry-d12 at 100 pg mL<sup>-1</sup>.

<sup>b</sup> Not quantifiable

<sup>c</sup> Nonlinear

**Table 2.4.** Comparison of proposed thin film extraction with other methods for the determination of PAHs.

Sorbent	Analytes	Conditioning	Extraction	Desorption	Analysis	LOD (pg mL <sup>-1</sup> )	Ref.
PDMS thin film membrane	7 PAH s	2 h at 250 °C	60 min, headspace extraction	Thermal desorption (250 °C)	GC-MS	2.5-19	[19]
PDMS/ $\beta$ -cyclodextrin membrane	7 PAHs	30 min washing with ACN	60 min, direct immersion	5 min (200 $\mu$ L ACN)	GC-MS	10-200	[32]
Carbon nanotubes/cellulose triacetate membrane	8 PAHs	30 min washing with MeOH	30 min, direct immersion	20 min (60 $\mu$ L MeOH)	HPLC-UV	20-90	[33]
Porous thin film	16 PAHs	-	60 min, direct immersion	5 min (1250 $\mu$ L hexane)	GC- MS/MS	1-100	This work

### **2.3.5. Matrix-matched calibration for real samples analysis**

Complex matrices interfere with analyte detection and quantification throughout the process. Co-extracted matrix components influence peak quality of targeted analytes [34], ion intensity in MS detection when caused by ion suppression [35] or reduce the extraction efficiency during sample preparation. Therefore, constructing calibration curves in synthetic blank samples and studying the effects of matrix components are necessary to develop non-exhaustive sample preparation techniques. Matrix-matched calibration curves of the 16 PAHs using thin film extraction were acquired in synthetic seawater and synthetic river water. The data summarized in Tables 2.5 and 2.6, show very good linearity with excellent correlation coefficients ( $R^2 > 0.990$ ) in both synthetic water samples. The method can quantify PAHs at trace levels in real matrices with LOQs in the 2-200  $\text{pg mL}^{-1}$  range. Moreover, the LDR obtained for the 16 PAHs is wide from 2 to 50000  $\text{pg mL}^{-1}$ , likely due to their different solubility in water. The slope values obtained in synthetic sea water and river water are in good agreement with those achieved in DI water for most PAHs. The difference in matrix between DI water (Table 2.3) and the synthetic water samples (Tables 2.5 and 2.6) cause differences in the extraction of the lately eluted PAHs, as reflected in the dissimilar slopes. These findings imply that matrix-matched calibration is required for real sample analysis to improve accuracy and precision of the measurement.

**Table 2.5.** Matched calibration data for analysing Waterford river sample (n=3).

PAHs	Linear range <sup>a</sup>	Function	R <sup>2</sup>	Accuracy (%)					Precision (%)				
				15	80	250	2500	25000	15	80	250	2500	25000
Naph	400-50000	y= 0.0013x - 0.26	0.9994	NQ <sup>b</sup>	NQ	NQ	94.2	105	-	-	-	1.1	4.9
Acy	20-50000	y = 0.00020x + 0.014	0.9997	NQ	109	116	102	105	-	9.9	4.8	1.1	3.5
Ace	40-50000	y = 0.0011x - 0.11	0.9995	NQ	108	106	88.8	82.9	-	1.6	1.1	1.1	2.2
Flu	200-20000	y = 0.0036x - 0.69	0.9975	NQ	NQ	116	115	112	-	-	19	1.5	1.9
Phen	100-50000	y = 0.0011x + 0.099	0.9999	NQ	NQ	112	98.3	103	-	-	5.3	0.20	3.3
Ant	100-50000	y = 0.00070x - 0.23	0.9995	NQ	NQ	141	102	107	-	-	10	0.50	3.5
Flut	20-10000	y = 0.0017x + 0.056	0.9999	NQ	117	104	79.3	NL <sup>c</sup>	-	15	7.8	4.0	-
Pyr	40-10000	y = 0.0017x + 0.058	0.9999	NQ	133	115	82.0	NL	-	17	9.2	4.6	-
BaA	4-2000	y = 0.013x - 0.89	0.9928	113	104	97.3	100	NL	2.3	1.1	4.6	1.0	-
Chry	2-1000	y = 0.012x - 0.037	0.9999	111	107	100	NL	NL	2.4	1.5	4.4	-	-
BbF	2-400	y = 0.0067x + 0.0015	0.9997	83.9	78.1	85.6	NL	NL	3.4	8.8	8.7	-	-
BkF	2-400	y = 0.0056x + 0.0028	0.9996	88.1	80.7	90.3	NL	NL	3.4	6.0	12	-	-
BaP	10-1000	y = 0.0033x - 0.057	0.9915	122	92.3	100	NL	NL	5.1	4.5	13	-	-
InP	4-1000	y = 0.0018x - 0.040	0.9917	82.9	80.4	71.2	NL	NL	4.2	7.6	11	-	-
D(ah)A	10-200	y = 0.0012x + 0.00070	0.9967	113	79.3	96.2	NL	NL	6.0	10	21	-	-
BGP	10-200	y = 0.0015x - 0.013	0.9971	101	79.3	86.3	NL	NL	2.1	19	17	-	-

<sup>a</sup> Spiked concentrations of PAHs in synthetic river water are from 1.0 to 50000 pg mL<sup>-1</sup>, and Naph-d8, Ace-d10 and Phen-d10 at 1000 pg mL<sup>-1</sup> and Chry-d12 at 100 pg mL<sup>-1</sup>.

<sup>b</sup> Not quantifiable

<sup>c</sup> Nonlinear

**Table 2.6.** Matched calibration data for analysing Harbour sample (n=3).

PAHs	Linear range <sup>a</sup>	Function	R <sup>2</sup>	Accuracy (%)					Precision (%)				
				15	80	250	2500	25000	15	80	250	2500	25000
Naph	100-50000	$y = 0.0012x - 0.27$	0.9990	NQ <sup>b</sup>	NQ	108	93.3	92.9	-	-	1.1	1.5	1.3
Acy	200-50000	$y = 0.00010x + 0.00070$	0.9997	NQ	NQ	137	117	108	-	-	2.0	2.6	2.4
Ace	200-50000	$y = 0.00080x + 0.11$	0.9992	NQ	NQ	126	105	99.5	-	-	1.4	2.6	1.5
Flu	200-20000	$y = 0.0036x + 0.28$	0.9998	NQ	NQ	123	109	95.4	-	-	6.6	3.5	5.4
Phen	100-50000	$y = 0.0010x + 0.49$	0.9981	NQ	NQ	117	105	94.9	-	-	1.8	2.3	2.6
Ant	400-50000	$y = 0.00050x + 0.28$	0.9961	NQ	NQ	NQ	135	119	-	-	-	2.7	2.3
Flut	40-50000	$y = 0.0014x + 0.55$	0.9989	NQ	125	120	108	90.9	-	6.6	4.0	3.3	4.6
Pyr	40-50000	$y = 0.0015x + 0.24$	0.9998	NQ	126	123	115	96.7	-	7.1	3.3	3.1	6.7
BaA	100-10000	$y = 0.017x - 5.9$	0.9932	NQ	121	89.0	80.1	89.4	-	7.4	2.1	0.50	5.5
Chry	20-2000	$y = 0.010x + 0.039$	0.9995	NQ	116	112	98.1	NL <sup>c</sup>	-	5.7	0.90	1.3	-
BbF	20-2000	$y = 0.0079x - 0.31$	0.9947	NQ	94.7	87.2	107	NL	-	16	5.7	4.7	-
BkF	20-1000	$y = 0.0057x - 0.015$	0.9996	NQ	89.7	97.1	99.5	NL	-	14	3.9	1.6	-
BaP	40-2000	$y = 0.0046x - 0.31$	0.9928	NQ	109	108	NL	NL	-	17	4.4	-	-
InP	40-2000	$y = 0.0017x - 0.10$	0.9940	NQ	117	81.2	81.8	NL	-	9.0	3.7	3.7	-
D(ah)A	2-200	$y = 0.0013x - 0.0033$	0.9977	93.2	88.0	98.3	NL	NL	5.8	23	5.3	-	-
BGP	2-200	$y = 0.0012x - 0.0049$	0.9966	107	76.5	79.4	NL	NL	9.2	15	5.0	-	-

<sup>a</sup> Spiked concentrations of PAHs in synthetic seawater are from 1.0 to 50000 pg mL<sup>-1</sup>, and Naph-d8, Ace-d10 and Phen-d10 at 1000 pg mL<sup>-1</sup> and Chry-d12 at 100 pg mL<sup>-1</sup>.

<sup>b</sup> Not quantifiable

<sup>c</sup> Nonlinear

To evaluate the applicability of the proposed thin film extraction using matrix-matched calibration, extraction tests in two different real samples including sea water and river water samples, were carried out. The samples were fortified with 15 pg mL<sup>-1</sup>, 80 pg mL<sup>-1</sup>, 250 ng mL<sup>-1</sup>, 2500 pg mL<sup>-1</sup> and 25000 pg mL<sup>-1</sup> of 16 PAHs pretreated under optimum extraction conditions. To calculate the enriched analytes in the real water samples, the matrix-matched calibrations (Table 2.5 and 2.6) obtained in synthetic river water and synthetic sea water were used. The results show that the extracted PAH amounts are in good correlation with the spiked amounts suggesting that these constructed calibration curves can be used for real sample analysis.

Furthermore, matrix effect was evaluated by defining relative error percentage for five spiking solutions (listed in Table 2.7) as shown below:

$$E\% = \frac{RC_{RS} - RC_{DW}}{RC_{DW}} \times 100$$

$RC_{RS}$  = Recovered concentration from real sample calculated by matrix-matched calibration curve

$RC_{DW}$  = Recovered concentration from real sample calculated by standard calibration curve

The relative error of recovered concentrations for real samples obtained by matrix-matched calibration was compared to the recovered concentration according to the calibration curves obtained in DI water. The matrix is more challenging for high MW PAHs which confirms using DI water as extracting solution, the external calibration curves contain major errors which can be eliminated by using synthetic water to spike the analytes and perform extraction and quantitation.

**Table 2.7.** Matrix effect assessment for real water samples.

PAHs	E%- Harbor sample					E%- Waterford river sample				
	15 (pg mL <sup>-1</sup> )	80 (pg mL <sup>-1</sup> )	250 (pg mL <sup>-1</sup> )	2.5 (ng mL <sup>-1</sup> )	25 (ng mL <sup>-1</sup> )	15 (pg mL <sup>-1</sup> )	80 (pg mL <sup>-1</sup> )	250 (pg mL <sup>-1</sup> )	2.5 (ng mL <sup>-1</sup> )	25 (ng mL <sup>-1</sup> )
Naph	-	-	18	11	11	-	-	-	5	5
Acy	-	-	22	14	13	-	-6	-9	-11	-11
Ace	-	-	29	10	8	-	15	-10	-18	-18
Flu	-	-	46	29	27	-	-	52	24	22
Phe	-	-	1	1	1	-	-	-2	-3	-3
Ant	-	-	-	25	23	-	-	3	-3	-4
Flut	-	3	-1	-2	-3	-	-	-9	-14	-16
Pyr	-	25	7	1	0	-	-	2	-9	-14
BaA	-	12	-11	-22	-23	5	-1	-2	-2	-
Chry	-	15	14	14	-	6	3	2	-	-
BbF	-	42	43	43	-	33	52	55	-	-
Bkf	-	83	85	85	-	71	83	85	-	-
BaP	-	120	108	-	-	126	114	111	-	-
InP	-	344	184	123	-	59	148	120	-	-
DB(ah)A	142	174	179	-	-	137	131	130	-	-
BGP	25	122	176	-	-	115	148	156	-	-

Natural river (Waterford River) and harbour water (St. John's Harbour) samples were analyzed for baseline contamination or interferences prior to the experiments to assess method recovery from real samples (see above). Although both samples showed PAHs levels below LOQ or LOD, one could expect to detect some PAHs in these samples. To provide an estimate of the amounts, relative peak area data for 2 pg PAHs mL<sup>-1</sup> in matched-matrices are presented in Figure 2.13 with data for the natural waters. Detectable amounts of all PAHs were seen in the urban river water sample, with Naph most prominent. The sample was collected during a rainy period in which- run-off from roads is a likely source of contamination. Similarly, the harbour samples show many of the PAHs, though with a different distribution than the river water sample. For example, none of the 3 heaviest PAHs were detected, and Naph was lower and Chry was higher than in the river water sample. St. John's harbour is a working harbour and one would expect to see inputs of PAHs from marine diesel and urban run-off.

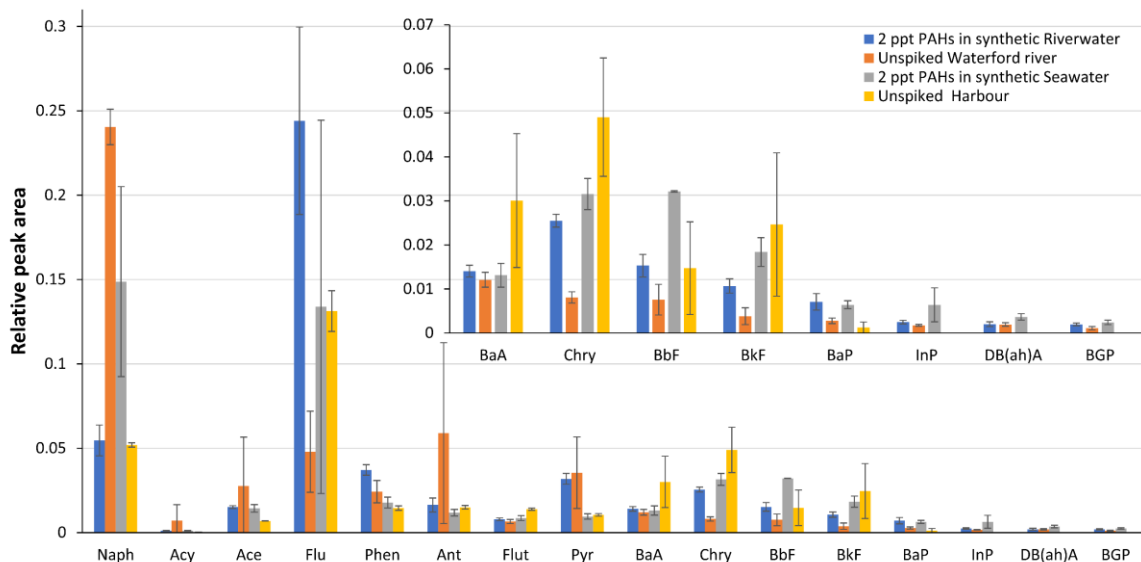


**Figure 2.13.** Comparison of relative peak area obtained for matched matrices at added concentration of 2 pg mL<sup>-1</sup> of PAHs and real samples.

## 2.4. Conclusion

A high throughput analytical method using a porous polymeric film was employed for the extraction of 16 PAHs in real water samples. The adsorptive coating was prepared via straightforward and inexpensive process in comparison to commercially-available thin film sorbents. The extraction and desorption processes optimized for efficiency and method sensitivity.

The extraction method affords high throughput and quick sample preparation, we prepared 18 samples (extraction, desorption, evaporation, and reconstitution) in 75 min, which would provide a sample for GC-MS/MS every 5 min. The only drawback of this method is that some specialized equipment, like a multi-position stirrer, are required to process many samples quickly. However, this is also an opportunity for flexible scale-up, for example, the sorption devices can be adapted for use with a 96-well plate sample system to automate this method and further increase throughput. Trace analysis of 16 Priority PAHs was achieved with good precision and accuracy at levels that easily meet regulatory criteria, with the added value of small sample volumes (20 mL) and reduced organic solvents ( $\leq 1.5$  mL) over current analytical protocols. Matrix-matched calibration was effective in the analysis of real sea and river waters, circumventing the requirement for tedious standard addition analysis. These thin film devices can be deployed for on-site sampling either using portable stirrers or in a flow through device.

Although intended for single use, reusability was also evaluated with good results for a minimum of 5 consecutive extractions. Arising from porous morphology of the

polymeric thin films, the desorption process is fast with no carry over; this eliminates the need for supplementary treatment steps to remove residual compounds before reuse.

## 2.5. References

- [1] O. World Health, Polynuclear aromatic hydrocarbons in Drinking-water, Background document for development of WHO Guidelines for Drinking-water Quality. Geneva: WHO (2003).
- [2] J. Godheja, S.K. Shekhar, D.R. Modi, Biodegradation of one ring hydrocarbons (benzene and toluene) and two ring hydrocarbons (acenaphthene and naphthalene) by bacterial isolates of hydrocarbon contaminated sites located in chhattisgarh: a preliminary study, *J. Pet. Environ. Biotechnol.* 6(1) (2015) 1.
- [3] K.-H. Kim, S.A. Jahan, E. Kabir, R.J.C. Brown, A review of airborne polycyclic aromatic hydrocarbons (PAHs) and their human health effects, *Environ. Int.* 60 (2013) 71-80.
- [4] J. Siemiatycki, L. Richardson, K. Straif, B. Latreille, R. Lakhani, S. Campbell, M.-C. Rousseau, P. Boffetta, Listing occupational carcinogens, *Environ. Health Perspect.* 112(15) (2004) 1447.
- [5] O. Water, Edition of the Drinking Water Standards and Health Advisories, EP Agency (ed.) (2012).
- [6] E.U. Parliament, Directive 2008/105/EC of the European Parliament and of the Council of 16 December 2008 on environmental quality standards in the field of water policy, amending and subsequently repealing, *Official Journal of the European Union*, L 348 (2008) 84-97.
- [7] C. Directive, 98/83/EC of 3 November 1998 on the quality of water intended for human consumption, ed, E. Union (1998).
- [8] D.M. Brum, R.J. Cassella, A.D.P. Netto, Multivariate optimization of a liquid-liquid extraction of the EPA-PAHs from natural contaminated waters prior to determination by liquid chromatography with fluorescence detection, *Talanta* 74(5) (2008) 1392-1399.
- [9] M. Biziuk, A. Przyjazny, J. Czerwinski, M. Wiergowski, Occurrence and determination of pesticides in natural and treated waters, *J. Chromatogr. A* 754(1-2) (1996) 103-123.

- [10] J.N. Brown, B.M. Peake, Determination of colloiddally-associated polycyclic aromatic hydrocarbons (PAHs) in fresh water using C18 solid phase extraction disks, *Anal. Chim. Acta* 486(2) (2003) 159-169.
- [11] J.J. Vreuls, A.J.H. Louter, U.A.T. Brinkman, On-line combination of aqueous-sample preparation and capillary gas chromatography, *J. Chromatogr. A* 856(1-2) (1999) 279-314.
- [12] N. Li, H.K. Lee, Solid-phase extraction of polycyclic aromatic hydrocarbons in surface water: negative effect of humic acid, *J. Chromatogr. A* 921(2) (2001) 255-263.
- [13] R.M. Smith, Before the injection—modern methods of sample preparation for separation techniques, *J. Chromatogr. A* 1000(1-2) (2003) 3-27.
- [14] R.-a. Doong, S.-m. Chang, Y.-c. Sun, Solid-phase microextraction for determining the distribution of sixteen US Environmental Protection Agency polycyclic aromatic hydrocarbons in water samples, *J. Chromatogr. A* 879(2) (2000) 177-188.
- [15] I. Domínguez, F.J. Arrebola, R. Gavara, J.L.M. Vidal, A.G. Frenich, Automated and simultaneous determination of priority substances and polychlorinated biphenyls in wastewater using headspace solid phase microextraction and high resolution mass spectrometry, *Anal. Chim. Acta* 1002 (2018) 39-49.
- [16] A. Naccarato, E. Gionfriddo, R. Elliani, J. Pawliszyn, G. Sindona, A. Tagarelli, Investigating the robustness and extraction performance of a matrix-compatible solid-phase microextraction coating in human urine and its application to assess 2–6-ring polycyclic aromatic hydrocarbons using GC–MS/MS, *J. Sep. Sci.* 41(4) (2018) 929-939.
- [17] Z. Qin, L. Bragg, G. Ouyang, V.H. Niri, J. Pawliszyn, Solid-phase microextraction under controlled agitation conditions for rapid on-site sampling of organic pollutants in water, *J. Chromatogr. A* 1216(42) (2009) 6979-6985.
- [18] J. Gao, C. Huang, Y. Lin, P. Tong, L. Zhang, In situ solvothermal synthesis of metal–organic framework coated fiber for highly sensitive solid-phase microextraction of polycyclic aromatic hydrocarbons, *J. Chromatogr. A* 1436 (2016) 1-8.
- [19] I. Bruheim, X. Liu, J. Pawliszyn, Thin-film microextraction, *Anal. Chem.* 75(4) (2003) 1002-1010.
- [20] R. Jiang, J. Pawliszyn, Preparation of a particle-loaded membrane for trace gas sampling, *Anal. Chem.* 86(1) (2013) 403-410.
- [21] F.S. Mirnaghi, Y. Chen, L.M. Sidisky, J. Pawliszyn, Optimization of the coating procedure for a high-throughput 96-blade solid phase microextraction system coupled with LC–MS/MS for analysis of complex samples, *Anal. Chem.* 83(15) (2011) 6018-6025.

- [22] E. Boyacı, J. Pawliszyn, Micelle assisted thin-film solid phase microextraction: a new approach for determination of quaternary ammonium compounds in environmental samples, *Anal. Chem.* 86(18) (2014) 8916-8921.
- [23] N. Reyes-Garcés, B. Bojko, J. Pawliszyn, High throughput quantification of prohibited substances in plasma using thin film solid phase microextraction, *J. Chromatogr. A* 1374 (2014) 40-49.
- [24] N. Reyes-Garcés, B. Bojko, D. Hein, J. Pawliszyn, Solid phase microextraction devices prepared on plastic support as potential single-use samplers for bioanalytical applications, *Anal. Chem.* 87(19) (2015) 9722-9730.
- [25] S.N. Egli, E.D. Butler, C.S. Bottaro, Selective extraction of light polycyclic aromatic hydrocarbons in environmental water samples with pseudo-template thin-film molecularly imprinted polymers, *Anal. Methods* 7(5) (2015) 2028-2035.
- [26] N. Kirschner, A.N. Dias, D. Budziak, C.B. da Silveira, J. Merib, E. Carasek, Novel approach to high-throughput determination of endocrine disruptors using recycled diatomaceous earth as a green sorbent phase for thin-film solid-phase microextraction combined with 96-well plate system, *Anal. Chim. Acta* 996 (2017) 29-37.
- [27] E.A. Souza-Silva, R. Jiang, A. Rodriguez-Lafuente, E. Gionfriddo, J. Pawliszyn, A critical review of the state of the art of solid-phase microextraction of complex matrices I. Environmental analysis, *TrAC, Trends Anal. Chem.* 71 (2015) 224-235.
- [28] H. Piri-Moghadam, M.N. Alam, J. Pawliszyn, Review of geometries and coating materials in solid phase microextraction: opportunities, limitations, and future perspectives, *Anal. Chim. Acta* 984 (2017) 42-65.
- [29] M.N. Alam, J. Pawliszyn, Numerical simulation and experimental validation of calibrant-loaded extraction phase standardization approach, *Anal. Chem.* 88(17) (2016) 8632-8639.
- [30] N. Zhang, C. Huang, P. Tong, Z. Feng, X. Wu, L. Zhang, Moisture stable Ni-Zn MOF/g-C<sub>3</sub>N<sub>4</sub> nanoflowers: A highly efficient adsorbent for solid-phase microextraction of PAHs, *J. Chromatogr. A* 1556 (2018) 37-46.
- [31] A.M.d. Almeida, M.M. Castel-Branco, A.C. Falcao, Linear regression for calibration lines revisited: weighting schemes for bioanalytical methods, *J. Chromatogr. B* 774(2) (2002) 215-222.
- [32] Y. Hu, Y. Yang, J. Huang, G. Li, Preparation and application of poly(dimethylsiloxane)/ $\beta$ -cyclodextrin solid-phase microextraction membrane, *Anal. Chim. Acta* 543(1-2) (2005) 17-24.

[33] N.H. Mukhtar, H.H. See, Carbonaceous nanomaterials immobilised mixed matrix membrane microextraction for the determination of polycyclic aromatic hydrocarbons in sewage pond water samples, *Anal. Chim. Acta* 931 (2016) 57-63.

[34] P.E. Grimmett, J.W. Munch, Development of EPA Method 525.3 for the analysis of semivolatiles in drinking water, *Anal. Methods* 5(1) (2013) 151-163.

[35] W. Ben, Z. Qiang, C. Adams, H. Zhang, L. Chen, Simultaneous determination of sulfonamides, tetracyclines and tiamulin in swine wastewater by solid-phase extraction and liquid chromatography–mass spectrometry, *J. Chromatogr. A* 1202(2) (2008) 173-180.

**Chapter 3: Thin film molecularly imprinted polymer (TF-MIP),  
a selective and single-use extraction device for high-throughput  
analysis of biological samples**

Fereshteh Shahhoseini, Evan Langille, Ali Azizi, Christina Sheila Bottaro. “Thin film molecularly imprinted polymer (TF-MIP), a selective and single-use extraction device for high-throughput analysis of biological samples” *Analyst*, 2021, 146, 3157–3168

### 3.1. Introduction

Demand for a reliable, sensitive, inexpensive and high-throughput method for biological sample analysis has spurred an explosion in bioanalytical research [1-3]. The presence of many exogenous and endogenous macromolecules in biological matrices complicates instrumental analysis, which, along with the need for high sensitivity in both targeted and nontargeted analysis, necessitates efficient and selective sample preparation methods [4]. Even with revolutionary advances in sample preparation, e.g., solid phase microextraction (SPME) and other miniaturized techniques, it is still a major bottleneck in biological analysis. Moreover, even with the advantages offered by the newer approaches, conventional exhaustive sample preparation methods such as liquid-liquid extraction (LLE), solid phase extraction (SPE) and protein precipitation (PP) are preferred for routine biological analysis. These techniques are attractive because they are simple, and straightforward calibration methods can be used for quantification. For example, protein precipitation is fast, using sample dilution, and the measurement is based mainly on instrumental calibration data, however, analytes can co-precipitate with the protein and other potential interferents may be left in the sample [5].

Recently developed biological sample preparation methods include SPME [6], stir bar sorptive extraction (SBSE) [7], microextraction by packed sorbent (MEPS) [8, 9], polymeric tablets [10], hollow fiber liquid phase microextraction (HF-LPME) [11], dispersive liquid-liquid microextraction (DLLME) [12], and electro membrane extraction (EME) [13]. The ultimate goals of all of the recent improvements in sample preparation are reducing the amount of solvent and sample, decreasing the sample processing steps and

time, and adding other labour-saving features, such as on-line and automatic coupling to chromatographic instruments [14]. Among these techniques, SPME is considered to be the leading microextraction technique because of its suitability for analysis of small sample volumes, ease of use, and direct sample introduction. This has driven demand for SPME devices giving rise to a range of commercially-available SPME fibers [15] and development of various formats such as thin film [16], and in-tube [17]. However, applications for routine clinical testing remains challenging due to the expense of the devices and demanding protocols for reuse [18]. Although single-use microextraction devices have been reported [19], reusable devices are more common due to their expensive fabrication costs and high inter-device variability [20], which has also hampered commercialization. Moreover, many microextraction techniques are non-selective, which can be inefficient for reduction of matrix effects from complex biological samples [21]. The chemistry of the sorptive material determines the selectivity of a sample preparation method, therefore, single use extraction devices made with selective adsorption phases are appealing.

Molecularly imprinted polymers (MIPs) have attracted great attention during the last two decades by providing a unique mode of selectivity for adsorption of analytes. These selective sorbents are generated by polymerizing functional monomers and crosslinkers around a template molecule(s) in the presence of a porogen. Following polymerization, the template is removed from the crosslinked polymer leaving cavities with size, shape, and functionalities complementary to the template or analogous compounds [22]. Besides the inherent selectivity of MIPs, these robust materials can be fabricated into different formats (i.e., bulk polymers, beads, particles, films) [23]. Consequently, MIPs have been

incorporated into SPE, SPME, MEPS, solid phase extraction in pipette tips (PT-SPE), and magnetic molecularly imprinted solid phase extraction (MMIPSPE) for pharmaceutical and biomedical analysis [24]. Of these techniques, SPME offers the greatest opportunity for high throughput methods with minimal sample manipulation and single-use devices free from the complications of carry-over. Traditionally lengthy and complex fabrication methods have impeded the development of single-use MIP-SPME devices, however, thin film MIPs introduced by our group are easy to fabricate reproducibly and have performed well in complex environmental samples [25-32]. The single-use application avoids memory effects, which is one of the main limitations of SPME fibers. In this study, we demonstrate the immense potential of thin film MIPs for biological analysis.

To the best of our knowledge, implementation of MIPs in thin film format has never been reported for the analysis of pharmaceuticals in biological samples, specifically human plasma. As a proof of concept, a thin film MIP developed for tricyclic antidepressants (TCAs) drugs was utilized for the analysis of their free concentration in human plasma. TCAs obstruct the reuptake of serotonin in presynaptic neurons [33]. Intoxication caused by TCAs can result in many serious symptoms such as sinus tachycardia, cardiac conduction abnormalities, vasodilation, arrhythmias, hypotension, delirium, drowsiness, coma, respiratory depression and seizure [34, 35]. Therapeutic drug monitoring (TDM) of TCAs is necessary to determine the optimum individual dose, increase the therapeutic efficiency, reduce the risk of intoxication and increases patient compliance. The necessity of TDM for these drugs can be justified by broad interindividual pharmacokinetic variability [36]. The therapeutic serum concentration ranges are relatively narrow: 20-300 ng mL<sup>-1</sup> for amitriptyline and nortriptyline [37], 15-500 ng mL<sup>-1</sup> for the sum of imipramine

and its active metabolite (desipramine) [38], 50-250 ng mL<sup>-1</sup> for doxepin [39], and 100-250 ng mL<sup>-1</sup> for clomipramine [40]; a threshold of 125 ng mL<sup>-1</sup> has been reported for desipramine alone [41]. The upper limits of these ranges are near to toxic concentrations, which have been reported at >250-1000 µg L<sup>-1</sup> [42].

The goal of this study is to introduce an efficient single-use, fast, user-friendly, robust, and selective extraction device by combining the advantages of an open-bed film geometry with a high-performance MIP sorbent for drug analysis in biological samples.

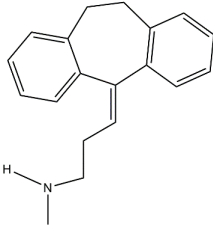
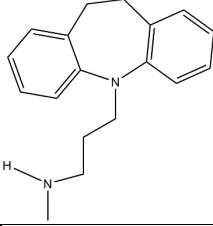
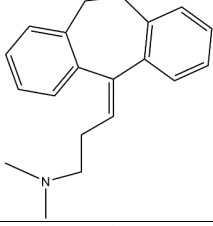
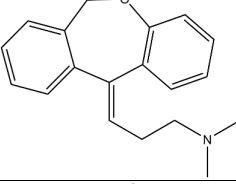
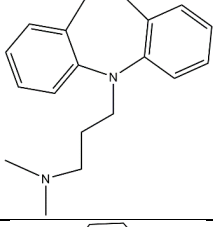
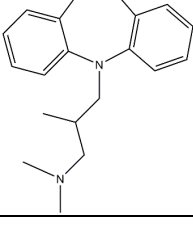
## **3.2. Experimental**

### **3.2.1. Materials and reagents**

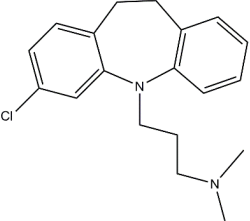
Standard solutions of amitriptyline (Ami), imipramine (Imi), clomipramine (Clo), desipramine (Des), doxepin (Dox), trimipramine (Tri), nortriptyline (Nor) 1 mg mL<sup>-1</sup> in acetonitrile (ACN) and imipramine-D3 (Imi-D3) reference solution with concentration of 0.1 mg mL<sup>-1</sup> were purchased from Cerilliant (Round Rock, TX, USA). The structures of the studied TCAs along with pK<sub>a</sub> and logP data are presented in Table 3.1. ACN, methanol (MeOH), and formic acid (FA), all Optima LC-MS grade, as well as reagent grade methacrylic acid (MAA), acetic acid, triethylamine (TEA) and ethylene glycol dimethacrylate (EGDMA) were obtained from Fisher Scientific (Whitby, Canada). 2,2-Dimethoxy-2-phenylacetophenone (DMPA, 99%), and 1-octanol (>99%) and desipramine hydrochloride (98%) were purchased from Sigma Aldrich (Oakville, Canada). Stainless steel substrate for producing thin film devices were purchased from McMaster Carr

(Douglasville, GA, US). Ultrapure water ( $18.2 \text{ M}\Omega \text{ cm}^{-1}$ ) was produced in-house with a Milli-Q purification system (Millipore, Sigma-Aldrich, Oakville, Canada).

**Table 3.1.** Target drugs and physical chemical properties

Compound	Structure	pKa	LogP*
Nortriptyline		10.1	4.51
Desipramine		10.4	4.90
Amitriptyline		9.4	4.92
Doxepin		8.96	4.29
Imipramine		9.4	4.80
Trimipramine		9.42	4.2

**Table 1.3.** (continued)

<b>Clomipramine</b>		8.98	5.19
---------------------	---	------	------

\* logP: log K<sub>o/w</sub>, (octanol–water partition coefficient)

Phosphate-buffered saline solution (PBS) contains 137 mM NaCl, 2.7 mM KCl, 8 mM Na<sub>2</sub>HPO<sub>4</sub>, and 2 mM KH<sub>2</sub>PO<sub>4</sub> (pH = 7.4) was purchased from Fisher Scientific (Whitby, ON, Canada) and diluted (×10) with ultra-pure water before usage. Lyophilized bovine serum albumin (BSA) from Hyclone laboratories Inc. (Whitby, ON, Canada) was prepared in diluted PBS to yield 5 % BSA (w/v). Dissolving the BSA with PBS solution can result in a more similar representative of biological fluidics. Human pooled and individual plasma and patient samples supplied from BioIVT (Westbury, United States). Health Research Ethics Authority (HREA) at Memorial University of Newfoundland has approved this work and deemed that this work is not subject to Health Research Ethics Board (HREB) ethics review.

### 3.2.2. Instrumentation and operating conditions

Separation and quantification of TCAs was performed using an Acquity ultra high-performance liquid chromatography (UHPLC) system with an Acquity BEH C<sub>18</sub> column (2.1 mm× 150 mm, 1.7 μm) maintained at 30.0 °C. The UHPLC was coupled to a Xevo TQ-S tandem MS (Waters Corporation) equipped with a Z-spray electrospray ionization (ESI) source. Samples were maintained in the autosampler at 4 °C and injections (1-μL) were made using a sample manager flow-through needle (SM-FTN). Separations were

achieved with isocratic elution at 50% ACN containing 0.1 % formic acid in water. MS/MS measurements were conducted in positive ionization mode under multiple reaction monitoring (MRM) conditions. MRM transitions, cone voltages and collision energy used for all compounds are included in Table 3.2. Nitrogen gas was supplied by a generator (Peak Scientific, Scotland, UK) and was used as both cone and desolvation gases, with flow rates of 150 and 1000 L h<sup>-1</sup>, respectively. Other important MS parameters were: capillary voltages, +3.5 kV; source temperature, 150 °C; and desolvation temperature, 500°C.

**Table 3.2.** Summary of tandem mass spectrometry parameters of TCAs using LC-MS/MS

TCAs	Precur sor ion ( <i>m/z</i> )	Cone voltage (V)	Product ion 1 ( <i>m/z</i> )	Collision energy (eV)	Product ion 2 ( <i>m/z</i> )	Collision energy (eV)
Nortriptyline	264.3	25	233.2	18	105.0	24
Desipramine	267.1	25	208.1	24	72.1	18
Amitriptyline	278.1	35	117.1	28	91.0	26
Doxepin	280.1	35	235.1	28	107.0	28
Imipramine	281.1	25	85.9	20	58.1	35
Imipramine-D3	284.2	30	208.2	30	89.1	15
Trimipramine	295.1	35	192.8	56	100.0	24
Clomipramine	315.1	35	85.9	24	58.0	42

Scanning electron microscopy (SEM) micrographs of thin films were obtained via a Quanta 650 FEG (field emission gun) SEM (Field Electron and Ion company, OR, USA). Nitrogen (N<sub>2</sub>) measurements were conducted at 77 K by a TriStar II Plus (Micromeritics, Norcross, GA, USA).

### 3.2.3. Preparation of the pseudo template

In a 500 mL round bottom flask, 15.00 g desipramine hydrochloride (1 eq, 0.05 mol) was dissolved in 200 mL THF and 85 mL 2 M NaOH with stirring under nitrogen. Benzyl Chloroformate (7.4 mL, 1.2 eq, 0.056 mol) was then added dropwise over ten minutes. The reaction was stirred overnight at room temperature under nitrogen. The biphasic mixture was transferred to a separatory funnel and allowed to separate. The organic phase was collected, and the aqueous phase was washed three times with 50 mL of ethyl acetate. The pooled organic phases were dried with anhydrous magnesium sulfate and evaporated to dryness under reduced pressure. The crude mixture was then purified by flash chromatography using a SiliaSep bare silica, 25  $\mu\text{m}$  (550 mesh), 90  $\text{\AA}$  cartridge. An isocratic elution consisting of 70:30 hexanes: ethyl acetate was used to elute the pure compound ( $R_f = 0.6$ ). The collected fractions were monitored for purity using thin layer chromatography (SiliaPlate 200  $\mu\text{m}$ , 3 x 6 cm, with F254 UV). The pure product, benzyl (3-(10,11-dihydro-5H-dibenzo[b,f]azepin-5-yl)propyl)(methyl)carbamate (CBZ-desipramine) (Figure 3.1) was obtained as a clear colorless oil (19.43g, 97%). The product was characterized by high resolution MS and  $^1\text{H}$  NMR. MS (ESI)  $m/z$  called. for  $[\text{C}_{26}\text{H}_{28}\text{N}_2\text{O}_2]^+$ : 400.21508  $[\text{M}+\text{H}]^+$ ; found: 400.21524;  $\delta = 0.41$  ppm.  $^1\text{H}$  NMR (500 MHz, Chloroform-d)  $\delta$  7.33 (tt,  $J = 11.1, 3.7$  Hz, 3H), 7.32 – 7.24 (m, 2H), 7.09 (dd,  $J = 16.5, 7.9$  Hz, 6H), 6.99 (d,  $J = 8.2$  Hz, 1H), 6.90 (td,  $J = 7.3, 1.3$  Hz, 2H), 5.09 (s, 1H), 4.99 (s, 1H), 3.72 (dt,  $J = 20.8, 5.8$  Hz, 2H), 3.35 – 3.27 (m, 2H), 3.15 (s, 1H), 3.11 (d,  $J = 5.3$  Hz, 2H), 2.78 (d,  $J = 12.1$  Hz, 3H), 1.79 (dt,  $J = 14.5, 7.1$  Hz, 2H).

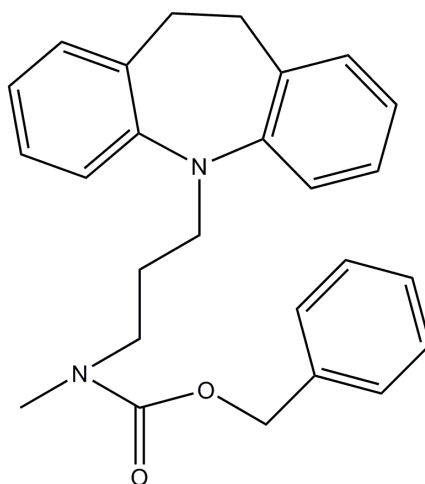


**Figure 3.1.** Chemical structure of benzyl (3-(10,11-dihydro-5H-dibenzo[b,f]azepin-5-yl)propyl)(methyl)carbamate

#### 3.2.4. Preparation of thin film MIPs

The drop casting method used here to fabricate the thin film MIPs has been reported in our previous papers [31], though the substrate is stainless steel rather than glass, and the shape of the device is modified ( $5 \times 25 \text{ mm}^2$  in a sword shape) to fit autosampler vials with a 750- $\mu\text{L}$  fused insert (micro-insert vials). Specifics of the fabrication method are as follows (See Figure 3.2). An aliquot of the pre-polymerization solution (3  $\mu\text{L}$ ) was pipetted onto the steel blades, which were cleaned with detergent and methanol and dried with nitrogen and covered with an 18  $\text{mm}^2$  cover glass. The pre-polymerization solution was prepared by dissolving 0.2 mmol of the template benzyl (3-(10,11-dihydro-5H-dibenzo[b,f]azepin-5-yl)propyl)(methyl)carbamate (a pseudo-TCA, CBZ-desipramine, 70  $\mu\text{L}$ ), 0.8 mmol (68  $\mu\text{L}$ ) of MAA (functional monomer), 4.8 mmol (906  $\mu\text{L}$ ) of EGDMA (crosslinker) in 1000  $\mu\text{L}$  1-octanol. MIPs commonly use the target analyte as the template for imprinting. However, for trace analysis this represents an unacceptable risk of false positive results due to

template bleeding even with exhaustive template removal steps. This is avoided by use of a pseudo-template. The photo initiator (DMPA, 16 mg) was added to the prepared solution followed by vortex mixing then degassing in an ultrasonic bath (5 min) to remove oxygen that can interfere with radical polymerization. The sandwiched layer of pre-polymer was exposed to UV (365 nm) for 30 min; then the cover glass was removed. The template was extracted from each batch of MIP films dynamically using a mixture of 0.1 % FA in 50% aqueous ACN until no template was detected in the wash solution. Template bleed was assessed for each batch using 3 MIP-coated blades each immersed in 700  $\mu\text{L}$  of 0.1 % FA in 50% aqueous ACN for 20 min agitated at 500 rpm, then the solution was analyzed by LC-MS/MS analysis. To assess the efficiency and selectivity of thin film MIPs, non-imprinted polymer (NIP) thin films were fabricated using the same procedure, but in the absence of the template molecule in pre polymerization solution.

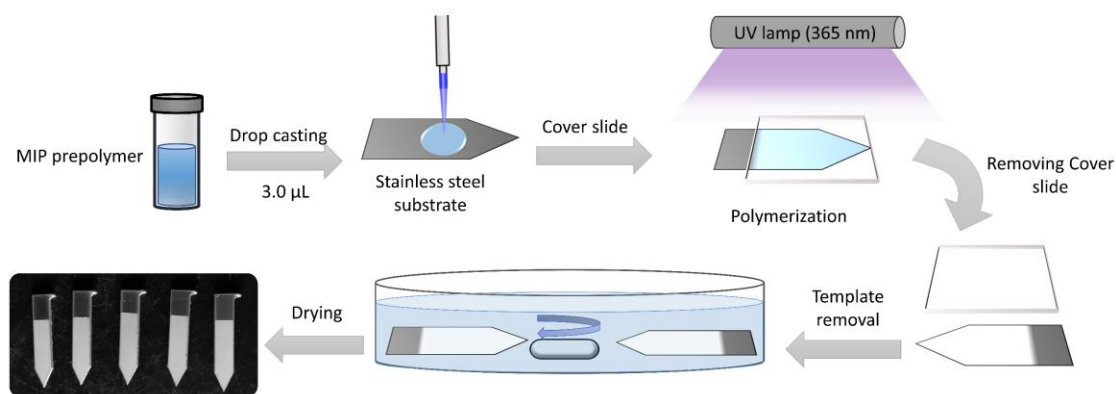


**Figure 3.2.** Fabrication of thin film MIP using drop casting technique

### 3.2.5. Optimization of MIP composition

The performance of the various MIP formulas was assessed by measuring extraction efficiency from 20 mL of TCA spiked (each at 50  $\text{ng mL}^{-1}$ ) aqueous TEA (1%). The

targeted TCAs are weakly basic (their hydrochloride salts are weakly acidic with  $pK_a$  values from 8.96 to 10.4), thus extraction efficiencies can be improved by adjusting the pH ( $> pK_a$ ) with TEA to yield the neutral form [43, 44]. Batch extractions using individual devices positioned with a plastic holder were carried out with a multi-position magnetic stirrer for 1-h stirring at 1000 rpm. After extraction, the thin films were rinsed with  $\sim 0.5$  mL ultrapure water then transferred into micro-insert vials containing 700  $\mu\text{L}$  of methanol for analyte desorption. Internal standard solution was spiked in the desorption solvent at the final concentration of 50  $\text{ng mL}^{-1}$  to verify for any error from the desorption and ionization process but not considered for calculation of presented data. The desorption was completed using a multi-vortex agitated at 1000 rpm for 30 min. Following the desorption, thin film MIPs were removed from the vial and the solution was analyzed using LC-MS/MS.

### **3.2.6. Extraction of TCAs from biological samples using thin film MIPs**

For plasma and standards in BSA, sample volumes were reduced, and all extraction and desorption steps were carried out in micro-insert vials. The method is illustrated in Figure 3.3. Thin films were inserted in the vials containing 700  $\mu\text{L}$  of the biological sample (BSA or plasma, with TEA at 1%). The batch extraction process was conducted by vortex-agitation for 60 min at 1500 rpm, then the thin films were washed by immersion in 1% aqueous TEA for 8 s. Following washing, the thin films were dried, and adsorbed analytes were desorbed into 700  $\mu\text{L}$  of 0.1 % FA in 50% aqueous ACN for 20 min at 500 rpm. Extracts were filtered with a 0.2  $\mu\text{m}$  syringe filter and analyzed by LC-MS/MS.

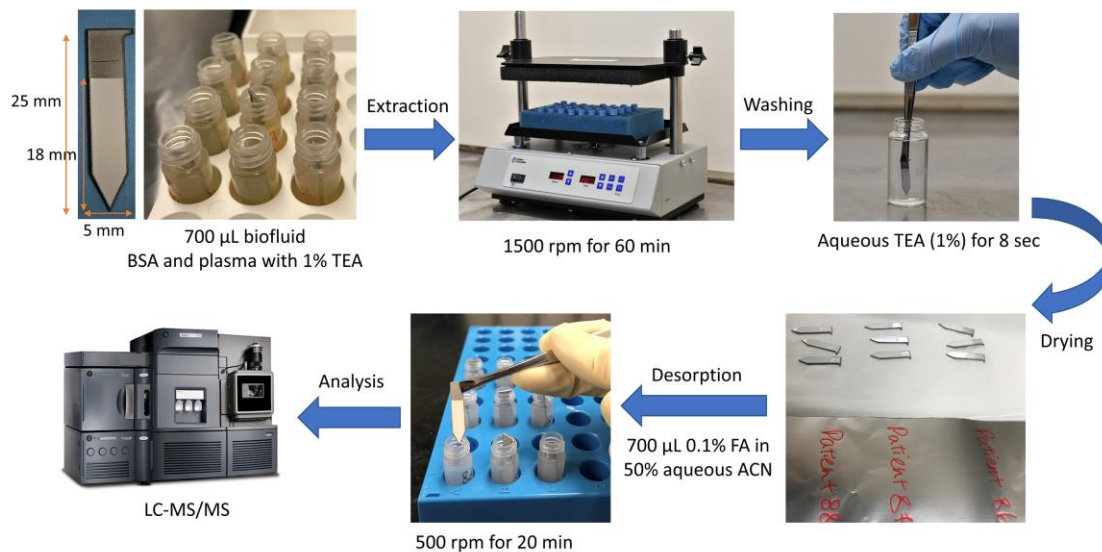


**Figure 3.3.** Experimental workflow for analysis of plasma samples using thin film MIPs.

### 3.3. Results and discussion:

#### 3.3.1. Preparation and characterization of thin film MIPs

Fabrication of the thin film extraction devices usually involves numerous tedious or lengthy processes, including preparation of substrate [45, 46], application of the prepolymer solution—which can be complex depending on the necessary format—and curing [47]. The last two steps frequently are repeated to build film thickness, improve coating homogeneity or introduce specialized selectivity [48]. However, in our approach casting thin film MIPs as thin porous monoliths allows for homogeneous film preparation in one cycle of prepolymer solution deposition and UV curing. We tested our thin film fabrication process on metal blades with no surface treatment as well as etched and sanded blades, with no difference in the quality of the coating. The stability of these coatings was also assessed using the harshest conditions we use for polymer preparation (methanol:

acetic acid, 9:1, v/v vortex mixed at 2000 rpm for 12 h) with no demonstrable damage e.g., no cracking or delamination from the substrate. The robustness of the coating is attributed to a well-controlled polymerization process achieved by the presented composition (high crosslinker ratio to monomer and other components in the prepolymer) and appropriate phase separation using octanol as porogen solvent. This crosslinked coating is stable and enables a uniform adhesion of the polymer to the substrate via physical attachment. This allowed us to prepare the thin films on an unmodified substrate eliminating the substrate preparation step and the need for corrosive reagents.

The main advantage of MIPs is the creation of selective binding sites that perform well in complex matrices. These sites are maximized with an optimal combination of functional monomer, template, and cross-linker in an optimal porogen. MAA was selected as the functional monomer because of its ability to establish hydrogen bonding with the pseudo-template (i.e., CBZ-desipramine). In this instance the MAA (pKa 4.8) forms the methacrylate anion at neutral pH and above, and the pseudo-template is cationic through protonation of the amine. This creates conditions for strong electrostatic interactions in the template-monomer complex. EGDMA, a water compatible crosslinker, improved porosity and film stability; MIPs made with MAA alone give a glassy non-porous coating. Octanol is an amphiphilic porogen chosen for its low volatility and its role in the formation of macro and mesoporous structures in the films [49]. Preliminary experiments identified the key factors influencing adsorption capacity and selectivity, which include the usual monomer-to-crosslinker and template-to-monomer ratios, but also the porogen volume relative to the amounts of monomer and crosslinker. Previous work by our group and others [50] has indicated that the relative volume of the porogen plays a significant role in polymer

porosity, binding site accessibility and surface area. The effect of diluting the prepolymer solution was investigated at fixed ratios of T:M:C (1:4:24) and a fixed mass of monomer and crosslinker, noting that the crosslinker mass (contributes most to the polymer mass, Table 3.3) is consistent for all films, except when varied in this study.

**Table 3.3.** Details of prepolymer solutions used for porogen dilution study.

Porogen volume	1000 $\mu\text{L}$	1200 $\mu\text{L}$	1300 $\mu\text{L}$
Monomer mass and volume	69.4 (68 $\mu\text{L}$ )		
Crosslinker mass and volume	950.3 mg (905 $\mu\text{L}$ )		
Total volume	1973 $\mu\text{L}$	2173 $\mu\text{L}$	2273 $\mu\text{L}$
Monomer + crosslinker mass /volume of prepolymerization solution (mg/ $\mu\text{L}$ )	0.52	0.47	0.45
Mass deposited on substrate (mg)	2.08	1.88	1.80

We found that films made using 800  $\mu\text{L}$  of porogen were glassy and unstable (cracked and delaminating), thus we compared only increased porogen volumes (i.e., 1200 and 1300  $\mu\text{L}$ ) relative to the initial conditions using 1000  $\mu\text{L}$ . Dilution leads to a slight reduction in the amount of polymer components deposited on the device (maximum estimated reduction in mass 15% Table 3.3), but has dramatic effects on selectivity (see imprinting factors (IF), Table 3.4) and adsorption capacity (Figure 3.4a and b). Looking first to Figure 3.4 a, the MIP and NIP films made with 1000  $\mu\text{L}$  showed the highest adsorption of the systems we studied, but the reproducibility was poor (high RSDs) and there was no evidence of imprinting (Table 3.4). Increasing the porogen volume to 1200  $\mu\text{L}$  resulted in a large decrease in the mass of analyte extracted (MIPs ~50%, NIPs>80%) across all targets, but impressive selectivity (IF 2.26 – 4.36). Further dilution to 1300  $\mu\text{L}$  yielded further loss in

adsorption and decreased selectivity. Even with the positive data for 1200  $\mu\text{L}$ , the error was higher than acceptable. Since the ionization of both the polymer and analytes depends on pH, we investigated extraction at higher pH. Increasing pH to  $\sim 11$  (1% TEA) will maximize the availability of anionic methacrylate moieties, while deprotonating the analytes to give their neutral form. Comparing the data in Figure 3.4 a and b, the mass of TCAs extracted is decreased for both MIPs and NIPs following pH adjustment regardless of porogen amount. This can be explained by the sorbent affinity (negative carboxylate anion) for the cationic form of the TCAs. Despite the decrease in extraction recoveries at pH 11, it is more important to evaluate repeatability and relative differences in extraction efficiencies between MIPs and NIPs as this reveals the degree of selectivity imparted by imprinting. The selectivity is essential in reducing non-selective interactions and interferences in analysis. For 1000  $\mu\text{L}$  of porogen, reproducibility was improved with increased pH from 30% to 10%. Though the extraction efficiency of the MIPs is decreased by a factor of two, the efficiency of the NIPs is reduced by four times. This suggests that pH adjustment reduces the non-selective electrostatic interactions in both MIPs and NIPs, but that the binding to imprinted sites in the MIPs is conserved. At higher dilutions (1200 and 1300  $\mu\text{L}$ ), similar losses in extraction recoveries are observed with pH adjustment but without the gains in selectivity or repeatability (Tables 3.4 and 3.5). For the balance of this work MIPs were made with 1000  $\mu\text{L}$  porogen.

**Table 3.4.** Effect of porogen volume on imprinting and repeatability of extraction of TCAs.

TCAs	Porogen volume					
	1000 $\mu$ L		1200 $\mu$ L		1300 $\mu$ L	
	No pH adj	pH adj	No pH adj	pH adj	No pH adj	pH adj
	IF ( $\pm$ SD)					
Nortriptyline	0.93 (0.35)	1.99 (0.24)	3.05 (1.32)	2.12 (0.61)	1.48 (0.51)	1.65 (0.49)
Desipramine	0.95 (0.33)	1.89 (0.27)	3.51 (1.58)	2.21 (0.63)	1.51 (0.55)	1.67 (0.48)
Amitriptyline	0.99 (0.34)	3.00 (0.42)	3.43 (1.63)	1.87 (0.86)	1.64 (0.61)	1.62 (0.49)
Doxepin	1.00 (0.33)	3.51 (0.65)	4.36 (2.24)	1.94 (0.89)	1.63 (0.67)	1.66 (0.48)
Imipramine	0.96 (0.33)	3.17 (0.48)	3.84 (1.78)	1.93 (0.85)	1.58 (0.57)	1.64 (0.46)
Trimipramine	0.96 (0.32)	2.76 (0.32)	3.78 (1.80)	1.73 (0.82)	1.52 (0.54)	1.60 (0.56)
Clomipramine	0.89 (0.34)	2.23 (0.19)	2.25 (0.97)	1.58 (0.84)	1.38 (0.46)	1.59 (0.59)

**Table 3.5.** Effect of porogen volume on recovery and repeatability of extraction of TCAs using MIPs and NIPs

TCAs	Porogen volume											
	1000 $\mu$ L				1200 $\mu$ L				1300 $\mu$ L			
	No pH adj		pH adj		No pH adj		pH adj		No pH adj		pH adj	
	MIP	NIP	MIP	NIP	MIP	NIP	MIP	NIP	MIP	NIP	MIP	NIP
Recovery% (RSD%)												
Nortriptyline	24.2(29.0)	26.0(24.7)	11.1(6.6)	5.6(10.4)	13.9(26.4)	4.6(34.6)	3.6(27.5)	1.7	5.6(18.1)	3.8(23.4)	3.6(25.8)	2.2(14.8)
Desipramine	23.3(27.2)	24.5(22.2)	10.4(8.1)	5.5(11.4)	13.3(26.4)	3.8(36.6)	3.3(26.6)	1.5	4.7(16.4)	3.1(14.8)	3.3(24.7)	1.9(14.8)
Amitriptyline	25.9(27.9)	26.3(21.1)	10.9(10.8)	3.6(8.8)	14.5(29.1)	4.2(37.6)	3.5(21.4)	1.9	5.8(18.2)	3.5(24.1)	3.3(21.1)	2.1(21.8)
Doxepin	27.0(26.9)	27.1(19.6)	8.7(15.7)	2.5(9.9)	14.3(31.2)	3.3(40.8)	2.3(20.4)	1.2	4.5(19.7)	2.8(23.3)	2.1(20.3)	1.3(20.2)
Imipramine	22.2(27.4)	23.1(21.1)	8.5(12.1)	2.7(9.0)	12.1(29.2)	3.1(36.0)	2.6(20.0)	1.3	4.1(18.1)	2.6(21.5)	2.4(19.9)	1.5(19.8)
Trimipramine	25.8(26.2)	26.9(21.3)	10.9(10.0)	3.9(6.1)	14.1(31.4)	3.7(35.7)	4.0(24.2)	2.3	4.9(18.8)	3.2(21.1)	3.9(24.6)	2.4(24.7)
Clomipramine	23.8(29.4)	26.6(24.0)	13.0(7.7)	5.8(3.3)	15.5(27.3)	6.9(33.0)	5.3(27.1)	3.3	8.1(17.0)	5.9(22.7)	5.4(27.0)	3.4(25.7)

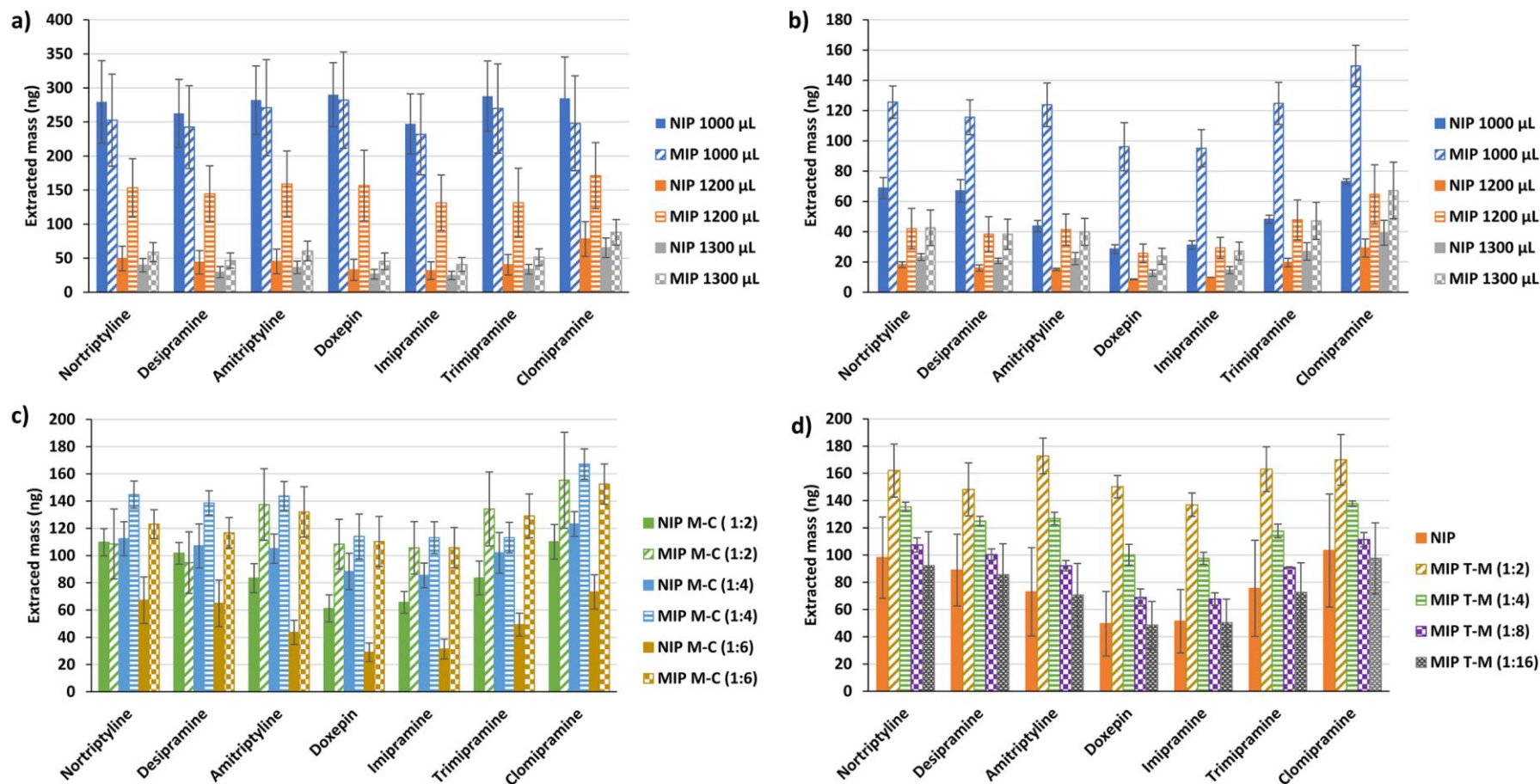


**Figure 3.4.** MIP formula development: a) Porogen volume effects, extraction at pH ~7 (T:M:C, 1:4:24); b) Porogen volume effects, extraction with 1% TEA at pH ~11 (T:M:C, 1:4:24); c) Optimization monomer-to-crosslinker ratio (T:M, 1:4); d) Optimization template-to-monomer ratio (M:C, 1:6). All extractions from 20 mL of 50 ng mL<sup>-1</sup> aqueous TCAs (n=3).

The mole ratios of M:C and T:M were also optimized. MIPs and NIPs with different ratios of M:C (1:2, 1:4, 1:6) were prepared with the amount of crosslinker fixed at 4.8 mmol in 1000  $\mu$ L octanol, and used for extraction of TCAs from aqueous solution containing 1% TEA (Figure 3.4c). Increasing the ratio of the crosslinker to monomer (by decreasing the monomer loading) resulted in better imprinting, which can be attributed to vital role of the crosslinker in the formation of a porous skeleton that conserves geometry of the templated binding sites. As a result, a ratio of 1:6 was chosen as the optimal monomer: crosslinker ratio. To determine the optimal ratio of T:M, 0.8 mmol monomer and 4.8 mmol of crosslinker were added to 0.05, 0.1, 0.2 and 0.4 mmol of template to prepare the ratios of 1:16, 1:8, 1:4 and 1:2. As can be seen in Figure 3.4d, decreasing the relative amount of template from 1:2 to 1:16 decreases the imprinting effect. Decreasing the amount of template ensures that it is completely bound in complexes with the functional monomer, but the excess functional monomer can increase the number sites available for non-selective interactions. Increasing the amount of template is thought to give more templated sites (specific cavities) by ensuring that more of the monomer is oriented for optimal interactions for the selective extraction of TCAs.

Fabrication of thin film MIPs by drop-casting method only requires a few microliters of pre-polymer solution. The pre-polymer mixture is stable and can be stored to prepare MIPs. However, we assessed the variability of MIPs formulae prepared on different by using 2 different batches of template. Three thin films from each batch were used for extraction of TCAs (Figure 3.5). The results depict that two batches of thin film MIPs are similar. A further investigation of the data was conducted by performing a t-test. The results

(Table 3.6) obtained at 95% of confidence level show that there was no difference between two batches and these batches were statistically identical.

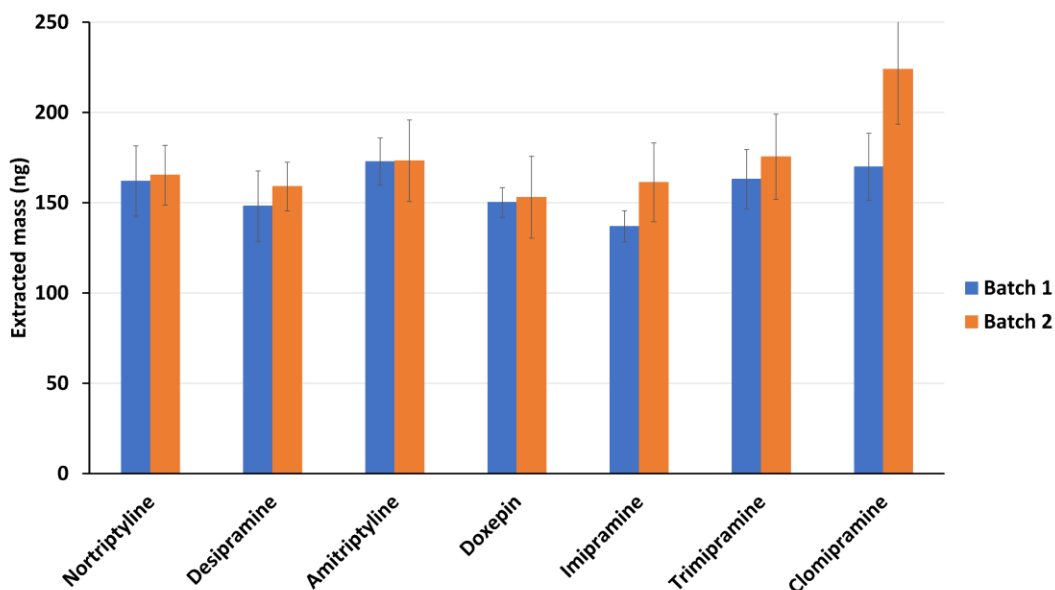


**Figure 3.5.** Inter-batch reproducibility of 2 sets of thin film MIPs. All extractions from 20 mL of 50 ng mL<sup>-1</sup> of TCAs with 1% TEA at pH ~11.

**Table 3.6.** T-test at a 95% confidence level for inter-batch reproducibility of thin film MIPs ( $T_{crit} = 2.776$ ).

TCAs	T-Value	P-Value
Nortriptyline	-0.22	0.835
Desipramine	-0.22	0.835
Amitriptyline	-0.03	0.976
Doxepin	-0.21	0.848
Imipramine	-1.8	0.147
Trimipramine	-0.75	0.497
Clomipramine	-2.62	0.059

SEM micrographs were collected for the optimal MIP (T:M:C, 1:2:12) and its corresponding NIP to assess the film thickness and morphology. In Figure 3.6, side-view

of prepared thin films are presented. As shown, both films have a thickness of  $\sim 20 \mu\text{m}$  obtained by depositing a  $3\text{-}\mu\text{L}$  portion of their pre-polymer.

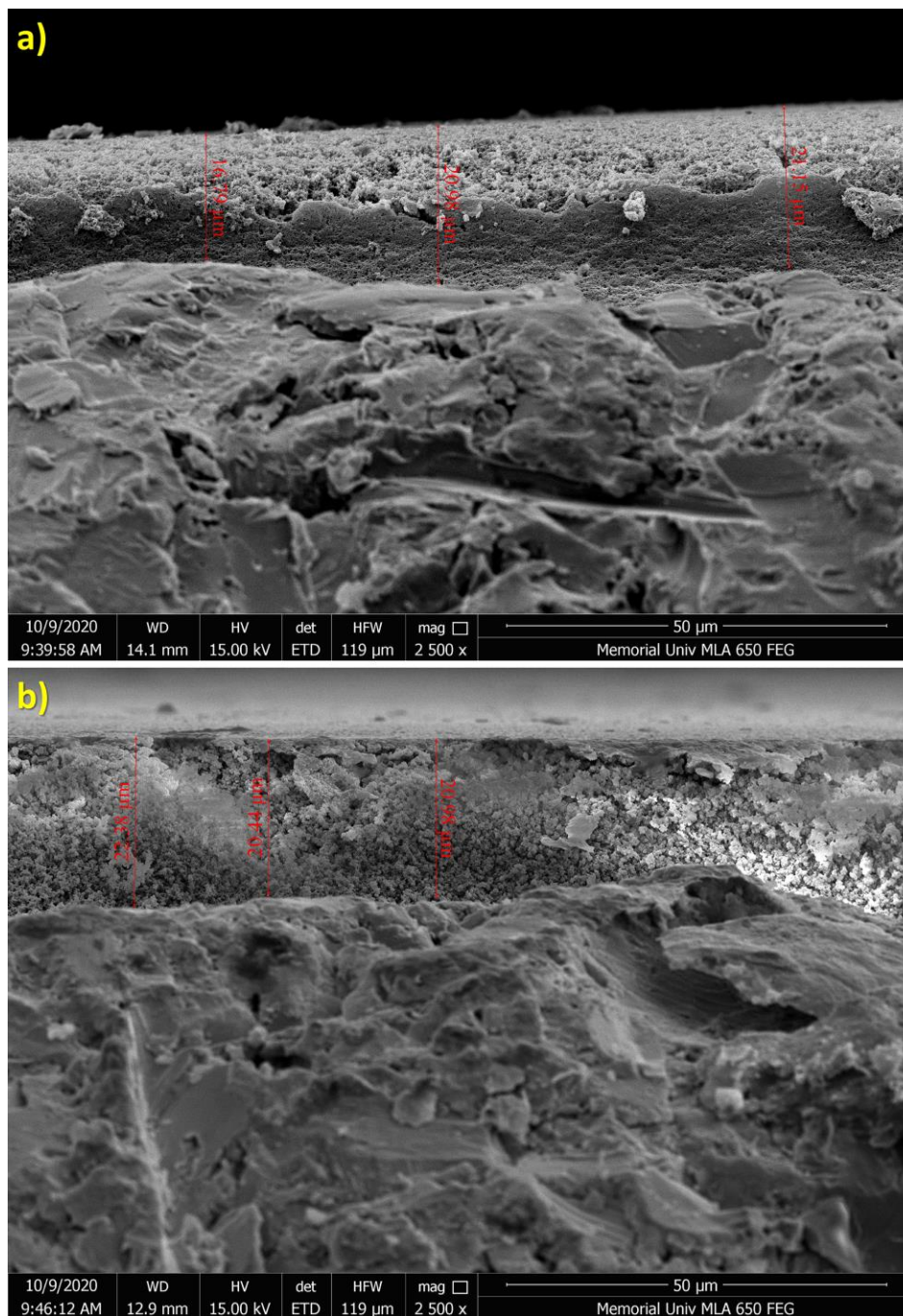


**Figure 3.6.** Side view of exemplary a) thin film MIP, and b) thin film NIP prepared on stainless steel substrates obtained at  $2500\times$  magnification.

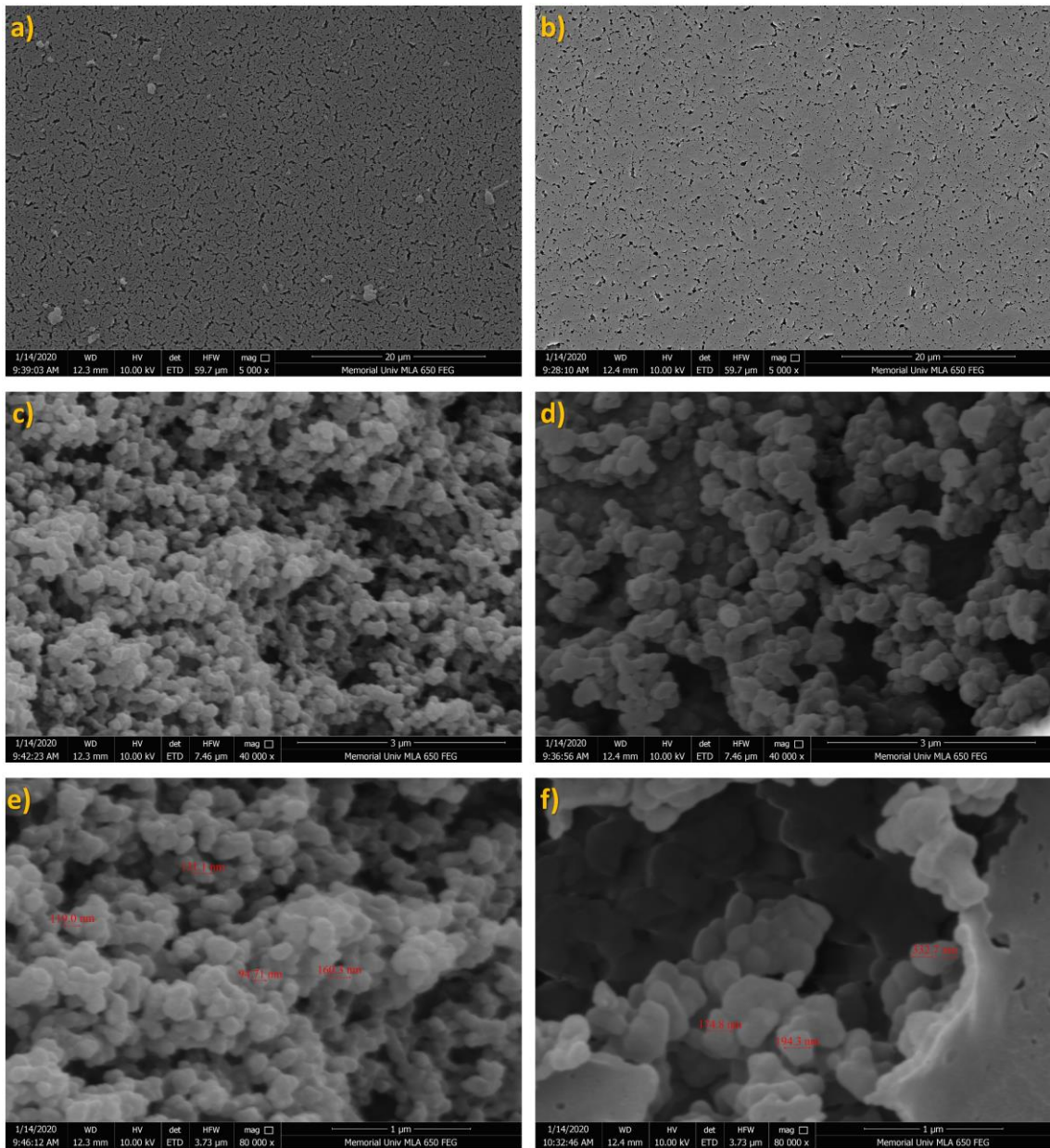


**Figure 3.7.** SEM of prepared thin film MIPs a) at 5000 $\times$ , c) at 40,000 $\times$ , and e) at 80000 $\times$ ; SEM of prepared thin film NIPs, b) at 5,000 $\times$ , d) at 40000 $\times$ , and f) at 80000 $\times$ . (T:M:C, 1:2:24)

The surface of prepared MIPs and NIPs also represent a homogeneous layer of polymer on the metal substrates (Figures 3.7a and b). The morphological differences

between the MIPs and NIPs can be seen at higher magnification (Figures 3.7c-f); with MIPs showing smaller particle-like structures. These differences suggest that the MIPs will have a higher surface area and thus a greater adsorption capacity than the NIPs. However, the study of pH effects showed similar adsorption behaviour at neutral pH, with MIPs outperforming NIPs when pH was adjusted (to >10). This suggests that surface areas may be similar for the MIPs and NIPs, but the conditions for the greatest selectivity are only achieved when the methacrylate moieties are ionized (net negative surface charge) and the analytes are neutral. By increasing pH and deprotonating the TCAs, the strength of the interactions with individual methacrylates, equally present in MIPs and NIPs, are reduced. This decreases the NIP performance while MIPs binding is maintained due to the entropic advantage associated with the templated sites.

Further characterization of thin films was performed via N<sub>2</sub> adsorption studies (Figure 3.8). The BET (Brunauer Emmet-Teller) analysis indicates that the specific surface area in MIP is  $29.06 \pm 0.36 \text{ m}^2 \text{ g}^{-1}$  and that of NIP is  $16.00 \pm 0.38 \text{ m}^2 \text{ g}^{-1}$ . Moreover, the total pore volume for MIP and NIP are  $0.0206$  and  $0.0057 \text{ cm}^3 \text{ g}^{-1}$ , respectively. The obtained data demonstrate that the presence of template molecules in prepolymer mixture yields in the formation of cavities containing binding sites and enhanced the specific surface area and pore volume in thin film MIPs versus NIPs.

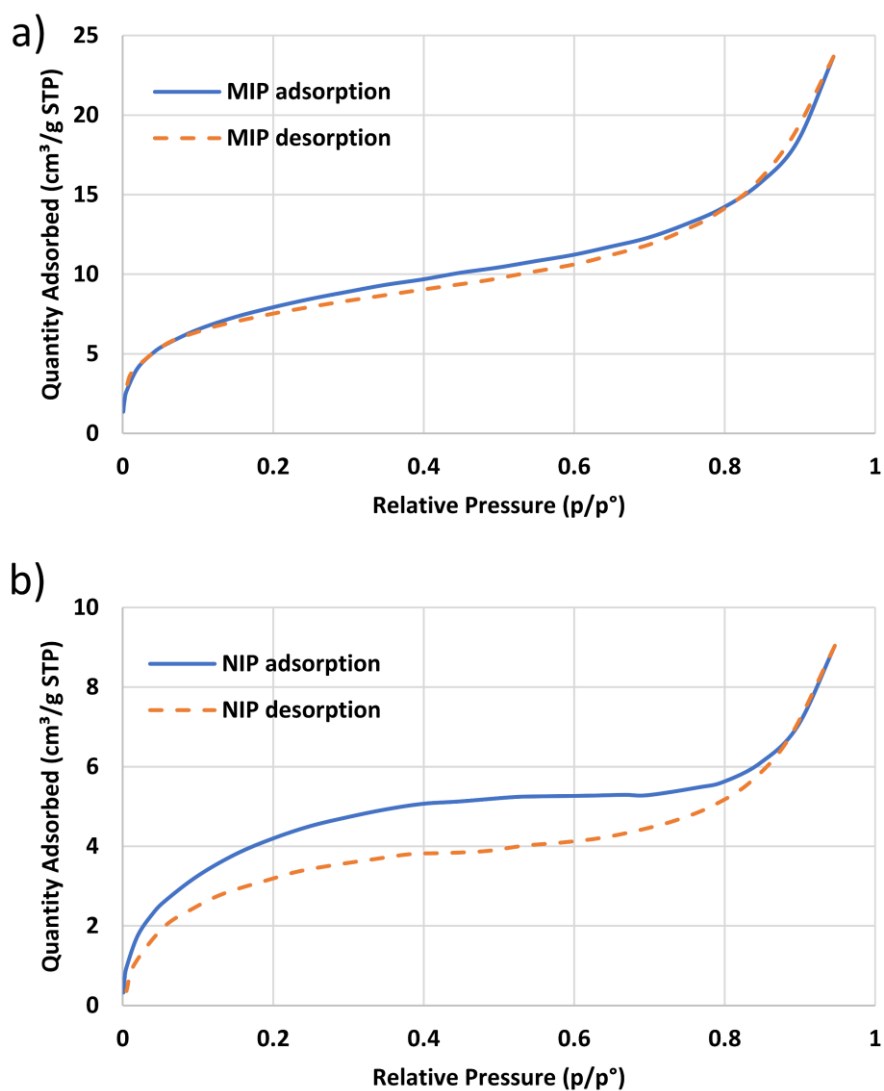


**Figure 3.8.** BET isotherm for a) optimized thin film MIP and b) its corresponding NIP

### 3.3.2. Considerations for the use of thin film MIPs for extraction of TCAs from biological matrices

Analyzing the free concentration of pharmaceuticals in plasma is essential since this form is most active in the pharmacokinetic processes [51]. For TCAs in biofluids the primary concern is their affinity for non-covalent interactions with plasma proteins. A

preliminary study of recoveries following spiking and incubation of TCAs at neutral pH showed excellent recoveries for TCAs in the presence of BSA (Figures 3.9 and 3.10). The results show that almost all the spiked concentrations of TCAs are in free format in BSA. Therefore, there is no binding between spiked TCAs and proteins. So, spiking solution can be used as the free concentration of drugs in calculations.

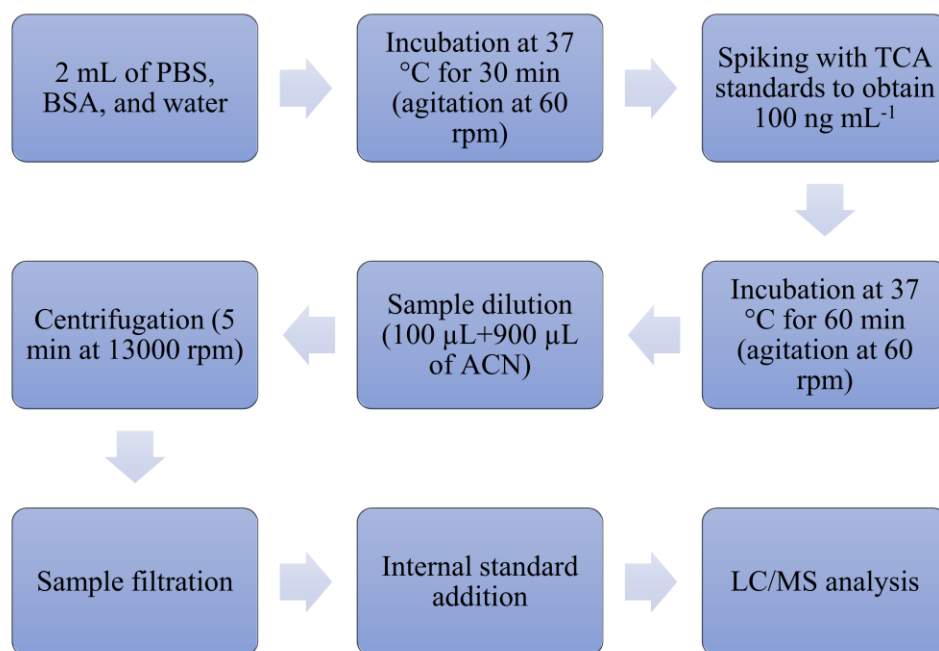


**Figure 3.9.** The summary process for assessment of protein binding of TCAs.

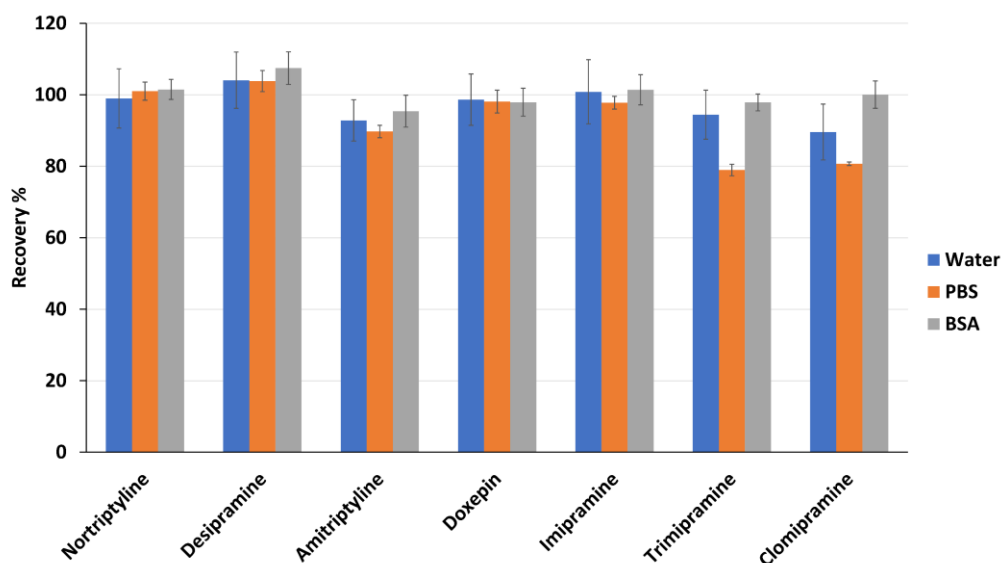


**Figure 3.10.** Effect of PBS and BSA on recoveries of TCAs following 1 h incubation at 37 °C at neutral pH (TCA are protonated under these conditions).

The alkaline pH is needed for optimal MIP selectivity and gives reproducible results by extraction of neutral form of the TCAs. Thus, we studied the effect of various bases used for pH adjustment on the recoveries of TCAs from distilled water, buffer solution (PBS), and BSA (Figure 3.11).

To determine if the type of base influences the method performance, different bases (ammonium hydroxide, sodium hydroxide, butylamine (BA), and TEA) were added at 1% in water, PBS, and BSA matrices spiked with TCAs at 100 ng mL<sup>-1</sup> and analyzed after incubation at 37 °C for 1 h under stirring at 60 rpm. NaOH led to precipitation of BSA which can also mean undesirable co-precipitation of the analytes; therefore, it was eliminated from this study.

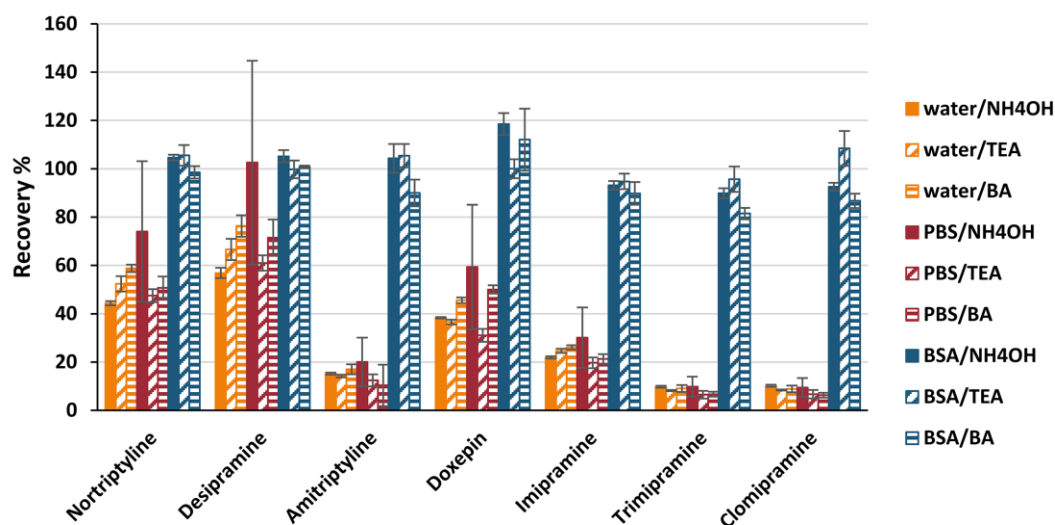


**Figure 3.11.** Effect of type of base on TCA recoveries following 1 h incubation at 37 °C of 100 ng mL<sup>-1</sup> of TCAs in 1% MS-compatible base with either water, PBS, or BSA solution. BA – butylamine

Figure 3.11 shows the TCA recoveries varied dramatically depending on the composition of the sample. For example, from water and PBS only 40-60 % of Nor and Des and <40 % of the other TCAs were recovered. Whereas TCAs were quantitatively recovered from BSA, with TEA showing the best performance in terms of recoveries and repeatability. We attribute the low recoveries to the decreased solubility of the TCAs in their hydrophobic neutral form ( $\log P \geq 4.2$ , Table 3.1). In basic solutions containing only water or PBS, TCAs seem to be adsorbed by the polypropylene vial, however, excellent recoveries were achievable from BSA solutions. This can be explained by interactions between the TCAs and the protein, which improves their solubility in the solution and avoids adsorption of these analytes by container. TEA was used for all further studies.

### **3.3.3. Optimization of extraction of TCAs from biological matrices**

Here the focus is on the optimization of the extraction process. However, other factors such as post-extraction, the sorbent washing and analyte desorption steps were also studied.

#### *3.3.3.1. Washing*

Thin film MIPs allow for sample clean-up after extraction. In the previous studies, this step was performed by washing the extraction devices after exposure to sample solution with ultrapure water [48]. This washing step reduces the co-adsorption of matrix components and interfering substances such as salts. In this step, three different washing solutions including ultra pure water, 0.1% aqueous FA, and 1% aqueous TEA were tested, and the results were compared with performing the extraction without any washing step (Figure 3.12). Performing desorption without rinsing the thin films has resulted in low efficiency due to co-extracted matrix components and ionization suppression. Although water has been recommended in the literature for rinsing step after direct immersion extraction, it can cause ionization of adsorbed TCAs on the thin film MIPs and facilitate these drugs desorption into the washing solution.

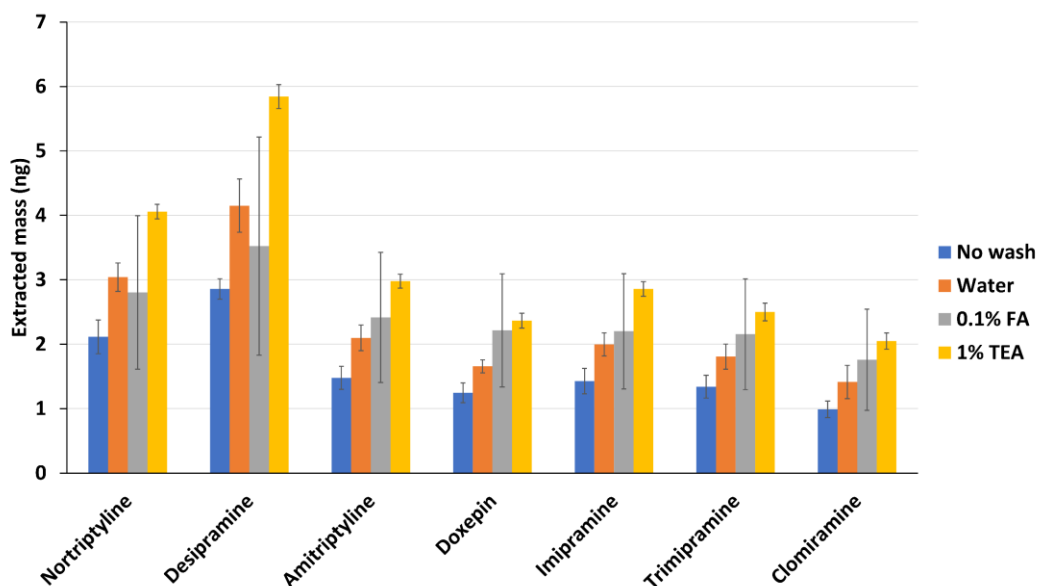


**Figure 3.12.** Wash optimization. Wash: 8 s immersion in 20 mL DI water, 0.1 % aqueous FA or 1% aqueous TEA. Sample extraction: 700  $\mu\text{L}$  of 100  $\text{ng mL}^{-1}$  of TCAs in BSA with 1% TEA, extraction for 20 min at 1000 rpm, Desorption conditions: 700  $\mu\text{L}$  MeOH, 20 min at 1000 rpm.

This idea was further demonstrated by the results of using of water with 0.1% FA as a washing solution leading to high %RSD values. These results can be explained by the basic nature of TCAs. These drugs are ionized in the neutral and acidic pH conditions which lead to wash them off the thin film MIPs. The highest efficiency and repeatability were obtained using immersion of thin films in 1% TEA in water as washing solution. Basic condition of 1% TEA can maintain the adsorbed analytes on the film and rinse co-extracted components.

### 3.3.3.2. Desorption

The composition of desorption solvent was optimized to ensure a reliable and efficient elution of analytes from thin film. TCAs are hydrophobic analytes needing organic solvent

(ACN or MeOH) to be desorbed. Additionally, due to the type of the interactions between the TCAs and the MIP sorbent which is mostly hydrogen binding, it was expected that adding FA and water can disturb these interactions and help to a better desorption of the drugs from the thin film MIP. Acidic conditions cause protonation of both the analytes and the MIP surface. Combination of solvents with different polarity is also effective in releasing the drugs which are trapped in the MIP's specific cavities. Figure 3.13 demonstrates the desorbed mass (ng) of the drugs using different desorption solvents.

As can be seen in Figure 3.13, desorption was improved by adding water (1:1 ratio) and FA (0.1%) to the pure solvent. Therefore, mixture of ACN/water (1:1) with 0.1%FA, which is also compatible with LC mobile phase, was used as the desorption solvent. Other factor which can be assessed to improve the desorption efficiency is the desorption time profile to find the equilibrium of analytes between thin film and desorption solvent. Figure 3.14 depicts that increasing the desorption time can improve the desorption efficiency. Based on these results, 20 minutes was selected as the optimum time for desorption.

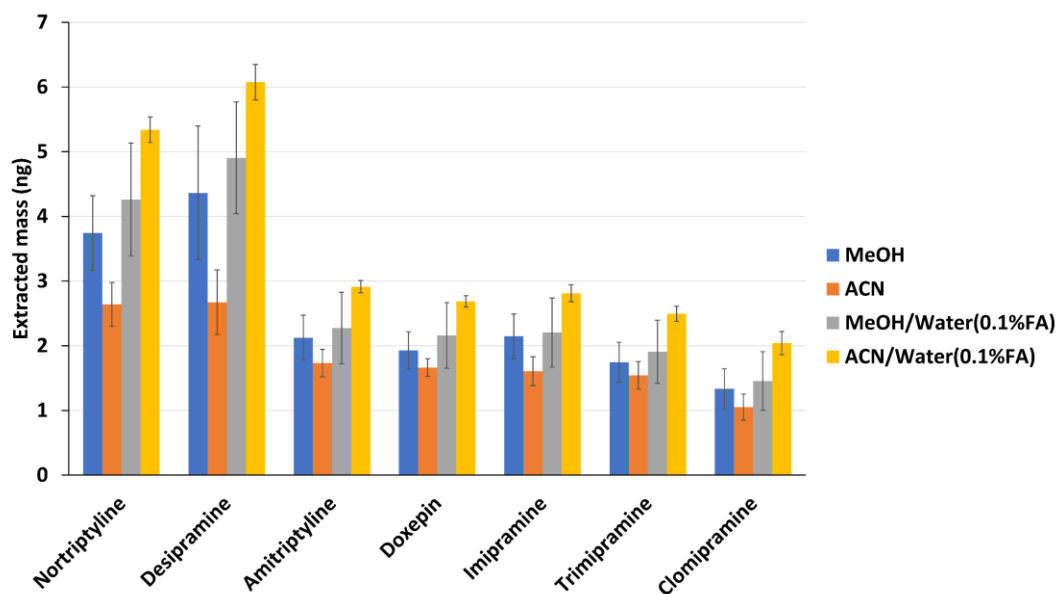


**Figure 3.13.** Comparison of the extracted mass of TCAs by using different solvents for desorption. Sample extraction: 700  $\mu\text{L}$  of 100  $\text{ng mL}^{-1}$  of TCAs in BSA with 1% TEA, extraction for 20 min at 1000 rpm, washing: 8 sec immersion in water with 1% TEA, Desorption conditions: 700  $\mu\text{L}$ , 20 min at 1000 rpm.

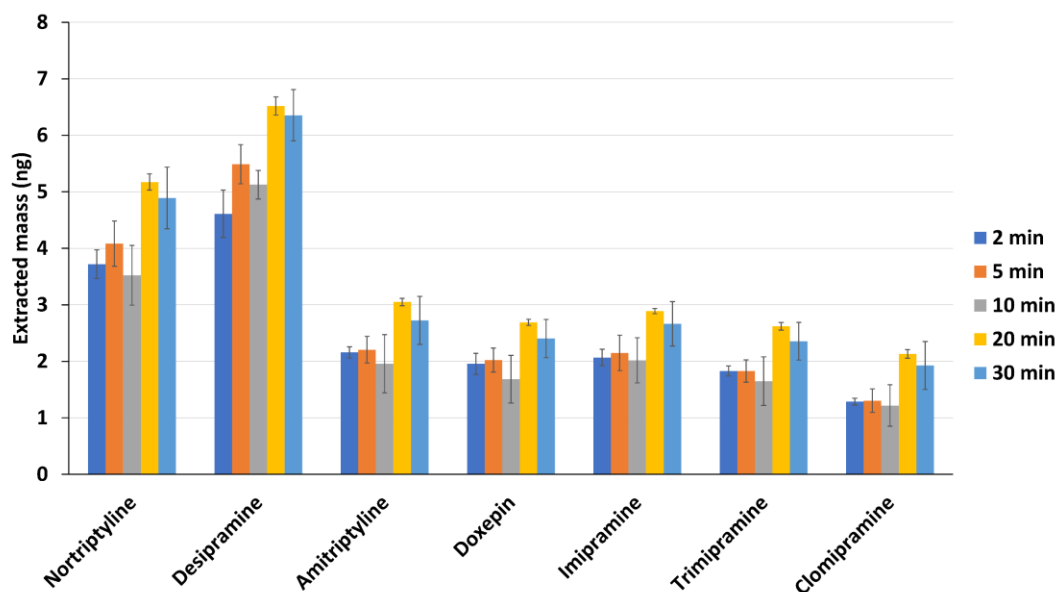


**Figure 3.14.** Desorption time profile. Sample extraction: 700  $\mu\text{L}$  of 100  $\text{ng mL}^{-1}$  of TCAs in BSA with 1% TEA, extraction for 20 min at 1000 rpm, washing: 8 sec immersion in water with 1% TEA, Desorption conditions: 700  $\mu\text{L}$  of ACN/water (1:1) with 0.1% FA at 500 rpm.

### 3.3.3.3. Extraction

Extraction of TCAs using thin film MIPs follows SPME theory where higher agitation of sample will lead to a faster equilibrium of analytes between the extraction phase and the solution and increased adsorption [52]. Increasing the agitation rate from 500 rpm to 2000 rpm enhanced the extraction efficiency by improving the mass transfer and thus shorten the equilibration time (Figure 3.15). Since the difference between 1500 and 2000 rpm was not significant and higher agitation leads to more wear on the equipment, 1500 rpm was selected for further study.

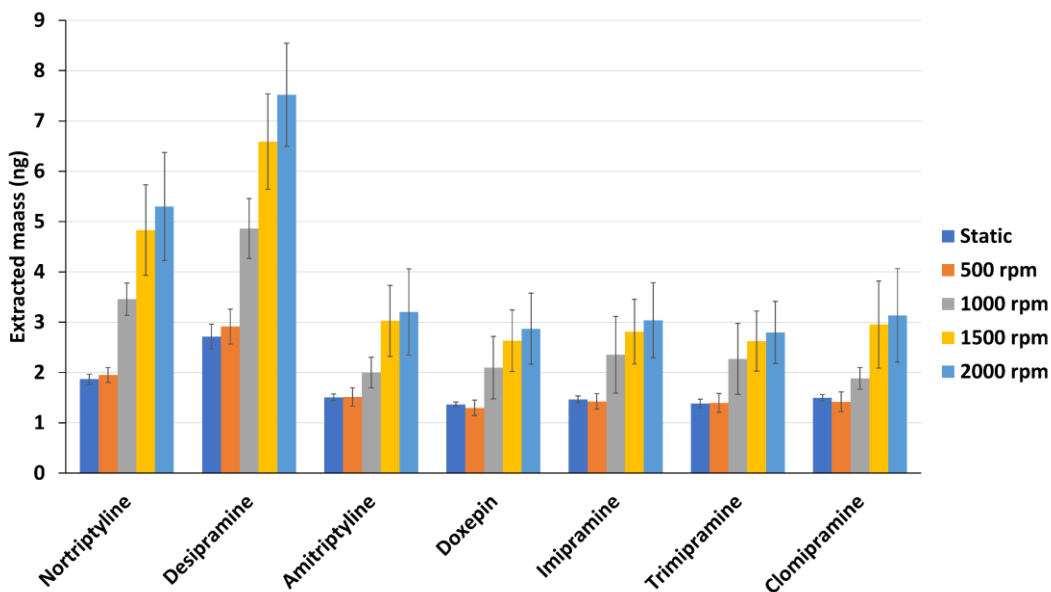


**Figure 3.15.** The effect of agitation on the recovered TCAs. Sample extraction: 700  $\mu\text{L}$  of 100  $\text{ng mL}^{-1}$  of TCAs in BSA with 1% TEA, extraction for 20 min at various agitation, washing: 8 sec immersion in water with 1% TEA, Desorption conditions: 700  $\mu\text{L}$  of ACN/water (1:1) with 0.1% FA, 20 min at 500 rpm.

In equilibrium-based extractions, time of extraction can have a dramatic effect on the precision and sensitivity of the method. To achieve repeatable results, extractions are

usually carried out at equilibrium and are preferred when higher sensitivity is needed. To improve throughput, extractions can be carried out at any time that falls within the linear region of the pre-equilibrium regime, though the specific time chosen should give precise results. Figure 3.16 illustrates the time profile for extraction of TCAs using thin film MIPs and NIPs.

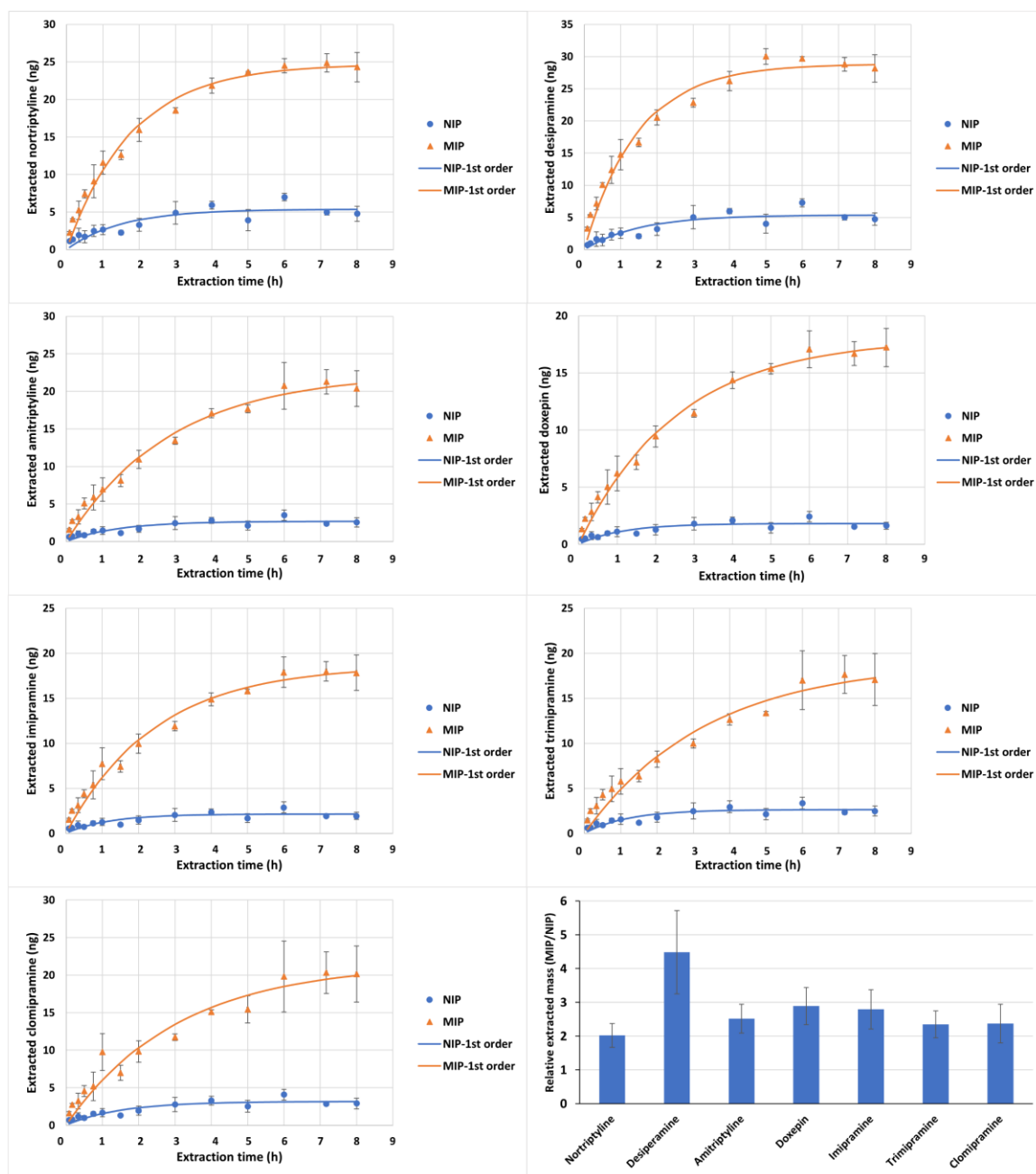


**Figure 3.16.** Adsorption Kinetics of TCAs. Extraction: 700  $\mu\text{L}$  of BSA sample spiked with 100 ng  $\text{mL}^{-1}$  of TCAs at 1500 rpm. Desorption: 700  $\mu\text{L}$  of 0.1 % FA in 50% aqueous ACN (20 min at 500 rpm).

These drugs reach equilibrium with the sorbent and a solution of 5% BSA within 5 h.

Considering throughput, sensitivity, repeatability, 60 min was selected for extractions.

Although a 60 min extraction may be considered long for routine analysis, the device format makes it easy to multiplex using a multi-vortex agitator. Use of an inexpensive 30 position agitator, allows for processing of 30 samples per h, which makes the LC-MS method the bottleneck in the process. The data (Figure 3.16) shows that MIP devices perform well in biological matrices even with long extraction times (e.g., 8 h). This highlights the broader potential of the MIP coating for analysis of biological samples over other microextraction devices where interactions with biological matrices lead to performance losses [53].

The effect of imprinting on the performance of polymeric adsorbents can be evaluated in terms of selectivity measured using different approaches such as kinetics and isotherm studies. In most studies, MIP and NIP performance is compared at equilibrium under high loading conditions, however this rarely reflects conditions relevant for trace analysis. Instead, we compared the MIP/NIP kinetics of adsorption (Figure 3.16) at relatively low analyte loadings ( $100 \text{ ng mL}^{-1}$ ).

MIPs are also usually characterized for selectivity and adsorption behaviour using isotherm studies under equilibrium. However, meaningful data can also be gained from such studies prior to complete equilibration provided that the time of exposure is well controlled. It is also necessary if the intent is to use the material under pre-equilibrium conditions, as is the case in this work. Adsorption (60 min interval) of TCAs by MIP and NIP sorbents was assessed using different initial concentration of TCAs ( $1\text{-}1000 \text{ ng mL}^{-1}$ ) in BSA. Representative chromatograms obtained after extraction of TCAs from BSA solutions ( $100 \text{ ng mL}^{-1}$ ) are shown in Figure 3.17, with data for extracted mass at each concentration provided in Figure 3.18.

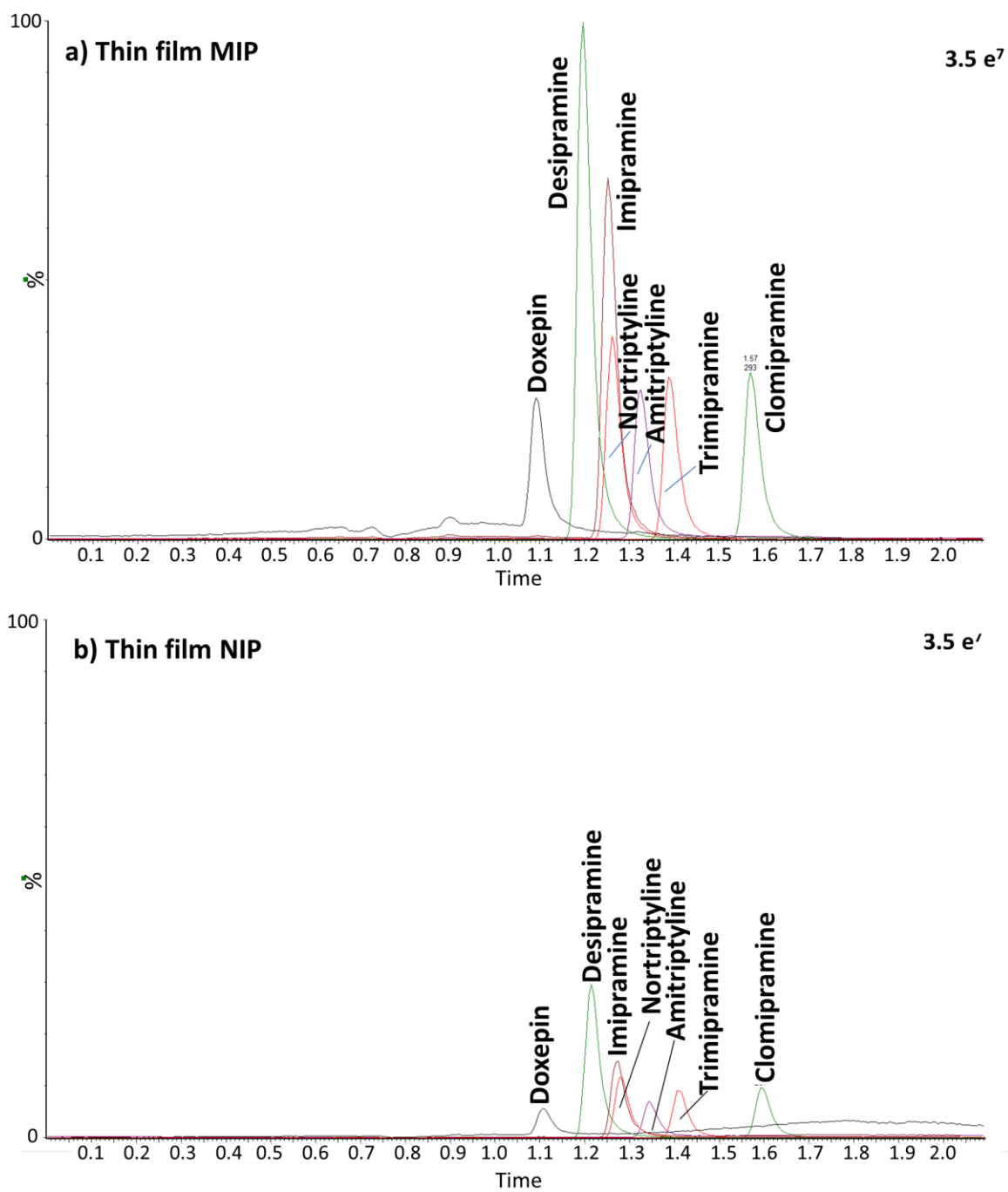


**Figure 3.17.** Comparison of the chromatograms of (a) thin film MIPs, and (b) thin film NIPs. Extraction: 700  $\mu\text{L}$  of BSA sample spiked with 100 ng mL<sup>-1</sup> of TCAs (60 min at 1500 rpm); Desorption: 700  $\mu\text{L}$  of 0.1 % FA in 50% aqueous ACN (20 min at 500 rpm).

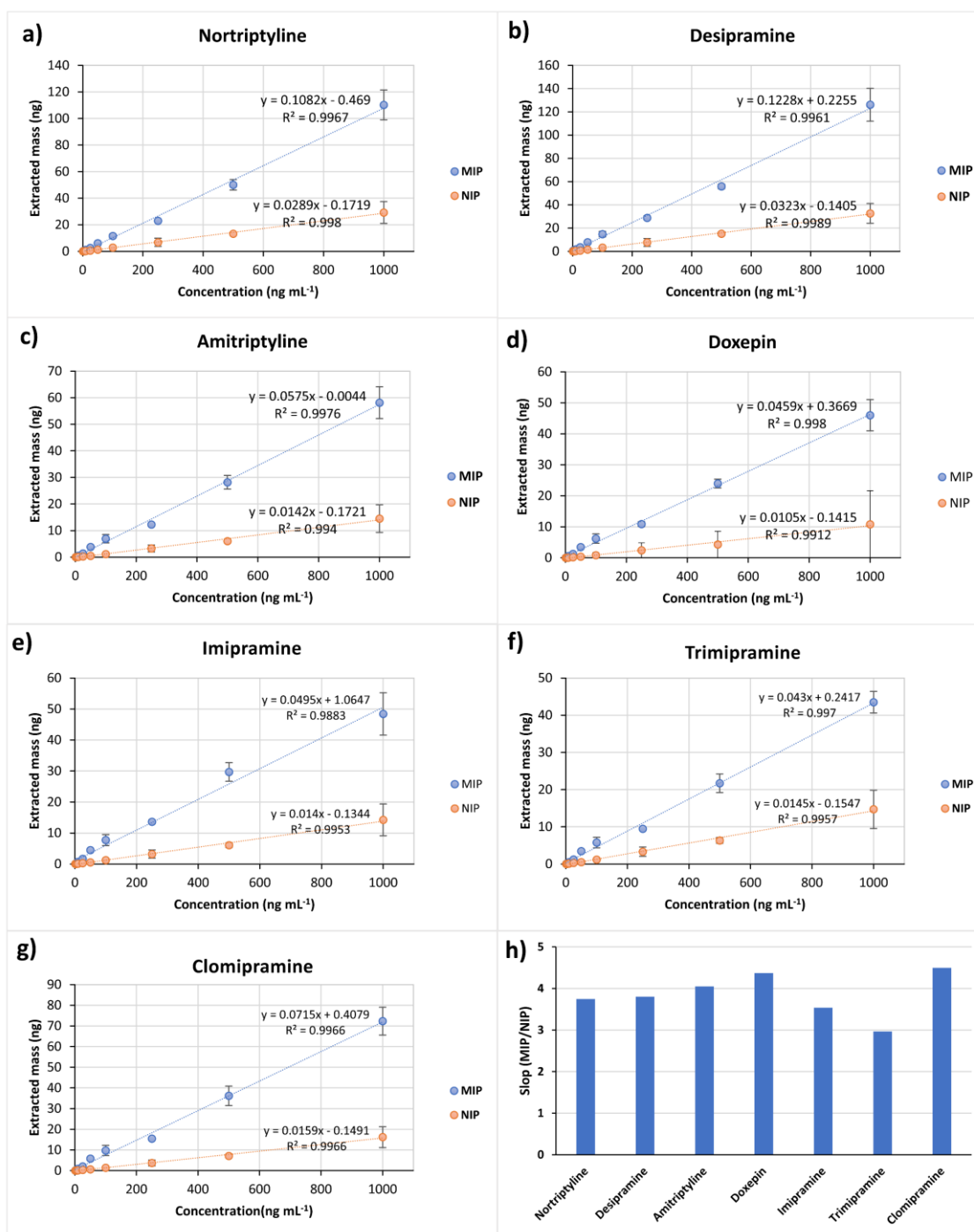


**Figure 3.18.** Calibration curves obtained for extraction of a) nortriptyline, b) desipramine, c) amitriptyline, d) doxepin, e) imipramine, f) trimipramine, and g) clomipramine; h) the ratio of slopes of calibration curve for TCAs using thin film MIPs versus NIPs for extraction from BSA.

The slope of extracted mass versus initial concentration is a measure of selectivity; comparing these, MIPs extracted between 3.0 (trimipramine) and 4.5 (clomipramine) times more of the target drugs compared to NIPs. The difference between TCAs is related to their structure and positioning towards imprinted sites. Moreover, their competition towards imprinted sites can be investigated by rebinding of analytes from individual and mix solutions [30, 54]. Higher slopes for the MIPs curves demonstrate that MIPs will yield a more sensitive method with lower detection limits.

As discussed in our previous work, thin films prepared with a drop-casting technique and optimized chemistry can be used as single-use extraction devices in environmental analysis without using internal standards [32]. To examine whether the device variability in biological analysis is acceptable, 15 unused thin film MIPs were evaluated for extraction of TCAs from BSA. The relative standard deviation (RSD%) of instrument responses (peak area) without and with normalization are provided in Figure 3.19. The RSD% ranged from 8.5 to 13.9, with an average of 11.5%. A significant proportion of the variability can be attributed to error in the instrument response. Use of an internal standard to normalize the MS response reduces the method variability to an average 5.2%.

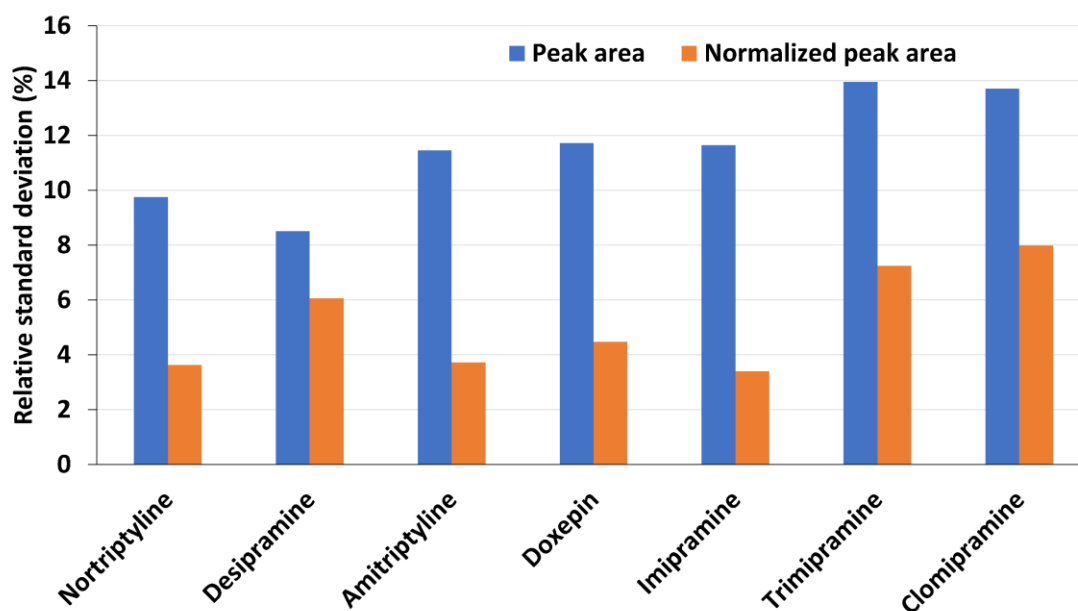


**Figure 3.19.** RSD percentage for extraction of TCAs using 15 individual devices with and without normalization

### 3.3.4. Method validation

#### 3.3.4.1. BSA

The performance of thin film MIPs for biological analysis were first assessed using a simple test of compatibility with samples containing high protein (5% BSA) prior to assessment of their efficiency in human blood plasma. Performance in BSA was also compared to performance in plasma for potential use in external matrix-matched calibration. BSA standard solutions were prepared by different concentration of TCAs (0.25-1000 ng mL<sup>-1</sup>). Imipramine-d3 (50 ng mL<sup>-1</sup>) was used as the internal standard and added to all sample solutions. Table 3.7 summarizes the figures of merit obtained in BSA solution.

Limits of quantification (LOQs) of free concentration of these drugs range between 0.25 and 5.0 ng mL<sup>-1</sup>, which are substantially lower than LOQs required for therapeutic

monitoring [55]. Linear dynamic ranges are also long enough to cover the toxic blood concentrations of TCAs with good linearity ( $R^2 > 0.99$ ). This indicates the suitability of proposed thin film MIPs for quantitative measurement of these antidepressant drugs in biofluids. The accuracy and precision of the proposed method were validated with low, mid, and high concentrations (0.8, 4, 80, 150 and 400 ng mL<sup>-1</sup>) to cover most of the linear range and includes therapeutic and toxic drug concentrations. The quantitation in BSA was assessed by comparing the response of TCAs spiked in BSA to a calibration in BSA (TCA calibration range 0.25-1000 ng mL<sup>-1</sup>) completed on another day. Accuracies were in the range of 95.3-117% with RSD% of 0.6-12%. The inter-day accuracy and precision were determined based on triplicate analyses on three subsequent days. The obtained inter-day accuracy figures ranged from 88.4% to 104% and RSD% in the range of 0.8-24% (most < 10%), which indicate the robustness of the proposed method for determination of TCAs in biofluids.

Matrix effect was evaluated by spiking the IS (imipramine-d3) (50 ng mL<sup>-1</sup>) into the desorption solvent that was used for desorbing TCAs from MIPs and comparing the peak area for IS for these samples with peak area obtained by spiking into neat solvent. The accuracy for this study was 98.3% with %RSD of 9.4 which are acceptable according to regulatory guidelines.

The dilution integrity was also calculated for BSA samples spiked with 1000 ng mL<sup>-1</sup> TCAs which was out of linear range of the instrument. A dilution factor of ten resulted in acceptable accuracy values in the range of 101-109 and RSDS between 6.7-13% (Table 3.8).

**Table 3.7.** Figures of merit for quantification of free concentration of TCAs in BSA using thin film MIPs (n=3).

TCAs	LR (ng mL <sup>-1</sup> )	Function	R <sup>2</sup>	Intra-day Accuracy (%) (%RSD)					Inter-day Accuracy (%) (%RSD)				
				0.8*	4.0	80	150	400	0.8	4.0	80	150	400
Nor	0.5-500	y = 0.004x - 0.0094	0.9993	95.7 (5.7)	95.3 (8.7)	102 (3.3)	112 (7.3)	96.2 (2.1)	96.3 (1.5)	89.6 (9.4)	97.6 (13)	103 (17)	89.7 (5.8)
Des	5.0-500	y = 0.0179x+0.0703	0.9959	<LOQ	<LOQ	105 (4.7)	117 (4.7)	99.1 (2.2)	<LOQ	<LOQ	102 (7.9)	102 (18)	88.4 (14)
Ami	0.5-500	y = 0.004x - 0.0102	0.9995	111 (12)	103 (3.2)	95.8 (1.6)	103 (3.5)	95.3 (3.5)	101 (24)	95.2 (8.3)	93.5 (5.7)	97.9 (8.1)	93.5 (4.8)
Dox	2.5-500	y = 0.0038x - 0.0033	1.0000	<LOQ	98.5 (5.3)	100 (1.4)	104 (1.3)	96.4 (1.2)	<LOQ	93.0 (7.8)	92.0 (6.3)	96.8 (5.8)	97.9 (3.5)
Imi	0.25-500	y = 0.0128x + 0.0018	1.0000	103 (5.6)	96.9 (2.6)	98.7 (0.6)	105 (2.4)	97.1 (1.3)	103 (0.8)	97.6 (2.7)	98.4 (5.7)	102 (4.4)	97.1 (3.4)
Tri	0.25-1000	y = 0.0055x - 0.0018	0.9999	102 (8.9)	99.8 (8.0)	102 (3.3)	104 (3.4)	102 (7.5)	102 (4.0)	94.0 (2.5)	104 (14)	104 (5.9)	104 (10)
Clo	0.5-1000	y = 0.0068x - 0.0032	0.9998	98.0 (7.8)	101 (5.3)	99.1 (4.0)	105 (2.6)	97.8 (8.1)	101 (9.8)	93.0 (4.3)	100 (12)	102 (6.2)	96.9 (8.4)

\*All the spiked concentrations are in ng mL<sup>-1</sup>

**Table 3.8.** Effect of dilution on the accuracy and precision of the results.

TCAs	Accuracy(%)	RSD(%)
Nortriptyline	109	10
Desipramine	101	13
Amitriptyline	101	11
Doxepin	103	12
Imipramine	104	11
Trimipramine	100	6.7
Clomipramine	102	9.2

#### 3.3.4.2. Plasma

The applicability of external matrix-matched calibration based on spiked BSA samples for TCAs in plasma was proven effective for five of the TCAs under study; Tri and Clo showed relative error of ca. -30%. Therefore, calibration curves were constructed (Figure 3.20) with a weighted calibration function (1/X) using data from TCAs spiked in pooled plasma (1.0-500 ng mL<sup>-1</sup>). Weighted calibration was used to obtain better fitting and accurate quantification, especially for lower ranges. Table 3.9 shows the figures of merit, with LOQs at 1 ng mL<sup>-1</sup> for all the TCAs, except Des (2.5 ng mL<sup>-1</sup>) and Ami (5 ng mL<sup>-1</sup>). Accuracy and precision (Table 3.9) were assessed by triplicate extractions from low (4 ng mL<sup>-1</sup>), mid (80 ng mL<sup>-1</sup>), and high (150 ng mL<sup>-1</sup>) concentrations of TCAs in the pooled plasma, as well as plasma samples from single individuals. This allows for assessment of pooled plasma calibration curves for matrix-matching against individual plasma samples required for therapeutic drug monitoring (Figure 3.20). The accuracy and precision should be  $\pm 15\%$  of nominal concentration ( $\pm 20\%$  for LLOQ), based on regulatory guidelines [56]. The obtained accuracy for plasma samples in this work was typically within  $\pm 10\%$ ,

particularly for the mid and high concentration ranges, with most of the low concentration data above 80%. On average, the precision was also acceptable at <10%. When compared with a method variability of ~5%, we conclude that the matrix associated variability for the MIP thin films is acceptable, making them well-suited for use in the analysis TCAs in human plasma without standard addition.

Although it is good practice to use an internal standard with these complex matrices, isotopically labelled internal standards can be costly. Previously, thin film extraction devices were found to be reproducible for analysis of water samples without using internal standards [32]. Uncorrected calibration curves using raw instrument response for pooled plasma are presented in Figure 3.21 along with recovery data points for individual plasma samples. The data shows excellent linearity ( $R^2 > 0.9988$ ), with high precision and good fit between different matrices. Thus, we demonstrate that thin film MIPs can enrich and adsorb quite similar mass of analytes regardless of individual device and matrix variability. Therefore, this method is reliable without the need for internal standards.

**Table 3.9.** Figures of merit for quantification of free concentration of TCAs in pooled plasma using thin film MIP extraction method.

TCAs	LR (ng mL <sup>-1</sup> )	Function	R <sup>2</sup>	Pooled plasma			Plasma 1			Plasma 2		
				4.0	80	150	4.0	80	150	4	80	150
Nor	1-500	$y = 0.0037x + 0.0087$	0.9995	98.8 (1.6)	96.9 (11)	102 (9.9)	88.5 (2.0)	96.1 (0.4)	94.7 (1.5)	89.2 (4.5)	103 (2.6)	88.6 (0.6)
Des	5.0-500	$y = 0.018x + 0.2406$	0.9985	<LOQ	103 (17)	113 (20.0)	<LOQ	103 (5.5)	97.4 (2.2)	<LOQ	107 (4.1)	90.2 (3.1)
Ami	2.5-500	$y = 0.0028x + 0.0033$	0.9998	83.2 (9.4)	94.2 (3.8)	98.6 (5.1)	89.4 (5.3)	102 (5.8)	103 (3.1)	90.7 (9.8)	97.9 (0.9)	101 (5.3)
Dox	1-500	$y = 0.0047x + 0.0022$	0.9999	70.1 (19)	99.2 (1.1)	101 (5.9)	105 (12)	97.2 (3.8)	90.1 (1.7)	83.6 (15)	94.2 (1.8)	96.8 (2.9)
Imi	1-500	$y = 0.0125x + 0.0133$	0.9999	117 (25)	98.1 (0.6)	99.6 (1.9)	97.1 (1.7)	95.8 (3.7)	95.5 (2.3)	96.5 (0.7)	96.0 (0.8)	98.6 (1.4)
Tri	1-500	$y = 0.0031x - 0.0009$	1.0000	88.7 (7.4)	100 (11)	108 (11.9)	101 (4.0)	104 (9.2)	104 (7.4)	105 (2.2)	96.0 (0.9)	111 (6.1)
Clo	1-500	$y = 0.0041x + 0.0009$	1.0000	93.7 (9.0)	90.7 (12)	99.5 (12.6)	107 (6.0)	104 (12)	111 (5.0)	107 (2.8)	94.9 (4.6)	104 (4.9)

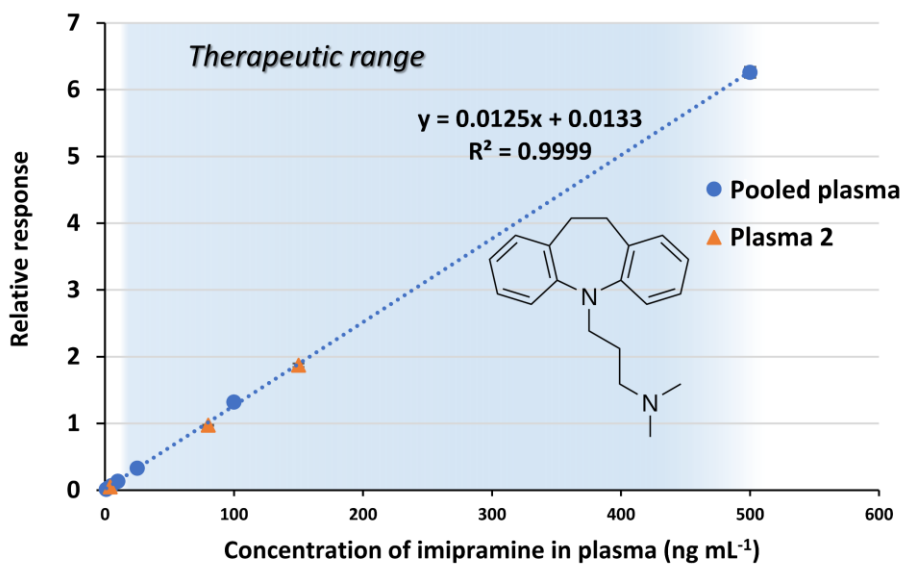
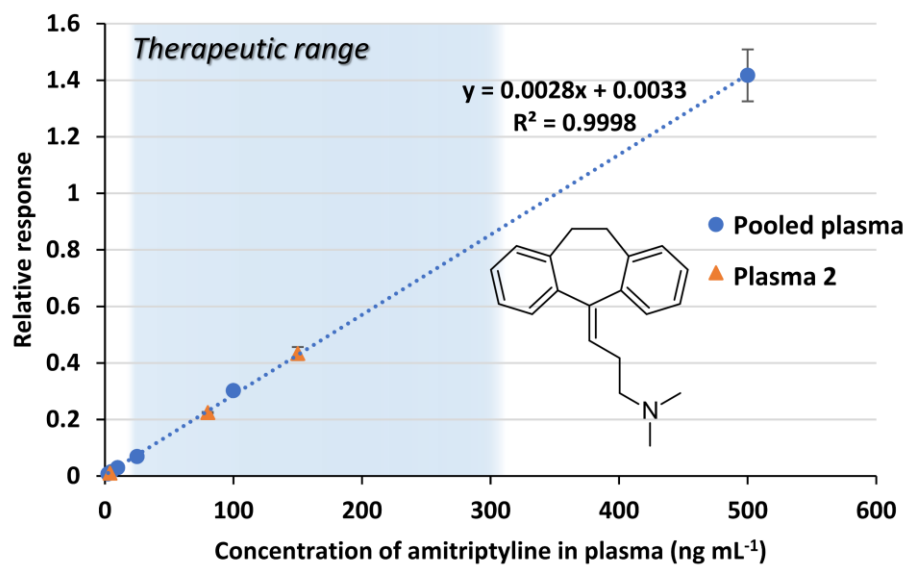


**Figure 3.20.** External calibration curve of thin film MIP device in pooled human plasma samples.

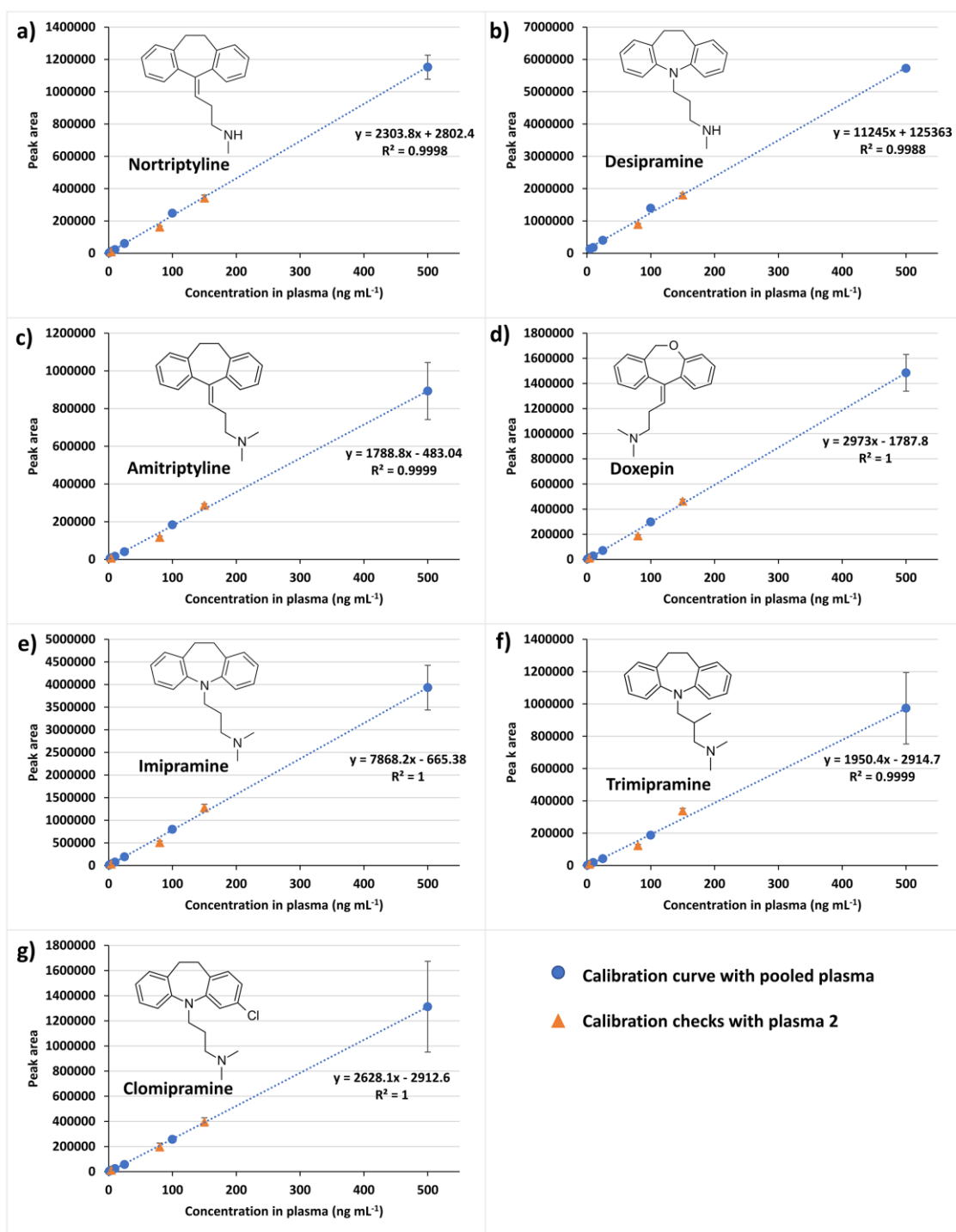


**Figure 3.21.** Calibration curves obtained for extraction of a) nortriptyline, b) desipramine, c) amitriptyline, d) doxepin, e) imipramine, f) trimipramine, and g) clomipramine using thin film MIPs from plasma solutions without internal standard correction.

### 3.3.5. Application to real patient samples for clinical validation

Ultimately any new analytical method must be validated on authentic samples, and for clinical applications this means analysis of patient samples. Three plasma samples from patients on TCA therapies were obtained and analyzed (with internal standard) using the thin film MIP devices. Concentrations presented (Table 3.10) are based on calibration data from extraction of TCAs from pooled plasma samples and correlate well to the patient therapies. In the case of Patient 3 who takes amitriptyline daily, nortriptyline was also detected. Nortriptyline is an N-dealkylated metabolite of amitriptyline. Because MIPs have complementary cavities for compounds which have similar structures and functionality, they can be used to extract and analyze metabolites with similar structures. Thus MIPs can be also be employed for idiosyncratic toxicity studies [57].

**Table 3.10.** Detected concentrations of TCAs in patient samples analyzed by thin film MIP extraction method.

TCAs	Detected concentration ( $\pm$ SD) (ng mL <sup>-1</sup> )			
	Negative control	Patient 1	Patient 2	Patient 3
Nor	0	0	28.4 (0.6)	16.6 (0.3)
Des	0	12.3 (2.4)	0	0
Ami	0	0	0	18.9 (0.7)
Dox	0	0	0	0
Imi	0	0	0	0
Tri	0	0	0	0
Clo	0	0	0	0

Patient dosing:

Patient 1: Desipramine 20 mg day<sup>-1</sup>;

Patient 2: Nortriptyline 50 mg day<sup>-1</sup>;

Patient 3: Amitriptyline 25 mg day<sup>-1</sup>

### 3.4. Conclusion

The growth of precision medicine and the complexity of modern therapeutic agents has driven the need for selective analytical methods that tolerate the wide range of patient blood chemistries. Here, we proved that our optimized MIP thin film is sufficiently selective to minimize the influence of matrix variations to the point where simple matrix-matched calibration gives reproducible and accurate data. The adsorption efficiencies for the MIPs 3 to 5 times better than for the analogous NIPs, which confirms that the use of the pseudo- template gives improved device performance. These single use MIP thin film devices give reliable results in water, solutions of BSA, and a range of human plasma samples. Clinical applications for the method were demonstrated by analyzing patient samples who regularly take TCAs. Although, the method reported here is already high throughput, it can be improved further with integration into modern automated sample processing systems, e.g., 96-well plate systems.

### 3.5. References

- [1] K. Gorynski, A critical review of solid-phase microextraction applied in drugs of abuse determinations and potential applications for targeted doping testing, *TrAC, Trends Anal. Chem.* 112 (2019) 135-146.
- [2] S. Seidi, M. Rezazadeh, R. Alizadeh, Miniaturized sample preparation methods for saliva analysis, *Bioanalysis* 11(02) (2019) 119-148.
- [3] S. Ansari, M. Karimi, Recent progress, challenges and trends in trace determination of drug analysis using molecularly imprinted solid-phase microextraction technology, *Talanta* 164 (2017) 612-625.
- [4] Z. Niu, W. Zhang, C. Yu, J. Zhang, Y. Wen, Recent advances in biological sample preparation methods coupled with chromatography, spectrometry and electrochemistry analysis techniques, *TrAC, Trends Anal. Chem.* 102 (2018) 123-146.

- [5] J.-P. Lambert, W.M. Mullett, E. Kwong, D. Lubda, Stir bar sorptive extraction based on restricted access material for the direct extraction of caffeine and metabolites in biological fluids, *J. Chromatogr. A* 1075(1-2) (2005) 43-49.
- [6] P.-K. So, B.-C. Yang, W. Li, L. Wu, B. Hu, Simple fabrication of solid-phase microextraction with surface-coated aluminum foil for enhanced detection of analytes in biological and clinical samples by mass spectrometry, *Anal. Chem.* 91(15) (2019) 9430-9434.
- [7] A. Taghvimi, H. Hamishehkar, Developed nano carbon-based coating for simultaneous extraction of potent central nervous system stimulants from urine media by stir bar sorptive extraction method coupled to high performance liquid chromatography, *J. Chromatogr. B* 1125 (2019) 121701.
- [8] R. Rahimpour, A. Bahrami, D. Nematollahi, F.G. Shahna, M. Farhadian, Facile and sensitive determination of urinary mandelic acid by combination of metal organic frameworks with microextraction by packed sorbents, *J. Chromatogr. B* 1114 (2019) 45-54.
- [9] M. Abdel-Rehim, S. Pedersen-Bjergaard, A. Abdel-Rehim, R. Lucena, M.M. Moein, S. Cárdenas, M. Miró, Microextraction approaches for bioanalytical applications: An overview, *J. Chromatogr. A* 1616 (2020) 460790.
- [10] A. El-Beqqali, L.I. Andersson, A.D. Jeppsson, M. Abdel-Rehim, Molecularly imprinted polymer-sol-gel tablet toward micro-solid phase extraction: II. Determination of amphetamine in human urine samples by liquid chromatography–tandem mass spectrometry, *J. Chromatogr. B* 1063 (2017) 130-135.
- [11] B. Mikova, M. Dvorak, L. Rysava, P. Kuban, Hollow fiber liquid-phase microextraction at-line coupled to capillary electrophoresis for direct analysis of human body fluids, *Anal. Chem.* 92(10) (2020) 7171-7178.
- [12] A. Golbabanezhadazizi, E. Ranjbari, M.R. Hadjmohammadi, H. Daneshinejad, Determination of selective serotonin reuptake inhibitors in biological samples via magnetic stirring-assisted dispersive liquid–liquid microextraction followed by high performance liquid chromatography, *RSC Adv.* 6(56) (2016) 50710-50720.
- [13] S. Pedersen-Bjergaard, Electromembrane extraction—looking into the future, *Anal. Bioanal. Chem.* 411(9) (2019) 1687-1693.
- [14] L. Nováková, H. Vlčková, A review of current trends and advances in modern bio-analytical methods: chromatography and sample preparation, *Anal. Chim. Acta* 656(1-2) (2009) 8-35.
- [15] S. Huang, N. Ye, G. Chen, R. Ou, Y. Huang, F. Zhu, J. Shen, G. Ouyang, A robust and homogeneous porous poly (3, 4-ethylenedioxythiophene)/graphene thin film for high-

efficiency laser desorption/ionization analysis of estrogens in biological samples, *Talanta* 195 (2019) 290-297.

[16] B. Onat, H. Rosales-Solano, J. Pawliszyn, Development of a biocompatible solid phase microextraction thin film coating for the sampling and enrichment of peptides, *Anal. Chem.* 92(13) (2020) 9379-9388.

[17] H.D. Ponce-Rodríguez, A.A. García-Robles, P. Sáenz-González, J. Verdú-Andrés, P. Campíns-Falcó, On-line in-tube solid phase microextraction coupled to capillary liquid chromatography-diode array detection for the analysis of caffeine and its metabolites in small amounts of biological samples, *J. Pharm. Biomed. Anal.* 178 (2020) 112914.

[18] E. Gionfriddo, D. Gruszecka, X. Li, J. Pawliszyn, Direct-immersion SPME in soy milk for pesticide analysis at trace levels by means of a matrix-compatible coating, *Talanta* 211 (2020) 120746.

[19] T. Vasiljevic, G.A. Gomez-Rios, J. Pawliszyn, Single-use poly (etheretherketone) solid-phase microextraction–transmission mode devices for rapid screening and quantitation of drugs of abuse in oral fluid and urine via direct analysis in real-time tandem mass spectrometry, *Anal. Chem.* 90(1) (2018) 952-960.

[20] K.-P. Huang, G.-R. Wang, B.-Y. Huang, C.-Y. Liu, Preparation and application of ionic liquid-coated fused-silica capillary fibers for solid-phase microextraction, *Anal. Chim. Acta* 645(1-2) (2009) 42-47.

[21] L.C. de Carvalho Abrão, E.C. Figueiredo, A new restricted access molecularly imprinted fiber for direct solid phase microextraction of benzodiazepines from plasma samples, *Analyst* 144(14) (2019) 4320-4330.

[22] V. Pichon, N. Delaunay, A. Combès, Sample preparation using molecularly imprinted polymers, *Anal. Chem.* 92(1) (2019) 16-33.

[23] A. Azizi, C.S. Bottaro, A critical review of molecularly imprinted polymers for the analysis of organic pollutants in environmental water samples, *J. Chromatogr. A* 1614 (2020) 460603.

[24] M.R. Gama, C.B.G. Bottoli, Molecularly imprinted polymers for bioanalytical sample preparation, *J. Chromatogr. B* 1043 (2017) 107-121.

[25] G. Van Biesen, J.M. Wiseman, J. Li, C.S. Bottaro, Desorption electrospray ionization-mass spectrometry for the detection of analytes extracted by thin-film molecularly imprinted polymers, *Analyst* 135(9) (2010) 2237-40.

[26] A.O. Gryshchenko, C.S. Bottaro, Development of molecularly imprinted polymer in porous film format for binding of phenol and alkylphenols from water, *Int. J. Mol. Sci.* 15(1) (2014) 1338-57.

- [27] H.Y. Hijazi, C.S. Bottaro, Selective determination of semi-volatile thiophene compounds in water by molecularly imprinted polymer thin films with direct headspace gas chromatography sulfur chemiluminescence detection, *Analyst* 143(5) (2018) 1117-1123.
- [28] H.Y. Hijazi, C.S. Bottaro, Analysis of thiophenes in seawater: Molecularly imprinted polymer thin-film extraction with desorption electrospray ionization mass spectrometry, *Int. J. Mass spectrom.* 443 (2019) 9-15.
- [29] H.Y. Hijazi, C.S. Bottaro, Molecularly imprinted polymer thin-film as a micro-extraction adsorbent for selective determination of trace concentrations of polycyclic aromatic sulfur heterocycles in seawater, *J. Chromatogr. A* 1617 (2020) 460824.
- [30] G.F. Abu-Alsoud, K.A. Hawboldt, C.S. Bottaro, Comparison of four adsorption isotherm models for characterizing molecular recognition of individual phenolic compounds in porous tailor-made molecularly imprinted polymer films, *ACS Appl. Mater. Interfaces* 12(10) (2020) 11998-12009.
- [31] F. Shahhoseini, A. Azizi, S.N. Egli, C.S. Bottaro, Single-use porous thin film extraction with gas chromatography atmospheric pressure chemical ionization tandem mass spectrometry for high-throughput analysis of 16 PAHs, *Talanta* 207 (2020) 120320.
- [32] A. Azizi, F. Shahhoseini, A. Modir-Rousta, C.S. Bottaro, High throughput direct analysis of water using solvothermal headspace desorption with porous thin films, *Anal. Chim. Acta* 1087 (2019) 51-61.
- [33] B.A. Baldo, M.A. Rose, The anaesthetist, opioid analgesic drugs, and serotonin toxicity: a mechanistic and clinical review, *Br. J. Anaesth.* 124(1) (2020) 44-62.
- [34] M. King, N. Ashraf, Tricyclic Antidepressant-Induced Anticholinergic Delirium in a Young Healthy Male Individual, *Drug Saf. Case Rep.* 5(1) (2018) 1-5.
- [35] S.M. Rombach, E.J. Wesselink, E.I. de Stoppelaar, E.R. Rijnsburger, C. Slagt, Glucagon in hemodynamic instability after tricyclic antidepressant overdose, *Netherlands J. Crit. Care* 24(1) (2016) 25-27.
- [36] M. Grundmann, I. Kacirova, R. Urinovska, Therapeutic monitoring of psychoactive drugs-antidepressants: a review, *Biomed. Pap. Med. Fac. Palacky Univ. Olomouc* 159(1) (2015).
- [37] D.N. Bailey, P.I. Jatlow, Gas-chromatographic analysis for therapeutic concentrations of amitriptyline and nortriptyline in plasma, with use of a nitrogen detector, *Clin. Chem.* 22(6) (1976) 777-781.

- [38] D.N. Bailey, P.I. Jatlow, Gas-chromatographic analysis for therapeutic concentration of imipramine and desipramine in plasma, with use of a nitrogen detector, *Clin. Chem.* 22(10) (1976) 1697-1701.
- [39] S. Leucht, W. Steimer, S. Kreuz, D. Abraham, P.J. Orsulak, W. Kissling, Doxepin plasma concentrations: is there really a therapeutic range?, *J. Clin. Psychopharmacol.* 21(4) (2001) 432-439.
- [40] R.S. Stern, I.M. Marks, D. Mawson, D.K. Luscombe, Clomipramine and exposure for compulsive rituals: II. Plasma levels, side effects and outcome, *Br. J. Psychiatry* 136(2) (1980) 161-166.
- [41] J.C. Nelson, P. Jatlow, D.M. Quinlan, M.B. Bowers, Desipramine plasma concentration and antidepressant response, *Arch. Gen. Psychiatry* 39(12) (1982) 1419-1422.
- [42] S.H. Preskorn, R.C. Dorey, G.S. Jerkovich, Therapeutic drug monitoring of tricyclic antidepressants, *Clin. Chem.* 34(5) (1988) 822-828.
- [43] A. Mohebbi, S. Yaripour, M.A. Farajzadeh, M.R.A. Mogaddam, Combination of dispersive solid phase extraction and deep eutectic solvent-based air-assisted liquid-liquid microextraction followed by gas chromatography-mass spectrometry as an efficient analytical method for the quantification of some tricyclic antidepressant drugs in biological fluids, *J. Chromatogr. A* 1571 (2018) 84-93.
- [44] M. Safari, M. Shahlaei, Y. Yamini, M. Shakorian, E. Arkan, Magnetic framework composite as sorbent for magnetic solid phase extraction coupled with high performance liquid chromatography for simultaneous extraction and determination of tricyclic antidepressants, *Anal. Chim. Acta* 1034 (2018) 204-213.
- [45] J.J. Poole, G.A. Gómez-Ríos, E. Boyacı, N. Reyes-Garcés, J. Pawliszyn, Rapid and concomitant analysis of pharmaceuticals in treated wastewater by coated blade spray mass spectrometry, *Environ. Sci. Technol.* 51(21) (2017) 12566-12572.
- [46] G.A. Gómez-Ríos, M. Tascon, N. Reyes-Garcés, E. Boyacı, J.J. Poole, J. Pawliszyn, Rapid determination of immunosuppressive drug concentrations in whole blood by coated blade spray-tandem mass spectrometry (CBS-MS/MS), *Anal. Chim. Acta* 999 (2018) 69-75.
- [47] N. Reyes-Garcés, B. Bojko, D. Hein, J. Pawliszyn, Solid Phase Microextraction Devices Prepared on Plastic Support as Potential Single-Use Samplers for Bioanalytical Applications, *Anal. Chem.* 87(19) (2015) 9722-9730.
- [48] F.S. Mirnaghi, Y. Chen, L.M. Sidisky, J. Pawliszyn, Optimization of the Coating Procedure for a High-Throughput 96-Blade Solid Phase Microextraction System Coupled

with LC–MS/MS for Analysis of Complex Samples, *Anal. Chem.* 83(15) (2011) 6018-6025.

[49] H. Zhang, X.-J. Ju, R. Xie, C.-J. Cheng, P.-W. Ren, L.-Y. Chu, A microfluidic approach to fabricate monodisperse hollow or porous poly(HEMA–MMA) microspheres using single emulsions as templates, *J. Colloid Interface Sci.* 336(1) (2009) 235-243.

[50] P.A.G. Cormack, A.Z. Elorza, Molecularly imprinted polymers: synthesis and characterisation, *J. Chromatogr. B* 804(1) (2004) 173-182.

[51] S.-B. Kim, T. Lee, H.S. Lee, C.K. Song, H.-J. Cho, D.-D. Kim, H.-J. Maeng, I.-S. Yoon, Development and validation of a highly sensitive LC–MS/MS method for the determination of acetaminophen in human plasma and its application to a protein binding study, *Arch. Pharmacol.* 39(2) (2016) 213-220.

[52] R. Jiang, J. Pawliszyn, Thin-film microextraction offers another geometry for solid-phase microextraction, *TrAC, Trends Anal. Chem.* 39 (2012) 245-253.

[53] S. Ulrich, Solid-phase microextraction in biomedical analysis, *J. Chromatogr. A* 902(1) (2000) 167-194.

[54] G.F. Abu-Alsoud, K.A. Hawboldt, C.S. Bottaro, Assessment of cross-reactivity in a tailor-made molecularly imprinted polymer for phenolic compounds using four adsorption isotherm models, *J. Chromatogr. A* 1629 (2020) 461463.

[55] S.C. Risch, L.Y. Huey, D.S. Janowsky, Plasma levels of tricyclic antidepressants and clinical efficacy: Review of the literature: I, Physicians Postgraduate Press, US, 1979, pp. 6-21.

[56] Bioanalytical Method Validation Guidance for Industry, 2018. <https://www.fda.gov/files/drugs/published/Bioanalytical-Method-Validation-Guidance-for-Industry.pdf>.

[57] B. Wen, L. Ma, M. Zhu, Bioactivation of the tricyclic antidepressant amitriptyline and its metabolite nortriptyline to arene oxide intermediates in human liver microsomes and recombinant P450s, *Chem. Biol. Interact.* 173(1) (2008) 59-67.

## **Chapter 4: Single-use porous polymer thin-film device: a reliable sampler for analysis of drugs in small volumes of biofluids**

Fereshteh Shahhoseini, Ali Azizi, and Christina S. Bottaro. "Single-use porous polymer thin-film device: A reliable sampler for analysis of drugs in small volumes of biofluids." *Analytica Chimica Acta*, 2022, 1203,339651.

## 4.1. Introduction

The growing demand for precision medicine has led to numerous new analytical protocols for analysis of biological materials [1]. Microsampling which requires only small amounts of biological material ( $<100\ \mu\text{L}$ ) from the human body has attracted much interest. This has led to miniaturization of diagnostic devices and less invasive sampling procedures [2]. Some exemplary microsampling techniques are volumetric absorptive microsampling, capillary microsampling, solid phase microextraction (SPME) and dried matrix spot (DMS) [3].

Dried blood spot (DBS) analysis, as the most common DMS, is user-friendly and cost effective for routine screening of drugs and biomarkers and in targeted preclinical and clinical studies that demand extensive pharmacokinetic and pharmacodynamic data [4]. However, DBS needs significant sample preparation to meet satisfactory levels of reliability, such as protein precipitation (PP), liquid-liquid extraction (LLE), solid phase extraction (SPE), and centrifugation before instrumental analysis [5]. Moreover, there are biases in the recovery and significant matrix effects with DBS caused by a non-homogeneous distribution of whole blood across the spot and viscosity related diffusion properties of blood [6]. Dried plasma spot (DPS) is better suited for clinical pharmacokinetic studies than DBS, even with the hurdle of blood processing to obtain plasma. Although much research has been conducted to improve the aforementioned spotting techniques [7], there are still some drawbacks such as co-extraction of matrix components and analyte dilution that reduce sensitivity and reproducibility [8, 9]. Spotting techniques also need several hours for the biofluids to dry to reduce the risks of infection

for analysts and sample contamination [10]. Additionally, the demand for room-temperature sample storage approaches has increased to allow extended storage in resource-poor settings or to accommodate delayed sample processing. However, DBS is not well-suited for preservation of extracted pharmaceuticals [11]. Therefore, it is imperative to develop simple microsampling devices that can resolve matrix related issues and preserve the analytes of interest.

SPME, which has simplified extraction and clean-up for a wide range of analytes in biological samples, is another technique for microsampling [12]. It is portable and automatable, and can be directly coupled with various detection systems for on site, sensitive, fast and high-throughput measurements [13]. Thin film SPME (TF-SPME) is a promising SPME geometry which has shown great potential to overcome the limitations of microsampling techniques. More congruent with spot sampling analysis, user-friendly TF-SPME devices employing a thin layer of polyacrylonitrile (PAN)-over C<sub>18</sub>-PAN SPME on mesh or metal blade substrates have been used for extracted blood spot (EBS) [14]. These devices have been used with routine analysis methods such as liquid chromatography (LC) by spot sampling from the blade or with direct introduction methods (i.e., direct analysis in real time (DART) with mesh geometry), though methods can be limited by lengthy desorption prior to LC and harsh conditions for drying the mesh before introduction to DART. In another effort, a thin film of PAN containing hydrophilic lipophilic balance (HLB) particles was employed for screening of biofluidic spots [15]. The authors showed that the pharmaceuticals were stable at room temperature for up to 7 days, and with freezing this could be extended to a month. Most SPME devices are intended to be used multiple times, requiring thorough cleaning to prevent carryover.

Porous thin films of organic polymers coated on glass substrates have been employed as single-use extraction devices for environmental analysis in our previous papers and showed high efficiency with minimum matrix effects [16, 17]. To the best of our knowledge, these devices have not been reported for small volume analysis of biological samples. In this paper, a new microsampling technique using porous thin films is introduced for analysis of human plasma. The polymer chemistry is optimized to be compatible for adsorption of tricyclic antidepressants (TCAs), as model compounds, from plasma spots. Determination of TCA concentrations in therapeutic drug monitoring (TDM) is a key to finding the optimum individual dose, improving efficiency, and decreasing the risk of intoxication [18]. The custom fabricated porous coating allows for various modes of interaction (i.e., electrostatic, hydrogen bonding and hydrophobic) and offers advantages for spot sampling versus previous approaches. These advantages include: 1) high porosity provides accessible binding sites for adsorption of analytes from plasma samples with high efficiency and limited barriers to fast mass transfer (loading and desorption) and also allows fast drying of the coating after the washing step; 2) requires no preconditioning; 3) easy fabrication with minimal inter-device variability makes the devices economical for single use in routine analysis of scarce biofluids; 4) facilitates fast and simple extraction of drugs from complicated samples with no complex sample processing; 5) devices can be integrated into routine bioanalysis workflows, including LC-MS/MS.

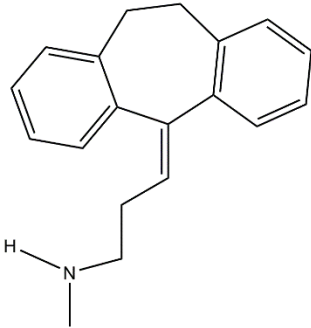
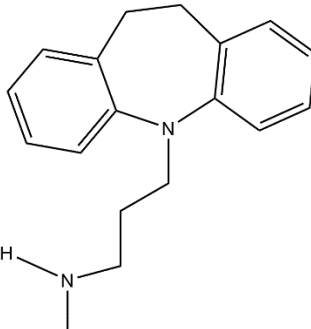
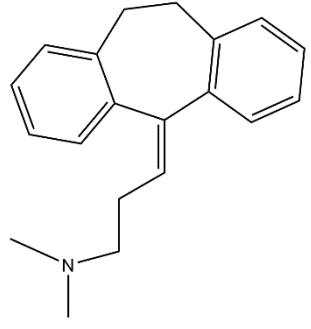
## 4.2. Experimental section

### 4.2.1. Chemicals and materials

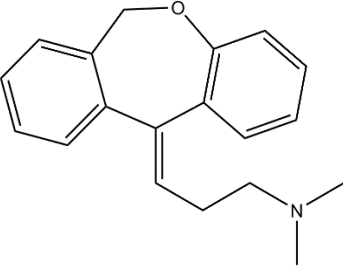
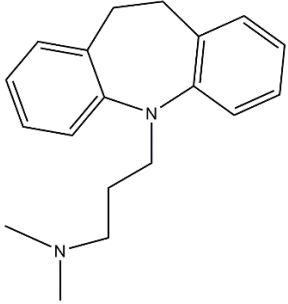
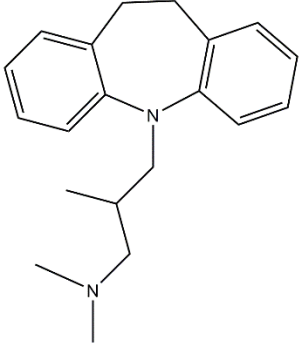
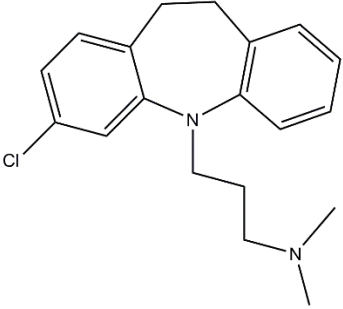
TCAs standard solutions were purchased from Cerilliant (Round Rock, TX, USA). The standards were individual solutions of amitriptyline, imipramine, clomipramine, desipramine, doxepin, trimipramine, nortriptyline at concentration of  $1 \text{ mg mL}^{-1}$  in acetonitrile (ACN) and  $0.1 \text{ mg mL}^{-1}$  of imipramine- $D_3$  reference solution. The structure and physicochemical properties of studied drugs (pKa and logP) are presented in Table 4.1. Ultrapure water ( $18.2 \text{ M}\Omega \text{ cm}^{-1}$ ) was produced using a Milli-Q purification system (Millipore, Sigma-Aldrich, Oakville, Canada). Optima LC-MS grade solvents (methanol (MeOH) and ACN) and reagents (formic acid (FA), methacrylic acid (MAA), acetic acid, triethylamine (TEA) and ethylene glycol dimethacrylate (EGDMA)) were obtained from Fisher Scientific (Whitby, ON, Canada). Allylamine (AAm), Styrene (Sty), 2,2-Dimethoxy-2-phenylacetophenone (DMPA, 99%), and 1-octanol (>99%) were purchased from sigma Aldrich (Oakville, ON, Canada). Stainless steel substrate for preparation of extraction devices were purchased from McMaster Carr (Douglasville, GA, US) and cut by Technical Services at Memorial University. Phosphate-buffered saline solution (PBS) contains  $2 \text{ mM KH}_2\text{PO}_4$ ,  $8 \text{ mM Na}_2\text{HPO}_4$ ,  $137 \text{ mM NaCl}$ , and  $2.7 \text{ mM KCl}$  (pH = 7.4) was purchased from Fisher Scientific (Whitby, ON, Canada). PBS was diluted ( $\times 10$ ) with ultra-pure water before preparing lyophilized bovine serum albumin (BSA) solutions. BSA was provided from Hyclone laboratories Inc. (Whitby, ON, Canada) and dissolved in prepared diluted PBS to yield 5 % BSA (w/v). Using diluted PBS for making BSA solution can help in better dissolving of BSA and result in a more similar representative of biological

fluidics. Human pooled plasma sample (K2 EDTA) was purchased from BioIVT (Westbury, NY, USA).

**Table 4.1.** Targeted TCAs with physical and chemical properties

Compound	Structure	pKa	LogP
Nortriptyline		10.1	4.51
Desipramine		10.4	4.90
Amitriptyline		9.4	4.92

**Table 4.1.** (Continued)

Compound	Structure	pKa	LogP
<b>Doxepin</b>		8.96	4.29
<b>Imipramine</b>		9.4	4.80
<b>Trimipramine</b>		9.42	4.2
<b>Clomipramine</b>		8.98	5.19

#### 4.2.2. Instrumentation

All the LC-MS/MS quantitation experiments were performed by an Acquity ultra performance liquid chromatography (UPLC) system coupled with a Xevo TQ-S from Waters Corporation (Milford, MA, USA) equipped with a Z-spray electrospray ionization (ESI) source. Separations of the TCAs were carried out on an Acquity BEH C<sub>18</sub> (1.7 μm) column (2.1×150 mm) maintained at 30.0 °C with an isocratic mobile phase of 50% ACN with 50% aqueous formic acid (0.1 %) at a flow rate of 0.4 mL min<sup>-1</sup> for a total separation time of 1.7 min. A sample manager flow-through needle (SM-FTN) was employed to inject 5 μL of sample; samples were kept at 4 °C while awaiting injection. Each drug was quantified in positive mode by multiple reaction monitoring (MRM); further details regarding MRM transitions, cone voltages and collision energy are presented in Table 4.2. Capillary voltage of +3.5 kV was applied and source temperature and desolvation temperature were set at 150°C and 500 °C, respectively. The cone and desolvation gases were set at flow rates of 150 and 1000 L h<sup>-1</sup>, respectively. Peak Scientific nitrogen generator (Scotland, UK) was employed to supply the required nitrogen for MS.

**Table 4.2.** Summary of tandem mass spectrometry parameters for determination of tricyclic antidepressants.

Drugs	Precursor ion (m/z)	Cone voltage (V)	Product ion (m/z)	Collision energy (eV)	Product ion (m/z)	Collision energy (eV)
Nortriptyline	264.3	25	105.0	24	233.2	18
Desipramine	267.1	25	72.1	18	208.1	24
Amitriptyline	278.1	35	91.0	26	117.1	22
Doxepin	280.1	35	107.0	28	235.1	15
Imipramine	281.1	25	58.1	35	85.9	20
Imipramine-D3	284.2	30	89.1	15	208.2	30
Trimipramine	295.1	35	100.0	24	192.8	56
Clomipramine	315.1	35	58.0	42	85.9	24

### **4.2.3. Manufacture of single-use porous polymeric thin film devices**

Porous polymeric thin films were made using our previously published drop-casting method [16, 17], and cast on a sword shape stainless steel substrate with a dimension of  $5 \times 25 \text{ mm}^2$ . The crosslinked polymer was produced by depositing  $3 \text{ }\mu\text{L}$  of the pre-polymerization solution on a blade, which is then covered with a glass cover slide ( $18 \times 18 \text{ mm}^2$ ) and exposed to UV light (365 nm) for 30 min (Figure 4.1). The pre-polymerization solution was prepared by vortex mixing of 1.2 mmol ( $102 \text{ }\mu\text{L}$ ) of methacrylic acid (MAA, functional monomer), 4.8 mmol ( $906 \text{ }\mu\text{L}$ ) of ethylene glycol dimethacrylate (EGDMA, crosslinker), 16 mg 2,2-dimethoxy-2-phenylacetophenone (DMPA, photoinitiator) in  $1000 \text{ }\mu\text{L}$  1-octanol (porogen). The solution was degassed in an ultrasonic bath (5 min) to remove oxygen that can interfere with radical polymerization. After formation of an opaque crosslinked polymer with the length of 18 mm, the cover glass was removed, and the thin film was washed with 10% acetic acid in MeOH for 2 h stirred at 500 rpm to remove unreacted components. The dry thin film devices can be stored at ambient conditions and no preconditioning is required prior to use.

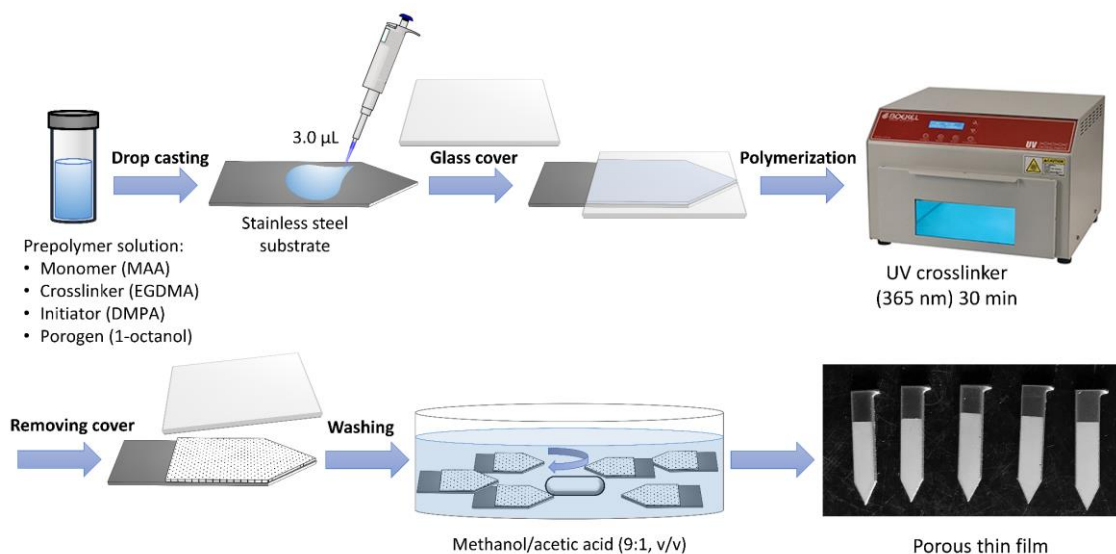


**Figure 4.1.** Schematic presentation for fabrication of porous thin films.

#### 4.2.4. Extracted biofluid spot procedure

Untreated pooled plasma was thawed, spiked with a mixture of TCA standards, and incubated for 1 h to establish equilibrium between the drugs and the plasma matrix prior to analysis. No internal standard (IS) was used during method development studies. To compensate for evaporation and instrumental errors, isotopically labelled imipramine (imipramine-D3) was used as IS for inter-device variability assessment. In validation studies, imipramine-D3 was used as a surrogate rather than an IS and spiked into the samples at the same time as the TCA standards. Processing of biofluids involves a simple three step workflow (Figure 4.2): i) deposition of a biofluid droplet (10  $\mu\text{L}$ ) on the film for a 3 min static extraction to isolate analytes; ii) washing the extraction device with 1 mL of 1% aqueous TEA for 10 s under 1000 rpm vortex agitation to remove unbound species, particularly matrix components, and air dried on a Kimwipe to avoid contamination (air

drying was relatively fast (~1 min) owing to the porous structure of the coating); iii) desorption of analytes by immersion in 200  $\mu$ L of 1% FA in ACN in polypropylene autosampler vials with a 300- $\mu$ L fused insert for 2 min under vortex agitation (1500 rpm). Prior to desorption, the dry devices can also be stored for later analysis, which allows time for transportation or for other circumstances where analysis is not carried out immediately (e.g., sample archiving). LC-MS/MS analysis was performed on 5  $\mu$ L of the desorbed solution. All the experiments were conducted in triplicate except for inter-device variability tests which were performed using 10 replicates.

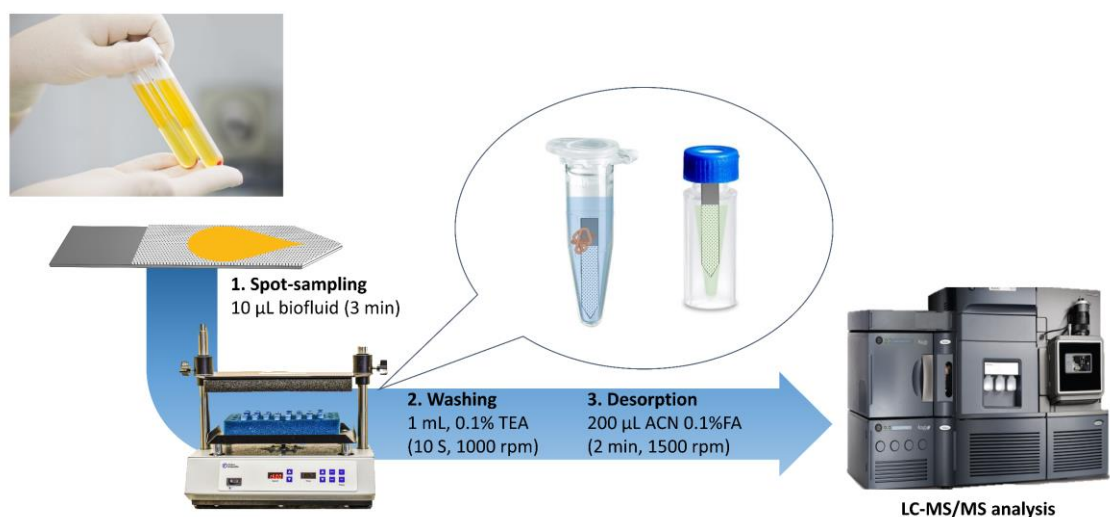


**Figure 4.2.** Analytical workflow for the developed biofluid spot procedure coupled with LC-MS/MS analysis.

## 4.3. Results and discussion

### 4.3.1. Porous thin film for extracted biofluid spot

The multifaceted behaviour of analytes in biofluids presents challenges particularly when considering droplet analysis. Phenomena can be complex, as in the case of analyte-protein interactions which reduce free analyte concentrations, or simple, as with viscosity

which impairs mass-transfer. The developed polymer used in this device is engineered to be wettable by aqueous solutions including plasma providing favourable conditions for analyte adsorption by improving contact between the sample solution and the adsorbent. Moreover, the porous nature of the device coating is highly efficient for adsorption from a viscous sample due to its large number of easily accessed adsorption sites and desorption using an organic solvent. A washing step after spotting removes matrix components (i.e., salts and proteins) from the polymer surface which can contaminate the ion source and reduce reproducibility. As part of method development, optimization of polymer composition and sampling procedure is discussed in this section.

#### *4.3.1.1. Evaluation of coating in extraction of TCAs:*

The extraction devices were prepared on stainless steel substrate as a robust material without chemical or physical treatment compared with glass in our initial research, which simplifies the fabrication of thin films [17, 19]. The steel substrate is also safe for operation during sample preparation and shipment for analysis. The high stability of the coating is because of the highly crosslinked polymer structure [20]. The thickness of the coating, which depends on the composition and volume of drop casted prepolymer, is ~15  $\mu\text{m}$  as shown in Figure 4.3.

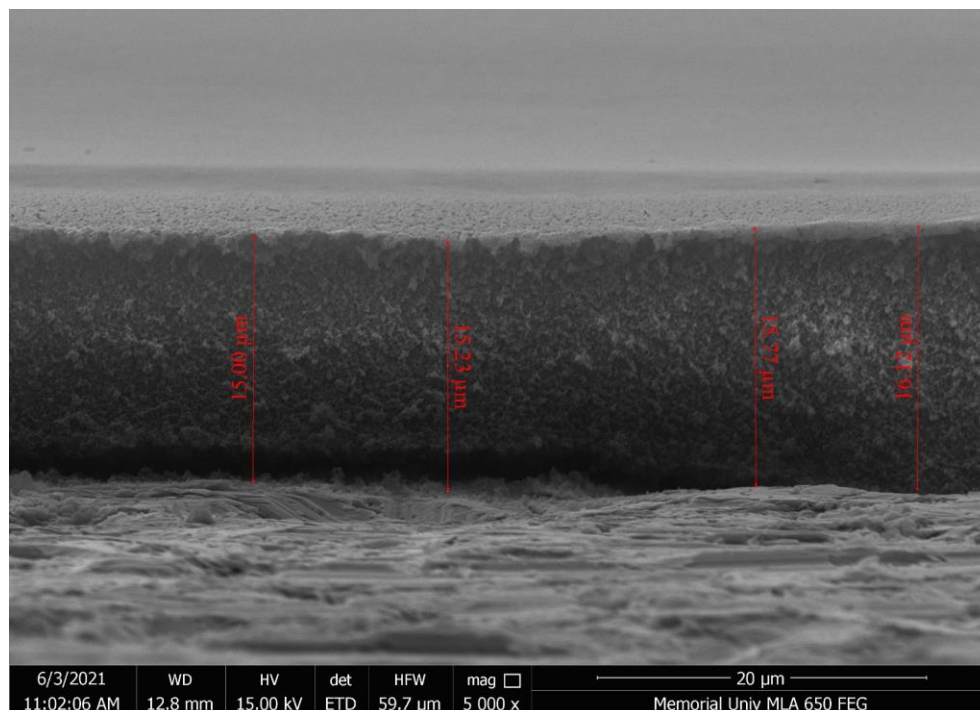


**Figure 4.3.** Side view of porous thin film prepared by MAA at 5000x magnification.

The analytes selected for this work are hydrophobic ( $\log P$ : 4.2-5.19) but are present in the water-soluble protonated form at physiological pH ( $pK_a$  8.96-10.4) and (Table 4.1). Since the purpose of this work is to perform the extraction of analytes with no sample manipulation, no pH adjustment of biological samples is desirable. Such basic drugs can be protonated at neutral pH and therefore a proper sorbent which can extract the charged forms of analytes should be developed. To investigate the significance of the functionality of the monomers at neutral pH values, three monomers with different functionalities that yielded stable polymers were used for extraction (Table 4.3).

Table 4.3. Details of prepolymer solutions used for monomer study.

<b>Monomer</b>	<b>Monomer amount</b>	<b>Crosslinker</b>	<b>porogen</b>	<b>Initiator</b>
MAA	1.2 mmol (102 $\mu$ L)	EGDMA	1-octanol	DMPA
Sty	1.2 mmol (140 $\mu$ L)	4.8 mmol	(1000 $\mu$ L)	(16 mg)
AAM	1.2 mmol (91 $\mu$ L)	(905 $\mu$ L)		

MAA, which is in its acrylate form, is a proton acceptor, Allylamine (AAM) can act as proton donor, and styrene (Sty) is a good monomer for hydrophobic and  $\pi$ - $\pi$  interactions were tested for extraction of TCAs from BSA solution in 5 min intervals (Figure 4.4). Although polymeric coatings with Sty and AAM as monomers were able to extract the target analytes, the recovery values were low with poor repeatability. Unreliable adsorption behaviour in these two porous films is attributed to non-selective interactions between the analytes and the polymer. However, porous films made of MAA yielded extraction efficiencies 2-3 times higher than either Sty or AAM. This result can be explained by electrostatic interactions between the positively charged drugs and negatively charged carboxylate functionality in MAA polymer in addition to hydrophobic interactions present in all the sorbents. However, sorbents with AAM and Sty provide only hydrophobic interactions and are not selective enough for adsorption of TCAs. Thus, MAA is chosen as the monomer to prepare the thin films for TCAs adsorption.

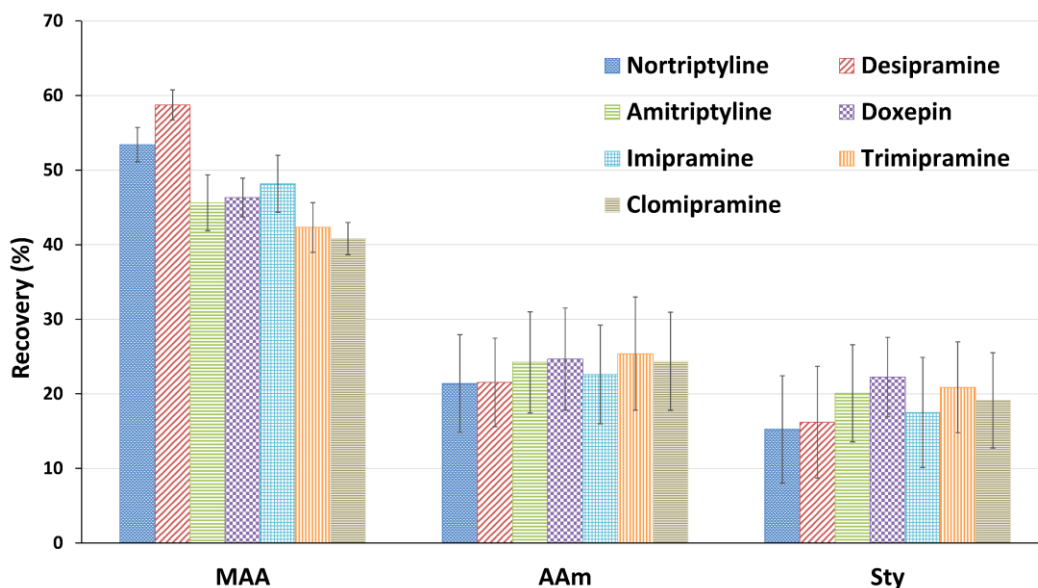


**Figure 4.4.** Effect of different monomers on recovery of TCAs. Extraction: 5 min from 100 ng mL<sup>-1</sup> TCAs in BSA solution, washing: 10 s immersion in 1 mL water 1% TEA, desorption: 300  $\mu$ L ACN/water 0.1% FA for 20 min at 500 rpm (n=3).

### 4.3.2. Optimization of extracted biofluid spot procedure

#### 4.3.2.1. Sample volume

The volume of biofluids that can be loaded onto the device should be maximized to ensure the best limits of detection and optimal exploitation of the available binding sites. We chose an upper limit of 20  $\mu$ L due to the size of the coated area of the device (5 $\times$ 18 mm<sup>2</sup>) including the tip and to keep sample sizes small. BSA solutions (5 % (w/v) in PBS) spiked with TCAs were spotted onto the device coatings with aliquot volumes ranging from 2 to 20  $\mu$ L. Figure 4.5 shows the extracted mass (pg) along with efficiency of the extraction (% recovery) with respect to sample loading on the thin films. Increasing the sample volume from 2 to 20  $\mu$ L increases the extracted mass from 142-168 pg at 2  $\mu$ L to 575-819 pg at 20  $\mu$ L due to higher analyte loadings. However, recoveries were decreased by increasing the sample volumes. Spotting using 2  $\mu$ L of BSA solution containing TCAs

showed recovery values in the range of 71.2-83.8%. Rising the sample volume up to 20  $\mu\text{L}$  decreases the extraction efficiency of TCAs (28.8-41.0%). Although higher volumes increase extracted mass and thus lower detection limits; loadings above 10  $\mu\text{L}$  result in a slight loss in reproducibility and increases in method sensitivity are not sufficient to justify higher sample consumption. Balancing sensitivity and precision, 10  $\mu\text{L}$  with recoveries ranged from 40.8% to 58.7% was chosen as the optimized volume for the rest of the study.

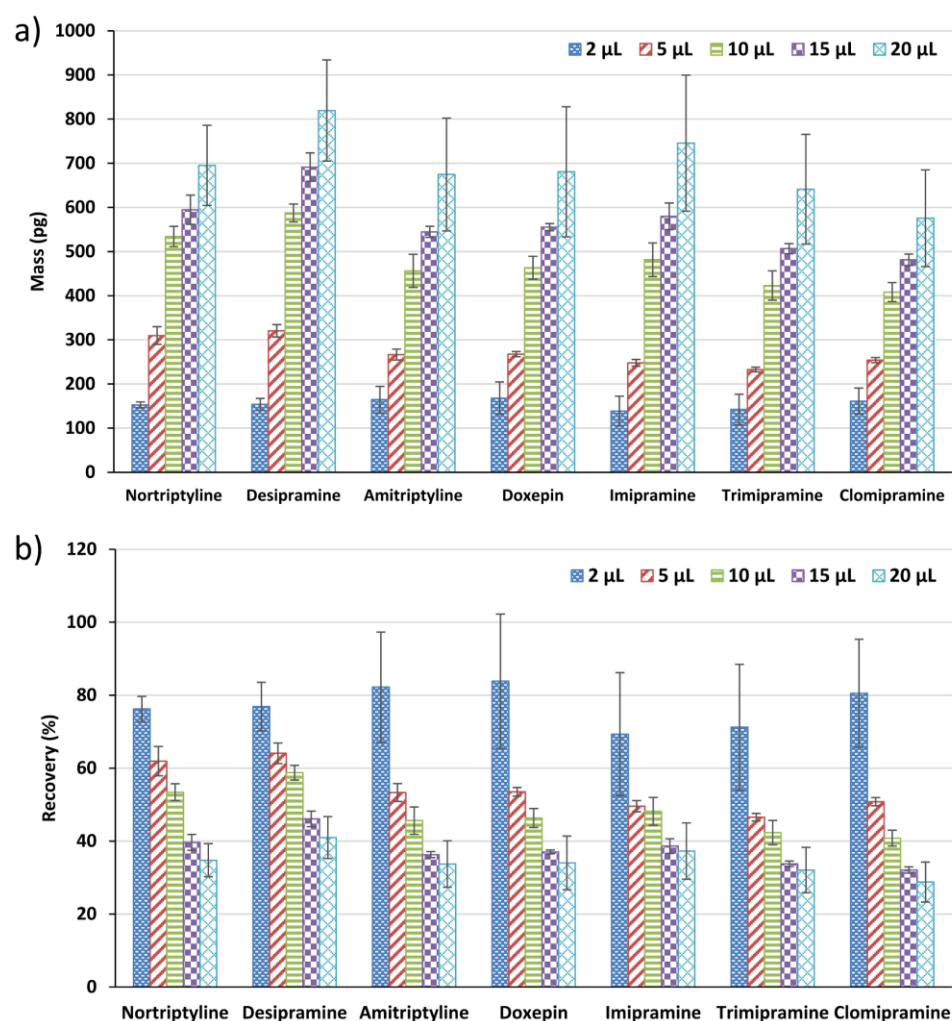


**Figure 4.5.** Effect of different sample volume on extracted mass (a) and recovery (b) of TCAs. Extraction: 5 min from 100  $\text{ng mL}^{-1}$  TCAs in BSA solution, washing: 10 s immersion in 1 mL water 1% TEA, desorption: 300  $\mu\text{L}$  of ACN/Water 0.1% FA for 20 min at 500 rpm (n=3).

#### 4.3.2.2. Solvent desorption

Efficient desorption of the extracted analytes using microsampling devices is necessary for a reproducible and sensitive analytical method. The influence of solvent type and volume, and time spent under vortex agitation were studied. Based on the nature of possible interactions governing the adsorption of TCAs and considering the compatibility with LC-MS/MS, the efficiency of a range of desorption solvent systems were investigated (Figure 4.6); specifically, ACN, MeOH, ACN/water (9:1, v/v), and ACN/water (1:1, v/v) all containing FA (0.1 %). The results showed that ACN with 0.1% FA performed best for desorbing TCAs from polymeric sorbent in terms of efficiency and repeatability compared with MeOH or the two mixtures of ACN with water. The desorption solvent performance also provides some insight into the type of the interactions between the sorbent and the bound analytes. The superiority of the ACN and MeOH with 0.1% FA for most of TCAs suggests that there are hydrophobic interactions for adsorption with this sorbent. The reduced efficiency of desorption and high standard deviations (except nortriptyline and desipramine) using the more polar mixtures of ACN and water confirms that the interactions with the sorbent are dominated by hydrophobic interactions, while the desorption of nortriptyline and desipramine is facilitated with water due to hydrogen bonding with secondary amines in these two molecules. Nevertheless, FA is also important as it supports the protonation of drugs to favour the positively charged form which increases their solubility in polar solvents; it also protonates the negatively charged carboxylate functionality in MAA polymer. As a result, ACN with 0.1% FA was selected over MeOH with 0.1%FA as the optimal desorption solvent due to the better compatibility with mobile phase system.

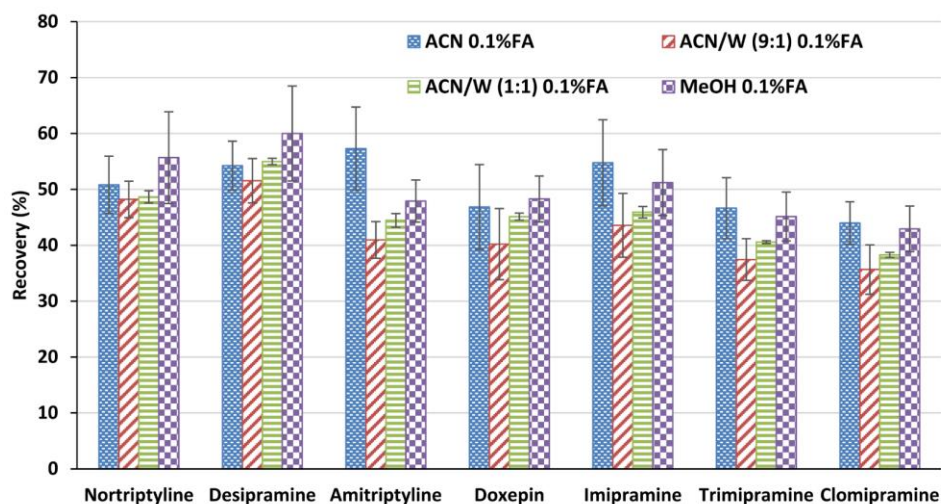


**Figure 4.6.** Desorption solvent study performed at 10 min at 1500 rpm using 500  $\mu\text{L}$  of ACN 0.1% FA at 1500 rpm; Extraction: 10  $\mu\text{L}$  of 100  $\text{ng mL}^{-1}$  TCAs in BSA solution for 5 min; Washing: 10 secs immersion in 1 mL water 1% TEA (n=3).

The solvent volume should be large enough for quantitative desorption of the drugs, balanced with the preference for small volumes to achieve the highest method sensitivity. Different volumes of ACN with 0.1% FA (100-700  $\mu\text{L}$ ) were used to desorb the TCAs from the thin films. As is consistent with a partition driven process, recoveries (Figure 4.7-a), improved with each increase in desorption solvent volume, with the most significant improvement seen with the increase from 100 to 200  $\mu\text{L}$ . For some of the analytes (imipramine, trimipramine and clomipramine) there is no distinct difference between 200 and 700  $\mu\text{L}$ . The rest of the drugs demonstrated  $\sim 15\%$  improvement by increasing the volume from 200 to 700  $\mu\text{L}$ . Despite improvements in absolute recovery, beyond 200  $\mu\text{L}$  dilution was the dominant influence and reduced the signal intensity significantly (Figure 4.7-b). To ensure subtle differences in performance would not be missed, 500  $\mu\text{L}$  was used to ensure maximal recoveries in optimization and qualitative studies. The final optimized

analytical method and reported figures of merit are based on use of 200  $\mu\text{L}$  of desorption solvent to minimize dilution.

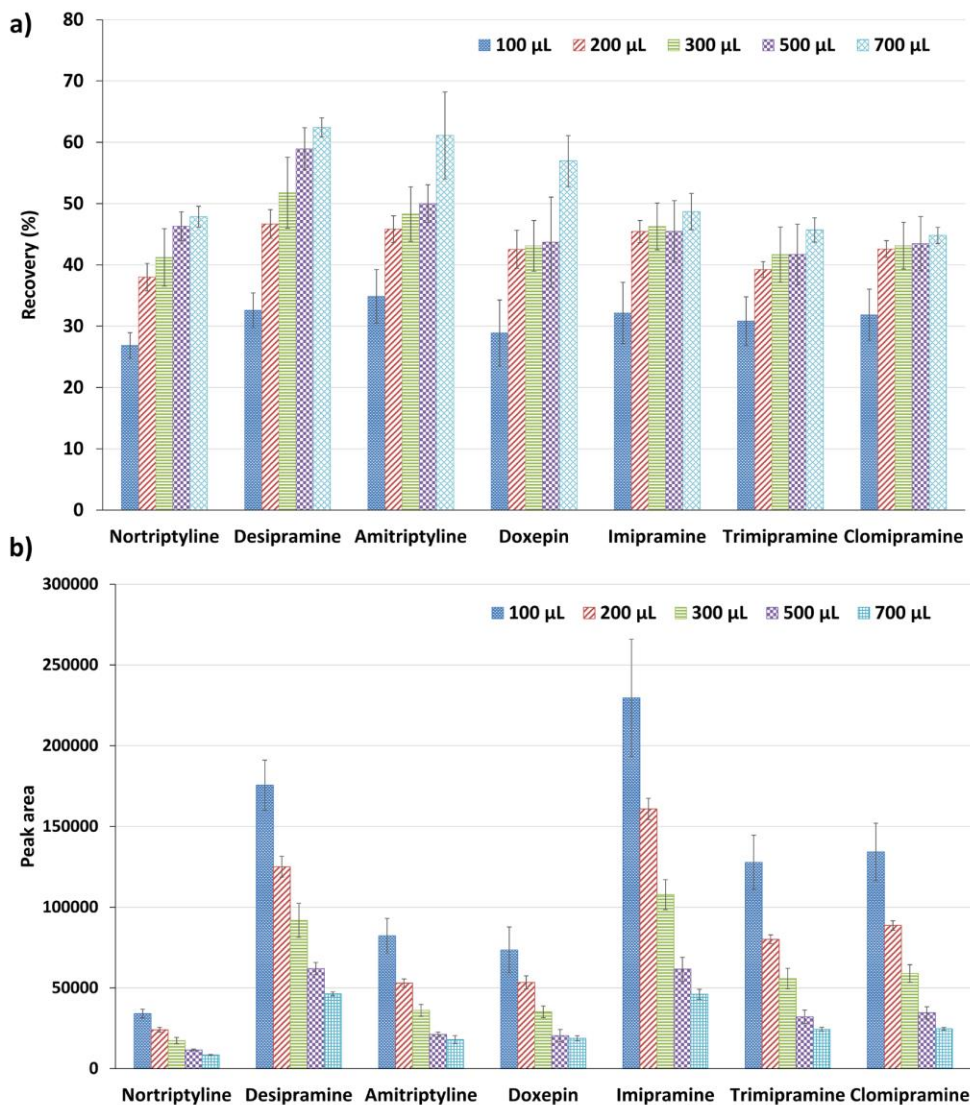


**Figure 4.7.** Desorption solvent volume effect on a) recovery and b) signal intensity (peak area) performed using ACN 0.1% FA at 1500 rpm for 10 min; Extraction: 10  $\mu\text{L}$  of 100  $\text{ng}\cdot\text{mL}^{-1}$  TCAs in BSA solution for 5 min; Washing: 10 secs immersion in 1 mL water 1% TEA (n=3).

New spot sampling methodologies must offer improvements on one or more fronts, such as sensitivity, sample handling, or throughput. Therefore, desorption time influencing both method efficiency and total analysis time was investigated. Desorption time profiles (Figure 4.8) illustrate that there is no significant difference between 2- and 30-min desorption times, which provides further evidence that the coating porosity observed translates to fast mass transfer. With the aim of introducing a quick analysis method, 2 min was selected as the optimal desorption time.

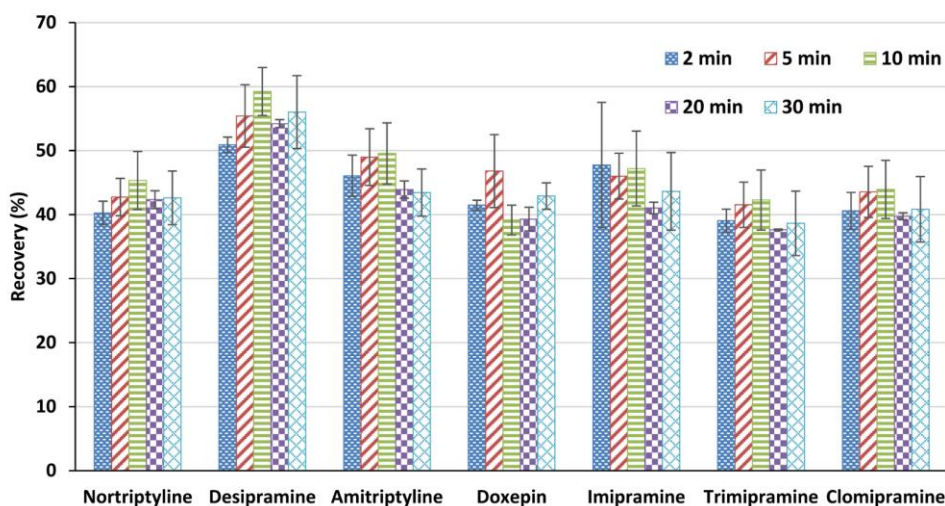


**Figure 4.8.** Desorption time profile using 500  $\mu\text{L}$  of ACN 0.1% FA at 1500 rpm; Extraction: 10  $\mu\text{L}$  of 100  $\text{ng mL}^{-1}$  TCAs in BSA solution for 5 min; Washing: 10 secs immersion in 1 mL water 1% TEA (n=3).

#### 4.3.2.3. Washing effect

Typically, methods employing solid phase extraction incorporate washing steps to remove undesirable matrix components, which can cause signal suppression/enhancement leading to positive or negative errors. This is considered as an advantage of polymer-based solid phase extraction compared to paper-based DBS methods, and is facilitated by

improved strength and specificity of the sorbent. Consequently, matrix effects following desorption directly from DBS cards are of the same magnitude as those observed following protein precipitation protocols [21]. Although incorporation of a washing step may also rinse away weakly bound analytes, the reduction in unpredictable analyte behaviour in complex matrices and resulting instrument contamination compensates for losses in sensitivity. Using our previous work, 1% aqueous TEA was found to be suitable for washing step following adsorption of TCAs from plasma [20]. In this study, recoveries following washing with 1 mL of 1% aqueous TEA under static conditions or with agitation (vortex mixing @1000 rpm) over different washing times (10 s - 60 s) were compared to analysis with no wash step. The experiment with no washing step includes a 3 min extraction, drying the surface of the film using a Kimwipe, and a desorption step. As can be seen in Figure 4.9, there is a significant drop in recoveries (~25%) even after a short 10 s static wash. This washing step might lead to a decreased method sensitivity, but it is crucial to reduce the influence of matrix components on MS performance and data reliability. More aggressive vortex washing for 10 s was not significantly worse than static washing for any TCAs. Even the most aggressive washing showed no differences in recoveries for nortriptyline and desipramine. For the others, losses using longer times ( $\geq 20$  s) were significant, but acceptable. Nevertheless, since some complex samples like whole blood might benefit from two separate cleanup steps, a second washing step was also carried out ( $2 \times 60$  s). There was no significant difference detected in comparison of data from the 60 s vortex wash to  $2 \times 60$  s, which suggests that analytes retained after washing interact strongly with the sorbent. In the interest of time and sensitivity, 10 s washing with 1000 rpm

agitation was used in the optimized method, noting that longer and more aggressive washing regimes are permissible for matrices with more intractable components.

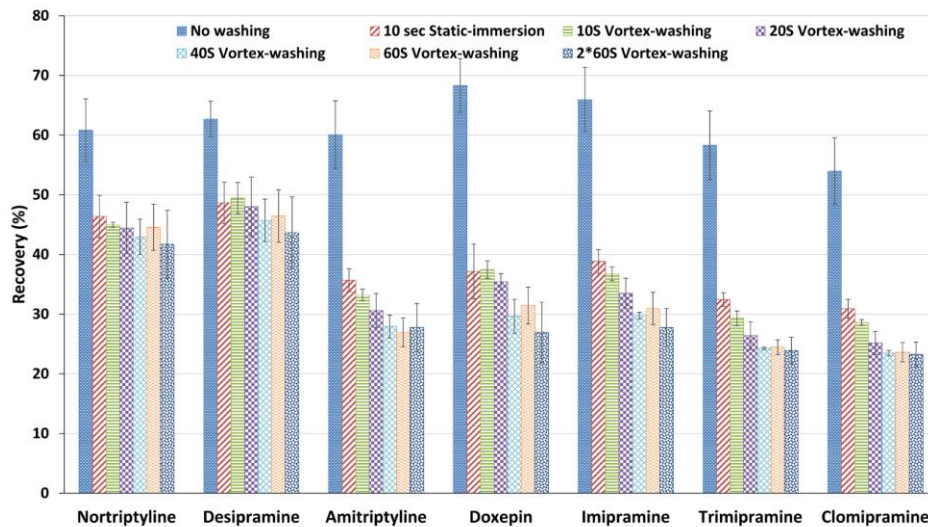


**Figure 4.9.** Washing effect on the percentage recovery of TCAs. Five min static extraction of 10  $\mu\text{L}$  of 100  $\text{ng mL}^{-1}$  TCAs in plasma solution for 5 min, desorption: 500  $\mu\text{L}$  of ACN 0.1% FA for 2 min at 1500 rpm. Washing with 1 mL of 1% TEA ( $n=3$ ).

#### 4.3.2.4. Extraction time profile:

The extraction time profile of analytes is key for SPME-based techniques used under non-equilibrium conditions where extraction efficiency is proportional to extraction time. Ideally, short extraction times are desirable to boost the pace of sample processing. Time profiles (30 s – 10 min) were obtained for TCAs spiked in BSA ( $100 \text{ ng mL}^{-1}$ ) and spotted on the porous thin films. At intervals longer than 10 min, samples spots dried completely, which can deteriorate the device performance. The data (Figure 4.10) demonstrated that static extraction from BSA samples reach the equilibrium within 10 min, before complete dryness. Recoveries for TCAs from BSA solutions reproducibly ranged from 50 to 62% (RSDs: 4.6 - 19%). To assess the thin-film device for analysis of real

biofluids, the extraction time profile was investigated in the spiked pooled plasma (100 ng mL<sup>-1</sup>). The extraction time profile in plasma (Figure 4.11), depicts lower recovery but a similar trend to that of BSA. The extraction equilibrium (plateau) was achieved at ~7 min with recoveries in the range of 32 and 51%, (RSDs: 4.9 - 10.1%). The similarity in kinetic behaviour indicates that the difference in matrix does not dramatically affect the analyte diffusion and partitioning behaviour with respect to these coatings. The obtained recovery values are satisfactory for an SPME-based technique, which is based on non-exhaustive partitioning of analyte between the coating and sample. Analyte quantitation can be performed at pre-equilibrium or equilibrium conditions [22]. Though extraction at equilibrium results in higher sensitivity, 3-min extractions were chosen for method validation as data at this time were reproducible and resulted in good method sensitivities along with fast sample processing, suitable for clinical applications.

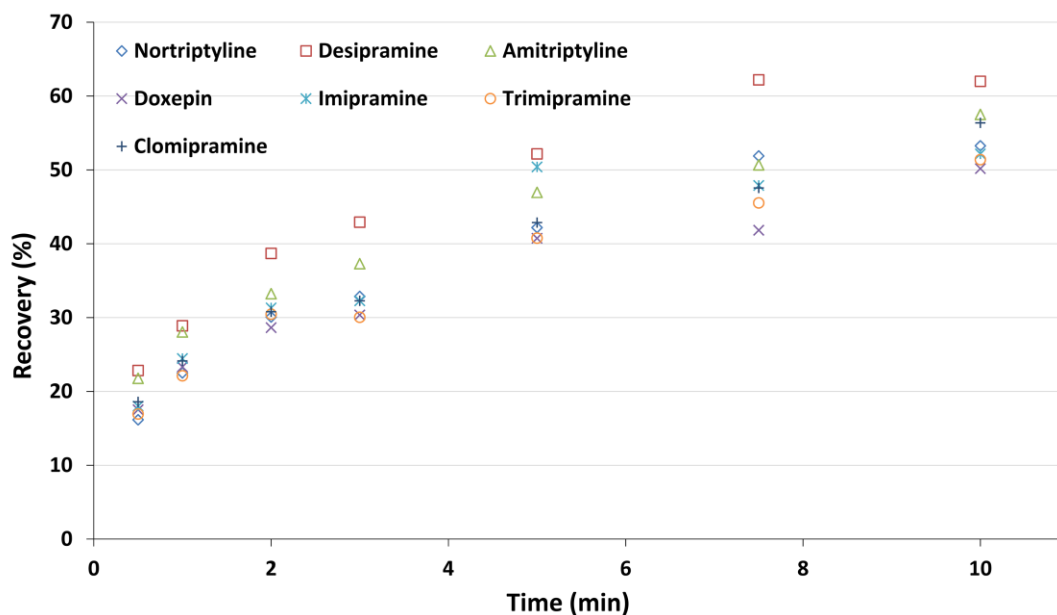


**Figure 4.10.** Extraction time profile TCAs in BSA solution. Static extraction of 10  $\mu\text{L}$  of 100  $\text{ng mL}^{-1}$ , washing: 10 s static wash in 1 mL water 1% TEA, desorption: 500  $\mu\text{L}$  ACN 0.1% FA, 2 mins at 1500 rpm (n=3).

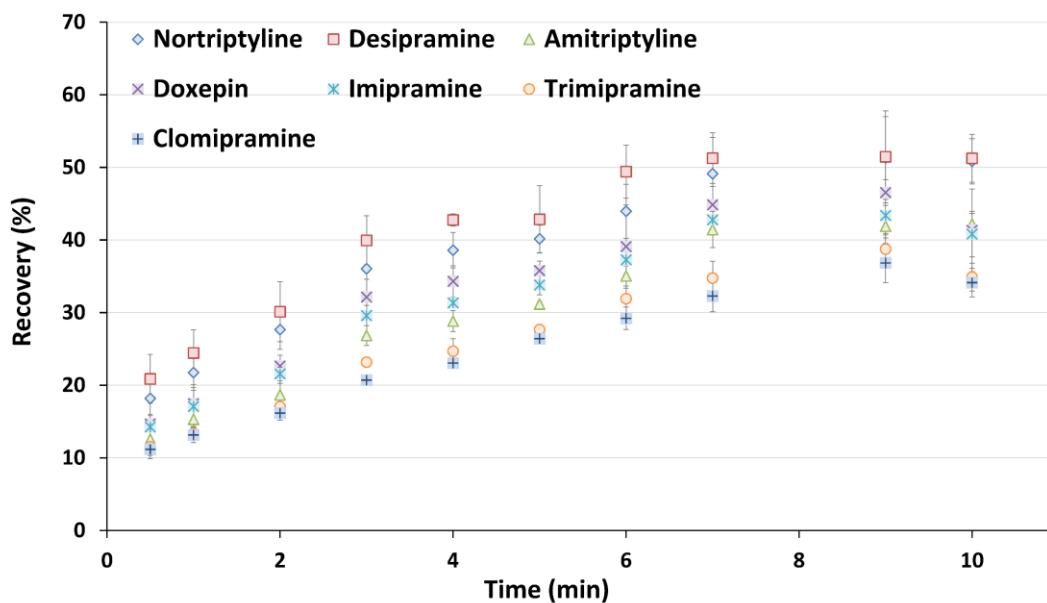


**Figure 4.11.** Extraction time profile in pooled plasma. Static extraction (3 min) of 10  $\mu\text{L}$  of 100  $\text{ng mL}^{-1}$  TCAs, washing: 10 s static wash in 1 mL water 1% TEA, desorption: 500  $\mu\text{L}$  ACN 0.1% FA, 2 min at 1500 rpm (n=3).

### 4.3.3. Matrix effects

Analysis of complex biofluids via ESI-MS can be challenging due to the presence of matrix components that can alter the ionization efficiency through competition for charge or by changing the rate of ion evaporation necessitating sample clean-up [23]. Sample clean-up to eliminate co-extracted matrix interferences is practical with solid sorbents, as with SPE [24] and SPME [25]. To investigate the effect of co-extracted components on method accuracy and precision, a matrix effect study was completed as recommended by Matuszewski et al. [26]. To create a solution containing extracted matrix components (blank extraction), the optimized sampling process was performed on 10  $\mu\text{L}$  of unspiked plasma. TCAs standards were spiked into the resulting solution and into neat solvent (ACN with 0.1% FA) at concentrations of 0.25, 2.5 and 25  $\text{ng mL}^{-1}$ , with no IS added. These concentrations were selected to show matrix effects at low, mid, and high concentrations within the linear range of the instrument. The matrix effect (ME) was calculated based on the following equation.

$$\% ME = \frac{A}{B} \times 100$$

Where A is the peak area of the TCAs drug after blank extraction and B is the peak area measured from standards in clean solvent. Any deviation from 100 percent indicates a matrix effect, though deviation within  $\pm 20\%$  are acceptable [27]. The majority of ME values obtained over all concentrations were within  $\pm 15\%$  (Table 4.4). Accordingly, we conclude that matrix effects associated with extractions using these devices are acceptable, particularly considering that no correction using an IS was used.

**Table 4.4.** Matrix effect study of spot sampling using porous thin-film device

Compound	ME (%) (n=3)			ME RSD % (n=3)		
	0.25 (ng mL <sup>-1</sup> )	2.5 (ng mL <sup>-1</sup> )	25 (ng mL <sup>-1</sup> )	0.25 (ng mL <sup>-1</sup> )	2.5 (ng mL <sup>-1</sup> )	25 (ng mL <sup>-1</sup> )
Nortriptyline	111	108.9	96.9	7.0	2.7	3.2
Desipramine	109	100.4	94.6	2.5	1.4	3.9
Amitriptyline	110	111.2	103	2.3	4.0	3.4
Doxepin	97.5	91.1	85.9	1.4	4.2	3.1
Imipramine	113	108.9	99.4	1.4	3.0	3.9
Trimipramine	131	118.6	106	2.9	1.9	4.3
Clomipramine	125	114.8	105	6.1	1.8	2.8

#### 4.3.4. Single-use sampling devices: suitability for collection, transport and storage

##### 4.3.4.1. Inter-device variability assessment:

Single-use microsampling devices are preferred for clinical analyses to allow for multi-patient sampling and replicate collections. Although this could be achieved with multi-use devices, such devices are typically more expensive, and users must adhere to strict clean-up protocols to eliminate carryover and concern over false-positive results. Nevertheless, single use devices are not without drawbacks. In particular, the performance of each device cannot be calibrated individually, therefore the inter-device variability must be low. Thus, ten thin-film devices were employed for extraction of TCAs from plasma without normalizing the response (Figure 4.12-a). The results (Figure 4.12-b) gave inter-device variabilities (%RSDs) in the range of 8.3 and 19.4 %, which is acceptable for routine screening. RSD can be improved to meet more rigorous standards of repeatability by incorporation of a surrogate or an IS into the method, as can be seen in Figure 4.12-a. The IS only compensates for the variability in the instrumental signal response and some variations in the sample handling after desorption. Addition of a surrogate will compensate for all of the variability throughout the process including variations in partitioning

behaviour during analyte extraction from the spot, but addition of deuterated surrogates to the sample prior to spotting for all analytes is expensive and obviates the value of a device like this for point-of-care applications. To assess the effect of deuterated surrogate in method variability, imipramine-D3 was added into plasma prior to spotting on the device. This procedure has reduced the average inter-device variability from 12.6 to 7.7%.

Since it is difficult to mix a surrogate into blood or plasma in a typical spot sampling environment, the possibility of pre-loading and post-loading of the IS to the device was investigated (Figure 4.12-a). In the pre-loading method, the IS solution is deposited onto the film and dried, then the plasma sample was applied onto to the device. For the post-loading approach, again the optimized sampling process was used; then the IS solution was applied onto the device and allowed to dry prior to desorption and analysis. The results (Figure 4.12-b) demonstrate that there is no significant difference between the precision of these methods. The average RSDs of both methods using IS are less than 10 %. The best agreement is between the conventional surrogate spiking data and the post-loading approach (7.7 and 7.1%, respectively). Although surrogates and IS serve somewhat different roles, it can be concluded that most of the device-to-device variability detected is related to the analytical method (LC-MS/MS) rather than the variability in the device performance. Most important, the application of the IS just prior to analysis improves the repeatability dramatically. As can be seen, imipramine and doxepin have shown the poorest results prior to IS normalization and this is reduced by at least half, even using a single deuterated IS. Moreover, the post-loading of the IS is operationally the simplest, and suitable for clinical applications and for remote sampling. For the present, we conducted

method validation using spiking the deuterated surrogate (imipramine-D3) into the samples.

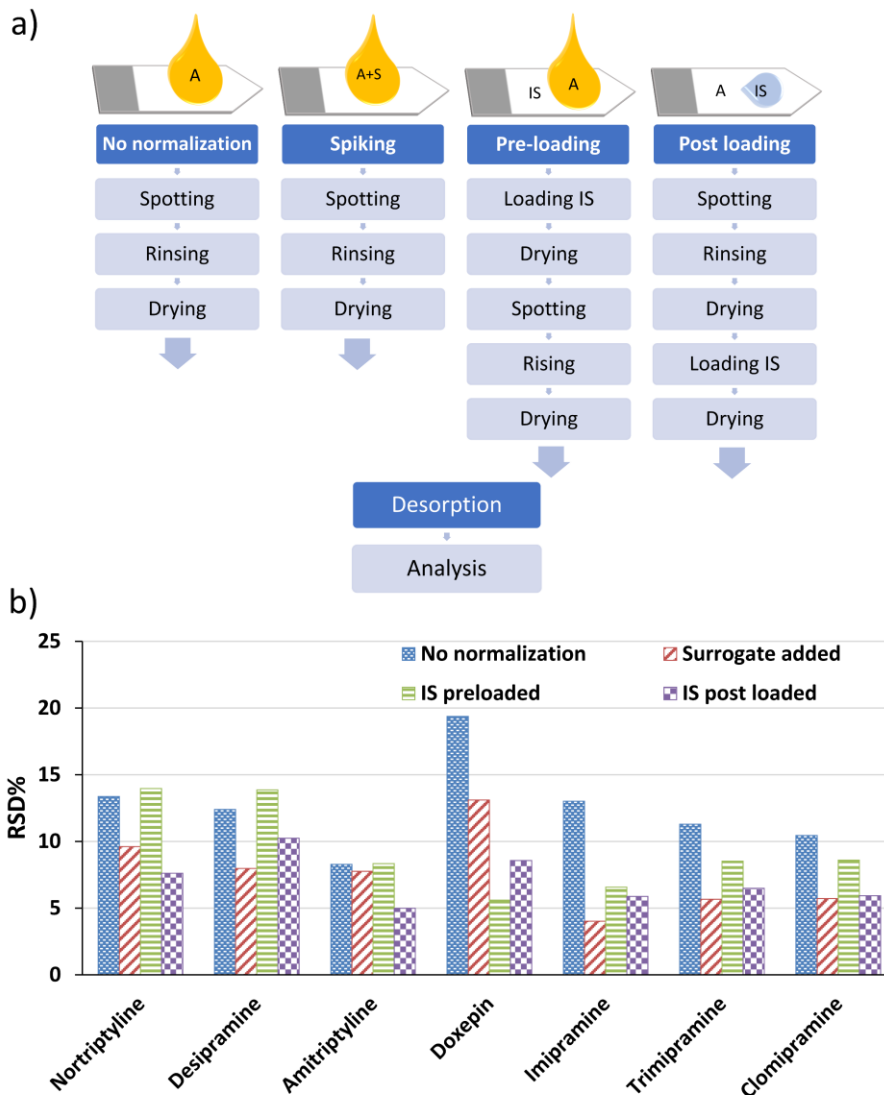


**Figure 4.12.** a) Effect of normalization using a deuterated standard applied into spot sampling method with different approaches (A: analyte, S: surrogate, IS: internal standard). b) acquired RSD values for inter-device variability without using IS and different approaches of loading IS. Extraction: static for 3 min, washing: 10 s in 1 mL water 1% TEA at 1000 rpm, desorption: 500  $\mu$ L ACN 0.1% FA, 2 min at 1500 rpm (n=10 for each method).

To assess the reproducibility of various batches of thin films, inter-batch assessment was conducted using two sets of films fabricated from independent prepolymer solutions

at different days (n=3 for each batch). These two batches showed similar recovery of TCAs from plasma without statistical differences (Figure 4.13 and Table 4.5).

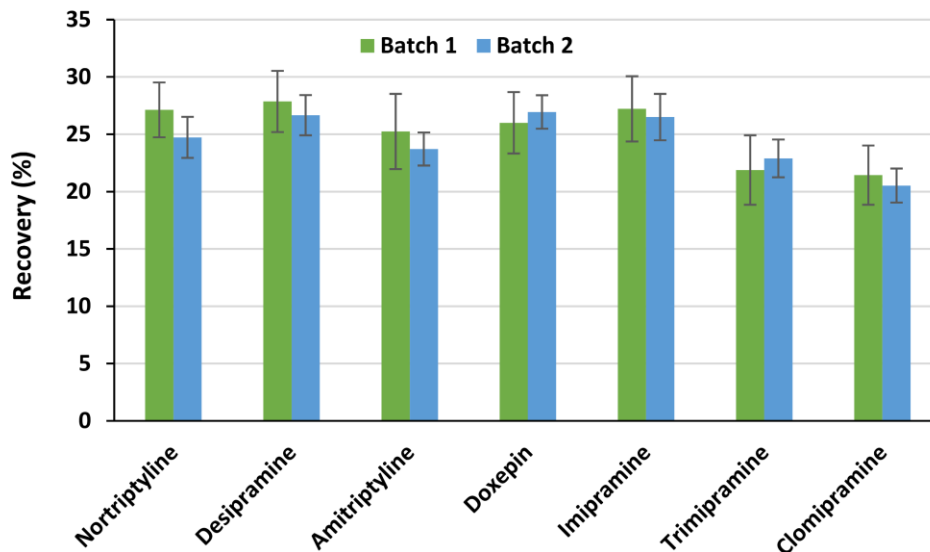


**Figure 4.13.** Inter-batch reproducibility of two different batches of porous thin films. Sample: 10  $\mu\text{L}$  of plasma spiked with TCAs ( $100 \text{ ng mL}^{-1}$ ) and imipramine-D3 ( $50 \text{ ng mL}^{-1}$ ); Extraction: 3 min static extraction by porous thin films; Washing: 1 mL 1% TEA in water at 1000 rpm for 10s; Desorption: 200  $\mu\text{L}$  ACN 0.1%FA at 1500 rpm for 2 min (n=3 for each batch).

**Table 4.5.** T-test at a 95% confidence level for inter-batch reproducibility of porous thin films ( $T_{\text{crit}} = 2.776$ ).

	Nortriptyline	Desipramine	Amitriptyline	Doxepin	Imipramine	Trimipramine	Clomipramine
T-Value	1.39	0.65	0.74	-0.54	0.35	-0.51	0.53
P-Value	0.237	0.55	0.501	0.62	0.742	0.638	0.626

#### 4.3.4.2. Preservation of drugs extracted onto the porous polymeric thin film:

The stability of analytes adsorbed to solid phase coatings depends on the type of adsorbent and the characteristics of the analytes; under the best circumstances the analytes should neither breakdown or volatilize between adsorption and analysis [28]. Devices with

good biopreservation capacity for the targeted analytes are ideal for remote sampling, as it allows for time to transport the samples to a centralized lab for analysis as well as potential for sample archiving. The ability of the porous thin film to preserve the extracted TCAs over time and the best storage temperature to minimize analyte losses were investigated. All extractions were carried out simultaneously to avoid variations in extraction. From this batch, three devices were chosen at random and analyzed immediately as a baseline measurement. The remaining films were divided into three groups for storage at different temperatures (room temperature (~21 °C), refrigerated (4 °C), or frozen (-21 °C)) and subdivided for assessment at 5 different storage times (1 day, 3 days, 7 days, 15 days, 30 days) for triplicate analysis. Extracted mass amounts for TCAs are presented in Figure 4.14. The data clearly show that the analytes are stable in the films at all temperatures and the study intervals, with no statistically relevant differences detected. Although there are a few data points with higher error, e.g., desipramine, nortriptyline and trimipramine @4 °C for 15 days, this behaviour appears to be an outlier and can be reduced using normalization. The findings from this investigation support the conclusion that the adsorption of analytes to the devices is a viable means of sample preservation.

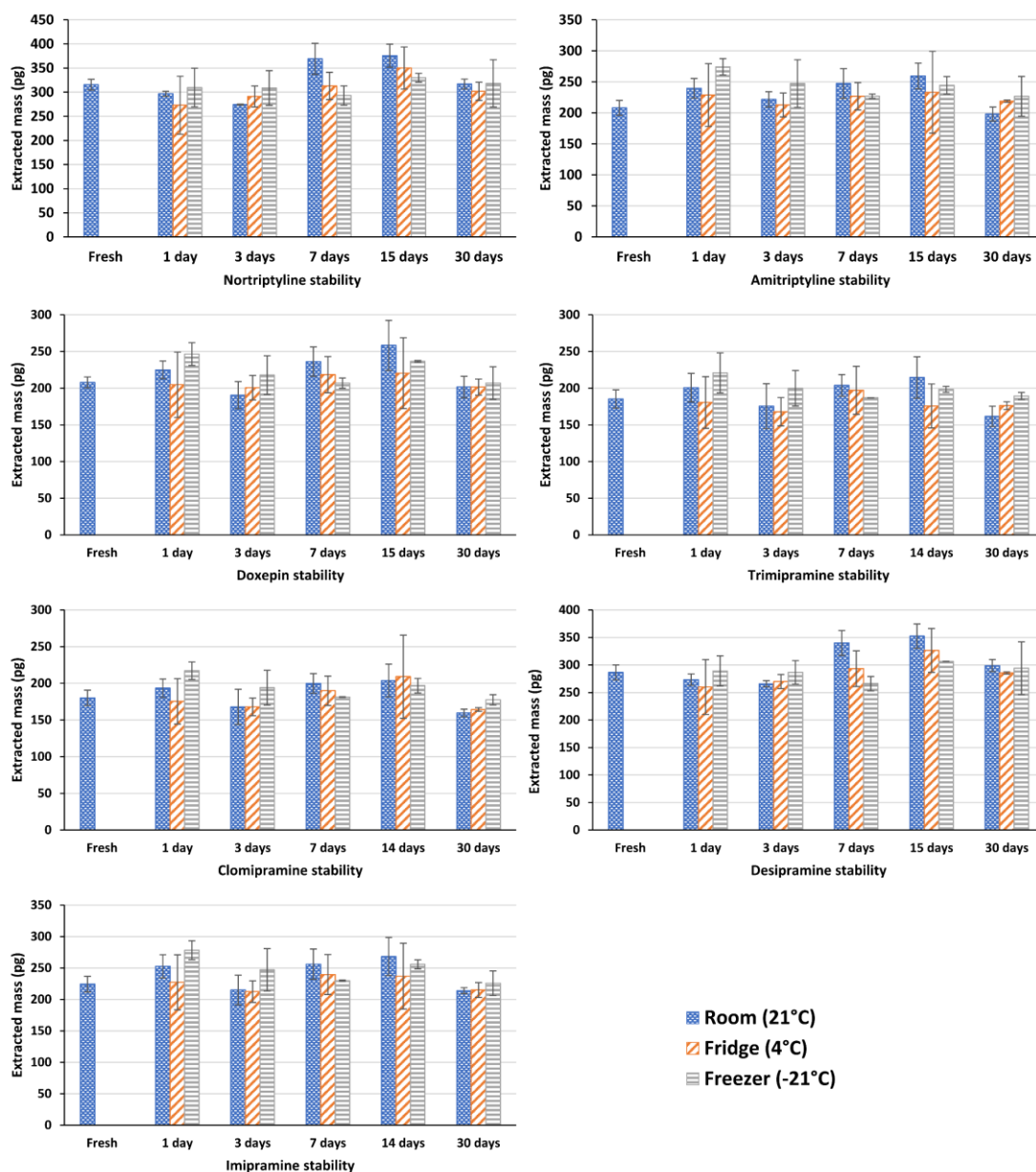


**Figure 4.14.** Stability assessment results using spot sampling obtained for a) desipramine and b) imipramine at various storage conditions; Sample: 10  $\mu\text{L}$  of plasma spiked with TCAs ( $100 \text{ ng mL}^{-1}$ ) and IS (imipramine-D3 at  $50 \text{ ng mL}^{-1}$ ); Extraction: 3 min static extraction by porous thin films; Washing: 1 mL 1% TEA in water at 1000 rpm for 10s; Desorption: 200  $\mu\text{L}$  ACN 0.1%FA at 1500 rpm for 2 min ( $n=3$ ).

TCAs have been shown to be stable at ambient temperature using a DBS technique, therefore their stability on thin films can be related to their chemical nature [29, 30].

Previous studies demonstrated that modified porous papers can be implemented for stabilizing labile compounds [31, 32]. Cocaine is a great example of these analytes and is not stable at ambient conditions. Therefore, we investigated the ability of thin films to preserve cocaine extracted from plasma drops. Two different coatings were prepared based on MAA and Sty as the monomers (Table 4.3) and employed for this experiment. The thin films with cocaine isolated from plasma were stored at room temperature and analyzed at different storage intervals up to 30 days (Figure 4.15). The detectable cocaine was consistent throughout the storage for both sorbents with higher reproducibility and recovery for Sty. The cocaine stability using these two sorbents implies that these porous coatings can be utilized for analysis of labile compounds without the need for refrigerated conditions during storage and transportation. The difference between Sty and MAA illustrates the importance of coating chemistry which suggests that compound-specific materials can be tailored for optimal efficiency of adsorption and method selectivity.

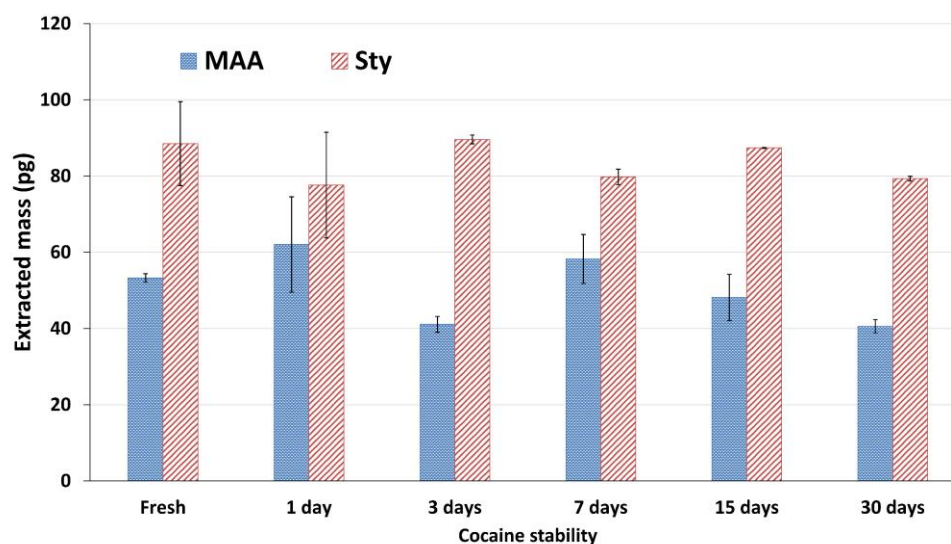


**Figure 4.15.** Stability assessment results using spot sampling obtained for cocaine at room temperature; Sample: 10 µL of plasma spiked with cocaine (100 ng mL<sup>-1</sup>); Extraction: 3 min static extraction by two different compositions of porous thin films; Washing: 1 mL water at 1000 rpm for 10s; Desorption: 200 µL MeOH 0.1%FA at 1500 rpm for 2 min (n=3).

#### 4.3.5. Reusability of porous thin films

Porous thin films developed in this work are intended to be single use, however, one might apply multiple uses when the coating is sufficiently stable and there is a protocol in place for an effective clean-up. Therefore, we evaluated the capability of developed coating for consecutive extractions/clean-ups (Figure 4.16). Following the first round, the devices were cleaned using a mixture of equal amounts of isopropanol: MeOH: ACN: water containing 0.1% FA (2×5 min, at 1500 rpm). The clean-up protocol was assessed by a blank desorption and LC-MS/MS analysis and no carryover was detected. The devices are stable and can be used for at least 15 extractions without a reduction in the efficiency.

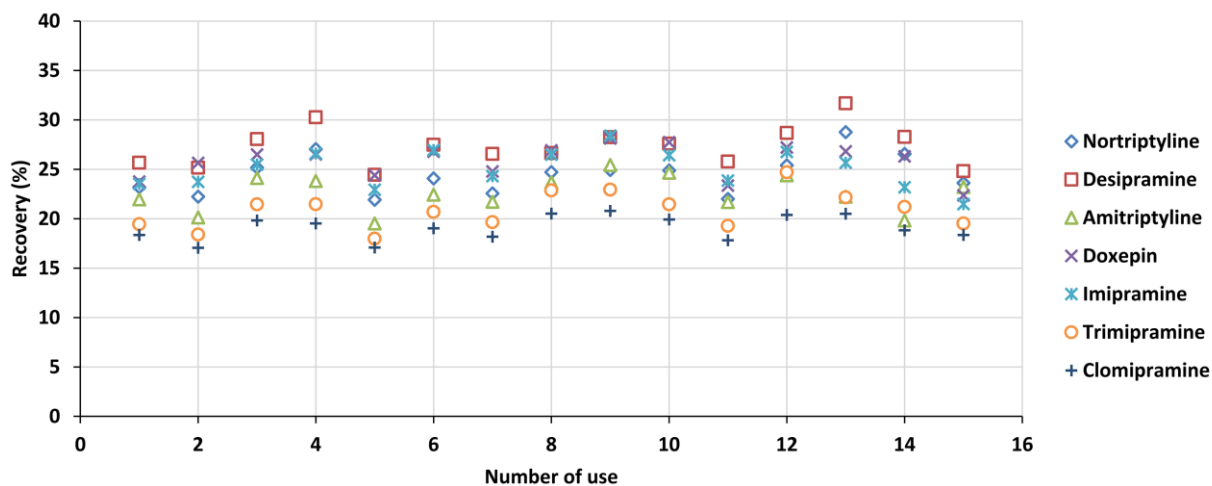


**Figure 4.16.** Reusability of porous thin films for spot sampling; Sample: 10  $\mu\text{L}$  of plasma spiked with TCAs ( $100 \text{ ng mL}^{-1}$ ); Extraction: 3 min static extraction by porous thin films; Washing: 1 mL 1% TEA in water at 1000 rpm for 10s; Desorption: 200  $\mu\text{L}$  ACN 0.1%FA at 1500 rpm for 2 min (n=3).

#### 4.3.6. Method validation

Data describing the analytical performance—linear range (LR), coefficient of determination ( $R^2$ ), accuracy, and precision—of these devices for the determination of

TCAs in plasma (10  $\mu\text{L}$ ) were obtained based on regulatory requirements of US FDA [33] and presented in Table 4.6. Addition of imipramine-D3 into plasma samples was to compensate for any matrix variability and competition in presence of other positively charged species with logP values similar to TCAs. Calibration curves (Figure 4.17) showed linearity ( $R^2 > 0.9978$ ) from the LOQ for each TCA (1-10  $\text{ng mL}^{-1}$ ) to 1000  $\text{ng mL}^{-1}$ . The choice of the upper limit was based on concentrations typical for clinical samples and well above the thresholds of toxicity; the brackets shown in orange represent the therapeutic range for each TCA. Although higher concentrations of TCAs can be adsorbed linearly due to the small volume of the sample and total loaded mass, higher concentrations would lead to non-linear ionization during ESI or detector saturation. Thus, such concentrations were not included for method validation. Non-weighted and weighted least-squares regression were used for fitting; each was tested for fit, and the best is reported in Table 4.6. To assess accuracy and precision, plasma samples were spiked with TCAs at three different concentrations of 30, 150 and 750  $\text{ng mL}^{-1}$  to cover the low, mid, and high linear range response of the drugs and the response compared to the calibration data (red triangles in Figure 4.17). Intra- and inter-day accuracies were in the ranges of 82.1-109 and 81.4-118%, respectively. The precision values were lower than 15% for the studied compounds and ranged from 0.7 to 9.5% for intra-day assay and from 0.6 to 12% for inter-day assay.

**Table 4.6.** Figures of merit obtained by spot sampling analysis using porous polymeric thin films (n=3).

Compound	Weighting factor	LR (ng mL <sup>-1</sup> )	Function	R <sup>2</sup>	Intra-day accuracy %, (RSD%, n=3)			Inter-day accuracy %, (RSD%, n=3)		
					30 (ng.mL <sup>-1</sup> )	150 (ng.mL <sup>-1</sup> )	750 (ng.mL <sup>-1</sup> )	30 (ng.mL <sup>-1</sup> )	150 (ng.mL <sup>-1</sup> )	750 (ng.mL <sup>-1</sup> )
Nortriptyline	1/X <sup>2</sup>	2.5-1000	y = 0.0026x + 0.0072	0.9986	92.8 (3.5)	97.2 (1.5)	91.7 (1.6)	85.8 (3.8)	85.5 (2.0)	81.4 (12)
Desipramine	1/X	1.0-1000	y = 0.0116x + 0.0197	0.9993	100 (6.0)	102 (2.4)	96.5 (5.1)	102 (6.1)	103 (1.7)	95.4 (9.7)
Amitriptyline	Non-weighted	10-1000	y = 0.0039x + 0.0193	0.9997	82.1 (5.8)	95.5 (2.6)	93.4 (2.7)	84.9 (5.4)	96.4 (3.2)	103 (4.1)
Doxepin	Non-weighted	10-1000	y = 0.0028x + 0.0071	0.9978	90.5 (4.3)	102 (2.1)	109 (6.2)	100 (3.4)	114 (4.3)	118 (2.4)
Imipramine	1/X	1.0-1000	y = 0.013x + 0.043	0.9997	103 (0.7)	101 (1.8)	98.9 (1.0)	105 (1.9)	103 (0.6)	101 (1.3)
Trimipramine	1/X	1.0-1000	y = 0.0062x + 0.0369	0.9996	100 (2.4)	91.5 (3.2)	89.2 (1.9)	104 (6.3)	99.1 (2.4)	105 (6.3)
Clomipramine	1/X <sup>2</sup>	1.0-1000	y = 0.006x + 0.0415	0.9993	99.7 (9.5)	95.2 (3.7)	97.6 (5.0)	96.1 (5.8)	103 (6.1)	106 (6.4)

\*All data normalized using imipramine-D3

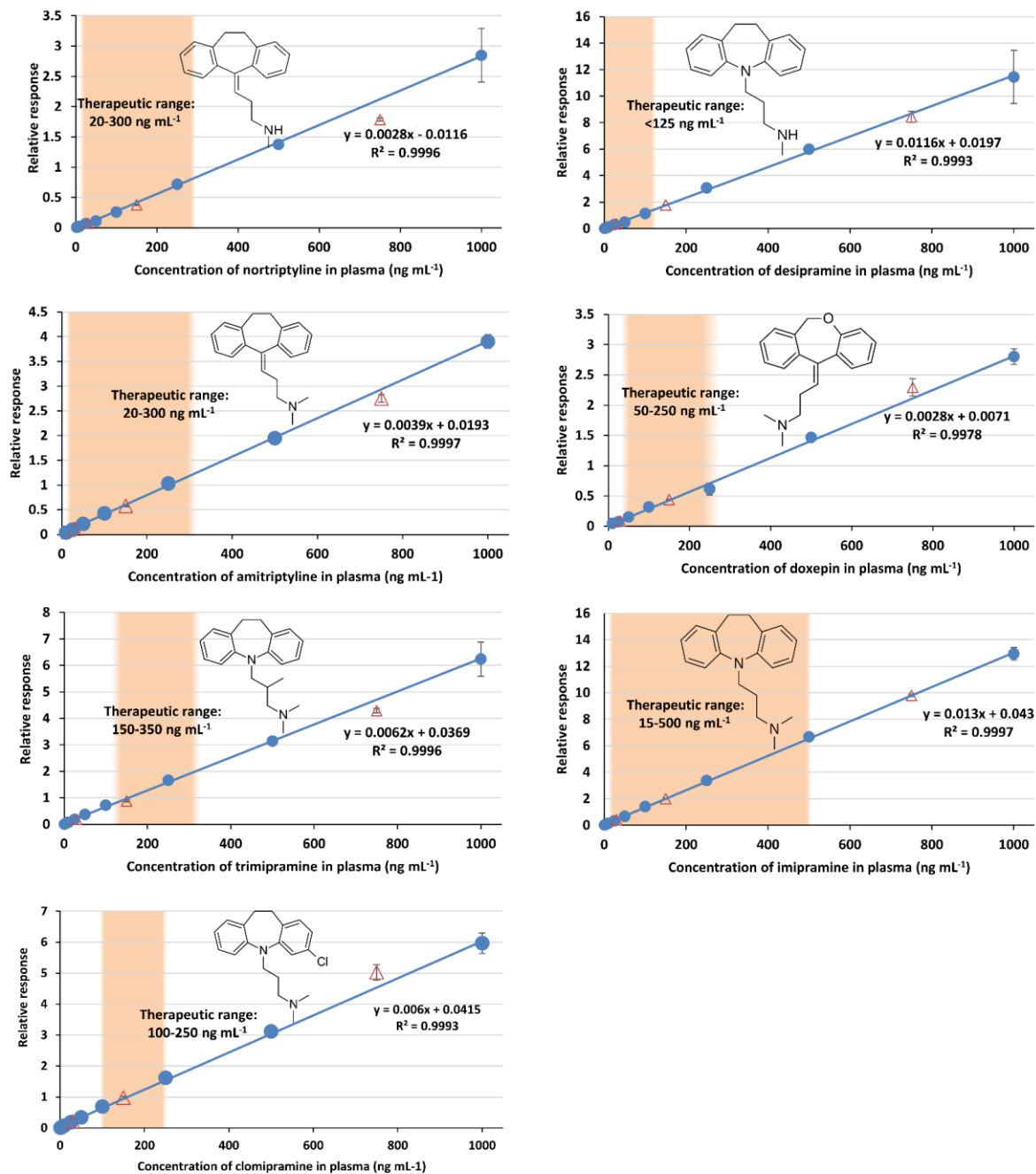


**Figure 4.17.** Quantitative analysis of plasma spiked with TCAs and imipramine-D3 (50 ng mL<sup>-1</sup>). Red triangles represent the obtained accuracy levels (30, 150 and 750 ng mL<sup>-1</sup>) (n=3).

To demonstrate the potential of these devices for use without normalization with an isotopically labelled surrogate, corresponding data without correction relative to imipramine-D3 is presented in Figure 4.18. Even without correction, the method provided excellent linearity ( $R^2 > 0.99$ ) and low errors for all analytes. Inter-day calibration checks (Figure 4.19) gave %RSD <20%, except trimipramine and clomipramine at 30 ng mL<sup>-1</sup> which gave %RSDs of ~24%. These results confirm that our devices are tolerant to matrix effects in mass spectrometry without use of IS. However, to account for the effect of patient sample variability on extraction efficiency, simple analyte analogues can be added as surrogates and be used rather than the costly deuterated standards to normalize MS data. These data prove the suitability of these devices with porous thin film coatings for biofluid analysis, such as that required for TDM studies.

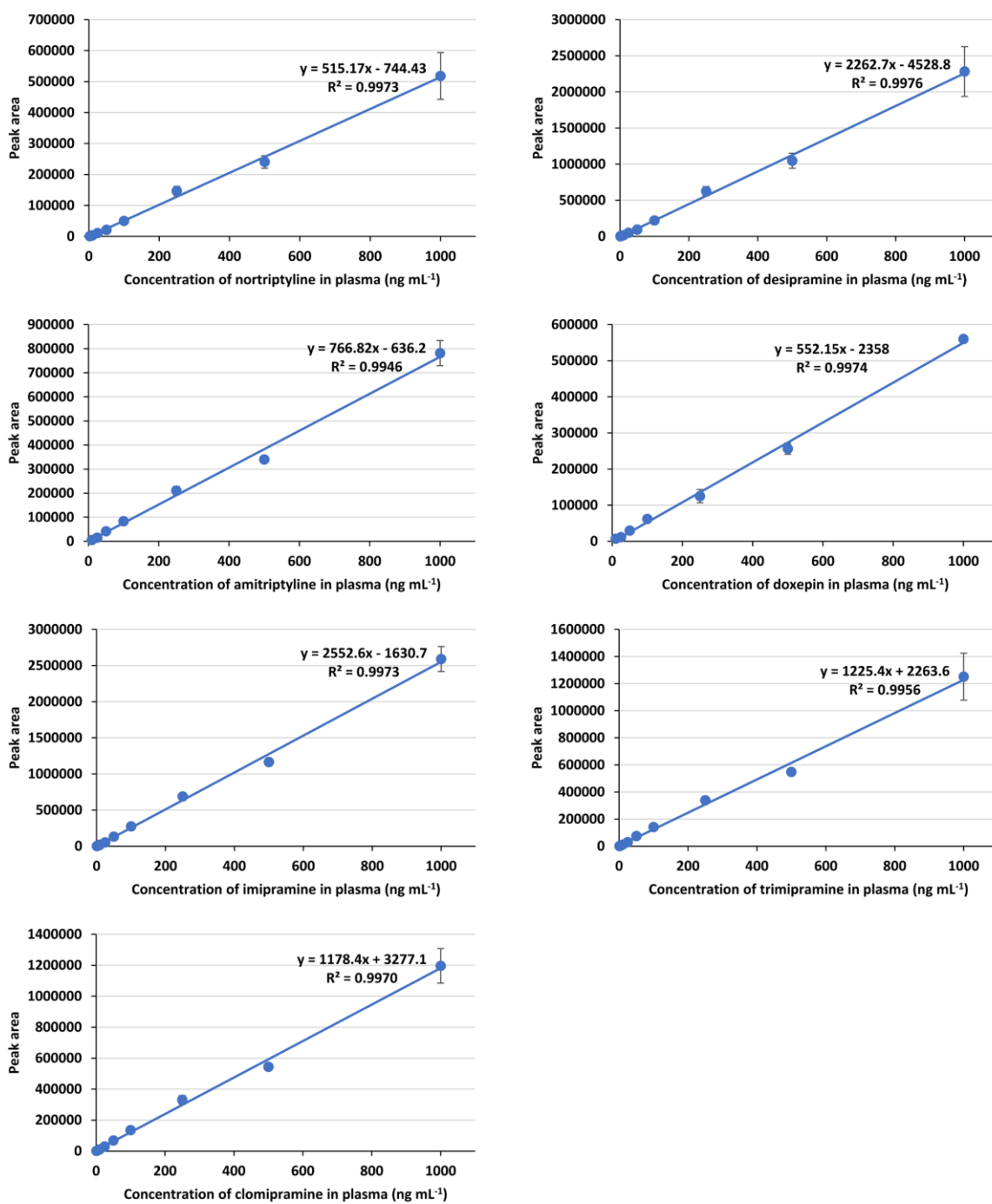


**Figure 4.18.** Quantitative analysis of plasma spiked with TCAs based on instrumental response (n=3).

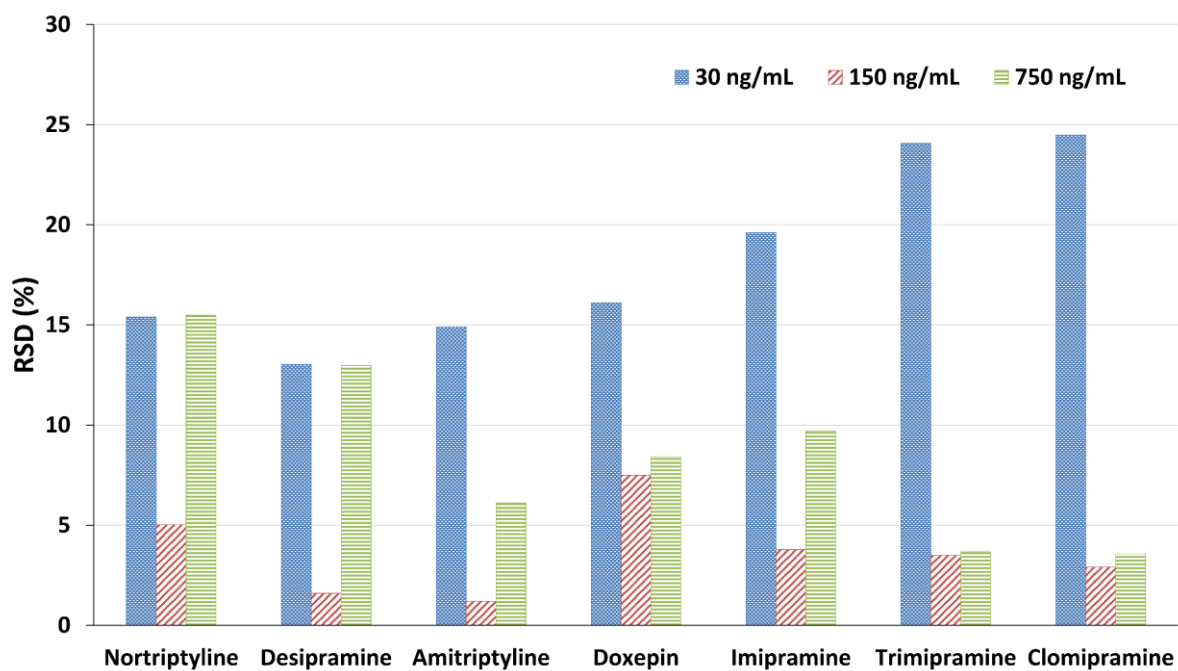


**Figure 4.19.** Variations of instrumental response (peak area) for extraction from plasma spiked with TCAs for inter-day validation experiments (n=3).

The spot sampling method was compared with previous work for extraction and analysis of TCAs in biological samples (Table 4.7) with an emphasis on methods using minimum amounts of sample. The presented work requires lower sample volume than all the methods including PP and DBS and provides similar or even better sensitivity. Our plasma spot sampling protocol is fast and simple (three steps in ~5 min) like PP while avoiding the matrix effect which is a common issue in PP and DBS. Furthermore, our method does not require long pre-conditioning or post-processing stages employed in other microextraction techniques.

**Table 4.7.** Comparison of extracted biofluid spot method with other methods for analysis of TCAs.

Method	Analytes	Matrix (volume)	Sample preparation (time)	Desorption	LOQ (ng mL <sup>-1</sup> )	Ref.
μSPE-HPLC-UV	Amitriptyline, desipramine, trimipramine	Urine (600 μL)	1- conditioning (30 mins) 2- loading (15 mins) 3- washing (5 mins) 4- Elution (12 mins)	MeOH (20 μL)	14-30	[34]
PP-HPLC-MS/MS	Amitriptyline, desipramine, imipramine, nortriptyline	Serum (500 μL)	1- Precipitation (5 mins) 2- Dilution: -	ACN (450 μL)	10-21	[35]
DBS-LC-MS/MS	Amitriptyline, nortriptyline, imipramine, clomipramine	15μL blood spot	1-Drying (overnight) 2-Back extraction (5 mins) 3- Centrifugation (5 mins)	ACN:MeOH (1:3, v/v) (250 μL)	40	[29]
SPME-LC-TOF-MS	Amitriptyline, desipramine, imipramine, nortriptyline	Blood (200 μL)	1-Cconditioning (45 mins) 2-Extraction (60 min) 3-Washing (5s) 4-Desorption: 30 min 5-Evaporation: 45 min 6-Preconcentration	ACN: MeOH:0.1% HCOOH (200 μL)	5.6-42.8	[36]
FPSE-HPLC-DAD	Amitriptyline, clomipramine	Serum (50 μL)	1-Conditioning: 5 mins 2-Rinsing: 5 mins 3-Extraction: 15 mins 4-Washing: -5-Elution: 5 mins	ACN: MeOH (500 μL)	500	[37]
HF-LPME-GC-MS	Amitriptyline, nortriptyline, desipramine, imipramine, clomipramine	Whole blood (500 μL)	1- Extraction: 30 min 2- Evaporation: NA 3- Dissolution	- 0.1 M FA (30 μL) - MeOH (30 μL)	20	[38]
EBS-LC-MS/MS	Nortriptyline, desipramine, amitriptyline, doxepin, imipramine, trimipramine, clomipramine	Plasma (10 μL)	1- Extraction: (3 mins) 2- Washing (10 s) 3- 2 mins desorption	200 μL ACN (0.1%FA)	1-10	This work

#### **4.3.7. Analysis of real samples**

Following the method validation, the developed method was used to analyze two individual plasma samples that did not contain any TCAs. After spiking these samples with TCAs (at three different concentrations) and surrogate, the extraction was performed using spot sampling followed by LC-MS/MS analysis. Quantitation in blood components using SPME devices can be conducted using matrix-matched calibration [12]. Thus, calibration curve obtained in pooled plasma was used to evaluate this approach for reliable quantitation of TCAs in two plasma samples. The relative recovery (RR%) values were determined by ratio of the found concentration to the spiked amount of analytes. As presented in table 4.8, the RR% ranged from 86.7% to 114% with RSD values of 0.1-10%. This study demonstrated the suitability of spot sampling technique using porous thin film for analysis of TCAs in real plasma samples.

**Table 4.8.** Application of spot sampling analysis using porous polymeric thin films for TCA quantitation in two plasma samples (n=3).

Compounds	Added concentration (ng mL <sup>-1</sup> )	Plasma 1			Plasma 2		
		Found concentration (ng mL <sup>-1</sup> ) ± SD	RR (%)	RSD (%)	Found concentration (ng mL <sup>-1</sup> ) ± SD	RR (%)	RSD (%)
Nortriptyline	0	ND	-	-	ND	-	-
	30	32.5 ± 0.8	108	2.4	31.5 ± 1.5	105	4.6
	100	106.2 ± 0.1	106	0.1	104.8 ± 6.5	105	6.2
	800	823.3 ± 26.7	103	3.2	819.1 ± 9.9	102	1.2
Desipramine	0	ND	-	-	ND	-	-
	30	32.2 ± 10.3	107	10	32.5 ± 5.9	108	5.9
	100	106.3 ± 0.9	106	0.9	105.3 ± 6.9	105	6.9
	800	817.5 ± 3.7	102	3.7	808.6 ± 1.9	101	1.9
Amitriptyline	0	ND	-	-	ND	-	-
	30	26.5 ± 0.5	88.2	1.8	26.0 ± 0.8	86.7	3.1
	100	97.9 ± 4.3	97.9	4.4	98.9 ± 9.2	98.9	9.3
	800	861.5 ± 29.4	108	3.4	839.8 ± 10.5	105	1.2
Doxepin	0	ND	-	-	ND	-	-
	30	31.5 ± 1.6	105	5.1	30.7 ± 1.3	102	4.3
	100	102.7 ± 2.7	103	2.6	102.0 ± 4.3	102	4.2
	800	776.8 ± 18.9	97.1	2.4	802.3 ± 29.1	100	3.6
Imipramine	0	ND	-	-	ND	-	-
	30	31.9 ± 0.3	106	0.9	34.2 ± 1.4	114	4.0
	100	105.2 ± 1.5	105	1.4	105.9 ± 3.7	106	3.5
	800	788.6 ± 21.0	98.6	2.7	788.3 ± 27.1	98.5	3.4
Trimipramine	0	ND	-	-	ND	-	-
	30	31.6 ± 1.5	105	4.7	32.7 ± 2.7	109	8.1
	100	104.4 ± 4.5	104	4.3	104.3 ± 4.5	104	4.4
	800	815.9 ± 27.3	102	3.4	789.9 ± 34.7	98.7	4.4
Clomipramine	0	ND	-	-	ND	-	-
	30	32.0 ± 2.2	107	7.0	30.9 ± 2.0	103	6.5
	100	98.2 ± 4.5	98.2	4.6	102.4 ± 1.3	102	1.3
	800	787.5 ± 27.7	98.4	3.5	748.8 ± 15.5	93.6	2.1

ND: not detected.

#### 4.4. Conclusion

This work describes the development of a spot sampling technique using a porous thin-film device for analysis of small volumes of biological samples. As a proof of concept, the presented method and customized porous thin-film device were employed for determination of TCAs in plasma samples. The high efficiency of extraction enables the use of broadly accessible instrumentation (e.g., LC-MS/MS), which is needed for use in demanding clinical environments that require fast and reliable sample processing. The fabrication technique is simple and fast, producing devices with a robust and consistent performance for microsampling. The porous structure of the coating provides high surface area for quick efficient extraction and pore-sizes needed for fast equilibration, which allows for the short sample processing times (3 min extraction and 2 min desorption). Washing the thin films after analyte enrichment assists with sample clean-up and avoids matrix effects observed in PP-based microsampling techniques. Although the method performance using this device is acceptable without use of surrogates or IS (<20%), variation can be reduced using a deuterated surrogate spiked into the samples or using an IS loaded onto the polymer coating before the sample spotting or just before desorption, or simply added to the desorption solvent. We also demonstrated that the analytes collected from biological samples onto these single-use devices are stable for at least 30 days at room temperature, refrigerated or frozen, allowing for various storage and shipping conditions. Single usage of the developed thin film is an advantage for fast and simple analyses; however, the performance of reused thin-film devices was also consistent up to 15 extractions. The method showed excellent figures of merit for all TCAs in plasma, i.e., sensitivity, linearity,

accuracy, and precision. In summary, porous thin-film devices performed well as microsampling devices due to the fast extraction process (no need for biofluid to be dried), reduced matrix effects due to possibility of washing after extraction, and good biopreservation and room storage capabilities. We anticipate similar performance for analysis of other biological fluids (i.e., blood and urine). These user-friendly devices have high potential for exploitation in automated sample preparation (e.g., 96-well plate systems) or in direct MS (e.g. blade-spray or DART). One of the limitations of the porous thin films is the reduced stability of the polymeric sorbent for the dried spots and thus biofluid needs to be removed or washed before dryness. Higher recovery values could be obtained by using polymer composition which can tolerate dried spots and be washed and analyzed after dryness.

## 4.5. References

- [1] S. Yang, Z. Yang, P.G. Wang, Bioanalysis for precision medicine, *Bioanalysis* 11(11) (2019) 1039-1043.
- [2] B.U.W. Lei, T.W. Prow, A review of microsampling techniques and their social impact, *Biomed. Microdevices* 21(4) (2019) 1-30.
- [3] V. Londhe, M. Rajadhyaksha, Opportunities and obstacles for microsampling techniques in bioanalysis: special focus on DBS and VAMS, *J. Pharm. Biomed. Anal.* 182 (2020) 113102.
- [4] J. Déglon, A. Thomas, P. Mangin, C. Staub, Direct analysis of dried blood spots coupled with mass spectrometry: concepts and biomedical applications, *Anal. Bioanal. Chem.* 402(8) (2012) 2485-2498.
- [5] H.Y. Tey, H.H. See, A review of recent advances in microsampling techniques of biological fluids for therapeutic drug monitoring, *J. Chromatogr. A* 1635 (2021) 461731.
- [6] S.L. Parker, J. Lipman, G. Dimopoulos, J.A. Roberts, S.C. Wallis, A validated method for the quantification of fosfomycin on dried plasma spots by HPLC–MS/MS:

Application to a pilot pharmacokinetic study in humans, *J. Pharm. Biomed. Anal.* 115 (2015) 509-514.

[7] G. Nys, M.G.M. Kok, A.-C. Servais, M. Fillet, Beyond dried blood spot: current microsampling techniques in the context of biomedical applications, *TrAC, Trends Anal. Chem.* 97 (2017) 326-332.

[8] C. Polson, P. Sarkar, B. Incledon, V. Raguvaran, R. Grant, Optimization of protein precipitation based upon effectiveness of protein removal and ionization effect in liquid chromatography–tandem mass spectrometry, *J. Chromatogr. B* 785(2) (2003) 263-275.

[9] J.-P. Lambert, W.M. Mullett, E. Kwong, D. Lubda, Stir bar sorptive extraction based on restricted access material for the direct extraction of caffeine and metabolites in biological fluids, *J. Chromatogr. A* 1075(1-2) (2005) 43-49.

[10] D.S. Kulyk, T. Sahraeian, S. Lee, A.K. Badu-Tawiah, Microsampling with a Solid-Phase Extraction Cartridge: Storage and Online Mass Spectrometry Analysis, *Anal. Chem.* 93(40) (2021) 13632-13640.

[11] B.S. Frey, D.E. Damon, D.M. Allen, J. Baker, S. Asamoah, A.K. Badu-Tawiah, Protective mechanism of dried blood spheroids: stabilization of labile analytes in whole blood, plasma, and serum, *Analyst* 146(22) (2021) 6780-6787.

[12] É.A. Souza-Silva, N. Reyes-Garcés, G.A. Gómez-Ríos, E. Boyacı, B. Bojko, J. Pawliszyn, A critical review of the state of the art of solid-phase microextraction of complex matrices III. Bioanalytical and clinical applications, *TrAC, Trends Anal. Chem.* 71 (2015) 249-264.

[13] G.A. Gómez-Ríos, T. Vasiljevic, E. Gionfriddo, M. Yu, J. Pawliszyn, Towards on-site analysis of complex matrices by solid-phase microextraction-transmission mode coupled to a portable mass spectrometer via direct analysis in real time, *Analyst* 142(16) (2017) 2928-2935.

[14] F.S. Mirnaghi, J. Pawliszyn, Reusable solid-phase microextraction coating for direct immersion whole-blood analysis and extracted blood spot sampling coupled with liquid chromatography–tandem mass spectrometry and direct analysis in real time–tandem mass spectrometry, *Anal. Chem.* 84(19) (2012) 8301-8309.

[15] G.A. Gómez-Ríos, M. Tascon, N. Reyes-Garcés, E. Boyacı, J. Poole, J. Pawliszyn, Quantitative analysis of biofluid spots by coated blade spray mass spectrometry, a new approach to rapid screening, *Sci. Rep.* 7(1) (2017) 1-7.

[16] A. Azizi, F. Shahhoseini, A. Modir-Rousta, C.S. Bottaro, High throughput direct analysis of water using solvothermal headspace desorption with porous thin films, *Anal. Chim. Acta* 1087 (2019) 51-61.

- [17] F. Shahhoseini, A. Azizi, S.N. Egli, C.S. Bottaro, Single-use porous thin film extraction with gas chromatography atmospheric pressure chemical ionization tandem mass spectrometry for high-throughput analysis of 16 PAHs, *Talanta* 207 (2020) 120320.
- [18] M. Grundmann, I. Kacirova, R. Urinovska, Therapeutic monitoring of psychoactive drugs-antidepressants: a review, *Biomedical Papers of the Medical Faculty of Palacky University in Olomouc* 159(1) (2015).
- [19] G.F. Abu-Alsoud, C.S. Bottaro, Porous thin-film molecularly imprinted polymer device for simultaneous determination of phenol, alkylphenol and chlorophenol compounds in water, *Talanta* 223 (2021) 121727.
- [20] F. Shahhoseini, E.A. Langille, A. Azizi, C.S. Bottaro, Thin film molecularly imprinted polymer (TF-MIP), a selective and single-use extraction device for high-throughput analysis of biological samples, *Analyst* 146(10) (2021) 3157-3168.
- [21] G. Liu, L. Patrone, H.M. Snapp, A. Batog, J. Valentine, G. Cosma, A. Tymiak, Q.C. Ji, M.E. Arnold, Evaluating and defining sample preparation procedures for DBS LC-MS/MS assays, *Bioanalysis* 2(8) (2010) 1405-1414.
- [22] K. Gorynski, A critical review of solid-phase microextraction applied in drugs of abuse determinations and potential applications for targeted doping testing, *TrAC, Trends Anal. Chem.* 112 (2019) 135-146.
- [23] W. Zhou, S. Yang, P.G. Wang, Matrix effects and application of matrix effect factor, *Bioanalysis* 9 (2017) 1839-1844.
- [24] I. González-Mariño, J.B. Quintana, I. Rodríguez, M. Gonzalez-Diez, R. Cela, Screening and selective quantification of illicit drugs in wastewater by mixed-mode solid-phase extraction and quadrupole-time-of-flight liquid chromatography-mass spectrometry, *Anal. Chem.* 84(3) (2012) 1708-1717.
- [25] X. Zhang, K.D. Oakes, D. Luong, C.D. Metcalfe, M.R. Servos, Solid-phase microextraction coupled to LC-ESI-MS/MS: evaluation and correction for matrix-induced ionization suppression/enhancement for pharmaceutical analysis in biological and environmental samples, *Anal. Chem.* 83(17) (2011) 6532-6538.
- [26] B.K. Matuszewski, M.L. Constanzer, C.M. Chavez-Eng, Strategies for the assessment of matrix effect in quantitative bioanalytical methods based on HPLC-MS/MS, *Anal. Chem.* 75(13) (2003) 3019-3030.
- [27] E. Boyacı, K. Gorynski, A. Rodriguez-Lafuente, B. Bojko, J. Pawliszyn, Introduction of solid-phase microextraction as a high-throughput sample preparation tool in laboratory analysis of prohibited substances, *Anal. Chim. Acta* 809 (2014) 69-81.

- [28] D. Marder, S. Dagan, L. Yishai-Aviram, D. Loewenthal, S. Chapman, R. Adani, S. Lazar, A. Weissberg, S. Gura, Instantaneous monitoring of free sarin in whole blood by dry blood spot–thermal desorption–GC–FPD/MS analysis, *J. Chromatogr. B* 1136 (2020) 121911.
- [29] E.J.J. Berm, J. Paardekooper, E. Brummel-Mulder, E. Hak, B. Wilffert, J.G. Maring, A simple dried blood spot method for therapeutic drug monitoring of the tricyclic antidepressants amitriptyline, nortriptyline, imipramine, clomipramine, and their active metabolites using LC-MS/MS, *Talanta* 134 (2015) 165-172.
- [30] M. Świądro, P. Stelmaszczyk, R. Wietecha-Posłuszny, D. Dudek, Development of a new method for drug detection based on a combination of the dried blood spot method and capillary electrophoresis, *J. Chromatogr. B* 1157 (2020) 122339.
- [31] E.L. Rossini, D.S. Kulyk, E. Ansu-Gyeabourh, T. Sahraeian, H.R. Pezza, A.K. Badu-Tawiah, Direct analysis of doping agents in raw urine using hydrophobic paper spray mass spectrometry, *J. Am. Soc. Mass. Spectrom.* 31(6) (2020) 1212-1222.
- [32] D.E. Damon, M. Yin, D.M. Allen, Y.S. Maher, C.J. Tanny, S. Oyola-Reynoso, B.L. Smith, S. Maher, M.M. Thuo, A.K. Badu-Tawiah, Dried blood spheroids for dry-state room temperature stabilization of microliter blood samples, *Anal. Chem.* 90(15) (2018) 9353-9358.
- [33] Bioanalytical Method Validation Guidance for Industry, 2018.  
<https://www.fda.gov/files/drugs/published/Bioanalytical-Method-Validation-Guidance-for-Industry.pdf>.
- [34] B. Fresco-Cala, Ó. Mompó-Roselló, E.F. Simó-Alfonso, S. Cárdenas, J.M. Herrero-Martínez, Carbon nanotube-modified monolithic polymethacrylate pipette tips for (micro) solid-phase extraction of antidepressants from urine samples, *Microchim. Acta* 185(2) (2018) 1-7.
- [35] A.R. Breaud, R. Harlan, M. Kozak, W. Clarke, A rapid and reliable method for the quantitation of tricyclic antidepressants in serum using HPLC-MS/MS, *Clin. Biochem.* 42(12) (2009) 1300-1307.
- [36] A. Majda, K. Mrochem, R. Wietecha-Posłuszny, S. Zapotoczny, M. Zawadzki, Fast and efficient analyses of the post-mortem human blood and bone marrow using DI-SPME/LC-TOFMS method for forensic medicine purposes, *Talanta* 209 (2020) 120533.
- [37] E. Zilfidou, A. Kabir, K.G. Furton, V. Samanidou, An improved fabric phase sorptive extraction method for the determination of five selected antidepressant drug residues in human blood serum prior to high performance liquid chromatography with diode array detection, *J. Chromatogr. B* 1125 (2019) 121720.

[38] M.F. dos Santos, C.C. Ferri, S.C. Seulin, V. Leyton, C.A.G. Pasqualucci, D.R. Munoz, M. Yonamine, Determination of antidepressants in whole blood using hollow-fiber liquid-phase microextraction and gas chromatography–mass spectrometry, *Forensic Toxicol.* 32(2) (2014) 214-224.

## **Chapter 5: Conclusion and future work**

## 5.1. Conclusion

MIPs have been used widely in sample preparation techniques including SPE and SPME devices [1]. However, SPE techniques are extensively used by analytical chemists, requirements in analytical chemistry, such as lower sample volume, less solvent consumption, and simpler sample preparation methods make SPME techniques more appealing[2]. Employing MIPs as sorbent for SPME devices can improve their performance for more selective extraction and reducing matrix effects [3]. Although many reviews have been published on the topic of MIPs in sample preparation, they do not provide details about SPME devices [4]. The first chapter of this thesis is a review about MIP SPME devices with a focus on their methods of fabrication, optimization and evaluation of MIP sorbents and their associated analytical method. The most common formats of MIP-SPME devices are covered: fiber, stir bar and thin film coated on a flat substrate. Many of the methods of fabrication of these devices are complicated and time consuming, which hinder the commercial viability and their widespread usage. MIP sorbents on SPME devices are fabricated by non-covalent imprinting and for them to be robust and yield reproducible performance, it is important to use the right MIP composition. The chemical components used in each MIP SPME device and some of important features of optimization of the MIP formula to gain a higher selectivity are summarized. MIP sorbents are fabricated in two different formats of particle or monolith. Particles are applied in SPME format by incorporating into a host (e.g. glue or other polymers) and this method of fabrication can cause many demerits such as reduced effectiveness of the MIP particles and the stability of the device; and change the partition behaviour. Preparation of MIP-

SPME devices as a monolith (stand alone device or coating) is performed in a single step and has a less complicated fabrication method. However, it is a very delicate process and many factors should be carefully optimized to achieve a highly selective MIP-SPME device with a favourable mass transfer and perfect robustness.

In Chapter 2, the details of the development and validation of a high throughput, reliable and precise method for analysis of the 16 priority PAHs listed by US EPA in water is presented. In this work, the MIP sorbent formulation which was previously developed in the Bottaro group [5], was modified. Some essential changes were made to the format of the thin film, fabrication method and the extraction and desorption process. A smaller size (size change from 25 ×25 mm<sup>2</sup> to 5×30 mm<sup>2</sup>) thin-film device was fabricated on frosted pre-cut glass without silanization. In previous papers pre-cut glass slides were silanized prior to deposition of the pre-polymerization solution on the substrate, but it was found that the polymer coating that was stable on a mechanically roughened surface and the derivatization step was unnecessary. In the method development the parameters affecting the extraction efficiency and recovery were studied, such as extraction agitation level (rpm), extraction time, desorption solvent, desorption agitation, and desorption time. The optimized method consisted of a 1 h extraction from a 20-mL water sample (1400 rpm), quick wash of the thin film devices and then desorption using multi-position vortex mixer (1000 rpm) in 1250 μL hexane following with evaporation and reconstitution in 100 μL of toluene and analysis with APGC-MS/MS. This resulted in sub-ppb LODs of 1 pg mL<sup>-1</sup> for BaA to 100 pg mL<sup>-1</sup> for Flu with good reproducibility (<20%). Linearity ( $R^2 > 0.997$ ) over the 2–50,000 pg mL<sup>-1</sup> was obtained for all the tested water matrices (DI water, synthetic river water and

seawater) and recovery was in the range of 19.0-40.6 %. Waterford River water and St. John's Harbour water samples (St. John's, NL) were analyzed using a matrix-matching technique, which uses calibration curves obtained in synthetic river water and synthetic seawater for analysis of real samples, showed acceptable accuracies (mostly in the range of 80-120%) and precision (<20%). Although the thin film device was introduced for single use purposes, reusability study showed that for a minimum of five consecutive extractions, there was no loss in the performance.

Chapter 3 and 4 describe thin film MIPs for bioanalytical purposes using TCAs compounds for proof-of-concept. For a more robust and safer device compared to one based on glass, stainless steel was cut into  $5 \times 25 \text{ mm}^2$  pieces and used as substrate for biological analysis projects. In Chapter 3, a thin film MIP was developed using a synthesized template, MAA as monomer, EGDMA as crosslinker, DMPA as initiator and 1-octanol as porogen. Optimization of the MIP formula was based on the results extraction of TCAs from 20 mL of water ( $50 \mu\text{gL}^{-1}$  of TCAs) containing 1% TEA for 1 h agitated at 1000 rpm and desorbed into 700  $\mu\text{L}$  methanol which was analyzed by UPLC-MS/MS. Based on our previous study [6], the ratio of porogen volume to the mass of the other components can have a huge effect on imprinting. Therefore, the MIP formula optimization in Chapter 3 was started by investigating the porogen volume. This investigation was performed under two conditions of adjusted pH and not adjusted pH. Results showed that although the extraction efficiency is higher in under the unadjusted conditions, the reproducibility is not satisfactory ( $\sim 30\%$ ). Adjusting pH revealed that the differences in extracted mass using both the MIP and NIP thin film formula using 1000  $\mu\text{L}$  of porogen

was higher and results were more reproducible, though extraction efficiency was halved, mostly by elimination of non-specific bindings. Further optimization of the template:monomer and monomer:crosslinker ratios led to a finalized formula of 1:2:12 of template:monomer:crosslinker. For analysis of plasma samples and other biological matrices involved immersion of the thin film MIP in 700  $\mu\text{L}$  of sample in propylene vials with a low-volume insert, then mixed with a multi-position vortex for 60 min at 1500 rpm; the films were then washed by submerging thin film MIPs in 20 mL 1% TEA aqueous solution followed by desorption in 700  $\mu\text{L}$  of 50% ACN aqueous solution for 20 min at 500 rpm. The solution then was analyzed by UPLC-MS/MS. The selectivity of the developed thin film MIP compared to NIP was determined for TCAs based on extraction time profiles and using the slopes of isotherms. There was a noticeable difference in MIP and NIP extraction time profiles, even at 5 min, the ratio of extracted amounts for MIPs over NIPs was from 2-4.5. The ratio of isotherm slopes was 3 to 4.5. Using the MIPs, inter-day and intra-day accuracy and precision were in the range of 90-117% and 0.6 - 18%, respectively in BSA solution. The method was also validated in pooled plasma with a linearity over at least 1.0-500  $\text{ng mL}^{-1}$  and an excellent accuracy (90%-110%) and precision (<15%). The validated method was used to monitor the concentration of TCAs in patient plasma samples who had been prescribed TCAs. The results correlated well with the patients' therapies. The inter-device variability was evaluated by calculating for TCAs from BSA solution using 15 thin film devices, the %RSD without normalization against an internal standard was <14% and by normalization decreased to <8%.

In the last chapter, the potential of thin film devices to be used as a micro -sampling technique was investigated. Micro-sampling techniques have the advantages of simplicity, remote sampling, and feasibility of archiving in the case of delayed analysis[7]. However, the current techniques still have some drawbacks, such as co-extraction of matrix components requiring sample clean-up, e.g., protein precipitation in which analyte dilution counteracts gains in sensitivity and reproducibility, moreover most of these techniques cannot preserve labile compounds [8, 9]. A porous thin film of MAA and EGDMA (1:4 ratio) in 1-octanol was coated on a stainless steel substrate ( $5 \times 18 \text{ mm}^2$ ) for spot plasma sampling for TCAs and analyzed using UPLC-MS/MS. To develop a reliable method, vital factors such as sampling volume, extraction time, matrix effects, and the desorption process were studied. The optimized analytical method was very fast and straightforward including: 3 min extraction of 10  $\mu\text{L}$  plasma sample spotted on the polymer coating, vortex washing (1000 rpm) for 10 s in 1 mL 1% TEA to remove extracted matrix salt and interferences, and quick 2 min desorption of thin film device in 200  $\mu\text{L}$  of ACN with 0.1% FA. The method of normalization used a deuterated TCA (imipramine-D3) with different spiking modes in human plasma: spiked in the sample, pre-loading (deposition on the film before extraction) and post loading (deposition on the film after extraction, washing and dryness) and compared with the precision of the method of analysis without normalization. Results showed even without normalization the precision was acceptable (less than 20%) however, using IS reduced this amount to less than 15%. Normalization using spotting IS solution after extraction is the best choice of normalization specially for the application of microsampling. Biopreservation of TCAs on the thin film device was studied by storing

devices containing extracted TCAs for 30 days in three different conditions of room temperature (25 °C), fridge (4 °C) and freezer (-20 °C). Results showed that TCAs were stable even at room temperature for one month. A bio-preservation study completed for cocaine, which is labile, used the thin-film for TCAs and another film customized for extraction of cocaine using Sty as monomer. Results obtained from the MAA thin film (for TCAs) had serious fluctuations, with extraction recovery from 40 % to 60%. However, the Sty thin-film had an excellent stability of extraction efficiency over 30 days from 80-90%. Reusability of the thin film device for extracting TCAs from plasma sample for 15 consecutive extraction showed no loss of performance and results were very consistent. Validation of the optimized method showed a good linearity ( $R^2 > 0.99$ ) in the range of 1-1000 ng mL<sup>-1</sup>, with good intra- and inter-day accuracy (81.4-118%) and precision ( $\leq 12\%$ ) in human plasma.

The outcome of the research and literature reviews completed during this PhD program has published in high ranked peer review journals, which is a proof of its success in the scientific field. However, the true value of a scientific research is determined by its applicability in solving the current issues that scientists are facing. Results obtained by comparing the performance of the developed MIP-thin during my PhD program with the other products available in the market for analysis of environmental and biological samples, made me confident that these devices are ready to be introduced to the sample preparation market. As a scientist who does not have any experience in the business, I faced many difficulties. However, learning from many awesome programs such as Lab2Market and Memorial Center for entrepreneurship helped me a lot during my entrepreneurship journey. Performing customer discovery and talking to analytical chemists in the industry revealed

the commercial viability of developed thin film MIPs. These devices can reduce the sample size and the hazardous solvent consumption while providing a more reliable analysis. Although the process of commercialization is hard and time-consuming but I believe in the future these thin film MIP devices are one of the products in the market.

## **5.2. Future work:**

Entrepreneurship activities and opportunity to have discussions with potential customers helped to understand many of the problems that analytical chemist are facing and also the commercialization trends exist in the current sample preparation market.

One of emerging pollutants that analysts have been facing many problems for determination in water is per and polyfluoroalkyl substances (PFAS) [10]. Although there are some standard methods tested by many labs for these compounds but there are still some uncertainties associated with the data quality in terms of accuracy, precision and sensitivity[11]. Beside all these issues, quick research can reveal that there are not any paper published with a topic on molecularly imprinted polymers for selective extraction of PFAS. Developing a thin film MIP for selective extraction and reliable analysis of PFAS was one of the interesting topics that cold be completed during this PhD program.

Commercialization trends in sample preparation market is toward providing labs with easier and faster analysis which needs less lab works and manpower. Scientists have introduced some devices that can be coupled to MS, such as paper spray [12], direct analysis in real time (DART) [13], and coated blade spray [14] to provide a fast analysis which needs any or very little sample treatment and preparation. The feasibility of

combining the sample preparation devices to the analytical instruments such as LC-MS or GC-MS for a simpler, faster and high throughput analysis is of interest to instrumentational companies. One of the future projects, can be the investigation of viability of thin film MIPs for direct analysis with MS and study the effect of thin film MIP in reducing biological matrix interferences which can enhance or suppress ionization in MS.

Results from this PhD research showed that even intensive washing can not remove the template from the thin film MIP completely. If the targeted pharmaceutical is used as template, leaching the remained template can cause positive error during trace analysis and determination [15]. To solve this problem, a pseudo template (or dummy template) is used which is a compound with similar structure to the targeted compound. Finding a proper template in developing a thin film MIP formula specially for pharmaceuticals with high mass is very challenging. The idea of partial imprinting is a topic of an exciting research to solve this problem. In this approach, some smaller organic compound that have similar chemical structure to a part of a bulkier pharmaceutical can be used separately to prepare thin film MIPs. Comparing the selectivity assessment result of these different thin film MIPs can help to select the most selective device. These results can also reveal some of the mechanism that can be employed for successful imprinting.

### **5.3. References:**

- [1] S. Tang, H. Zhang, H.K. Lee, Advances in sample extraction, *Anal. Chem.* 88(1) (2016) 228-249.
- [2] V. Jalili, A. Barkhordari, A. Ghiasvand, A comprehensive look at solid-phase microextraction technique: A review of reviews, *Microchem. J.* 152 (2020) 104319.

- [3] E. Turiel, A. Martín-Esteban, Molecularly imprinted polymers for sample preparation: a review, *Anal. Chim. Acta* 668(2) (2010) 87-99.
- [4] E. Turiel, A. Martín-Esteban, Molecularly imprinted polymers-based microextraction techniques, *TrAC, Trends Anal. Chem.* 118 (2019) 574-586.
- [5] S.N. Egli, E.D. Butler, C.S. Bottaro, Selective extraction of light polycyclic aromatic hydrocarbons in environmental water samples with pseudo-template thin-film molecularly imprinted polymers, *Anal. Methods* 7(5) (2015) 2028-2035.
- [6] A. Azizi, F. Shahhoseini, E.A. Langille, R. Akhoondi, C.S. Bottaro, Micro-gel thin film molecularly imprinted polymer coating for extraction of organophosphorus pesticides from water and beverage samples, *Anal. Chim. Acta* 1187 (2021) 339135.
- [7] B.U.W. Lei, T.W. Prow, A review of microsampling techniques and their social impact, *Biomedical microdevices* 21(4) (2019) 1-30.
- [8] D.S. Kulyk, T. Sahraeian, S. Lee, A.K. Badu-Tawiah, Microsampling with a Solid-Phase Extraction Cartridge: Storage and Online Mass Spectrometry Analysis, *Anal. Chem.* 93(40) (2021) 13632-13640.
- [9] B.S. Frey, D.E. Damon, D.M. Allen, J. Baker, S. Asamoah, A.K. Badu-Tawiah, Protective mechanism of dried blood spheroids: stabilization of labile analytes in whole blood, plasma, and serum, *Analyst* 146(22) (2021) 6780-6787.
- [10] A. Podder, A.H.M.A. Sadmani, D. Reinhart, N.-B. Chang, R. Goel, Per and poly-fluoroalkyl substances (PFAS) as a contaminant of emerging concern in surface water: a transboundary review of their occurrences and toxicity effects, *J. Hazard. Mater.* 419 (2021) 126361.
- [11] S. Taniyasu, L.W.Y. Yeung, H. Lin, E. Yamazaki, H. Eun, P.K.S. Lam, N. Yamashita, Quality assurance and quality control of solid phase extraction for PFAS in water and novel analytical techniques for PFAS analysis, *Chemosphere* 288 (2022) 132440.
- [12] J. Liu, H. Wang, N.E. Manicke, J.-M. Lin, R.G. Cooks, Z. Ouyang, Development, characterization, and application of paper spray ionization, *Anal. Chem.* 82(6) (2010) 2463-2471.
- [13] E.S. Chernetsova, G.E. Morlock, I.A. Revelsky, DART mass spectrometry and its applications in chemical analysis, *Russ. Chem. Rev.* 80(3) (2011) 235.
- [14] G.A. Gómez-Ríos, J. Pawliszyn, Development of Coated Blade Spray Ionization Mass Spectrometry for the Quantitation of Target Analytes Present in Complex Matrices, *Angew. Chem. Int. Ed.* 53(52) (2014) 14503-14507.

[15] J. Yin, Z. Meng, Y. Zhu, M. Song, H. Wang, Dummy molecularly imprinted polymer for selective screening of trace bisphenols in river water, *Anal. Methods* 3(1) (2011) 173-180.